SYNTHETIC AND STRUCTURAL INVESTIGATION INTO HOMO- AND HETERO-, DI- AND TRI-NUCLEAR COMPLEXES CONTAINING OSMIUM

A thesis submitted to the

UNIVERSITY OF CAPE TOWN

in fulfilment of the requirements for the degree of

DOCTOR OF PHILOSOPHY

by

ELIZABETH ELDRED SUTTON
M.Sc. (Natal)

Department of Inorganic Chemistry
University of Cape Town
Rondebosch
South Africa

January 1986

TO MY MOTHER

without whom this would have been impossible

There is a beauty and an order to clusters and cluster structures that provides sufficient aesthetic and intellectual content for justification of molecular metal cluster research, be it theory, structure or exploratory synthesis.

E L MUETTERTIES

TABLE OF CONTENTS

Page

ACKNOWLEDGEMENTS

My sincere thanks and appreciation are extended to:

Professor J R Moss for his supervision and guidance;

Professor L R Nassimbeni and, especially, Dr M Niven for her very able and enthusiastic assistance in the X-Ray crystallographic research;

Dr G Jackson for helpful discussions in the nmr research;

Professor D A Thornton for financial assistance in the form of a lecturing post;

all colleagues, for their interest, help and friendship and, in particular, Phillip Hall for proofreading and drawings, Cheryl Walker, Bridget Williamson, Zayed Brown and William Hendricks;

the University of Cape Town and the South African Council for Scientific and Industrial Research for financial assistance;

Mrs Janet Longman for her patience and perseverance with the typing of this thesis;

my parents and family for their tremendous encouragement, help and support and, especially, my husband, Gordon, for unselfishly giving me this time, and my son, Andrew William, who will hopefully one day understand.

ABBREVIATIONS

Bu	butyl (superscript n, i, t, normal iso or tertiary butyl)
CDT	all trans-1,5,9-cyclododecatriene
dppm	bis(diphenylphosphino)methane
Et	ethyl
EXAFS	extended X-Ray absorption fine structure
hp	2-hydroxypyridine anion
IR	infrared
L	ligand
M	central (usually metal) atom in compound
Me	methyl
nmr	nuclear magnetic resonance
pdma	o-phenylenebis(dimethylarsine)
Ph	phenyl, C_6H_5
$[PPN]^+$	$[(Ph_3P)_2N]^+$
Pr	propyl (superscripts, n or i)
py	pyridine
R	alkyl or aryl group
THF	tetrahydrofuran
tht	tetrahydrothiophen
TMEDA	N N'N' N'-tetramethylethylenediamine
TMGH	tetramethylguanidine
TTF	tetrathiofulvalenium

ABSTRACT

Chain cluster complexes have been largely neglected in the general discussion on metal cluster complexes. The first chapter of this thesis has been devoted to an updated review of the synthetic and structural aspects of chain cluster complexes, classifying species of this type in a group of their own, as a sub-set of the large class of compounds loosely referred to as metal cluster complexes.

The reaction of $Os_3(CO)_{12}$ with X_2 (X = Cl, Br or I) in benzene, in direct, bright sunlight or a Hanovia photochemical reactor, has been studied. The nature of the products of the reactions depends critically on the experimental conditions employed. $Os_2(CO)_8X_2$ (X = Br or I), among other products, are obtained in reasonable yield, directly from $Os_3(CO)_{12}$. $Os_2(CO)_6I_2$ has been prepared from $Os_2(CO)_8I_2$ in 80% yield and the reactivity of the hexacarbonyl derivative with CO, PPh_3, PMe_2Ph, I_2, H_2 and C_2H_4 has been studied. The new species, $Os_2(CO)_6(PPh_3)_2I_2$ and $Os_2(CO)_6(PMe_2Ph)_2I_2$, are obtained. Cis-$Os(CO)_4X_2$ (X = Cl, Br or I) are thermally converted into $Os_2(CO)_6X_4$ (X = Cl, Br or I) species.

The X-Ray crystal structure of $Os_3(CO)_{12}Cl_2$ has been determined. Crystals of the compound are monoclinic, space

group C2/m, with a = 12.105(3) Å, b = 10.612(3) Å, c = 8.798(1) Å, β = 117.02(2)° and Z = 2. Intensities were obtained using ω-2θ scan techniques with a CAD4 diffractometer, using graphite-monochromated MoK$_\alpha$ radiation. The data were Lp processed and an empirical absorption correction applied. The structure was solved by conventional heavy-atom methods and least-squares refinements of structural parameters led to a R factor of 0.036 (R_w = 0.037, w = $(\sigma^2F)^{-1}$) for 821 observed reflections. The molecular structure of $Os_3(CO)_{12}Cl_2$ shows a linear triosmium chain with the three osmium atoms joined by single osmium-osmium bonds, of bond length 2.893(1) Å. The two terminal chloride ligands are situated in equatorial positions on the terminal osmium atoms. The equatorial ligands on the terminal osmium atoms adopt a staggered conformation with respect to the equatorial carbonyl ligands on the central osmium atom. The osmium-chlorine distance is 2.43(1) Å.

The structure of the compound, $Os_2(CO)_6I_2$, has been determined by X-Ray crystallography. Crystals of the compound are monoclinic, space group $P2_1/m$, with a = 6.453(3) Å, b = 14.017(7) Å, c = 7.328(4) Å, β = 91.03(2)° and Z = 2. Intensities were obtained using ω-2θ scan techniques with a Phillips PW1100 four-circle diffractometer, using graphite-monochromated MoK$_\alpha$ radiation. The structure was solved by conventional heavy-atom methods and

least-squares refinements of the structural parameters led to a convenitional R factor of 0.079 (R_w = 0.086, w = (σ^2F + 2 x $10^{-3}F^2$)$^{-1}$) for 1048 observed reflections. The molecular structure of $Os_2(CO)_6I_2$ shows a butterfly-type arrangement, with two six-coordinate osmium atoms joined by a metal-metal bond and two bridging iodide ligands at the apices of the wings. Three terminal carbonyl groups are attached to each osmium atom.

The X-Ray crystal structure of the compound, $Os_2(CO)_8Cl_2$, has been determined. Crystals of the compound are orthorhombic, space group $P2_12_12_1$, with a = 9.3599(9) Å, b = 9.879(2) Å, c = 16.014(3) Å and Z = 4. Intensities were obtained using ω-2θ scan techniques with a CAD4 diffractometer, using graphite-monochromated MoK_α radiation. The data were Lp processed and an empirical absorption correction applied. The structure was solved by conventional heavy-atom methods and least-squares refinements of structural parameters led to a R factor of 0.038 (R_w = 0.038, w = (σ^2F)$^{-1}$), for 1270 observed reflections. The molecular structure of $Os_2(CO)_8Cl_2$ shows two formally equivalent halves joined by a single osmium-osmium bond, of length 2.897(1) Å, and existing in a staggered conformation. Each osmium atom, in the +1 oxidation state with one terminal equatorial chlorine ligand and four

terminal carbonyl ligand, is six-coordinate with the six occupancy sites lying in a near-perfect octahedral configuration. The two osmium-chlorine distances are 2.452(6) and 2.442(6) Å, respectively.

The X-Ray crystal structure of the compound, $Os_2(CO)_8I_2$, has been determined. Crystals of the compound are tetragonal, space group $I4_1cd$, with a = 11.793(2) Å, c = 23.583(4) Å and Z = 8. Intensities were obtained using ω-2θ scan techniques with a CAD4 diffractometer, using graphite-monochromated MoK_α radiation. The data were Lp processed and an empirical absorption correction applied. The structure was solved by conventional heavy-atom methods and least-squares refinements of structural parameters led to a R factor of 0.0477 (R_w = 0.0424, w = $(\sigma^2F)^{-1}$), for 578 observed reflections. The molecular structure of $Os_2(CO)_8I_2$ shows two crystallographically identical halves, joined by a single osmium-osmium bond, of length 2.947(3) Å, and existing in a staggered conformation. Each osmium atom in a +1 oxidation state bonded to a terminal equatorial iodide ligand and four terminal carbonyl ligands, is six-coordinate, displaying near-perfect octahedral geometry. The osmium-iodine distance is 2.767(3) Å.

The X-Ray crystal structure of the complex, $[HOsRe(CO)_8Br]PPN$ has been determined. The crystals are

triclinic, space group $P\bar{1}$, with a = 11.762(2) Å, b = 14.206(2) Å, c = 14.333(2) Å, α = 117.75(1)°, β = 92.68(1)°, γ = 95.55(1)° and Z = 2. Intensities were obtained using ω-2θ scan techniques with a CAD4 diffractometer, using graphite-monochromated MoK_α radiation. The data were Lp processed and an empirical absorption correction applied. The structure was solved by conventional heavy-atom methods and least-squares refinements of structural parameters led to a R factor of 0.043 (R_w = 0.039, w = $(\sigma^2F)^{-1}$), for 3072 observed reflections. The structure of the anion, $[HOsRe(CO)_8Br]^-$, shows the two parts joined by a single osmium-rhenium bond, of length 2.995(1) Å, and existing in a staggered conformation. There are four terminal carbonyl ligands and one terminal equatorial hydride ligand bonded to the osmium atom and four terminal carbonyl ligands and one terminal equatorial bromide ligand bonded to the rhenium atom. The osmium-hydrogen and rhenium-bromine bond lengths are 1.66(8) Å and 2.646(2) Å, respectively.

The reaction of $[Os(CO)_4]Na_2$ with $M(CO)_5Br$ (M = Mn or Re) in a 1:1 or 1:2 molar ratio, respectively, in THF at room temperature, has been studied. The reactions are exceedingly complex and the nature of the products obtained depends upon the purity of $[Os(CO)_4]Na_2$ employed as the primary reactant. Isolation of individual anionic

species from the complex mixtures formed is difficult and it has only proved possible, to obtain the species, [HOsRe(CO)$_8$Br]PPN and [OsRe(CO)$_9$]PPN, on the addition of [PPN]Cl, in an analytically pure condition. Apart from the formation of the previously reported products, $M_2Os(CO)_{14}$ (M = Mn or Re) and HOsRe(CO)$_9$, which were incompletely characterised, evidence for the formation of HOsMn(CO)$_9$ is also obtained.

The reaction of [Os(CO)$_4$H]PPN with M(CO)$_5$Br (M = Mn or Re) in an equimolar ratio, in THF at room temperature, has been studied. As for the above reaction, these reactions are complex and the nature of the products obtained depends on the purity of [Os(CO)$_4$H]PPN employed as the primary reactant. The neutral hydride complexes, HOsM(CO)$_9$ (M = Mn or Re) are obtained pure, uncontaminated by $M_2(CO)_{10}$ (M = Mn or Re) species and are characterised by ^{1}H nmr, IR and mass spectroscopy. The anionic species, [HOsRe(CO)$_8$Br]PPN is isolated and fully characterised by ^{1}H nmr and IR spectroscopy and elemental analysis. Further evidence for the molecular formulation of this complex is obtained from the protonation reaction employing CF_3COOH in CH_3CN, where $Os(CO)_4H_2$ and $[Re(CO)_4Br]_2$ are obtained as products. The presence of [HOsMn(CO)$_8$Br]PPN, although obtained analytically impure, is postulated on the basis of ^{1}H nmr and Far IR spectroscopy. A second anionic product from the

reaction with $Mn(CO)_5Br$ is isolated, but due to its instability it remains uncharacterised. From the nature of the products obtained in these reactions, it is possible to deduce some of the reaction paths which are probably involved in the formation of these heteronuclear complexes.

The reaction of $[Os(CO)_4H]PPN$ with $Re(CO)_5I$ in an equimolar ratio, in THF, at room temperature has also been studied. The neutral iodo derivative, $IOsRe(CO)_9$ is obtained in low yield, contaminated with $Re_2(CO)_{10}$, and is identified by IR and mass spectroscopy. The major product of this reaction, $[HOsRe(CO)_8I]PPN$, is isolated and fully characterised by ^1H nmr and IR spectroscopy and elemental analysis. From the similarity of the $\upsilon(CO)$ bands in the IR spectrum of the complexes, $[HOsRe(CO)_8X]PPN$ (X = Br or I), it is suggested that $[HOsRe(CO)_8I]PPN$ adopts a similar structure to that determined in this present work for the bromo analogue.

The reactivity of $HOsRe(CO)_9$ with various reagents, namely, CH_3I, CBr_4 and CCl_4 has been investigated and the halo derivatives, $XOsRe(CO)_9$ (X = Cl, Br or I) are obtained and characterised by IR and mass spectroscopy. Evidence for halogen cleavage of the osmium-rhenium bond is obtained from the reaction of $HOsRe(CO)_9$ with I_2.

The reactivity of $[HOsRe(CO)_8Br]PPN$ with various reagents,

namely, CH_3I, CBr_4, $AgBF_4$, $AuPPh_3Cl$, PPh_3, py and CO has been investigated. Several new products $[XOsRe(CO)_8Br]PPN$ (X = I or Br), $[Os(CO)_4(AuPPh_3)ClRe(CO)_4]PPN$, $[Os_2Re_2(CO)_{12}(AuPPh_3)_2]PPN$ and $[Os(CO)_3HLRe(CO)_4Br]PPN$ (L = PPh_3 or py) are believed to have been obtained, and evidence for their formation is presented. However, only an X-Ray structural determination of crystals of each of these products would enable unequivocal characterisation to be made.

^1H nmr spectra of hydrido osmium species show low intensity satellites due to coupling to natural abundance ^{187}Os. The high resolution ^1H nmr spectra of the homologous series of hydrido osmium complexes, $[Os(CO)_4]_nH_2$ (n = 1, 2 or 3) as well as three heteronuclear hydrido species, $HOsRe(CO)_9$ and $[HOsRe(CO)_8X]PPN$ (X = Br or I) have been determined. $^1J(^{187}Os-^1H)$ has been observed for all the complexes studied, while a 'secondary' coupling constant, $^2J(^{187}Os-^1H)$, for a hydride ligand coupling to an adjacent osmium atom two bonds away, has been observed for $Os_2(CO)_8H_2$ and $Os_3(CO)_{12}H_2$.

CHAPTER 1

INTRODUCTION

1.1 A Discussion on Metal Cluster Complexes with Particular Reference to Chain Cluster Complexes

There are two types of catalytic reactions. The homogeneous catalytic reaction is, by definition, one in which all the constituents of the reaction are present in the same phase.[1] Generally, the reactants and the catalyst are present in a common liquid phase, i.e. in solution. The heterogeneous catalytic reaction, on the other hand, is one in which one or more of the constituents are in different phases. In heterogeneous catalysis, the catalyst is usually present as a solid and the reactants as liquids or, more frequently, as gases. The catalysed reaction then takes place at the phase interface, i.e. on the catalyst surface.[1] Both types of catalytic systems have their advantages and disadvantages. The solid state heterogeneous catalytic system is often preferred purely from engineering considerations. These considerations include ease of product separation or dictates of the reaction temperature where no liquid phase is feasible and/or where the catalyst is required to have very high thermal stability.[2] However, whereas the intimate details of reaction mechanisms in catalytic reactions are very difficult to assess for reactions taking place on a surface, these reactions occurring in solution are relatively well-understood.[2] It has been suggested that reaction mechanisms which have been established for homogeneous catalytic reactions may also be applied to those reactions occurring on metal surfaces. However,

specific properties exhibited by metal surfaces have not as yet been observed in discrete coordination or organometallic compounds.

A class of compounds, commonly referred to as metal clusters,[3] retain all the experimentally desirable features of simple mononuclear homogeneous catalysts for the definition of structure, stereochemistry, dynamic stereochemistry (ligand mobility) and the mechanistic details of catalytic chemistry,[4] because they are discrete molecular entities, soluble in a variety of non-reactive solvents. It is commonly believed that metal clusters may be far more meritorious models of surfaces of chemisorption and heterogeneous catalytic processes than molecular or homogeneous catalysts.[4] In no way is a metal cluster, like $Os_3(CO)_{12}$, a model of a clean metal surface, but the cluster may be a reasonable approximation of chemisorbed species on a metal surface, in this case, chemisorbed carbon monoxide molecules. There is a view that studies of reactions of small substrates with metal clusters may shed light on the interactions which occur on the metallic surface.[3] The bonding modes which CO, H_2 and small organic molecules adopt on reaction with small clusters may be identified with certainty and their spectroscopic properties often identified with those of chemisorbed species.[3]

Requisite data for a comparison of metal-metal bond

strengths between metal atoms at the metal surface and metal atoms in a cluster are not available.[2] However, a comparison of the average metal-metal bond energy in bulk metal with metal bond energies in dinuclear metal complexes, commonly referred to as cluster prototypes, has been determined[5] and this clearly suggests that the energies in the two limiting cases for a given metal, will be quite similar. In both metals and metal clusters, the metal-metal bond energy increases within a group as the size or atomic weight of the metal increases and parallel changes in bond energy are found with variation in the electronic character of the metal.[2]

A metal atom 'cluster' may be defined as a "group of two or more metal atoms in which there are substantial and direct bonds between the metal atoms, even though there may be some non-metal atoms associated intimately with the cluster".[6] There have been many definitions of 'metal clusters' put forward.[3] However, in general, a cluster consists of a metallic framework surrounded by ligands.[7] Therefore, the metallic backbone may exist as either an open structure with a linear or bent framework, or closed with a cage-type structure, within the more general definition provided by Cotton.[6] Reviews on metal cluster chemistry, through to 1983, have dealt mainly with closed or cage structures where a polyhedral array of metal atoms is held together by metal-metal bonds with at least two metal-metal bonds to each metal atom.[8-12] Open or chain clusters, of which there are many known, appear to be a

forgotten or neglected class of cluster compounds. However, chain clusters may also provide good models for metal surfaces. They may be useful for investigating the interaction between groups on adjacent metal atoms.

Homogeneous catalytic reactions, which incorporate reactions such as hydrogenation, isomerization, dimerization and polymerization of olefins, olefin metathesis, oxidations, and conversion of olefins to aldehydes and vinyl acylates, to mention but a few, have been shown to traverse reaction intermediates in transition metal catalysts encompassing a wide variety of metal bonding interactions. These so-called "functionalities" which involve single metal centres, have been previously mentioned.[2] The potential "functionalities" for surface chemical reactions have also been listed[2] where more than one metal atom may be involved in the bonding interaction. The scheme below illustrates the difference between these "functionalities" for the homogeneous and the heterogeneous catalytic systems, respectively, using the metal carbonyl bonding interaction as an example.[2]

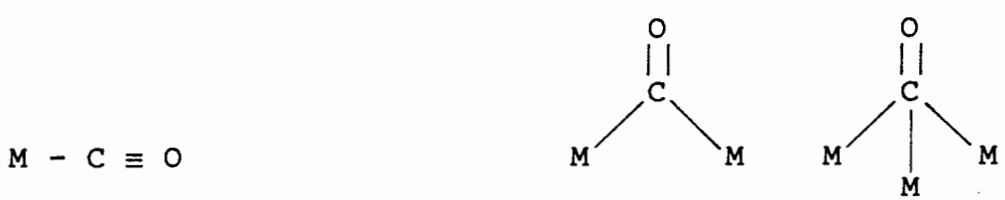

Homogeneous catalyst Heterogeneous catalyst

Since metal clusters are believed to be models for metal surfaces, such "functionalities" would also be expected to be found for this class of complexes. A third possible bonding interaction for carbon monoxide was found to be present in the cluster prototype, $Mn_2(CO)_5(Ph_2PCH_2PPh_2)_2$,[13] where one carbonyl ligand was shown to be involved in an unusual bridging arrangement, as shown in figure 1.1.

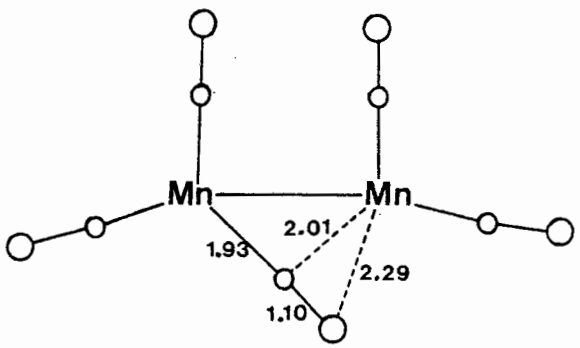

Figure 1.1 Diagrammatic representation of $Mn_2(CO)_5(Ph_2PCH_2PPh_2)_2$, showing unusual bridging carbonyl arrangement.

In this structure, there is a strong Mn-O interaction which, perhaps, anticipates

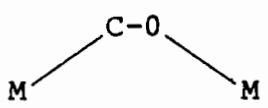

bonding on metal surfaces, a feature which may be critical in the catalytic reduction of carbon monoxide by hydrogen.[2]

Consider the hydrogenation of an olefin where both H_2 addition and olefin complexation to the metal surface occurs. It is unlikely that both these attachments could ensue at a single metal atom on the metal surface. A more plausible mechanistic scheme would be to involve adjacent metal atoms on the surface and assume high mobility for hydrogen atoms,[2] as illustrated in the scheme below:

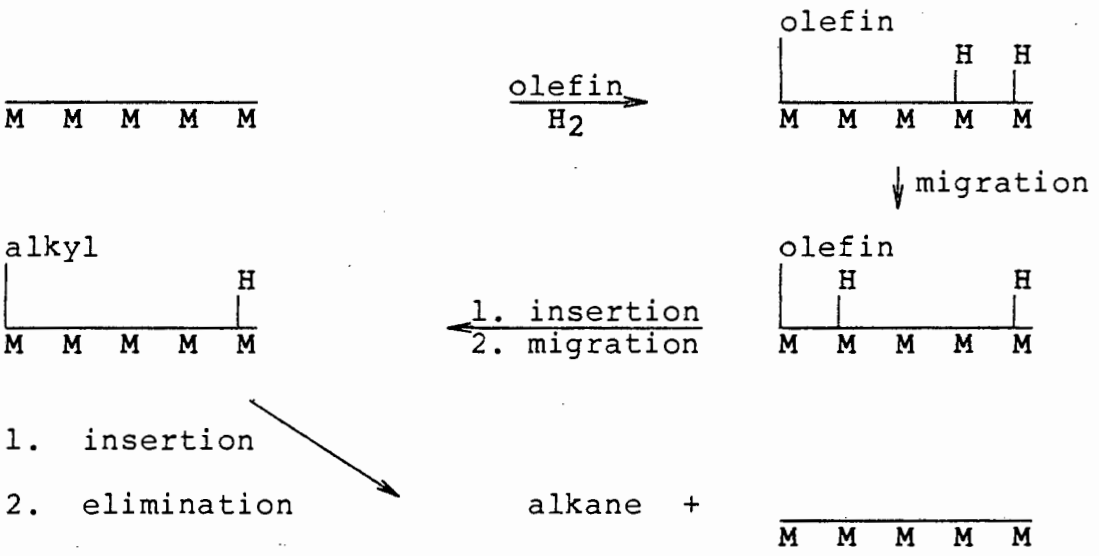

In this specific case, hydrogen migration on a surface may be simply viewed as a large amplitude bending motion which converts a terminally bonded hydrogen atom to a bridge bonded hydrogen atom, or vice versa, as can be seen in the scheme below:[2]

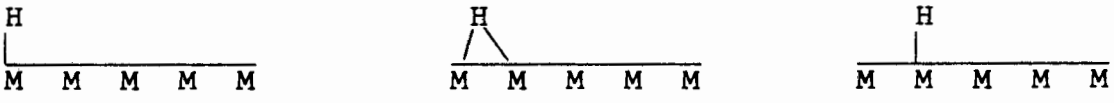

Similar 'surface walks' have been observed for hydrogen atoms on metal clusters. For example, in the complex,

$H_2Os_3(CO)_{11}$,[14] which has one terminal and one bridging hydride ligand, the hydride ligands seem to readily traverse edge or edge-vertex positions of the cluster. Ligand mobility over the metal cluster was first suspected by Cotton.[15] Similar behaviour for carbon monoxide molecules on the metal surface, as outlined below,

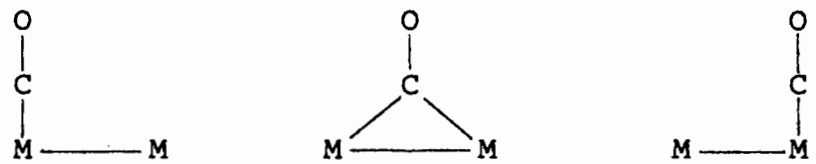

has been frequently observed in metal cluster chemistry, through ^{13}C dynamic nmr studies. These data establish that rapid intramolecular exchange of all carbonyl groups in many metal carbonyl complexes occurs. An essential feature for this exchange must be the process which interconverts terminal and bridging carbonyl positions and allows for facile traverse of the cluster periphery by a carbonyl group.[2] Clusters have been shown to exhibit a full range of ligand bonding as would seem necessary for a valid cluster-surface analogy, since both terminal and bridge bonding have been reasonably defined for hydrogen and carbon monoxide ligands on some metal surfaces.[6]

Since the discovery of the Fischer-Tropsch reaction, i.e. the conversion of CO and H_2 to hydrocarbons, principally a mixture of linear alkanes and alkenes, by passage over heterogeneous transition metal catalysts, several

proposals as to the mechanism of the reaction have been presented.[17,18] It is currently believed that surface-bound CH_2 species are involved in the reaction.[19,20] Bridging methylene ligands bound to metal cluster complexes have received much attention in recent years. Their IR vibrational assignments have been compared with the frequencies assigned to methylene species chemisorbed on metal surfaces and have been found to be very similar.[21] Bridging methylene ligands were reported[21] to bind to the Os_3 triangle in the complexes $Os_3(CO)_{10}(\mu_2\text{-}H)_2(\mu_2\text{-}CH_2)$ - figure 1.2 a)- and $Os_3(CO)_{10}(\mu_2\text{-}CO)(\mu_2\text{-}CH_2)$ - figure 1.2 b).

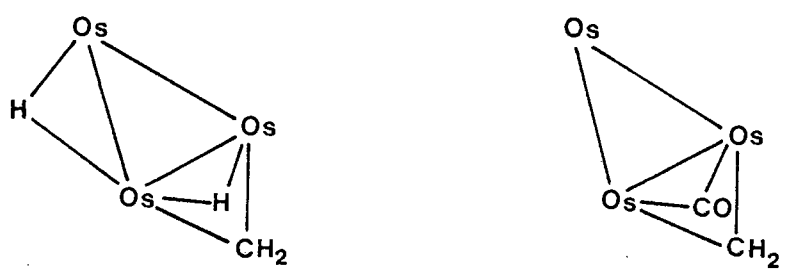

a) b)

Figure 1.2 Diagrammatic representation of
a) $Os_3(CO)_{10}(\mu_2\text{-}H)_2(\mu_2\text{-}CH_2)$ and
b) $Os_3(CO)_{10}(\mu_2\text{-}CO)(\mu_2\text{-}CH_2)$

It has also been suggested that a methylene species is involved in the hydrogenation of surface-bound carbide

atoms during the methanation reaction.[19]

Metal cluster complexes are thus believed to be miniature versions of a surface, discrete entities, the detailed structures of which may be ascertained. Their stoichoimetric chemisorption analogues and catalytic reactions may be probed effectively in a mechanistic context through kinetic and spectroscopic analysis. Thus, they offer a template on which reactions believed to be occurring on metal surfaces, can be more effectively studied.

Chemists have become increasingly involved in the synthesis of inorganic and organometallic chain and layer compounds, because physicists wanted to look at magnetic and optical properties in one or two dimensions only. This collaboration resulted in a wide range of novel compounds with unusual physical properties, e.g. molecular superconductors,[23] where 'superconductivity' has been described as a "cooperative phenomenon of electrical conductivity. It is displayed when the normal process of scattering between electrons and the lattice, which gives rise to electrical resistance, are removed; a superconductor shows no impediment to a steady electrical current."[24] This phenomenon has only recently been observed in the compound $Hg_{2.86}AsF_6$.[25]

Two-dimensional metals can be defined as those compounds

which possess metal atoms bound by a layer-type linkage while 'one-dimensional metals' are compounds which have chain-like linkage of the metal atoms.[12] Particular interest in 'one-dimensional metals' lies in the fact that in the ideal case they represent minute electrical conductors with their own insulation.[26,27] Nevertheless, in spite of the large number of chemical and physical studies carried out on these compounds,[28,29] the desired high-temperature 'superconductivity' did not materialise until 1974. The use of these compounds as current carriers is limited by the difficulty of obtaining ideal crystals of suitable size.[12]

Many substances are now known which have crystal structures in which the nearest neighbour ions or molecules are much more closely spaced in some directions than others. Layers and chains are, therefore, a common feature in structural inorganic chemistry.[23] Two properties appear to be necessary for a complex to exhibit high and anisotropic electrical conductivity properties. These are, firstly, that square coplanar complexes must form a columnar stack structure with a short intrachain metal-metal separation and, secondly, that the metal atom or complex as a whole must adopt a non-integral formal oxidation state. This was the conclusion of a study made on the one-dimensional conductor $Li_{0.75}$-$[Pt\{S_2C_2(CN)_2\}_2].2H_2O$.[30]

Ginsberg et al[31] have investigated the compounds $K_{0.60}Ir(CO)_2Cl_2.0.5H_2O$, $(TTF)_{0.61}Ir(CO)_2Cl_2$ (TTF = tetrathiofulvalenium), $K_{0.57}Ir(CO)_2Br_2.0.2CH_3COCH_3$ and $Cs_{0.60}Ir(CO)_2Br_2$ - figure 1.3 - by various physical techniques and have found that conducting linear chains of cis-$[Ir(CO)_2X_2]^{0.60-}$ (X = Cl, Br) units are present in the three compounds studied. Since conductivity is proportional to the density of charge carriers, materials with a high degree of partial oxidation might show enhanced conductivity. The analytical data of these compounds showed that the oxidation state of the iridium in the anionic complexes is in the range 1.39 - 1.44. This corresponds to 3.9 - 4.4 charge carriers for every ten iridium atoms. The conductivity behaviour of the complexes and their morphological and optical anisotropy (dichroism) - see later - is strong evidence that they are linear-chain conductors. The magnetic susceptibility measured for the compound $(TTF)_{0.61}Ir(CO)_2Cl_2$ was found to be particularly interesting. Since TTF^+ has an unpaired spin it cannot be present in the salt as a simple monocation but must form clusters or linear stacks in which the spin is quenched. The possibility that TTF is stacked and that the unpaired spins are delocalised along the stack structure is unlikely because of the very similar appearance (colour, morphology, dichroism) and conductivity behaviour of the TTF and the alkali metal salts of $[Ir(CO)_2Cl_2]^{0.6-}$.

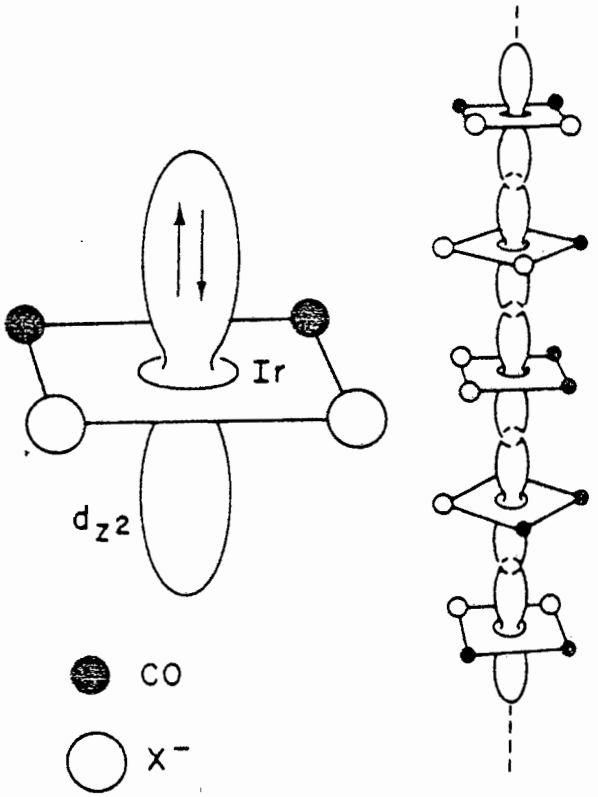

Figure 1.3 Linear chain structure of $[Ir(CO)_2X_2]^{0.6-}$ showing overlap of d_z2 orbitals.[31]

These two criteria, necessary for electrical conductivity, were also found for the compound $K_2Pt(CN)_4Br_{0.30}.3H_2O$[32] - see figure 1.4. This compound was prepared early in the 19th century by partially oxidising $K_2Pt(CN)_4$ with Br_2. Although the Pt(IV) salt, $K_2Pt(CN)_4Br_2$, does not conduct electricity, it has the ability to act as a metal in one direction, that being parallel to the $Pt(CN)_4$ stacks. The conductivity arises from overlap between the $5d_z2$ orbitals on neighbouring complexes which are broadened into a band. Partial oxidation means that the band is partly filled as required for metallic conductivity. Between the chains the separation is nearly 8 Å but within the chains it has

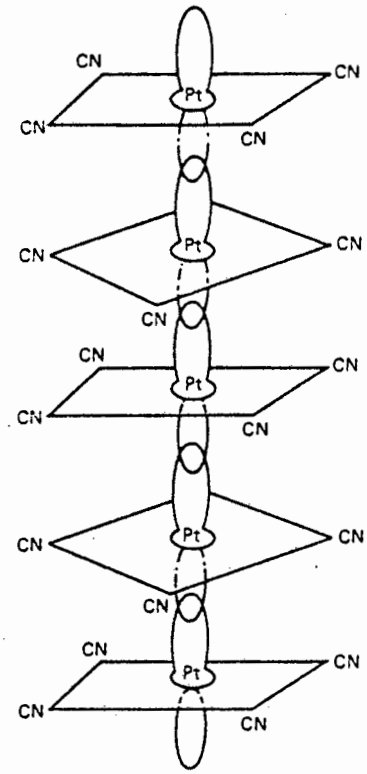

Figure 1.4 Diagram of the stacking of $[Pt(CN)_4]^{n-}$ ions showing how metal d_z2 orbitals can overlap.[32]

been found to be only 2.89 Å, hence the one-dimensionality. However, the compound $K_2Pt(CN)_4Br_{0.30}.3H_2O$ was only found to be metallic (in that the conductivity decreases with increasing temperature), in the region of room temperature.[23] At lower temperatures, the dependence becomes similar to that of a semiconductor.

A recent study[33] on the charge overlap of multiple metal-metal bonding and conjugation in linear chains of transition metal atoms presented some interesting findings. The study concentrated on linear digonal bonding, using only spectroscopically observed real states such as the d^nsp state, which is pertinent for digonal sp or dp hybridization and attempted to determine whether the

excitation energy was compensated for by the bond stabilization energy, assuming an infinite linear chain. The analysis showed that for an infinite linear chain of metal atoms, because of the need to reserve electrons to bond to neighbours on two sides, for chain extension, the bond orders for the $-M_2-$ in the chain are generally one order less than those of dinuclear metal complexes. The bonding in a chain should be much stronger because electron repulsion is reduced by digonal hybridization and by excitation to the d^nsp hybridized configuration. This stabilization should be further enhanced by resonance conjugation over an infinite chain, which is not possible for di- or tri-nuclear complexes. Obviously, the multiple bonding concept would enhance 'superconductivity'. It is pertinent to this area of study that the mode of bonding in the metal chain be understood, since the high and anisotropic electrical conductivity properties, which tetracyanoplatinate and **bis**(oxalato)platinate display, can be explained completely in terms of the charge carrier being confined to the metal atom chain. The coordinating ligands do not participate directly in the conduction mechanism.[31]

Whereas closed or cage-type clusters appear to have been more widely studied in terms of catalytic behaviour, attention has been focussed more on linear or chain structures of metal atoms in terms of the search for uni-dimensional conducting properties. Catalytic aspects of cage-type cluster chemistry have been reviewed on

numerous occasions.[3,22,34] However, chain clusters, as a group, which potentially holds exciting possibilities for investigation of adjacent metal atoms, have never been formally discussed. It is also of prime importance that the solid-state properties of 'one-dimensional' metals be understood. If they should prove to be highly anisotropic conductors, their possible technological applications are vast.[23] A review of chain cluster complexes covering the literature up to 1979 has been written.[35] What follows herein is a second review on the same topic, filling in omissions and updating the information to March 1983, along the same guidelines as the first review.

1.2 Review of Chain Cluster Complexes

1.2.1 Introduction

Several workers, in view of the interesting uni-dimensional electron transport properties associated with intermetallic chains in certain crystal lattices, have concentrated their efforts on the synthesis of linear molecular polymers with backbones comprised entirely of covalently bonded metal atoms. One form of strategy has been to prepare collinear trimetallic monomers of octahedral transition metal complexes which might then be further elaborated into oligomers or polymers.[36] Oligomers formed from linear trimetallic segments would have to become quite large in order to cycle back on themselves and thus would be expected to have a higher

probability of growing linearly.[36] However, the chain cluster compounds mentioned in this review have not, with one or two exceptions, been studied in terms of electrical conductivity properties, since the majority of chain clusters discussed are trinuclear complexes. Consider the molecule, $Mn_2Os(CO)_{14}$[37] (figure 1.5) quoted in the first review[35] which is an example of a linear trinuclear chain cluster complex.

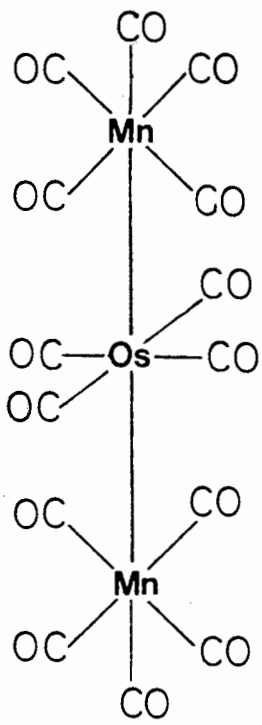

Figure 1.5 The structure of $Mn_2Os(CO)_{14}$.

The carbonyl groups are staggered around the metal atoms in a quasi-square planar configuration, as are the cyano groups in $K_2Pt(CN)_4Br_{0.30}.3H_2O$. However, the molecule exists as a discrete diamagnetic entity. It does not exist in an extended metallic array, as does

$K_2Pt(CN)_4Br_{0.30}.3H_20$, nor does the molecule adopt a non-integral formal oxidation state. Furthermore, the intermolecular separations are probably too great to enable meaningful interchain interactions to take place. Therefore, these linear trimetallic complexes would not be expected to exhibit electrical conductivity properties. They do, however, represent a 'building block' for metal chain extension since they contain the essential metallic framework and, therefore, a collective study of their syntheses and properties is warranted.

The review to follow will cover two broad categories, namely, those chain clusters containing only transition metal atoms and those containing both transition metal and main group metal atoms. The discussion will follow the order of the Periodic Table as closely as possible. It has been necessary to adhere to a specific definition of a 'chain cluster' and the following criteria have been set:

1. At least one transition metal must be incorporated in the chain.

2. The cluster may contain more than two metals atoms (by our definition).

3. The cluster must be held together only by metal-metal bonds. No clusters containing metal-metal bonds supported by bridging groups have been included; and

4. No clusters containing elements on the borderline between metal and non-metal, for example, germanium, arsenic, selenium, have been included, although many are known to exist.

1.2.2 Chain Cluster Complexes Incorporating Only Transition Metal Atoms

Since 1979, homonuclear chain cluster complexes have, been reported only for osmium. The compounds $Os_3(CO)_{12}(SiXCl_2)_2$ (where X = Me,Cl), have been isolated[38] from the reaction of $Os_3(CO)_{12}$ with the appropriate silane, Cl_2XSiH, at 140°C, under carbon monoxide pressure (80 atm). The crystal structure of $Os_3(CO)_{12}(SiCl_3)_2$ - figure 1.6 - has been determined by X-Ray methods. The molecule was found to have a crystallographic centre of symmetry. The carbonyl groups on the terminal osmium atoms were found to be staggered with respect to those on the central osmium atom. The osmium-osmium distance of 2.912(1) Å found, is somewhat longer than usual unbridged Os-Os bond

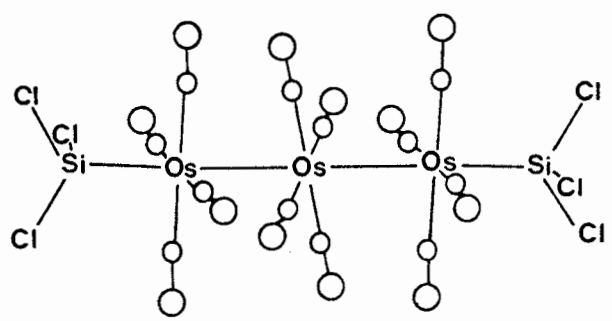

Figure 1.6 The structure of $Os_3(CO)_{12}(SiCl_3)_2$.

lengths, e.g. in $Os_3(CO)_{12}$[39] the mean value is 2.877(13) Å, but comparable with the corresponding distance in $Os_3(CO)_{12}I_2$[40] of 2.935(2) Å. The ^{13}C nmr spectrum of the compound showed that the linear $SiOs_3Si$ chain is maintained in solution. The carbonyl signals in an approximate 2:1 ratio were unambiguously assigned to the carbonyl ligands of the terminal and central osmium atoms, respectively. The staggered conformation of the carbonyl groups is typical and has previously been found in such molecules as $Os_3(CO)_{12}I_2$,[40] and $[Mn_3(CO)_{14}]^-$ [41], (discussed in the first review[35]).

Evans and Sheline[42] reported the photochemical synthesis of $ReFeMn(CO)_{14}$ - figure 1.7 - which is the most unique member of the general series of trinuclear carbonyls $MM'Fe(CO)_{14}$ (M and M' = Group VIIA metals, Mn and Re). The osmium and ruthenium analogues (M = M') are also known. The compound, $ReFeMn(CO)_{14}$, was obtained by the irradiation of a n-hexane solution of $Fe(CO)_5$ and $ReMn(CO)_{10}$. After 30 minutes, the solution changed from light yellow to bright orange and the compound was crystallised as an orange, needle-like substance, from acetone. This compound is believed to contain a linear sequence of metal atoms, on the basis of IR spectral data.[43]

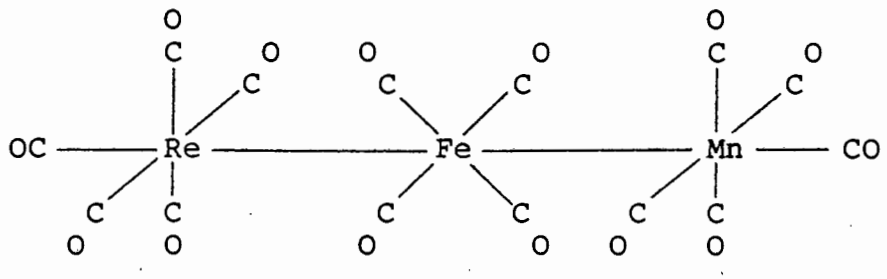

Figure 1.7 The structure of $ReFeMn(CO)_{14}$.

The tetrahydrothiophen group (tht) in $Au(C_6F_5)_3(tht)$ has been reported to be readily replaced by the carbonylmetalate, $[M(CO)_n]^-$ (M = Co, n = 4, M = Mn, n = 5) or $[M(\eta\text{-}C_5H_5)(CO)_3]^-$ (M = Mo or W), to give bimetallic complexes. However, the reaction of these carbonylmetalates with $Au(C_6F_5)(tht)$ gives rise to disproportionations affording $[Au\{M(\eta\text{-}C_5H_5)(CO)_3\}_2]NBu^n_4$, $[Au\{M(CO)_n\}_2]PPN$ (PPN = bis(triphenylphosphine)iminium) and $[Au(C_6F_5)_2]Q$ (Q = PPN or NBu^n_4) which are stable at room temperature.[44] The presence of a linear unit, Co-Au-Co, in $[Au\{Co(CO)_4\}_2]PPN$ - figure 1.8 - has been established by a single crystal structure determination. The cation was found to lie on a crystallographic centre of symmetry with a Co-Au bond length of 2.509(2) Å. The idealised trigonal-bipyramidal geometry at cobalt is distorted by the bending of the CO groups towards the Co-Au metal-metal bonds. The same effect has been noted, to a lesser extent, in $[Hg\{Co(CO)_4\}_2]$,[45] which is isoelectronic with this anion and also possesses a

staggered conformation. This has also been noted in the dinuclear complex, $Ph_3PAuCo(CO)_4$.[46]

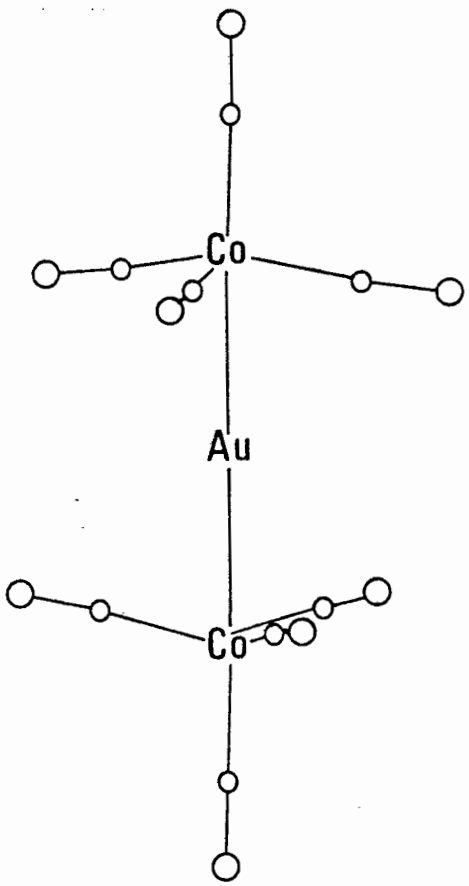

Figure 1.8 The structure of $[Au\{Co(CO)_4\}_2]PPN$.

Reaction of the carbonyl anions $[Mn(CO)_5]^-$, $[Co(CO)_4]^-$ and $[(\eta\text{-}C_5H_5)Mo(CO)_3]^-$ on the substrate trans-PtL_2Cl_2 have been carried out and the crystal structures of trans - $Ptpy_2[Mn(CO)_5]_2$ and trans-$Ptpy_2[Co(CO)_4]_2$ (py = pyridine) have confirmed the trans square-planar configuration of the platinum atom.[47] The molecular structure of these compounds has been shown, however, to depend very much on the nature of the ligand, L. If L is pyridine, a linear

trimetallic chain containing the Co-PtL_2-Co unit is obtained,[48] whereas if L is triphenylphosphine, a tetrameric $Pt_2Co_2(CO)_5(\mu_2\text{-}CO)_3(PPh_3)_2$ butterfly cluster is formed.[49,50]

Braunstein[51] showed that for the family of trimetallic complexes, M-PtL_2-M (M = $Co(CO)_4$, $Fe(CO)_3NO$, $Mo(CO)_3(\eta\text{-}C_5H_5)$, $W(CO)_3(\eta\text{-}C_5H_5)$ and $Mn(CO)_5$) there is an increase in π-back donation from Pt to the ligand L following the above series of the M varieties. He explained this trend as being a consequence of the increased electron density on the Pt on going from the Co to the Mn complex.[51]

The abovementioned series of linear trimetallic complexes were reduced on Pt and Au electrodes in nonaqueous media to examine their electrochemical behaviour.[52] All of these complexes were found to undergo irreversible one-electron reductions which result in the rupture of one Pt-M bond and the liberation of one $[M]^-$ ion per mole of complex reduced. Coupled ESR spectroscopy and coulometry indicated that a radical is generated during the reduction of the trimetallic species. This behaviour was compared with the analogous series of $[M\text{-}Au\text{-}M]^-$ (where M = $Cr(CO)_3(\eta\text{-}C_5H_5)$, $Mo(CO)_3(\eta\text{-}C_5H_5)$, $W(CO)_3(\eta\text{-}C_5H_5)$ and M-Hg-M (where M = $Mn(CO)_5$, $Co(CO)_4$) complexes and while the Pt complexes resulted in the formation of an unexpected paramagnetic Pt(I) species, the gold and

mercury complexes showed predictable metal-metal bond cleavage. The proposed reduction schemes were given as follows:

$$M\text{-}PtL_2\text{-}M + 1e^- \longrightarrow M^- + M\text{-}PtL_2^{\bullet}$$

$$(M\text{-}Au\text{-}M)^- + 1e^- \longrightarrow Au^{\circ} + 2M^-$$

$$M\text{-}Hg\text{-}M + 2e^- \longrightarrow Hg + 2M^-$$

The ligands L (isocyanide ligands) introduce a strong π-acceptor character able to stabilise the otherwise unstable Pt(I) radical, $M\text{-}PtL_2^{\bullet}$. The half-wave reduction potential values recorded for the $Co(CO)_4$ and $Fe(CO)_3NO$ complexes of Pt which were found to be more cathodic on going from Co to Mn, agree with these two moieties being better leaving groups than the other carbonylmetalate anions, as described previously.[51]

The reaction between $cis\text{-}PtCl_2(PPh_2Cl)_2$ with $NaMn(CO)_5$ in THF has been reported to yield a series of new trimetallic Pt-Mn complexes.[53] The substitution of the Pt-Cl bonds was accompanied by a redox reaction and a labilization of the Pt-P bonds, as exemplified by the isolation of complexes in which such bonds have been broken or created. $Pt(CO)_2[Mn(CO)_5]_2$ - figure 1.9 - one of the products of this reaction, was separated out by column chromatography from other products and is most likely to possess a linear Mn-Pt-Mn arrangement. Pt-Mn bonds have been shown to be

intrinsically strong enough to allow the isolation of trimetallic open $(OC)_5Mn-PtL_2-Mn(CO)_5$ complexes.

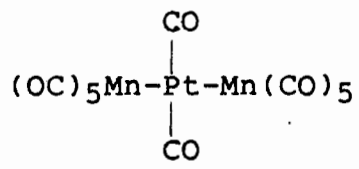

Figure 1.9 Diagrammatic representation of $Pt(CO)_2[Mn(CO)_5]_2$

The electrochemical behaviour of the linear trinuclear platinum-cobalt complex, $(OC)_4Co-PtL_2-Co(CO)_4$ (L = cyclo-$C_6H_{11}CN$) has recently been compared with that of closed, cage-structured platinum-cobalt complexes.[54] It was found that one-electron reduction took place in both cases and that $[Co(CO)_4]^-$ was the common species produced. These observations led these workers to the reasonable assumption that the overall electroreduction scheme of both types of clusters is very similar, whether the metallic skeleton be open or closed, and occurs through the intermediate generation of radicals.

1.2.3 Chain Cluster Complexes Incorporating Transition Metal and Main Group Metal Atoms

1.2.3.1 Zinc, Cadmium and Mercury

The complexes $[(\eta-C_5H_5)_2Mo][(\eta-C_5H_5)Zn]_2$ and $[(\eta-C_5H_5)_2W]-[(\eta-C_5H_5)Zn]_2$ have been reported[55] to be obtained in

quantitative yield when the appropriate transition metal hydride is treated with an excess of $(\eta\text{-}C_5H_5)_2Zn$ in benzene at room temperature according to the following stoichiometry:

$$2(\eta\text{-}C_5H_5)_2Zn + 2MH \rightarrow [(\eta\text{-}C_5H_5)Zn]_2M + C_5H_6 + H_2$$

where $M = Mo(\eta\text{-}C_5H_5)_2$, $W(\eta\text{-}C_5H_5)_2$

These compounds are thermally stable solids which are soluble in benzene. Molecular weight determinations have shown them to be monomeric. Although their crystal structures have not been determined, they are believed to exist as a chain of metal atoms.

The synthesis and reactivity of $(ClZn)_2Fe(CO)_4.C_6H_{14}O_3$ has been described.[56] This compound was formed from $(ClHg)_2Fe(CO)_4$,[57] powdered zinc and diglyme. Investigations of the reactivity of $(ClZn)_2Fe(CO)_4.C_6H_{14}O_3$ with triphenyltin halide in diglyme were carried out and the product $(Ph_3Sn)_2Fe(CO)_4$ was isolated in 67% yield.

When $(NH_3)_3ZnFe(CO)_4$ was added to a THF solution of 1% Na/Hg amalgam, a yellow orange solution of $[Na(THF)_2]$-$[Zn\{Fe(CO)_4\}_2]$ - figure 1.10 - was obtained.[58] This complex was isolated in 63% yield as very air-sensitive colourless crystals, with a light pink tint, which formed on standing in a toluene/THF solution. The crystal structure showed that the Zn atom is located at a site of 2/m

symmetry with the Fe atom and CO ligands of the independent $[Fe(CO)_4]$ fragments lying on a crystallographic mirror plane.

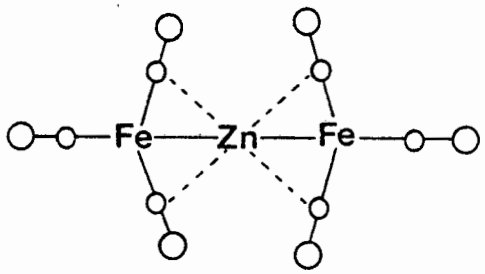

Figure 1.10 The structure of $[Zn\{Fe(CO)_4\}_2]$ where the dotted lines represent the square-planar geometry about the zinc atom.

The Zn-Fe bond length was found to be 2.317 Å which is nearly 0.25 Å shorter than expected, as calculated from the sum of the van der Waal's radii of Zn and Fe. The structure of the dianion is highly novel in that it represents an example of a zinc-capped iron tetrahedron which is intermediate between face-capping and edge-capping. A major distortion from a regular trigonal-bipyramidal geometry is found for the axial carbonyl ligand C_1O_1 and two equatorial carbonyl ligands C_3O_3 and $C_3'O_3'$- which are bent in towards the zinc atom or the Fe-Zn metal-metal bond. Bond angles of trans-Zn-Fe-C(1) = 162.3(2)° and cis-Zn-Fe-C(3) = 74.8° indicate the extent of the distortion. The C_3 and three symmetrically related carbonyl carbon atoms form a square-planar geometry about the zinc atom, represented by the dotted lines in figure 1.10.

The electrochemical synthesis of linear trimetallic complexes has been achieved.[59] The electrochemical oxidation of a Zn, Cd or In electrode was performed in the presence of $Co_2(CO)_8$ or $Mn_2(CO)_{10}$ in an organic solvent mixture containing a neutral bidentate donor ligand such as bipyridine. The heteronuclear complexes $M[M'(CO)_n]_m$ (M = Zn,Cd or In; M' = Co or Mn; n = 4 or 5; m = 2 or 3), were thus obtained. A mechanism involving discharge of $[Mn(CO)_5]^-$ and $[Co(CO)_4]^-$ anions to radicals at the anode surface was proposed.

The synthesis and characterisation of a number of cyclopentadienylzinc-transition metal compounds have been reported and have been found to be stable to disproportionation, unlike their organozinc analogues. The preparation of $[(\eta\text{-}C_5H_5)Zn]_2Co(\eta\text{-}C_5H_5)PPh_3$ has been reported and its structure determined.[60] The complex was obtained from the reaction of $(\eta\text{-}C_5H_5)_2Zn$ with $HCo(N_2)(PPh_3)_3$ in benzene. The crystal structure of the compound - figure 1.11 - consists of four discrete molecular units in a monoclinic unit cell. The molecule consists of a central cobalt atom which is surrounded in a roughly tetrahedral fashion by two zinc atoms, a phosphorus atom and a η-bound cyclopentadienyl group. The

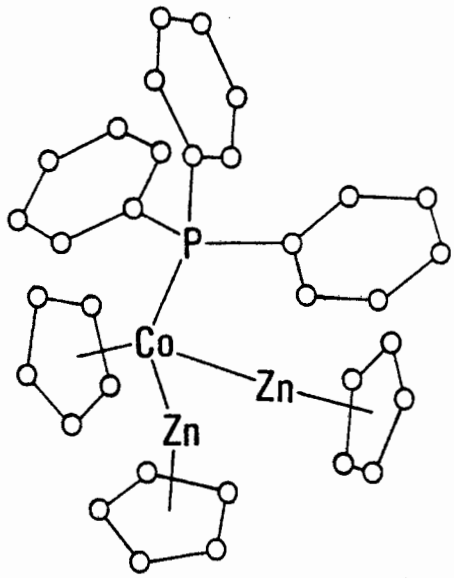

Figure 1.11 The structure of $[(\eta\text{-}C_5H_5)Zn]_2Co(\eta\text{-}C_5H_5)PPh_3$.

average Zn-Co distance of 2.289(1) Å is slightly smaller than that reported previously for the linear trimetallic chain, $Zn[Co(CO)_4]_2$,[61] where the mean Zn-Co distance was found to be 2.305 Å.

In view of the ease of disproportionation of alkyl- and arylzinc transition metal compounds, the stability of their cyclopentadienyl analogues is surprising. A possible explanation involves the '18-electron rule'.[62] The cyclopentadienyl group is a 5-electron ligand while $Co(CO)_4$ functions as a 1-electron ligand. Thus, in the reaction of $Zn[Co(CO)_4]_2$ with $(\eta\text{-}C_5H_5)_2Zn$, two molecules of the 18-electron complex, $(\eta\text{-}C_5H_5)ZnCo(CO)_4$, are formed from a 14-electron complex, $Zn[Co(CO)_4]_2$, and a formally 22-electron complex, $(\eta\text{-}C_5H_5)_2Zn$. This explanation has been adopted rather tentatively due to the polar character of the $(\eta\text{-}C_5H_5)$-Zn bond indicated by the two rather long

(η-C_5H_5)-Zn bonds of 2.018(5) and 2.2028(5) Å, respectively in [(η-C_5H_5)Zn]$_2$Co(η-C_5H_5)PPh_3 and by the ^1H nmr spectra of these compounds. While the (η-C_5H_5) proton resonance is usually located at δ 3.5-5 ppm when bound to the transition metal, it is found at δ 6.3 ppm in [(η-C_5H_5)Zn]$_2$Co(η-C_5H_5)PPh_3 where it is bound to zinc, the latter value being much closer to the position of the proton resonance of a free cyclopentadienide anion.

The reactions of allylic and propargylic amines and ethers with $Zn[Co(CO)_4]_2$ have been investigated.[63] The allylic C-N bond of CH_2=$CHCH_2NEt_2$ is cleaved by $Zn[Co(CO)_4]_2$ producing (η-C_3H_5)$Co(CO)_3$. The propargylic amine, HC≡CCH_2NEt_2, undergoes an unusual catalytic dimerization to Et_2NCH_2C≡$CCH(Me)N(Et)CH_2CH$=CH_2, which implies activation of an ethyl C-H bond. Comparison with the reactions of the corresponding ethers indicates that Zn-N coordination plays an important role in these reactions. An investigation of a system of this type was of interest because while transition metal compounds play an important role as activators of carbon-carbon multiple bonds in many catalytic processes, zinc behaves as a typical main group metal in activating mainly carbon-heteroatom single and multiple bonds.[63] Likewise, the amines and ethers were selected as reagents in the investigation as they contain an isolated carbon-carbon multiple bond and a carbon-heteroatom single bond. The reaction of bis(triphenylgermyl)cadmium with

nickelocene proceeds through the displacement of a cyclopentadienyl ring, and the formation of a polynuclear compound, $[GePh_3Cd]_2[Ni(\eta\text{-}C_5H_5)GePh_3]_2Cd$ - figure 1.12 - containing five metal atoms in a bent chain structure and which is solvated with one toluene molecule.[64] These workers presented this compound as the longest known polymetallic chain where they included germanium as a metal atom, of nine metal atoms in all. However, in this review, germanium is not considered to be metallic and hence the chain is here classified as consisting of five metal atoms.

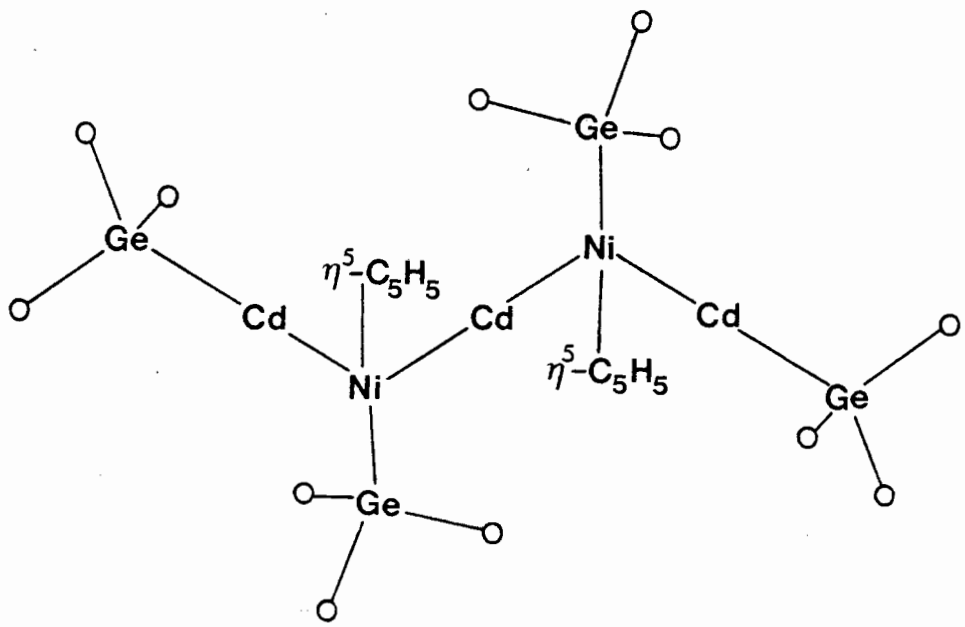

Figure 1.12 Diagrammatic representation of the polymetallic backbone of $[Ge(Ph)_3Cd]_2$-$[Ni(\eta\text{-}C_5H_5)Ge(Ph)_3]_2Cd$.

The most interesting structural feature is the presence of metal-metal bonds between nickel and cadmium which are not reinforced by bridging ligands. The red crystals of the compound are oxidised rapidly in air and decompose at

190°-194°C. The compound is very soluble in aromatic solvents and insoluble in hexane. The mercury analogue, $[GePh_3Hg]_2[Ni(\eta\text{-}C_5H_5)GePh_3]_2Hg$ - figure 1.13 - was obtained in 30% yield from the reaction of nickelocene with $(Ph_3Ge)_2Hg$; it has similar physical and chemical properties and an identical crystal structure. Both molecules were found to be crystallographically centrosymmetric.

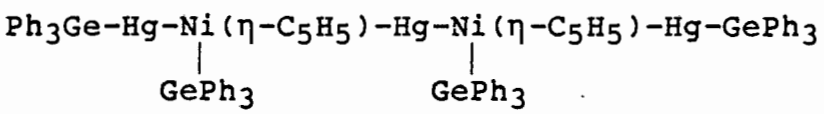

Figure 1.13 Diagrammatic representation of the polymetallic backbone of $[Ge(Ph)_3Hg]_2$-$[Ni(\eta\text{-}C_5H_5)Ge(Ph)_3]_2Hg$.

The Ni atoms have a "piano stool" configuration and an 18-electron shell but the Ge-Ni-Cd and the Cd-Ni-Cd angles in the formal structure - figure 1.13 - between the stool legs are decreased to ca 86° (instead of an ideal value of 90°) due to the bulkiness of the cyclopentadienyl ligand on the Ni atom. Covalent metal-metal bonds in these polynuclear organometallic compounds are strongly shielded by all ligands from the external influences and form a metallic 'skeleton' inside an 'organic case' which seems to be responsible for an increased stability of polymetallic chains. In the reaction of $(Et_3Ge)_2Cd$ with $(\eta\text{-}C_5H_5)_2Ni$, it is interesting to note that no polynuclear organometallic compounds have been isolated, perhaps

because of weakly shielded metal-metal bonds by ethyl substituents.

The symmetrical transition metal complexes $[(\eta\text{-}C_5H_5)(CO)_3M]_2Hg$ (M = Cr, Mo or W) were prepared by King and Stone[65] by treatment of a diglyme solution of $[(\eta\text{-}C_5H_5)(CO)_3M]Na$ (M = Cr, Mo or W) with an aqueous solution of mercury(II) cyanide. A ^{199}Hg Fourier Transform nmr study on these complexes has been carried out in order to further explore their properties.[66] These workers concluded, on measuring $^1J(^{199}Hg\text{-}^{183}W)$ for several compounds, that increasing charge on the mercury atom caused an increase in coupling between the directly bonded nuclei, Hg and W, because of orbital contraction. Mercury salts which are more polar are more shielded, while the symmetrically covalently bound systems are deshielded.

Glocking et al[67] reported the preparation and reactivity of the series of trimetallic iron-mercury complexes, $cis\text{-}[Fe(CO)_4(HgR)_2]$

(where R = CH_2SiMe_3,
$CH(SiMe_3)_2$
or $C(SiMe_3)_3$).

These complexes are believed to have a similar crystal structure to that reported for the compound

$[Fe(CO)_4(HgBr)_2]$[68] i.e. an octahedral type structure containing two cis-oriented Fe-HgX bonds, with the Hg-Fe-Hg bond angle = 78.0° and a mean Fe-Hg distance of 2.59 Å. $Fe(CO)_4[Hg\{C(SiMe_3)_3\}]_2$ resists thermal symmetrisation. It reacts with $HgBr_2$ and with $[Fe(CO)_4(HgBr)_2]$ to form $HgBr[C(SiMe_3)_3]$ and $[\{HgFe(CO)_4\}_n]$, probably via the intermediate $Fe(CO)_4(HgBr)[Hg\{C(SiMe_3)_3\}]$. At 60°C the carbonyl groups in cis-$Fe(CO)_4[Hg\{C(SiMe_3)_3\}]_2$ are fluxional, whereas at -55°C, the axial and equatorial carbonyl groups can be distinguished.[67]

The reaction of octacarbonyldicobalt with the dichlorocarbene precursor, $Hg(CCl_3)Ph$, at 60°C in hexane afforded the closed cluster $[Co_3(CCl)(CO)_9]$ in 49% yield. It has been postulated that the reaction may proceed through intermediates which contain a trimetallic Hg-Co-Co chain[69] as shown in figure 1.14.

Figure 1.14 Diagrammatic representation of intermediates containing a trimetallic Hg-Co-Co chain.

One of the two possible mechanistic pathways for the reaction is outlined in the scheme below. The first involves a four-centre reaction between the mercury compound and $Co_2(CO)_8$ to afford unstable intermediates

which are not depicted here since the intermediates are not of a chain-type nature. The second pathway, shown in the scheme, namely oxidative addition of $Hg(CCl_3)Ph$ to $Co_2(CO)_8$ could occur to give the intermediate (1) which could then either decompose to the intermediates $Co(CCl_3)(CO)_4$ and $Co(HgPh)(CO)_4$ or it could decompose via a 1,2-chlorine shift with elimination of dichlorocarbene to form intermediate (2). Intermediate (2) might be expected to undergo further breakdown as shown in the scheme.

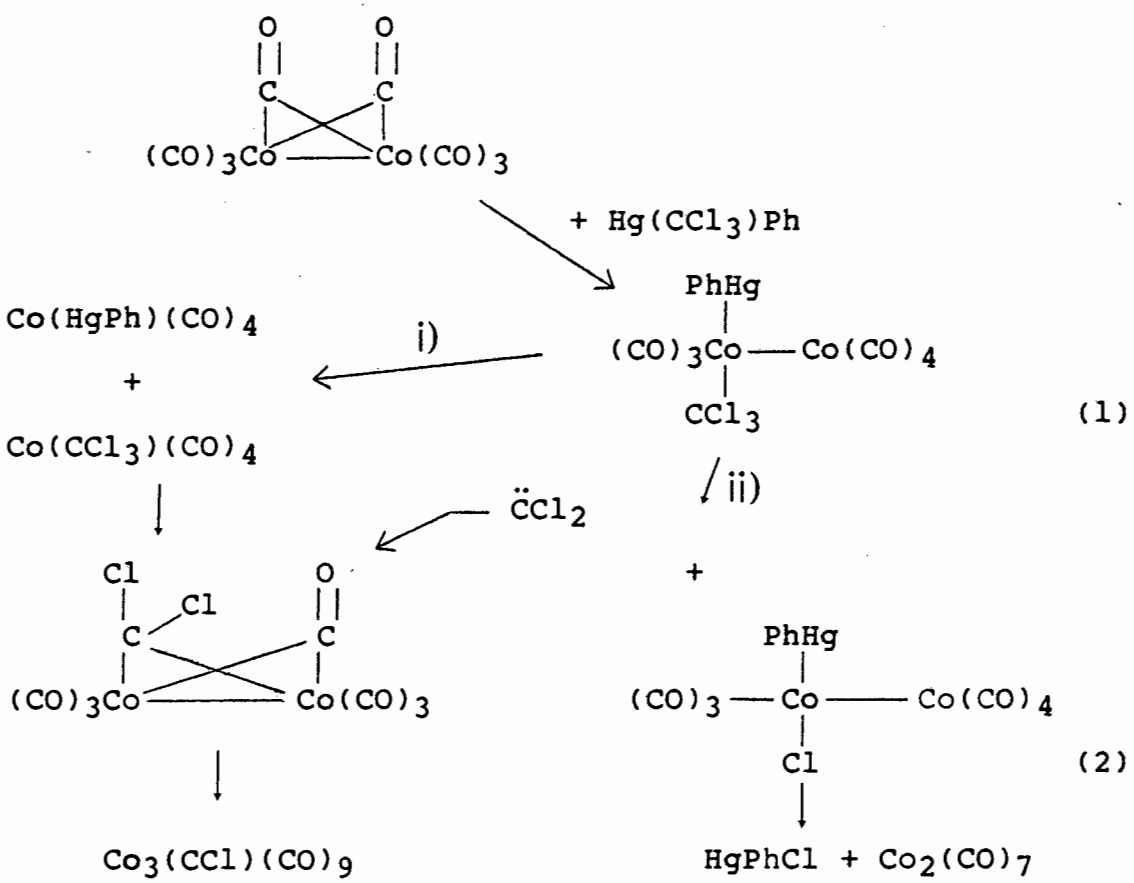

These proposed intermediates have also been prepared by the reaction of HgBrPh with $Co_2(CO)_8$[70] in THF under

nitrogen at room temperature with stirring for two hours. Carbon monoxide was evolved during the reaction.

Bis[pentafluorophenyltin]mercury(II) has been reported to react rapidly with $Pt(PPh_3)_3$ to give complexes of the type $(C_6F_5)_3Sn\text{-}Pt(PPh_3)_2\text{-}HgSn(C_6F_5)_3$ which involve a four-atom heterometallic chain.[71] The nature of the group co-ordinated to the tin atom appears to determine to a considerable extent, the rate of reaction and the stability of the complex. The analagous complex, i.e. the insertion product $(C_6F_5)_3Sn\text{-}Pt(PPh_3)_2\text{-}HgGe(C_6F_5)_3$, formed from $(C_6F_5)_3Sn\text{-}Hg\text{-}Ge(C_6F_5)_3$ and $Pt(PPh_3)_3$ has been characterised by means of an X-Ray structural determination,[72] which has shown that the molecule has a square-planar structure - figure 1.15 - with the phosphine ligands cis to each other.

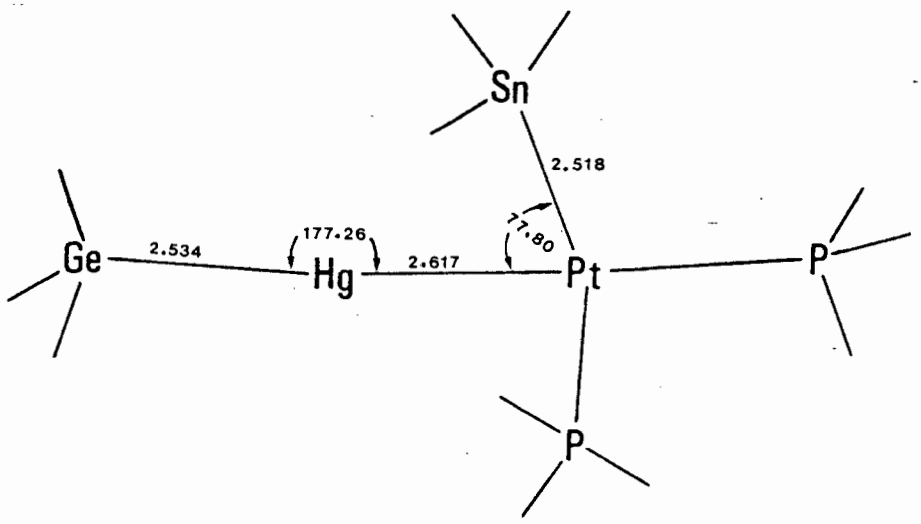

Figure 1.15 Diagrammatic representation of $(C_6F_5)_3Sn\text{-}Pt(PPh_3)_2\text{-}HgGe(C_6F_5)_3$.

The Hg-Pt (2.617 Å) and the Sn-Pt (2.518 Å) bond lengths are a little shorter than the sums of the covalent radii of the relevant atoms (2.73 Å and 2.83 Å) respectively, while the Ge-Hg (2.53 Å) bond length is almost equal to the sum of the covalent radii of Hg and Ge. These complexes are both crystalline, air-stable solids but are, however, photolabile and react with Br_2, HCl and H_2 according to the following stoichiometry:

$$R_3Sn\text{-}Pt(PPh_3)_2\text{-}Hg\text{-}Ge(C_6F_5)_3 + 2Br_2 \xrightarrow{C_6H_6} R_3SnPt(PPh_3)_2Br + BrGe(C_6F_5)_3 + Hg_2Br_2$$

Boiling in CF_3COOH for 4 hours or irradiation with UV light in benzene was found to break the molecule, shown in figure 1.15, apart and separate the metallic Hg completely. The analogous cadmium and zinc derivatives have also been obtained[71] and they are all oxidised by air. A distinctive feature of all studied reactions of trinuclear compounds $R_3M\text{-}M'\text{-}MR_3$ of the type discussed above, with triphenylphosphine complexes of nickel, palladium or platinum, is the formation of only tetranuclear products and not any higher nuclearity compounds, resulting from further insertion. The insertion of NiL_2, PdL_2 or PtL_2 moieties into one of the M-M' bonds, completely deactivates the second M-M' bond in

the compound towards the starting triphenylphosphine complexes.[71]

1.2.3.2 Thallium

The thallium compound $Tl[Mo(CO)_3(\eta\text{-}C_5H_5)]_3$ was originally prepared by King.[73] The reaction between thallium(I) cyclopentadienide with $Mo(CO)_6$ gave the unexpected thallium(III) derivative. The red-green dichroic appearance of $Tl[Mo(CO)_3(\eta\text{-}C_5H_5)]_3$ resembles that of certain solid 16-electron square-planar complexes of rhodium(I), e.g. $[C_5H_7ORh(CO)_2]$, platinum(II), e.g. $[Pt(CN)_4]^{2-}$ and iridium, e.g. $[Ir(CO)_2X_2]^{0.6-}$ - see figure 1.3 - which can form stacked polymeric crystal structures with metal-metal δ-bonding on an axis perpendicular to the coordination square.[26] The thallium atom in the Tl-Mo complex has a coordination number of 3 with planar trigonal sp^2 hybridization as determined by X-Ray crystallography.[74] Furthermore, the thallium atom has a 16-electron configuration like the central metal atoms mentioned above. The coplanarity of the three Tl-Mo bonds and the 16-electron configuration of the three-coordinate thallium atom makes possible a similar stacked polymeric structure for $Tl[Mo(CO)_3(\eta\text{-}C_5H_5)]_3$ in the solid state with Tl-Tl bonding between layers. The molybdenum atoms in successive layers would then be relatively close together thereby, possibly accounting for the facile decomposition in solution to give $[Mo(CO)_3(\eta\text{-}C_5H_5)]_2$. Attempts to

obtain some single-crystal conductivity measurements on $Tl[Mo(CO)_3(\eta\text{-}C_5H_5)]_3$ in order to detect any relationship between the axis of prominent dichroism and possible anisotropic conductivity failed since the crystals were too small and too brittle for such measurements.[74]

1.2.3.3 Tin

Reaction between SnX_2 (X = Cl, Br) and the dimeric manganese complex, $[(OC)_4Mn(\mu\text{-}AsMe_2)Mn(CO)_2(\eta\text{-}C_5H_5)]$,[75] resulted in the Mn-Mn bond being broken and a linear Mn-Sn-Mn system resulting via an insertion reaction. For the $SnCl_2$ complex, the average Mn-Sn distance was found to be 2.635(1) Å, while for the analogous bromo-complex, it was found to be 2.642(3) Å.[76]

The synthesis and crystal structure of the first transition metal substituted ditin dihydride, $H[Mn(CO)_5]_2Sn\text{-}Sn[Mn(CO)_5]_2H$ - figure 1.16 - has been reported.[77]

This orange crystalline cluster compound was also obtained as an unexpected product from the reaction of dicyclopentadienyltin and $HMn(CO)_5$ in benzene at room temperature.

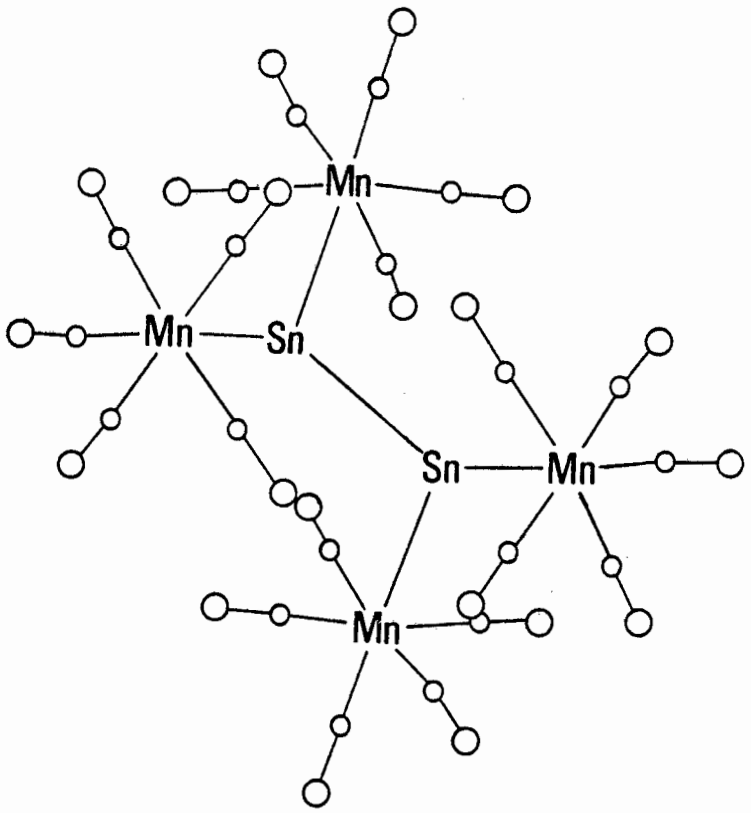

Figure 1.16 The structure of $H[Mn(CO)_5]_2Sn\text{-}Sn[Mn(CO)_5]_2H$

The following reactions of the compound were also reported:

$$H_2Sn_2[Mn(CO)_5]_4 \xrightarrow[-CHX_3]{CX_4} X_2Sn_2[Mn(CO)_5]_4 \quad (X = Cl, Br)$$

The tin atoms in $H_2Sn_2[Mn(CO)_5]_4$ are in a strongly distorted tetrahedral environment, the Mn-Sn-Mn angle being 119.8° and the Mn-Sn-Sn bond angles being 107.7° and 121.9°, respectively. The Sn-Sn distance was reported as 2.89 Å while the Sn-Mn distances were found to be 2.67 and

2.73 Å, respectively. For clarity, the two hydrogen atoms have been omitted from the diagram. These latter atoms were not located in the crystal structure refinement. Rather, their presence was inferred from the mass spectrum which showed a polyisotopic parent peak pattern with the most abundant peak at 1020 rather than at 1018 as would be expected for the dimer $[Sn\{Mn(CO)_5\}_2]_2$. Analytical data also pointed to the presence of two hydrogen atoms and chemical evidence was obtained for the presence of a M-H bond from the reaction with CX_4 (X = Cl or Br) which gave chloroform or $CHBr_3$ and resulted in the formation of the corresponding dichloro- or dibromo-complex, respectively. In the IR spectrum, the absorption at 1725 cm^{-1}, which is notably absent in the IR spectrum of $Cl_2Sn_2[Mn(CO)_5]_4$ is assigned to the Sn-H stretching frequency. The low value of ν(Sn-H), the lowest value reported for a tin hydride, may be explained by the enhanced p-character of the Sn-H bond in this transition metal tin-hydride complex. The complexes $X_2Sn[Re(CO)_5]_2$ (X = Cl, Br or I) were formed during the preparation of clusters of the type $Re_2(CO)_8[\mu\text{-}SnXRe(CO)_5]_2$ (X = Cl, Br or I) from the reaction of Sn(II) halides with $Re_2(CO)_{10}$.[78] This indicated that insertion of SnX_2 into the Re-Re bond was the primary step in the reaction.

Phthalocyaninato- and porphinatotin(IV)- dichlorides have been reported[79] to react with $Re_2(CO)_{10}$ to afford the trimetallic chain cluster complex shown in the scheme below:

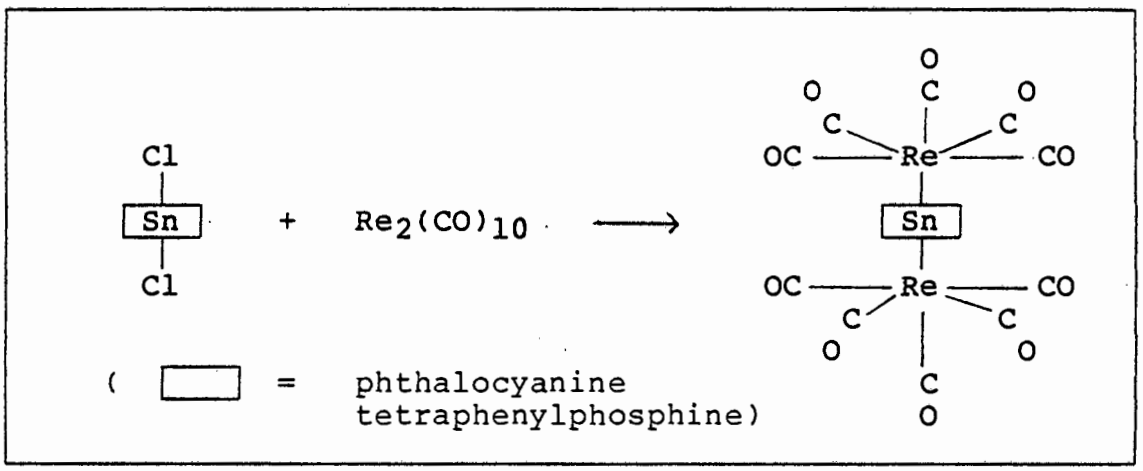

The compound $[Ru(SnMe_3)(CO)_4]_2$, was isolated in very low yields from the reaction of trimethyltin chloride with the anion $[Ru(CO)_4]^{2-}$.[80] The crystal structure of this compound has revealed the carbonyl ligands adopting an eclipsed configuration with a Ru-Ru bond length of 2.943 Å [80] - figure 1.17. Any suggestion that the eclipsed configuration adopted by the carbonyl groups, might be accounted for by multiple bonding can certainly be dismissed as the Ru-Ru bond is rather long for a single bond.[81] Arguments relating to eclipsed versus staggered configurations of carbonyl groups in linear polynuclear carbonyls have been fully presented,[41] but it is evident that the energy of interconversion of the two forms must be of the same order of magnitude as that of the crystal packing forces. The possibility obviously exists that the very neat packing of the molecules in the eclipsed configuration is, in the case of the Ru-Sn compound, the over-riding factor.[41] In any event, the interactions

between the antibonding orbitals of the carbonyl groups on one Ru atom and the d orbitals on the other metal atom, sometimes believed to constrain equatorial carbonyl groups into a staggered configuration are likely to be unimportant in this structure - figure 1.17. This is because of the unusually long Ru-Ru bond and because of the bending of the carbonyl groups away from the molecular centre.

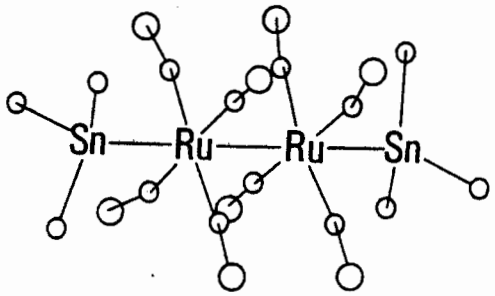

Figure 1.17 The structure of $[Ru(SnMe_3)(CO)_4]_2$.

The preparation of a number of new pentanuclear hetero-atomic compounds which have a linear structure and contain a fragment composed of three osmium atoms in the metal chain have been reported.[82] These pentanuclear clusters of the type, $Os_3(CO)_{12}Cl\text{-}SnCl_2\text{-}M(CO)_nL$ - figure 1.18 - were obtained by replacing the halogen atom in the compound $Cl(CO)_4Os\text{-}Os(CO)_4\text{-}Os(CO)_4\text{-}SnCl_3$[83] by metal carbonyl groups.

$$Cl(CO)_4Os\text{-}Os(CO)_4\text{-}Os(CO)_4\text{-}SnCl_2\text{-}M(CO)_nL$$

(where $M(CO)_nL = W(CO)_3(\eta\text{-}C_5H_5)$, $Re(CO)_5$, $Fe(CO)_2(\eta\text{-}C_5H_5)$.)

Figure 1.18 Diagrammatic representation of $Os_3(CO)_{12}Cl\text{-}SnCl_2\text{-}M(CO)_nL$.

The reaction was carried out in THF at ca 20 °C using a 1:1 molar ratio of the reactants. These complexes are yellow crystalline compounds that are sparingly soluble in polar organic solvents and practically insoluble in aliphatic hydrocarbons or water. They are all stable when stored in the air and decompose without melting when heated to about 150 °C. The IR spectra of the compounds correspond to their postulated structure and contain, in the absorption region of the carbonyl stretching vibrations, the bands of both the $Os_3(CO)_{12}$ fragment and the $M(CO)_n$ group. A number of bands in the 2150-1990 cm^{-1} region are present, which are characteristic of a linear grouping composed of three $Os(CO)_4$ groups. The reaction was monitored by polarographic reduction of $ClOs_3(CO)_{12}SnCl_3$ at a dropping mercury electrode in acetonitrile. It was established that the reaction took place in several steps in which two clearly expressed waves were observed, the first corresponding to initial cleavage of the Sn-Cl bond.

The X-Ray crystal structure of the tin-cobalt complex $[(\eta^4\text{-}C_7H_8)(CO)_2Co]_2SnCl_2$ - figure 1.19 - has been determined.[84]

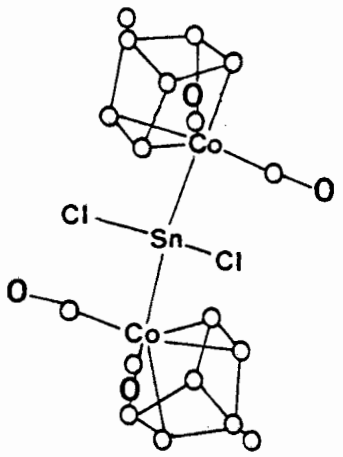

Figure 1.19 The structure of $[(\eta^4\text{-}C_7H_8)(CO)_2Co]_2SnCl_2$.

The compound was isolated as a result of studies of the $X_2Sn[Co(CO)_4]_2$ system which indicated that these complexes actively catalyse the dimerization of norbornadiene, but in a manner remarkably sensitive to the substituent X (where X = Cl(I); X = Ph(II)).[85] Coordination at tin may be described in terms of distorted tetrahedra with Co-Sn-Co angles = 128.3(1)° in (I) and 118.3° in (II). The Sn-Co bond distances for (I) are 2.498(2) and 2.499(2) Å and for (II) are 2.573(3) and 2.556(3) Å. Bond distances to tin are 2.498(2) and 2.499(2) Å for Sn-Co in (I) and 2.575(3) and 2.556(3) Å in (II). The cobalt atoms exhibit distorted trigonal-bipyramidal geometries, where the norbornadiene double bonds chelate

one apical and one equatorial site and the carbonyl groups occupy the remaining two equatorial positions. These structures were the first reported for cobalt-norbornadiene η-complexes.[84]

The displacement of trimethylsilyl groups by $SnHMe_3$ in $Pt-SiMe_3$ bonded complexes was reported to produce compounds containing $Pt-SnR_3$ (R = Me) groupings. Subsequent reaction with additional $HSnMe_3$ gave linear and bent trinuclear Sn-Pt-Sn complexes.[86] The reactions are believed to proceed through successive oxidative addition and elimination stages, and if equilibrium constants are determined largely by the M-H bond strength of the displaced hydride, then organoplatinum complexes would be expected to undergo similar reactions. The reactions between $HSnMe_3$ and $PtR_2(PPh_2CH_2PPh_2)$ (R = Me or Et) take place with quantitative displacement of the R group, as RH, at room temperature. The diphenylplatinum complex (R = Ph) is less reactive, but at 50 °C both phenyl groups are converted into benzene. With an excess of $HSnMe_3$, the complex $Pt(SnMe_3)_3(H)(PPh_2CH_2PPh_2)$ - figure 1.20 - is produced, the low value of the ν(Pt-H) (1968 cm^{-1}) indicative of the hydride ligand being trans to the $SnMe_3$ group, and thereby defining the stereochemistry.

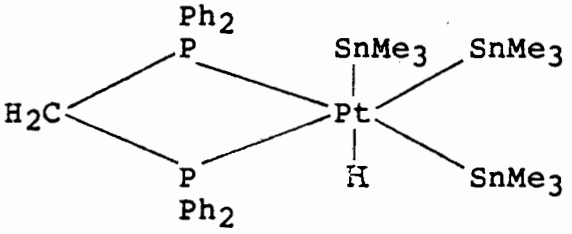

Figure 1.20 Diagrammatic representation of $Pt(SnMe_3)_3(H)(PPh_2CH_2PPh_2)$.

This complex was found to be stable in air for up to six months in the solid state but reversibly dissociated in benzene solution according to the following sequence:

$$Pt(SnMe_3)_3(H)(PPh_2CH_2PPh_2) \xrightarrow{C_6H_6} Pt(SnMe_3)_2(PPh_2CH_2PPh_2) + HSnMe_3$$

These exchange reactions provide one of the cleanest and simplest methods for the formation of Pt-Sn bonded complexes.

Dichloro{bis(diphenylphosphino)methane}platinum(II), $PtCl_2(PPh_2CH_2PPh_2)$ was also found to add trimethylstannane but via a complex reaction mechanism since $H_2SnClMe_3$ and Sn_2Me_6 were formed.[86] The product was assigned the following structure - figure 1.21:

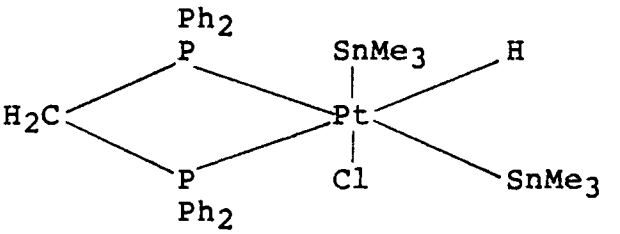

Figure 1.21 Diagrammatic representation of $Pt(SnMe_3)_2HCl(PPh_2CH_2PPh_2)$.

based on the values of ν(Pt-H) and ν(Pt-Cl) stretching frequencies and on its ready conversion to a complex formulated as $PtCl(SnMe_3)(PPh_2CH_2PPh_2)$. The di-tin compound, shown in figure 1.21, was found to be considerably more stable than the tri-tin compound shown in figure 1.20 and comparison of ν(Pt-H) in the two compounds, 1968 cm^{-1} in the tri-tin compound and 2002 cm^{-1} in the di-tin compound, suggested that the difference in stability may be related to the lower trans-labilizing effect of phosphorus relative to that of the trimethylstannyl group.[87]

The reactions between tetraorganotin compounds $SnMe_{4-n}R_n$ (R = aryl, n = 1-3) and $Pt(C_2H_4)(PPh_3)_2$ have been reported to form cis-$PtR(SnMe_{4-n}R_{n-1})(PPh_3)_2$ (n = 1 or 2).[88] Reactions between these products and $SnMe_3R$ produce cis-$PtR(SnMe_{4-n}R_{n-1})(PPh_3)_2$ with elimination of $SnMe_4$ and $SnMe_2R_2$ respectively, as shown below:

$$cis - PtR(SnMe_3)(PPh_3)_2 + SnMe_3R \rightleftharpoons cis - PtR(SnMe_2R)(PPh_3)_2 + SnMe_4$$

$$\text{and } cis - PtR(SnMe_2R)(PPh_3)_2 + SnMe_3R \rightleftharpoons cis - PtR(SnMe_3)(PPh_3)_2 + SnMe_2R_2$$

The above compounds have been proposed to involve platinum(IV) intermediates whose structures have not been established, but can be written as shown in figure 1.22 below, assuming that the PPh_3 ligands remain cis throughout.

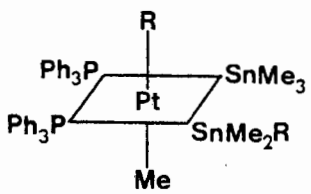

a)

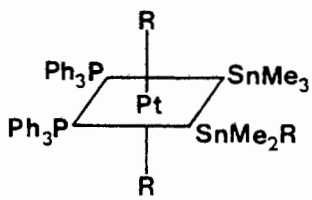

b)

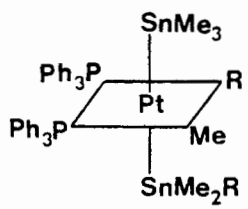

c)

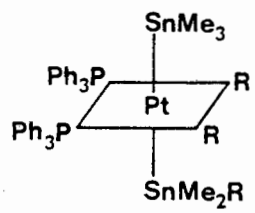

d)

Figure 1.22 Diagrammatic representation of proposed platinum(IV) intermediates.

The symmetry of the complexes would allow for the possible exchange processes, required in these reactions, to occur. Platinum(IV) complexes of this type have not been isolated or detected prior to this work and, thus, choice of a structure from the above by comparative purposes cannot be achieved. The dihydride derivative[89], $PtL_2H_2(SnR_3)_2$ (L = PEt_3 or PMe_2Ph; R = Ph, C_6H_4Me-2,-3,-4) - figure 1.23 - obtained by oxidative addition of $HSnR_3$ to a transient platinum(0) species has the following configuration:

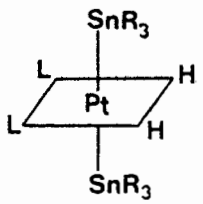

Figure 1.23 Diagrammatic representation of $PtL_2H_2(SnR_3)_2$

The balance of evidence, therefore, perhaps favours the structures shown in figures 1.22 c) and d) for the intermediates in these reactions.[88]

Treatment of the complexes, $Cl_3SnMn(CO)_5$, $Cl_3SnMn(CO)_4(PEt_2Ph)$ and $Cl_3SnFe(CO)(\eta\text{-}C_5H_5)$ with $TlCo(CO)_4$ and $TlCr(CO)_3(\eta\text{-}C_5H_5)$ afforded the new mixed dichlorobis(carbonylmetalato)tin(IV) complexes, Cl_2SnXY (X = $Mn(CO)_5$, $Mn(CO)_4(PEt_2Ph)$ or $Fe(CO)_2(\eta\text{-}C_5H_5)$; Y = $Co(CO)_4$ or $Cr(CO)_3(\eta\text{-}C_5H_5)$), which are believed to all possess bent-chain structures.[90]

Treatment of **trans**-$(ClBu_2Sn)_2Os(CO)_4$ with the $[Re(CO)_5]^-$ anion gave a good yield of pentametallic Re-Sn-Os-Sn-Re chain[36] (which is a viscous liquid at room temperature) according to the following sequence:

$$2HRe(CO)_5 + \textbf{trans}\text{-}(ClBu_2Sn)_2Os(CO)_4 \xrightarrow{Et_2NH} [(CO)_5ReSnBu_2]_2Os(CO)_4$$

Branched-chain clusters involving tin as the central metal atom have been reported.[91]

$[(\eta\text{-}C_5H_5)(CO)_2Fe][(\eta\text{-}C_5H_5)(CO)Ni][(CO)_4Co]SnCl$ - figure 1.24 a) - and $[(\eta\text{-}C_5H_5)(CO)_3Mo][(\eta\text{-}C_5H_5)(CO)_2Fe]$-$[(CO)_4Co]SnCl$ - figure 1.24 b) - were prepared by the reaction of

$[(\eta\text{-}C_5H_5)(CO)_2Fe][(\eta\text{-}C_5H_5)(CO)Ni]\ SnCl_2$ or

$[(\eta\text{-}C_5H_5)(CO)_3Mo][(\eta\text{-}C_5H_5)(CO)_2Fe]SnCl_2$ with

$Co_2(CO)_8$ or $TlCo(CO)_4$, respectively, in THF.

These compounds were believed to have the following polymetallic backbones:

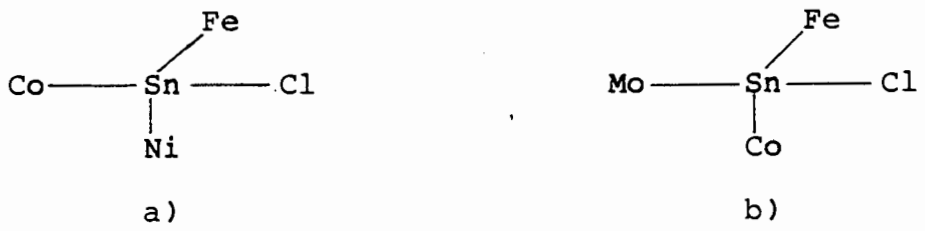

Figure 1.24
a) Diagrammatic representation of the polymetallic backbone of $[(\eta\text{-}C_5H_5)(CO)_2Fe]$-$[(\eta\text{-}C_5H_5)(CO)Ni][(CO)_4Co]SnCl$.

b) Diagrammatic representation of the polymetallic backbone of $[(\eta\text{-}C_5H_5)(CO)_3Mo]$-$[(\eta\text{-}C_5H_5)(CO)Fe][(CO)_4Co]SnCl$.

The nature of the metal has been found to be important in successive substitutions at the tin atom.[92]

When $[(\eta\text{-}C_5H_5)(CO)Ni]_2$ was refluxed with $[(\eta\text{-}C_5H_5)(CO)_2Fe][(CO)_4Co]SnCl_2$ in benzene[91] rather than in THF as above, rupture of the tin-cobalt bond rather than the tin-chloride bond occurred:

$$[(\eta\text{-}C_5H_5)(CO)_2Fe][(CO)_4Co]SnCl_2 + [(\eta\text{-}C_5H_5)(CO)Ni]_2 \xrightarrow{\Delta} [(\eta\text{-}C_5H_5)(CO)_2Fe][(\eta\text{-}C_5H_5)(CO)Ni]SnCl_2$$

$[(\eta\text{-}C_5H_5)(CO)_2Fe][(\eta\text{-}C_5H_5)(CO)Ni]SnCl_2$ has also been prepared[93] by the reaction of nickelocene with $[(\eta\text{-}C_5H_5)(CO)_2Fe]SnCl_3$. Reaction of $[(\eta\text{-}C_5H_5)(CO)_2Fe]SnCl_3$ with $Co_2(CO)_8$ in the 1:2 molar ratio used by Manning et al[94] to obtain $[(\eta\text{-}C_5H_5)(CO)_2Fe][(CO)_4Co]SnCl_2$, gave the complex $[(\eta\text{-}C_5H_5)(CO)_2Fe][(CO)_4Co]_2SnCl$, described by Behrens et al[95] and the expected product was obtained using a 1:0.65 molar ratio.

The crystal structure of the complex, $[(\eta\text{-}C_5H_5)(CO)_2Fe]$-$[(\eta\text{-}C_5H_5)(CO)Ni][(CO)_4Co]SnCl$ - figure 1.25 - was recently reported.[91] The chlorine atom and the metallic groups are arranged around the tin in a tetrahedral geometry with some distortion caused by steric hindrance. The

Cl-Sn-(Fe,Co and Ni) bond angles, respectively, were found to be significantly less than 109.5°. The value of 2.493 Å is the first reported Ni-Sn bond length. The Fe-Sn and Co-Sn distances were reported as 2.544 Å and 2.651 Å respectively.

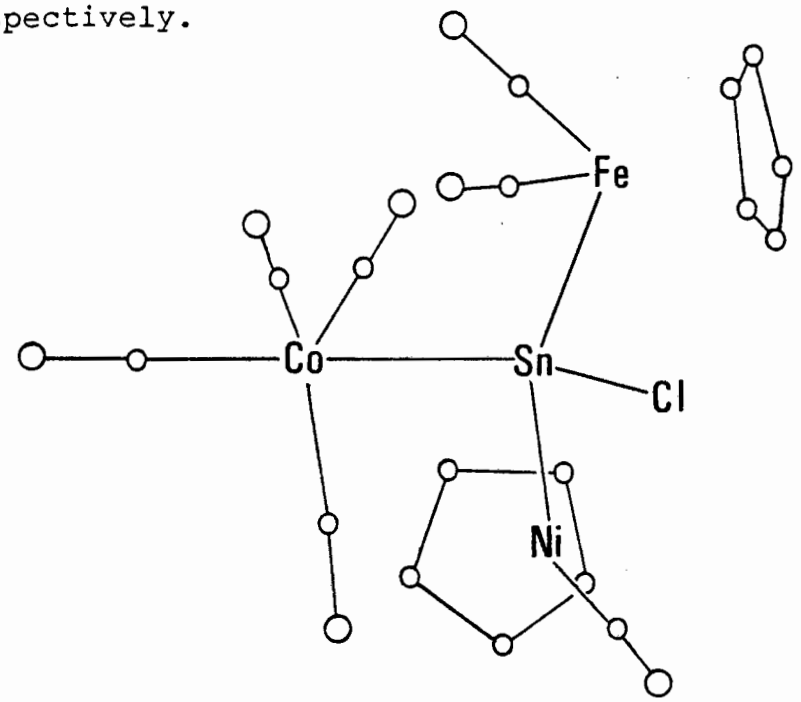

Figure 1.25 The structure of $[(\eta\text{-}C_5H_5)(CO)_2Fe]$-$[(\eta\text{-}C_5H_5)(CO)Ni][(CO)_4Co]SnCl$.

1.2.3.4 Miscellaneous

The direct reaction of alkali metals, e.g. $Li(TMEDA)_2$ (TMEDA = N,N,N',N'-tetramethyl-EDA), with transition metal complexes, e.g. Ni(CDT) (CDT = all trans-1,5,9-cyclododecatriene) was reported to produce the trimetallic lithium-nickel complex, bis(lithium-N,N,N',N'-tetramethylethylenediamine)(all trans-1,5,9-cyclododecatriene-nickel).[96] The adduct formation can be attributed to the tendency of the coordinatively unsaturated CDT.Ni°

(16-electron shell) to achieve a noble gas configuration in which the two additional electrons come from the two lithium atoms. This compound displays a slight electrical conductivity in THF, apparently due to partial dissociation. It is also readily soluble in pentane or benzene. The crystal structure of the compound has been determined by X-Ray techniques[97] - figure 1.26 - where two unique and essentially identical molecules possessing no crystallographic symmetry were found to exist. The trigonal-bipyramidal geometry of the nickel atom, the centres of the three olefinic double bonds in the trigonal plane and the lithium atoms in apical positions, is distorted. The average Ni-Li distance was found to be 2.400(6) Å which is shorter than expected, and this is probably due to some Ni-Li $d\pi$-$p\pi$ backbonding in this structure. The average Li-Ni-Li angle is 164(2)°.

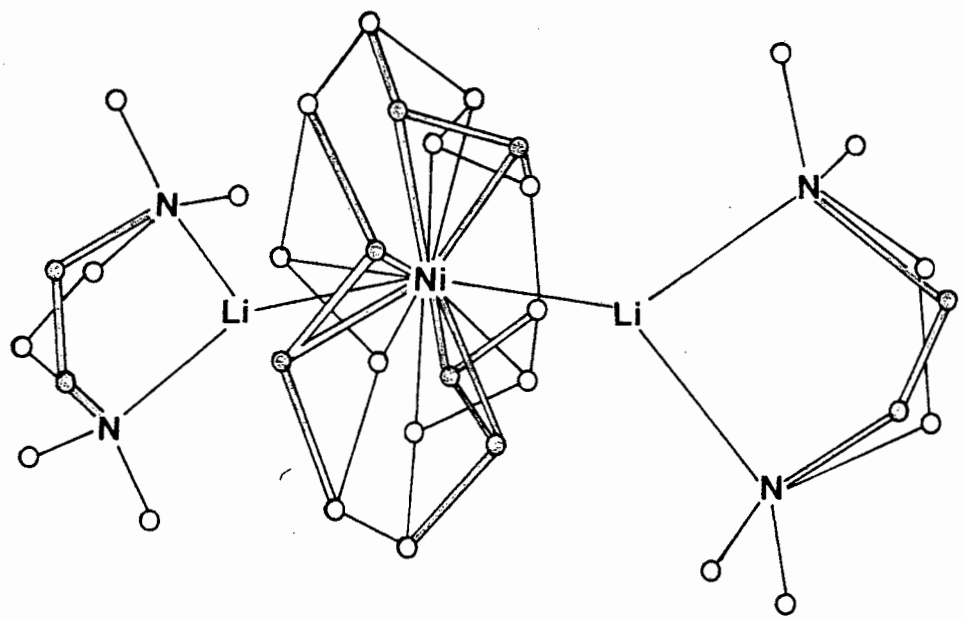

Figure 1.26 The structure of $[Li(TMEDA)_2]_2Ni(CDT)$ where TMEDA = tetramethylenediamine and CDT = cyclododecatriene.

1.2.4 Conclusion

Chain cluster complexes have in the above, as well as in the first, review[35] been classified in a separate group of their own, apart from closed cluster complexes and as a subgroup of the class of complexes generally referred to as 'metal clusters'. It is believed that chain clusters may offer an alternative model of a metal surface to cage or closed cluster complexes.

It was suggested that in the chain clusters discussed in the first review[35], where the central metal atom was a transition metal, the chain cluster was generally found to have a linear structure.[98] A recent study was carried out by Wadt[99] on the linear and bent geometries of the triatomic chain complexes, UO_2^{2+} and ThO_2, respectively. These workers presented evidence for this difference in geometry having its origin in the relative ordering of the 5f and 6d levels on the central metal atoms, respectively. The study concentrated on relativistic core potential calculations carried out on UO_2^{2+} and the isoelectronic ThO_2 complex. The analyses showed that it was not the 6p levels which determined the linear geometry of UO_2^{2+}, as previously proposed.[100] For uranium, the 5f levels are lower in energy and dominate the backbonding from the oxygen in UO_2^{2+}, while for thorium, the 6d levels are lower in energy and dominate the backbonding in ThO_2. The 5f levels prefer linear geometries while the 6d levels prefer bent geometries; hence the difference which exists between UO_2^{2+} and ThO_2.

Thus it appears that in the case of UO_2^{2+} and ThO_2, it is the nature of the orbitals on the central metal atom, used in bonding to the oxygen atoms, which determines the preferred geometry of the molecule. For similar reasons, this may also be the case in trinuclear chain cluster complexes, where the orbitals on the central metal atom may largely dictate the geometry that the chain cluster eventually adopts.

It is hoped that the potentially interesting features of chain cluster complexes, whether of linear or bent structure, have been highlighted in the above review which has dealt mainly with individual molecular structures of chain cluster complexes. These complexes have not been fully investigated catalytically, nor in terms of unidimensional conductivity properties. The emphasis in research conducted recently[71,82] in this field appears to have concentrated on synthesising chain clusters with an ever-increasing number of metal atoms in the chain. This is most likely an attempt to create an analogy to the extended metallic array of the metal surface. In addition, in this extended array, these chain clusters are more likely to exhibit some form of electrical conductivity property since close metallic contacts would be established. It

would be beneficial to this search for compounds with electrical conductivity properties, if chain clusters could be tailored to incorporate 'growth points', i.e. readily replaceable ligands, coaxial with the metal backbone. Should these ligands be replaced by additional metal fragments, the desired extension of the metal chain might be effected.

CHAPTER 2

DINUCLEAR OSMIUM CARBONYL HALIDE COMPLEXES

2.1 Introduction

The presence of adjacent metal sites in polynuclear complexes offers additional possibilities to bonding and reactivity studies which cannot be shown at a single metal site. Collman et al[102] have discussed this topic in a recent report. They include as examples the following possibilities: (i) the binding of a single substrate to two or more metal atoms; (ii) the attachment of substrate fragments to adjacent metal atoms; (iii) the migration of ligands from one metal atom to another, and (iv) reactions of the metal-metal bonds.

Dinuclear complexes are the simplest type of complex with more than one metal atom. These complexes have been considered to be cluster prototypes, but are often excluded from discussions on cluster complexes. Although they are excluded from the cluster group by definition, their chemistry is obviously relevant to cluster chemistry.[103]

Several dinuclear complexes have also been shown to possess catalytic activity themselves, examples of which are presented below. Some dinuclear rhodium complexes possess a very high reactivity to olefins yet have an impressive resistance to fragmentation.[104] The dinuclear complex, $\{HRh[P(O\text{-}i\text{-}C_3H_7)_3]_2\}_2$[104] catalysed the hydrogenation of 1-hexene at catalyst:substrate ratios of 1:10 000 with rates

that exceeded one turnover per second at 24°C. In fact, these workers[104] reported that the rate was so high that an upper limit was difficult to establish.

Recently, the dinuclear osmium carbonyl halide complex, $Os_2(CO)_6Br_4$ was isolated in the catalytic hydrogenation of carbon monoxide, using $Os_3(CO)_{12}$ as a catalyst precursor and BBr_3 as a solvent, catalyst promoter and reactant.[105] In this study, $Os_3(CO)_{12}$ was rapidly converted to $Os_2(CO)_6Br_4$ and the latter was believed to be the more enduring catalyst precursor. Using relatively mild conditions (2 atm, 180°C), the major products isolated from this reaction were methyl- and ethyl-bromides.

A large number of dinuclear complexes containing bridging methylene groups are now known.[106] Methylene intermediates have been proposed in the Fischer Tropsch reaction and thus complexes containing bridging methylene groups are of considerable interest. Such complexes often have high stability, for example, the rhodium methylene complex $[(\eta^5\text{-}C_5H_5)Rh(CO)]_2(\mu\text{-}CH_2)$ has been found to be remarkably stable to thermolysis and photolysis, thus providing one possible model for a methylene group on a metal surface. The reactivity of the methylene bridge in $Fe_2(CO)_8(\mu\text{-}CH_2)$ has been studied and of particular interest to catalysis are reactions with hydrogen and olefins.[107] Olefin insertion

into the metal-methylene bond in $Fe_2(CO)_8(\mu\text{-}CH_2)$ seems to be a facile process in these complexes, indicating the high reactivity of the methylene bridge.[107] A diruthenium complex, $(\eta\text{-}C_5H_5)_2Ru_2(CO)_2(\mu\text{-}CO)(\mu\text{-}CH_2)$[108] containing a bridging methylene group is known and a diosmium complex containing a methylene bridge has also recently been reported.[109] Treatment of the complex, $Os_2(CO)_8(\mu\text{-}CH_2)$, with ethylene has been shown to produce the diosmacyclopentane species via olefin insertion into the osmium-methylene bond - see scheme below. This reaction was found to be reversible.

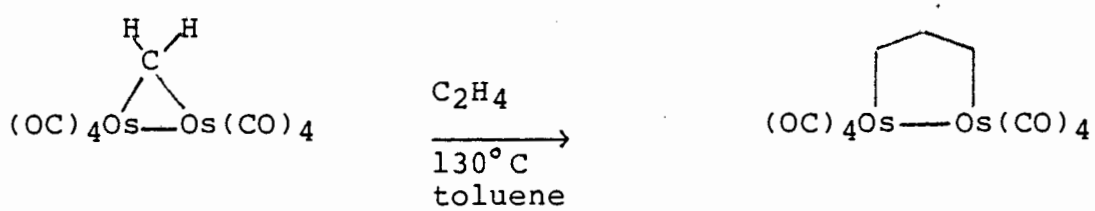

The formation of propene from the diosmacyclopentane species offers direct evidence in support of the Bergman[110] mechanism for the formation of propene from ethylene and methylene-bridged dinuclear complexes.

Dinuclear complexes are also believed to be potentially interesting in terms of 'one-dimensional' metal chains. The stacking of dinuclear cluster prototypes into 'one-dimensional' chains is believed to be an alternative to mononuclear cluster stack structures.[27] The types of dinuclear complexes purported to display the above potential

- see figure 2.1 - may or may not possess metal-metal bonds. The two atoms in the dinuclear cluster could be different or possess different oxidation states, which would impart interesting additional properties to the chain, which could not be imparted by mononuclear cluster stack structures.

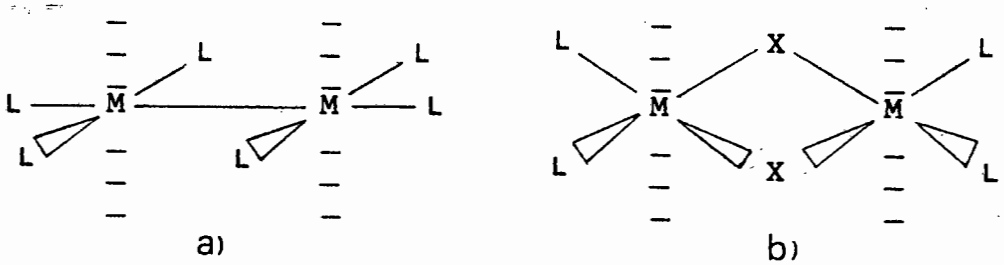

Figure 2.1 Two possible diagrammatic representations of dinuclear metal complexes a) with, or b) without metal-metal bonds, which may form 'one-dimensional' metal chains.

2.1.1 Dinuclear Osmium Carbonyl Halide Complexes

Osmium, being a third-row transition metal, would be expected to form strong metal-metal bonds. Calculated "bonding" energies[111(a)] in kcal/mol for the iron triad have been reported as Fe(16), Ru(29) and Os(31).[111(b)] Therefore, osmium is expected to form relatively thermally stable dinuclear complexes. Yet, due to the difficulty of preparing dinuclear osmium carbonyl complexes, reactivity studies involving these complexes have been limited. Dinuclear osmium carbonyl halides could be used as starting materials for many other dinuclear osmium derivatives.

Dinuclear osmium carbonyl halides have been prepared by several routes. These complexes were first prepared by Manchot and König[112] as early as 1925. These workers passed CO over heated $OsCl_3$ and obtained a white compound to which they assigned the formula, "$Os(CO)_3Cl_2$". Hieber and Stallman,[113] who carried out similar investigations on the effect of CO at high temperature and pressure on osmium halides, also assigned the formulae "$Os(CO)_3X_2$" (X = Cl, Br or I) to some of the products they obtained. The molecules were considered to be dimeric although molecular weights were not measured at the time. Hieber and Stallman[113] suggested structures involving bridging carbonyl ligands. However, Hales and Irving[114] refuted this suggestion since the IR spectrum of "$Os(CO)_3X_2$" showed only two ν(CO) stretching bands above 2 000 cm^{-1}. Reasonable structures were proposed[114] to involve two bridging halogen ligands if osmium is to be hexacoordinate and the complex diamagnetic. It was proposed,[114] using local symmetry arguments, that the expected CO stretching frequencies should correspond with those observed for monomeric fac- or mer-$ML_3(CO)_3$ complexes, namely, two or three bands, respectively. These workers[114] found that osmium tricarbonyl dihalides of the type $[Os(CO)_3X_2]_2$ (X = Cl, Br or I) were the major products of the reactions of CO at 100 atm with osmium trichloride, diosmium enneabromide and osmium oxyiodide, respectively. They reported that the IR spectrum observed for $[Os(CO)_3X_2]_2$

(X = Cl, Br or I) exhibited two absorption bands and suggested a symmetrical structure for these complexes - shown in figure 2.2(a).

Reaction between $Os_3(CO)_{12}$ and hydrogen chloride[115] produced a white chlorocarbonyl product in 81% yield which, as deduced from analytical data, had the empirical formula $Os(CO)_3Cl_2$. However, mass spectral evidence suggested the compound to be dimeric, i.e. $Os_2(CO)_6Cl_4$. This reaction was carried out in a sealed evacuated tube in cyclohexane at 170°C for 40 hours. Interestingly, these workers noticed two different sets of ν(CO) bands in the IR spectrum of this product and assigned each set to either an α- or a β-isomer of $Os_2(CO)_6Cl_4$, respectively - see figure 2.2(a) and (b) (X = Cl).

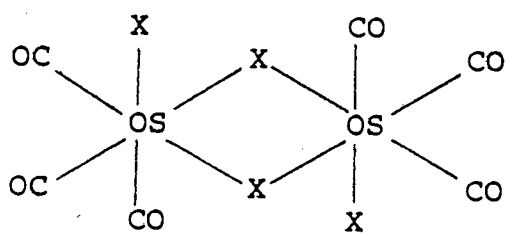

(a)

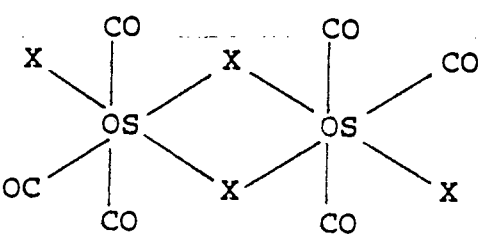

(b)

Figure 2.2 Diagrammatic representation of proposed a) α-, and b) β- isomeric forms of $Os_2(CO)_6X_4$

The analagous ruthenium complex, $Ru_2(CO)_6Br_4$, was obtained from the reaction of $Ru_3(CO)_{12}$ with $CHBr_3$[116] and has been shown by an X-Ray study[117] to have the structure shown in figure 2.3, i.e. the so-called α-form.

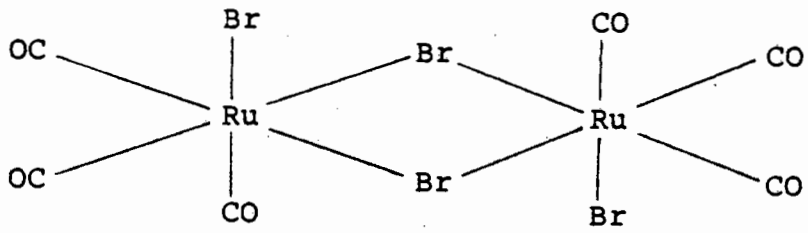

Figure 2.3 Diagrammatic representation of the structure of α-$Ru_2(CO)_6Br_4$.

The low pressure carbonylation of $RuCl_3$ afforded the dimeric carbonyl chloride $[Ru(CO)_3Cl_2]_2$.[118] The reaction of $Ru_3(CO)_{12}$ with halogens was found to form $[Ru(CO)_3X_2]_2$ or cis-$Ru(CO)_4X_2$ (X = Cl, Br or I), depending on reaction conditions.[119]

The reaction of $Os_3(CO)_{12}$ and BBr_3, (where the latter was employed as the solvent, the Lewis acid and a reactant) produced $Os_2(CO)_6Br_4$, as mentioned, page **58**. Irradiation of a CCl_4 solution of $Os_3(CO)_{12}$ at room temperature yielded only $Os(CO)_4Cl_2$.[120] This product was also obtained when the photolysis was carried out using $CHCl_3$ or CH_2Cl_2 as the solvent. Prolonged photolysis in these solvents[120] gave an additional product which was identified by its IR spectrum as $[Os(CO)_3Cl_2]_2$ and which was considered to form from the photolysis of $Os(CO)_4Cl_2$. Indeed, on irradiation of a CCl_4 solution of $Os(CO)_4Cl_2$, $[Os(CO)_3Cl_2]_2$ was obtained.[120]

Recently, a convenient and reproducible synthesis of cis-$Os(CO)_4Cl_2$ and its quantitative thermal conversion to $[Os(CO)_3Cl_2]_2$ was reported.[121]

Hales and Irving[114] observed that the compound $Os(CO)_4I_2$ was not particularly stable and when heated in benzene was found to slowly lose carbon monoxide to form the tricarbonyl iodide "$Os(CO)_3I_2$". These workers[114] obtained $Os(CO)_4I_2$ in small yield as a sublimate on the lid of the autoclave during the preparation of "$Os(CO)_3I_2$". $Os(CO)_4I_2$ was also found to sublime in small amounts when a stream of carbon monoxide at atmospheric pressure was passed over osmium oxyiodide and copper turnings at 200°C. In a similar way, the complexes $Re(CO)_5X$ (X = Cl, Br or I) have also been found to thermally dimerise, to give $[Re(CO)_4X]_2$ species with loss of CO.[122]

The dinuclear fragments, $Os_2(CO)_6X_4$ and $Os_2(CO)_8X_2$, have been detected in the mass spectrum of $Os_3(CO)_{12}X_2$,[114] consistent with the fragmentation of this trinuclear compound into mono and dinuclear fragments.

The detailed mechanism of the reaction of $Os_3(CO)_{12}$ with halogens appears complicated[123] and it has been shown that, in the case of chlorine, the rate of reaction was dependent on halogen concentration.[124] The reaction of $Os_3(CO)_{12}$ with iodine in decalin was found to be photochemically

initiated.[124] The kinetics of these reactions were not studied in benzene, since the photochemical reaction between benzene and halogen prevented accurate determination of halogen concentration.[124]

In a separate study,[115] reaction between $Os_3(CO)_{12}$ and iodine or CF_3I in benzene solution in a sealed evacuated tube at 170°C for 2 and 3 days, respectively, gave $Os_2(CO)_6I_2$ and $Os_2(CO)_8I_2$, in varying amounts. In the iodine reaction, only 50% of the $Os_3(CO)_{12}$ was consumed, giving $Os_2(CO)_6I_2$ (2%) and $Os_2(CO)_8I_2$ (73%) while the CF_3I reaction gave $Os_2(CO)_6I_2$ (10%) and $Os_2(CO)_8I_2$ (15%), respectively. Recently, Geoffroy et al[125] have reported a high yield synthesis of $Os_2(CO)_6I_2$ via the reaction of $Os_3(CO)_{12}$ with iodine in a Carius tube in toluene at 175°-180°C for 24 hours. These workers[125] found that the yield of $Os_2(CO)_6I_2$ was highly dependent upon reaction conditions, particularly temperature. They found that when the reaction temperature dropped to 165°-175°C, mixtures of $Os_2(CO)_6I_2$ (ca 70%) and $Os_2(CO)_8I_2$ (ca 30%) were obtained. This mixture could be upgraded to give essentially pure $Os_2(CO)_6I_2$ by reheating in a Carius tube at 175°-180°C for 12 hours. These workers[125] also reported the high yield conversion of $Os_2(CO)_6I_2$ to $Os_2(CO)_8I_2$ by pressurising a reaction vessel, containing a hexane solution of $Os_2(CO)_6I_2$, to 90 psi with CO and subsequently stirring the solution at

room temperature for 24 hours.

The dinuclear octacarbonyl dihalide complexes $Os_2(CO)_8X_2$, (X = Cl, Br or I) were first reported by Hieber and Stallman[113] who assigned the formulae, $[Os(CO)_4X]_2$ to some of the products they obtained from the reaction of CO with osmium trihalides. More recently,[126] the complexes $Os_2(CO)_8X_2$ (X = Cl or Br) were obtained by reaction of the corresponding hydride complex, $Os_2(CO)_8H_2$ with CX_4 (X = Cl or Br). $Os_2(CO)_8H_2$ was obtained as one of the products of the reaction of OsO_4 with CO (40 atm) and H_2 (37 atm) and a temperature of 433K, in 21% yield.[127]

The hexacarbonyl dinuclear dihalide complexes of the type $Os_2(CO)_6X_2$ (X = Cl or Br) have also been reported to be formed by heating the corresponding octacarbonyl derivatives $Os_2(CO)_8X_2$ under reflux in heptane for 40 minutes.[126] The structures of $Os_2(CO)_6X_2$ (X = Cl, Br or I) were believed,[115,126] on the basis of the IR spectra, to contain bridging halide ligands and a single metal-metal bond.

The reported synthetic methods and properties of osmium carbonyl complexes, including the dinuclear carbonyl halide complexes, have recently been discussed.[128] Diosmium octacarbonyl diiodide has been shown to be a useful precursor to the dianion, $[Os_2(CO)_8]Na_2$.[109] This dianion

reacts with alkyl halides to give dialkyl compounds.[109] Addition of an excess of methyl iodide to the dianion $[Os_2(CO)_8]Na_2$, as a solution in THF, readily gives $Os_2(CO)_8(CH_3)_2$; addition of the dianion solution to 1-2 equivalents of dihaloalkane gives the 1,2-diosmacycloalkanes, $(OC)_4\overline{Os(CH_2)_nOs}(CO)_4$ (n = 1,2,3).[109]

When the present work commenced, there was no convenient route in the literature for the preparation of $Os_2(CO)_8X_2$ or $Os_2(CO)_6X_2$ from readily available starting materials. The objectives of the present study were, firstly, to attempt to find a high yield and convenient synthetic route to dinuclear osmium carbonyl halide complexes from $Os_3(CO)_{12}$; secondly, to then investigate their reactivity and, thirdly, to investigate the crystal and molecular structures of some of the dinuclear complexes by X-Ray crystallographic techniques.

2.2 Results and Discussion

2.2.1 Dinuclear Octacarbonyl Dihalide Complexes prepared in the reaction of $Os_3(CO)_{12}$ with Halogens

2.2.1.1 Reaction of $Os_3(CO)_{12}$ with Chlorine

(a) A benzene solution of chlorine was added to a benzene solution of $Os_3(CO)_{12}$ at 80°C in a 3.5:1 molar ratio and the resulting solution placed in direct, bright sunlight for 3-5 minutes. The reaction was stopped when the bright yellow colour of the solution paled, indicative of the consumption of $Os_3(CO)_{12}$ in its reaction with chlorine. This reaction resulted in the isolation of three major products, i.e. $Os_3(CO)_{12}Cl_2$ (20%),[119] $Os_2(CO)_8Cl_2$[126] and $Os_2(CO)_6Cl_2$.[126] The latter two products could not be separated by chromatography.

(b) An identical experiment to 2.2.1.1(a) above was carried out, except that a Hanovia photochemical reactor was used in the place of the sunlight and the reaction solution was irradiated for 2 minutes. An IR spectrum of the reaction solution taken immediately after the addition of Cl_2 showed that $Os_3(CO)_{12}Cl_2$ had been formed, while an IR spectrum run after 2 minutes showed that new species were

present in solution. From this reaction, the major products isolated were $Os_3(CO)_{12}Cl_2$,[119] cis-$Os(CO)_4Cl_2$[129] and $Os_2(CO)_8Cl_2$.[126] $Os_2(CO)_6Cl_2$[126] was also obtained in low yield. Pure $Os_2(CO)_8Cl_2$ (24%) was obtained by washing the mixture of $Os_2(CO)_8Cl_2$ and $Os_2(CO)_6Cl_2$ with a minimum of hexane.

On the basis of the products isolated, the reaction of $Os_3(CO)_{12}$ with chlorine, under the conditions described above, can be represented by the following equations:

(i) $$Os_3(CO)_{12}+Cl_2 \xrightarrow{C_6H_6} Os_3(CO)_{12}Cl_2$$

(ii) $$Os_3(CO)_{12}Cl_2+Cl_2 \xrightarrow[h\nu]{C_6H_6} Os_2(CO)_8Cl_2 + \text{cis-}Os(CO)_4Cl_2$$

(iii) $$Os_2(CO)_8Cl_2 \xrightarrow[h\nu \text{ or } \Delta]{} Os_2(CO)_6Cl_2 + 2CO$$

In 2.2.1.1(a) above, some cis-$Os(CO)_4Cl_2$ may have formed but was possibly converted to $Os_2(CO)_6Cl_4$ which may have been lost during column chromatography.

Since $Os_2(CO)_8Cl_2$ was obtained in only 24% yield, the above reaction cannot be regarded as a good

method for the preparation of $Os_2(CO)_8Cl_2$ from $Os_3(CO)_{12}$. The reaction of $Os_3(CO)_{12}$ with chlorine takes place very rapidly to initially form $Os_3(CO)_{12}Cl_2$.[119] Since $Os_3(CO)_{12}Cl_2$ precipitated out of solution on cooling, reaction of $Os_3(CO)_{12}Cl_2$ with Cl_2 to produce the di- and mono-nuclear compounds outlined in equation (ii) above, was restricted. This could possibly explain the low yield of $Os_2(CO)_8Cl_2$ obtained. Previously, $Os_2(CO)_8Cl_2$ was reported to have been obtained from $Os_2(CO)_8H_2$ by reaction with CCl_4 in 86% yield.[126] Although this yield is high, the drawback of this synthesis of $Os_2(CO)_8Cl_2$ is the somewhat lengthy preparation of $Os_2(CO)_8H_2$.

2.2.1.2 Reaction of $Os_3(CO)_{12}$ with Bromine

(a) A similar procedure to 2.2.1.1(a) above was carried out for the reaction of $Os_3(CO)_{12}$ with bromine (1:3.5 molar ratio), except that a longer time of 5-10 minutes for the exposure of the reaction solution to direct, bright sunlight was used. The yellow benzene solution of $Os_3(CO)_{12}$ turned orange on the addition of bromine and the reaction was stopped when the colour of the solution changed to

pale yellow, indicative of the consumption of bromine. The major products isolated in the reaction were $Os_2(CO)_8Br_2$[126] and cis-$Os(CO)_4Br_2$.[129] The halogen concentration was found to be a critical factor in the yield of $Os_2(CO)_8Br_2$ obtained. In a series of experiments, molar ratios of 2.5, 3.0, 3.5, 4.0 and 6:1 of bromine to $Os_3(CO)_{12}$ were used. Highest yields of $Os_2(CO)_8Br_2$ for reactions using a 3.5:1 molar ratio of bromine to $Os_3(CO)_{12}$ were obtained when the reaction solution was placed in the brightest sunlight. Since this molar ratio gave the highest yields of $Os_2(CO)_8Br_2$, this ratio was also used for the reactions of $Os_3(CO)_{12}$ with chlorine and iodine, respectively.

It was found that both UV light and elevated temperatures, i.e. above room temperature, were necessary for the success of the reactions to give $Os_2(CO)_8Br_2$, since:

(i) the irradiation with UV light of a benzene solution of bromine and $Os_3(CO)_{12}$ (3.5:1 molar ratio) for 3.5 hours at room temperature, was investigated and the reaction monitored by IR spectroscopy. The reaction was stopped when additional ν(CO) bands, other than those

corresponding to $Os_3(CO)_{12}Br_2$, were observed in the IR spectrum, indicating that $Os_3(CO)_{12}Br_2$ was no longer the only species present. The products obtained were separated on the basis of their solubility in n-hexane and were identified as $Os_3(CO)_{12}Br_2$[119] (67%) and $Os_2(CO)_8Br_2$[126] (33%);

(ii) the addition of bromine to a benzene solution of $Os_3(CO)_{12}$ in a 3.5:1 molar ratio at 80°C and allowing the reaction solution to stand in the dark, at room temperature, produced crystals of $Os_3(CO)_{12}Br_2$[119] (87%) and $Os_2(CO)_8Br_2$[126] (13%).

(b) The reaction of bromine with $Os_3(CO)_{12}$ (3.5:1 molar ratio) in an identical experiment to 2.2.1.2(a) above, was carried out except that a Hanovia photochemical reactor was used in the place of sunlight and the reaction solution was irradiated for 7 minutes. The reaction was monitored by IR spectroscopy and was stopped when the ν(CO) bands in the IR spectrum indicated that $Os_3(CO)_{12}Br_2$ was no longer the major species present in solution. Three main products isolated in this reaction were separated by column chromotography and were identified as $Os_2(CO)_8Br_2$[126] (46%),

cis-$Os(CO)_4Br_2$[129] (12%) and $Os_2(CO)_6Br_4$[105] (18%). $Os_2(CO)_6Br_2$[126] (3%) was obtained in low yield. $Os_2(CO)_6Br_4$ was identified by its mass spectrum but its IR spectrum differed from that reported in the literature,[105] showing two strong bands at ν(CO) bands at 2120 and 2032 cm^{-1}. Since it was eluted off the column using methanol as the eluent, we believe that an interaction between $Os_2(CO)_6Br_4$ and methanol had occurred, producing $Os(CO)_3Br_2(MeOH)$ in solution.

We believe that the procedure outlined in 2.2.1.2(b) above is a convenient, one-step method for obtaining $Os_2(CO)_8Br_2$ from $Os_3(CO)_{12}$ in reasonable yield. From a series of separate reactions employing different irradiation times, an irradiation time of 7 minutes was found to produce the optimum yield of $Os_2(CO)_8Br_2$. Previously, $Os_2(CO)_8Br_2$ was obtained from the reaction of $Os_2(CO)_8H_2$ with CBr_4 in 70% yield.[126] As mentioned above, although this yield is high, the drawback of this synthesis of $Os_2(CO)_8Br_2$ is the somewhat lengthy preparation of $Os_2(CO)_8H_2$.

2.2.1.3 Reaction of $Os_3(CO)_{12}$ with Iodine

(a) A similar experiment to 2.2.1.1(a) and 2.2.1.2(a) above was carried out for the reaction of $Os_3(CO)_{12}$ with iodine (1:3.5 molar ratio), except that a time of 20 minutes for the exposure of the reaction solution to direct, bright sunlight, was used. The reaction was carried out several times using various exposure times of the reaction solution to sunlight, and 20 minutes was found to produce the optimum yield of $Os_2(CO)_8I_2$. Varying amounts of $Os_2(CO)_8I_2$,[115] $Os_2(CO)_6I_2$,[115] cis-$Os(CO)_4I_2$[114] and trans-$Os(CO)_4I_2$[130] were obtained from this reaction and these results may be attributed to the somewhat variable room temperature and also the intensity of the sunlight.

(b) The reaction of iodine with $Os_3(CO)_{12}$ (3.5:1 molar ratio) in an identical experiment to 2.2.1.3(a) above, was carried out, except that a Hanovia photochemical reactor was used in the place of the sunlight, as in 2.2.1.1(b) and 2.2.1.2(b) above, and the reaction solution was irradiated for 15 minutes. The reaction was monitored by IR spectroscopy and was stopped when additional ν(CO) bands, other than

those corresponding to $Os_3(CO)_{12}I_2$, were observed, indicating that $Os_3(CO)_{12}I_2$ was no longer the major species present in solution. The products isolated in the reaction were separated by column chromotography and fractional recrystallisation and were identified as $Os_2(CO)_8I_2$[115] (42%), **cis**-$Os(CO)_4I_2$[130] (5%), **trans**-$Os(CO)_4I_2$[130] and $Os_2(CO)_6I_4$[114] (23%). The IR spectrum of $Os_2(CO)_6I_4$ agreed with that reported in the literature[114] but differed from that obtained in this present work for the product of the reaction of $Os_2(CO)_6I_2$ with I_2, also believed to be $Os_2(CO)_6I_4$. In reaction 2.2.1.3(b), however, $Os_2(CO)_6I_4$ was eluted off the column using methanol as the eluent. We believe that $Os_2(CO)_6I_4$, identified by its mass spectrum, interacted with the methanol, producing $Os(CO)_3I_2(MeOH)$ in solution, as for $Os_2(CO)_6Br_4$ in reaction 2.2.1.2(b) above. It is possible that the IR spectrum previously reported for $Os_2(CO)_6I_4$[114] was actually that of $Os(CO)_3I_2(H_2O)$, formed by the interaction of $Os_2(CO)_6I_4$ with an impurity, possibly H_2O, in the CCl_4 solvent. The mass spectrum of $Os_2(CO)_6I_4$ was not previously[114] reported.

The interaction of $[Ru(CO)_3X_2]_2$ species with ethanol present in commercial chloroform, as the stabiliser,

has previously been observed and the IR spectra studied.[131,132] The products identified from the reactions of $Os_3(CO)_{12}$ with bromine or iodine can be represented by the following equations (X = Br or I) and see discussion in 2.4 below:

(i) $Os_3(CO)_{12} + X_2 \xrightarrow{C_6H_6} Os_3(CO)_{12}X_2$

(ii) $Os_3(CO)_{12}X_2 + X_2 \xrightarrow[h\upsilon]{C_6H_6} Os_2(CO)_8X_2 + \textbf{cis}\text{-}Os(CO)_4X_2$

(iii) $Os_2(CO)_8X_2 \xrightarrow[h\upsilon \text{ or } \Delta]{} Os_2(CO)_6X_2 + 2CO$

(iv) $2\ \textbf{cis}\text{-}Os(CO)_4X_2 \xrightarrow[h\upsilon \text{ or } \Delta]{} Os_2(CO)_6X_4 + 2CO$

(v) $Os_2(CO)_6X_2 + X_2 \longrightarrow Os_2(CO)_6X_4$

(vi) $Os_2(CO)_8X_2 + X_2 \longrightarrow 2\ \textbf{cis}\text{- or }\textbf{trans}\text{-}Os(CO)_4X_2$

(vii) $Os_2(CO)_6X_4 + MeOH \longrightarrow 2\ Os(CO)_3X_2(MeOH)$

(viii) $\textbf{trans}\text{-}Os(CO)_4I_2 \xrightarrow{h\upsilon} \textbf{cis}\text{-}Os(CO)_4I_2$

$Os_2(CO)_6I_2$ may have formed in reaction 2.2.1.3(b) above but may then have reacted with I_2 to produce $Os_2(CO)_6I_4$, as has been demonstrated in this present work - section 2.2.2.2.3. **Trans**-$Os(CO)_4I_2$ has previously been reported[130] to be converted to

cis-$Os(CO)_4I_2$ when exposed to sunlight, whereas **trans**-complexes could not be obtained by the action of sunlight on hexane solutions of **cis**-$Os(CO)_4I_2$.[130] The very low yield of **trans**-$Os(CO)_4I_2$ obtained in the reaction of $Os_3(CO)_{12}$ with I_2, identified by IR and mass spectroscopy only, could possibly be explained in terms of this previous observation.[130] It is possible that **trans**-$Os(CO)_4I_2$ is the kinetically favoured product which is formed initially and this is mostly converted to **cis**-$Os(CO)_4I_2$, the thermodynamically favoured isomer, in the presence of UV radiation.

We believe that the procedure outlined in 2.2.1.3(b) above is a convenient, one-step method for the preparation of $Os_2(CO)_8I_2$ from $Os_3(CO)_{12}$. From a series of separate experiments, an irradiation time of 15 minutes was found to produce the optimum yield of $Os_2(CO)_8I_2$. $Os_2(CO)_8I_2$ has previously been obtained by various routes, as mentioned previously in section 2.1.

2.2.1.4 Conclusion

The initial step in the reaction of $Os_3(CO)_{12}$ with halogens has been shown to be the cleavage of one osmium-osmium bond,

resulting in the formation of $Os_3(CO)_{12}X_2$ (X = Cl, Br, I). Three strong ν(CO) bands corresponding to $Os_3(CO)_{12}X_2$ (X = Cl, Br, I) are observed in the IR spectrum of the reaction solution run immediately after the addition of halogen to $Os_3(CO)_{12}$. Indeed, these trinuclear dihalide derivatives can be isolated in high yield if the reaction is carried out for a short time.[119] If the reaction with halogens is allowed to continue beyond this stage and in the presence of UV radiation, we have found that the major products obtained are $Os_2(CO)_8X_2$ and $Os(CO)_4X_2$ (X = Cl, Br or I). Thus, a logical next step based on the formation of these products, would be the cleavage of a second osmium-osmium bond in $Os_3(CO)_{12}X_2$ (X = Cl, Br, I) to produce the di- and mono-nuclear derivatives. Indeed, the products of the reaction of bromine with $Os_3(CO)_{12}Br_2$ in an equimolar ratio are $Os_2(CO)_8Br_2$ and **cis**-$Os(CO)_4Br_2$, as we have shown in a separate experiment - see Experimental Section. The detailed mechanism of the reaction of $Os_3(CO)_{12}$ with halogens is not well understood and has been previously described as complicated.[123] However, we have found that the major products isolated in the ensuing reactions are as expected and can be rationalised. Only two moles of halogen are theoretically required for the cleavage of two osmium-osmium bonds to obtain the desired octacarbonyl derivatives - see scheme below (CO ligands are omitted for clarity):

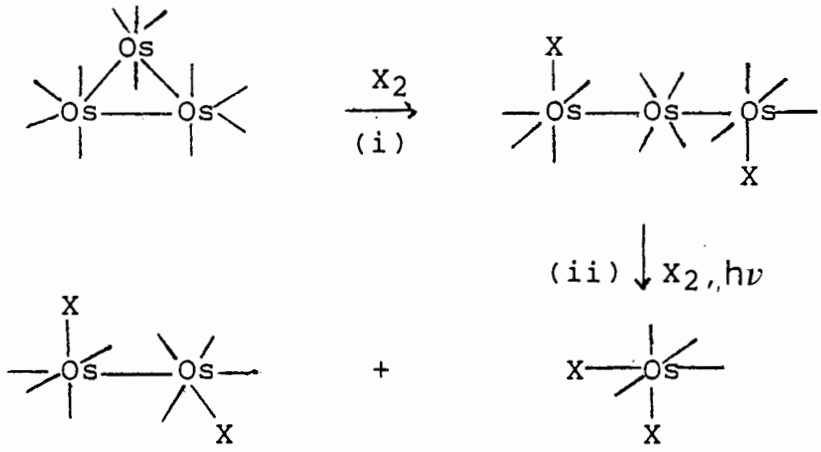

However, in the presence of heat or UV radiation, these products, $Os_2(CO)_8X_2$ and $Os(CO)_4X_2$ (X = Cl, Br or I) undergo decarbonylation to produce $Os_2(CO)_6X_2$ and $Os_2(CO)_6X_4$ (X = Cl, Br or I) - see equations (iii) and (iv):

(iii) 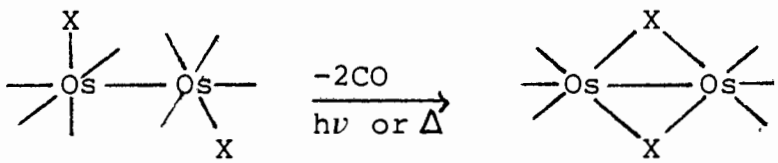

(iv) 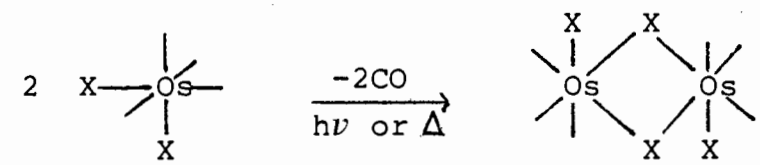

$Os_2(CO)_6I_2$ has been shown in this present work - see section 2.2.2.2.3 - to react with I_2 to form $Os_2(CO)_6I_4$. Therefore, $Os_2(CO)_6X_2$ species could react with a further mole of

halogen to produce $Os_2(CO)_6X_4$ species (X = Cl, Br or I) - see equation (v). Although the reaction has not been demonstrated, it is also probable that $Os_2(CO)_8X_2$ could react with a further mole of halogen to form $Os(CO)_4X_2$ (X = Cl, Br or I) - see equation (vi).

(v) 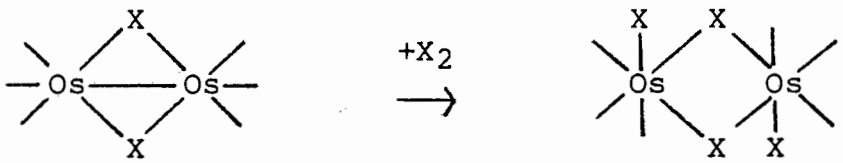

(vi) 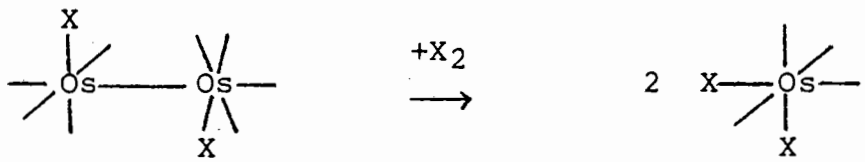

Reactions outlined in equations (iii) to (vi) are believed to occur simultaneously but at various reaction rates. For example, the decarbonylation of $Os_2(CO)_8X_2$ species - equation (iii) - is known to proceed readily and reaction of the hexacarbonyl derivatives with halogen - equation (v) - is known to proceed almost immediately to form $Os_2(CO)_6X_4$ species, whereas the decarbonylation of $Os(CO)_4X_2$ species is known to be slower - equation (iv). Equations (v) and (vi) illustrate further reactions which would involve the consumption of further moles of halogen. Thus, the addition of an amount of halogen in excess of the two moles required to cleave two osmium-osmium bonds - see equations (i) and

(ii) above - was necessary to produce the desired octacarbonyl derivatives in optimum yield. Indeed, a series of experiments - as mentioned in 2.2.1.2(a) above - employing different molar ratios of bromine to $Os_3(CO)_{12}$ concluded that a 3.5:1 molar ratio led to optimum yields of $Os_2(CO)_8Br_2$ being obtained. Irradiation times of 2, 7 and 15 minutes, respectively, were required for the reactions of $Os_3(CO)_{12}$ with chlorine, bromine or iodine, respectively, to produce optimum yields of $Os_2(CO)_8X_2$ (X = Cl, Br or I).

It is interesting to note that $Os_3(CO)_{12}X_2$ loses two moles of CO to give $Os_3(CO)_{10}X_2$ (X = Cl, Br or I)[133] but we did not find any evidence for $Os_3(CO)_{10}X_2$ species in our reactions. Presumably, the reaction of $Os_3(CO)_{12}X_2$ with X_2 to cause osmium-osmium bond cleavage is much faster than the reaction to lose CO.

The procedures outlined in section 2.2.1 above, for the preparation of $Os_2(CO)_8X_2$ (X = Cl, Br or I) from $Os_3(CO)_{12}$ are far simpler and less time-consuming than previously reported synthetic methods for $Os_2(CO)_8X_2$, which all involve two-step procedures. Although the procedure outlined in this present work cannot be regarded as a good method for the synthesis of $Os_2(CO)_8Cl_2$, both $Os_2(CO)_8Br_2$ (46%) and $Os_2(CO)_8I_2$ (42%) were obtained in reasonable yield directly from $Os_3(CO)_{12}$.

2.2.2 Dinuclear Hexacarbonyl Dihalide Complexes

2.2.2.1 Synthesis

The octacarbonyl derivatives, $Os_2(CO)_8X_2$, (X = Br or I) were converted into the hexacarbonyl compounds, $Os_2(CO)_6X_2$, (X = Br or I) by heating under reflux for 40 minutes, as has been previously reported[126] for X = Cl or Br. In this present work, $Os_2(CO)_6I_2$ was obtained from $Os_2(CO)_8I_2$ in 80% yield and, therefore, in 40% overall yield from $Os_3(CO)_{12}$.

The conversion of $Os_2(CO)_8I_2$ to $Os_2(CO)_6I_2$ was previously carried out in vacuo.[115] $Os_2(CO)_6I_2$ was also previously obtained[114] from the reaction of $Os_3(CO)_{12}$ with iodine or CF_3I in benzene solution in a sealed evacuated tube at 170°C for 2 and 3 days, in 1% and 10% yields, respectively. More recently,[125] $Os_2(CO)_6I_2$ has been obtained in 80% yield from the reaction of $Os_3(CO)_{12}$ with I_2 under conditions of high temperature and 6 atm CO pressure for 24 hours.

The conversion route may be represented by the following equation:

$$Os_2(CO)_8I_2 \xrightarrow[\text{n-heptane}]{\Delta} Os_2(CO)_6I_2 + 2CO$$

2.2.2.2 Investigation of the reactivity of $Os_2(CO)_6I_2$

The complex, $Os_2(CO)_6I_2$, i.e. 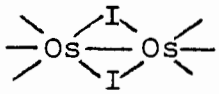

has two iodine bridges spanning the two osmium atoms, as we have shown by X-ray crystallography[134] - section 3.3. A common reaction of dinuclear compounds with halogen bridges is the cleavage of the bridges by neutral ligands, commonly called a "bridge-splitting" reaction.

e.g. 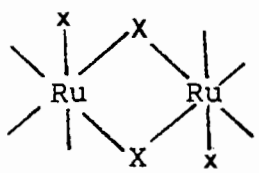 $\xrightarrow{py}$ $2\ RuX_2(CO)_3py$ [131]

e.g. 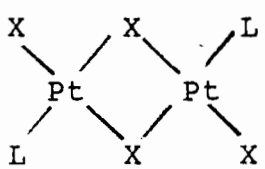 $\xrightarrow{2CO}$ $2\ cis\text{-}PtL(CO)X_2$ [135]

(X = halogen; L = tertiary phosphine)

In these two above examples, there is no metal-metal bond in the dinuclear starting complexes and mononuclear complexes result. However, for $Os_2(CO)_6I_2$, there is an osmium-osmium bond in addition to the two iodine bridging ligands, as we have shown by X-Ray crystallography.[134] We might expect that two ligands would add to $Os_2(CO)_6I_2$ to give complexes of the type, $Os_2(CO)_6L_2I_2$, with retention of the osmium-osmium bond and splitting of the iodine bridges. We

have shown that the complex, $Os_2(CO)_6I_2$ does readily undergo addition reactions with neutral ligands as discussed below for L = CO, PPh_3 and PMe_2Ph.

2.2.2.2.1 Reaction of $Os_2(CO)_6I_2$ with CO

Carbon monoxide was bubbled through a n-hexane solution of $Os_2(CO)_6I_2$ for 20 minutes. The solution was then stirred in a closed Schlenk tube, under an atmosphere of CO, at room temperature, for 2 days. An IR spectrum of the reaction solution after this time showed ν(CO) bands of both $Os_2(CO)_6I_2$ and $Os_2(CO)_8I_2$, indicative of some reaction of the hexacarbonyl complex with CO having occurred. Complete conversion to $Os_2(CO)_8I_2$ under these conditions was not observed and possibly more vigorous conditions were required. However, this conversion was recently reported[125] by workers who carried out the reaction under 90 psi of CO and an 85% yield of $Os_2(CO)_8I_2$ from $Os_2(CO)_6I_2$ was obtained but also with some unreacted $Os_2(CO)_6I_2$ remaining. Interestingly, even under conditions of high pressure, total conversion to $Os_2(CO)_8I_2$ was not apparently observed.

2.2.2.2.2 Reaction of $Os_2(CO)_6I_2$ with Tertiary Phosphines

(a) With PPh_3

The addition of 2 moles of PPh_3 to a n-hexane solution of $Os_2(CO)_6I_2$, at room temperature, resulted in the almost immediate precipitation of a yellow solid. This compound was formulated as $Os_2(CO)_6(PPh_3)_2I_2$ on the basis of IR and ^1H nmr spectroscopy, microanalysis and a solution molecular weight determination which confirmed the dimeric nature of the molecule - see Experimental Section.

(b) With PMe_2Ph

As with the triphenylphosphine reaction above, the addition of 2 moles of PMe_2Ph to a n-hexane solution of $Os_2(CO)_6I_2$ resulted in the almost immediate precipitation of a slightly oily, yellow product. Trituration of this solid with n-hexane produced a bright yellow solid formulated as $Os_2(CO)_6(PMe_2Ph)_2I_2$ on the basis of IR and ^1H nmr spectroscopy and microanalysis - see Experimental Section. The ^1H nmr spectrum showed a complex multiplet at 2.46 τ for for the phenyl protons and a doublet at 8.25 τ [$J(^{31}P-^1H)$ = 13 Hz], for the methyl protons. The fact that only one doublet was observed suggests that the two PMe_2Ph ligands are in identical environments. On this basis then, possible structures for $Os_2(CO)_6(PMe_2Ph)_2I_2$ can be drawn - see figure 2.4. Structures where two iodines are coordinated to

one osmium atom were not considered since it is unlikely that one osmium atom exists in a +II oxidation state and the other osmium atom in a zero oxidation state. Structure d - see figure 2.4 - is also unlikely since in a similar complex

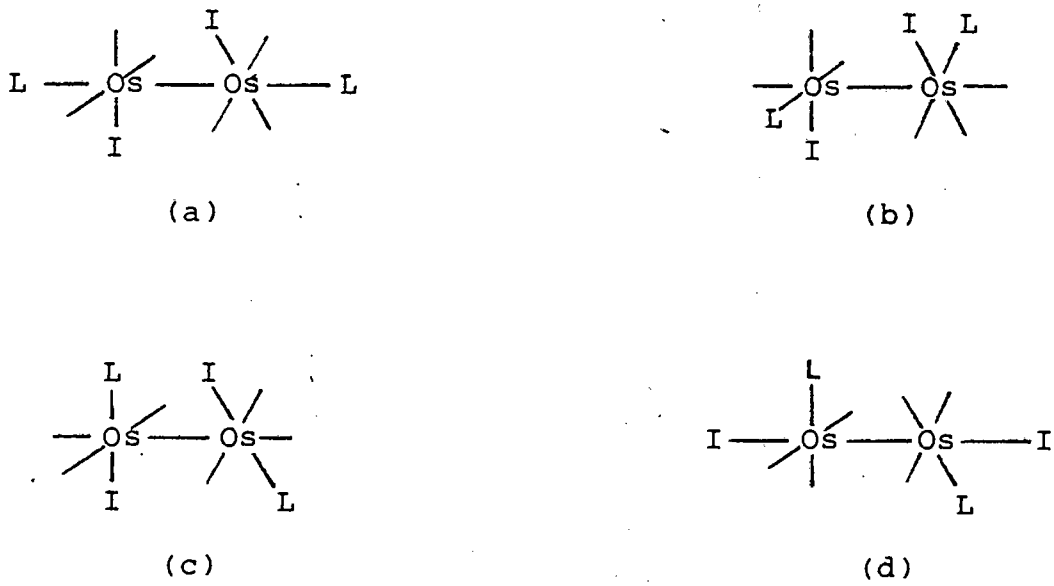

Figure 2.4 Diagrammatic representations of the possible structures for $Os_2(CO)_6(PMe_2Ph)_2I_2$

$Os_2(CO)_6(PPh_3)_2H_2$ it was proposed that the hydride ligands were in equatorial positions.[126] Also, the structural determinations of the complexes, $Os_2(CO)_8X_2$, (X = Cl or I) have shown the halide ligands to be in equatorial positions - sections 3.4 and 3.5, respectively. Interestingly, the structure of $Re_2(CO)_8(CNC_6H_3Me_2\text{-}2,6)_2$ also adopts a configuration where the two $(CNC_6H_3Me_2\text{-}2,6)$ ligands are

situated in equatorial positions.[136] The ^1H nmr spectrum of $Os_2(CO)_6(PPh_3)_2H_2$[126] was reported to yield a phosphorus-hydrogen coupling constant of 18.5 Hz. On the basis of this measurement, the most likely structures proposed for this hydride complex were those with the PPh_3 ligands **cis** to the hydride ligands - see figure 2.5.

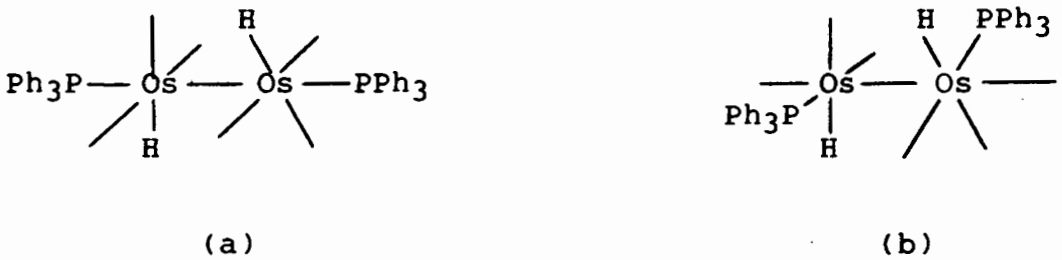

(a) (b)

Figure 2.5 Diagrammatic representations of the most likely structures proposed for $Os_2(CO)_6(PPh_3)_2H_2$

The structures (a), (b) and (c) drawn in Figure 2.4 do not possess simple mer- or fac-$Os(CO)_3L_3$ geometry which on local symmetry grounds would be expected to display two or three υ(CO) bands in the IR spectra, respectively. On local symmetry grounds, each osmium atom in structures (a) and (c) has an approximate mer-$Os(CO)_3LXY$ configuration, while in structure (b), each osmium atom has an approximate fac-$Os(CO)_3LXY$ configuration. The IR spectra of $Os_2(CO)_6L_2I_2$ (L = PMe_2Ph or PPh_3) species show the maximum number of υ(CO) bands expected for a hexacarbonyl species; the 7 υ(CO) bands observed for the PPh_3 complex may be due to the presence of more than one isomer.

Local symmetry arguments were not applicable for the complex, 1,2-$Mn(CO)_8(Bu^tNC)_2$[137] either, which showed five ν(CO) bands in the IR spectrum. Thus, we suggest that $Os_2(CO)_6(PMe_2Ph)_2I_2$ adopts either structure (a) or (b) depicted in figure 2.4. We suggest that the complex, $Os_2(CO)_6(PPh_3)_2I_2$, adopts a similar structure to the PMe_2Ph complex on the basis of the similarity of their IR spectra in the ν(CO) region. Of the structures (a) or (b), structure (b) would be more likely on electronic grounds since CO groups prefer to adopt positions cis to each other. However, on steric grounds, structure (a) would be favoured. It is possible that since even CO stretches are observed in the IR spectrum, that a mixture of isomers is present.

The addition reactions of $Os_2(CO)_6I_2$ with neutral ligands, CO, PPh_3 and PMe_2Ph, are illustrated in the following equation:

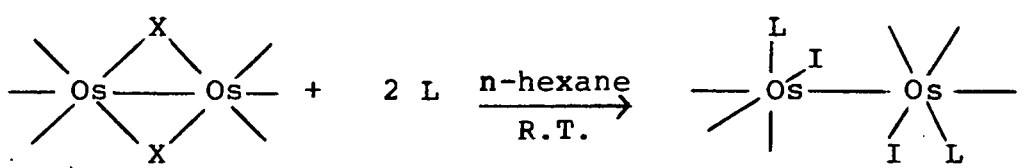

or

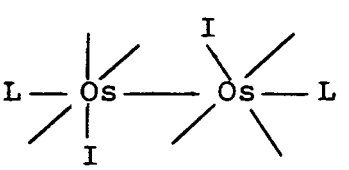

(L = CO, PPh_3 or PMe_2Ph)

The above addition reactions of $Os_2(CO)_6I_2$ with CO, PPh_3 or PMe_2Ph were shown to proceeds readily at room temperature, although the reaction with CO did not proceed to completion. Since $Os_2(CO)_6I_2$ undergoes addition reactions with neutral ligands, it can therefore be considered to be "unsaturated".

2.2.2.2.3 Reaction of $Os_2(CO)_6I_2$ with I_2

We have shown that $Os_2(CO)_6I_2$ has both an osmium-osmium bond and two iodide ligands by X-Ray crystallography.[134] As part of our studies on the reactivity of this complex, we were interested in investigating the possibility of cleaving the osmium-osmium bond of $Os_2(CO)_6I_2$ while still retaining the dimeric nature of the molecule via the bridging iodide ligands. We have shown above that $Os_2(CO)_6I_2$ will undergo addition reactions with the neutral ligands CO, PPh_3 and PMe_2Ph that result in the cleavage of the iodide bridges but with retention of the osmium-osmium bond. Halogens are known to cleave metal-metal bonds in polynuclear complexes. Thus, the reactions of $Os_3(CO)_{12}$ with halogens results in the formation of $Os_3(CO)_{12}X_2$ (X = Cl, Br or I) by the fission of an osmium-osmium bond.[119] Similarly, the reaction of $Mn_2(CO)_{10}$ with iodine produces $Mn(CO)_5I$.[138]

The addition of one mole of iodine in the solid state to

$Os_2(CO)_6I_2$ as a solution in n-hexane, at room temperature, resulted in the almost immediate precipitation of a bright yellow, microcrystalline product. The product was formulated as $Os_2(CO)_6I_4$ on the basis of its mass spectrum which gave a molecular ion at m/e 1058, corresponding to $[Os_2(CO)_6I_4]^+$ with sequential loss of six carbonyl groups to give a positive ion at m/e 890, corresponding to $[Os_2I_4]^+$. The IR spectrum of the product in the ν(CO) region showed two strong bands at 2115 and 2025 cm^{-1}. The carbonyl stretching frequencies for $Os_2(CO)_6I_4$ were reported in the literature[115] to occur at 2119 and 2051 cm^{-1}. However, we believe these latter two bands are possibly due to $Os(CO)_3I_2(H_2O)$ formed in solution, from the interaction of $Os_2(CO)_6I_4$ with an impurity, possibly H_2O, present in the CCl_4 solvent.

The reaction of $Os_2(CO)_6I_2$ with I_2 represents a novel type of oxidative addition reaction which can be illustrated by the following equation:

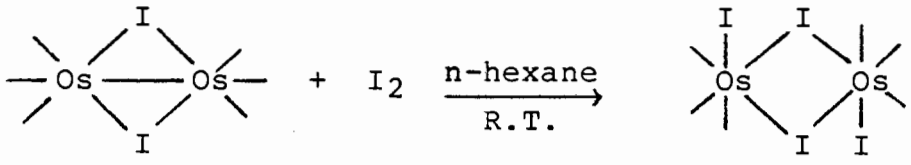

This addition reaction is an example of the reactivity potential offered by dinuclear complexes which cannot be shown by mononuclear complexes.

2.2.2.2.4 Reaction of $Os_2(CO)_6I_2$ with H_2 or C_2H_4

Since $Os_2(CO)_6I_2$ undergoes addition reactions with CO, PPh_3, PMe_2Ph and I_2, it can be considered to be "unsaturated". We decided, therefore, to investigate whether $Os_2(CO)_6I_2$ would add small molecules, e.g. H_2 or C_2H_4. H_2 was bubbled through a hexane solution of $Os_2(CO)_6I_2$ for 20 minutes, at room temperature, and the solution stirred for 12 hours in a closed Schlenk tube, under an atmosphere of H_2. An identical experiment was carried out, except that C_2H_4 was bubbled through a solution of $Os_2(CO)_6I_2$. No change in the IR spectra of either reaction solution was observed, indicating that no reactions had occurred, under the conditions employed. The above reactions may have succeeded under more vigorous conditions of high temperature and pressure. Thus, H_2 and C_2H_4 were not found to add to $Os_2(CO)_6I_2$ as readily as tertiary phosphines and iodine, respectively.

2.2.3 Dinuclear Hexacarbonyl Tetrahalide Complexes

The mononuclear tetracarbonyl dihalide complexes, cis-$Os(CO)_4X_2$ (X = Cl, Br or I) were dissolved in light petroleum (bp 100°-120°C) by heating under reflux. Refluxing was continued for 3 to 5 hours. The products which precipitated out of solution, on cooling, in all three

reactions were recrystallised from boiling chloroform or benzene and were obtained pure in near quantitative yield. The products were shown to be $Os_2(CO)_6X_4$ (X = Cl, Br or I) by IR and mass spectroscopy.[105,114,115] The thermal conversion of **cis**-$Os(CO)_4Cl_2$ to $Os_2(CO)_6Cl_4$ was also found to proceed in CH_2Cl_2 by heating under reflux for 3 hours. The products, $Os_2(CO)_6X_4$ (X = Cl, Br or I) have previously been obtained by various routes,[105,114,115] as discussed in section 2.1 above. The above reactions can be represented as follows:

$$\text{cis-}Os(CO)_4X_2 \xrightarrow{\Delta} Os_2(CO)_6X_4 + 2\ CO$$

Reaction conditions:

(a) X = Cl, Br or I : reflux, light petroleum (bp 100°-120°C), 3-5 hours

(b) X = Cl : reflux, CH_2Cl_2, 3 hours

2.3 Conclusion

Metal carbonyl halides, as has been discussed previously, are convenient starting materials for the synthesis of many other metal carbonyl derivatives. In this present work, we have established a convenient, one-step procedure for preparing the dinuclear carbonyl halides, $Os_2(CO)_8X_2$ (X = Br or I) from $Os_3(CO)_{12}$ in reasonable yields. We have concluded that UV radiation is necessary for the cleavage

of the osmium-osmium bond in initially formed $Os_3(CO)_{12}X_2$ (X = Br or I) to obtain the octacarbonyl derivatives, $Os_2(CO)_8X_2$ (X = Br or I). The above procedure provides a new synthetic route, whereby the complexes, $Os_2(CO)_8X_2$ (X = Br or I) are more readily available for reactivity studies and as starting materials for the synthesis of other new dinuclear complexes.

The reactivity of $Os_2(CO)_6I_2$ towards neutral ligands, CO, PPh_3, PMe_2Ph and I_2 has been investigated. These addition reactions, and in particular, a novel oxidative addition reaction of $Os_2(CO)_6I_2$ with I_2, were all found to proceed readily. The new complexes, $Os_2(CO)_6L_2I_2$ (L = PPh_3 or PMe_2Ph) have been synthesised and possible structures proposed for these complexes on the basis of IR and ^1H nmr spectroscopic data.

CHAPTER 3

X-RAY CRYSTALLOGRAPHIC STUDIES OF SOME OSMIUM(I) HALIDE AND HYDRIDE COMPLEXES

3.1 General Experimental Procedures used in the Crystallographic Analysis

3.1.1 Single Crystal Analysis[139-142]

Experimental details of crystal preparation, X-Ray photography and the data collections are presented independently with each crystal structure.

3.1.2 Computation

All computations were carried out on a Sperry 1100/81 computer system at the University of Cape Town. The programme SHELX[143] was employed for the solution and refinement of the structures. Features of the programme utilised include data reduction, full-matrix least-squares refinements, analysis of variance and automatic optimisation of weighting schemes, Fourier syntheses with peak search and structure factor listings.

The agreement between observed (F_o) and calculated (F_c) structure factors is expressed by the conventional residual index R defined as:[140]

$$R = \frac{\Sigma \| F_o | - | F_c \|}{\Sigma | F_o |} = \frac{\Sigma | \Delta |}{\Sigma | F_o |}$$

or expressed as

$$R_w = \frac{\sum w^{\frac{1}{2}} |\Delta|}{\sum w^{\frac{1}{2}} |F_o|}$$

where $w = K/[\sigma^2(F) + gF^2]$ upon introduction of a weighting scheme. K was redetermined after each structure factor calculation. The value of g was chosen to give the smallest variation of $w\Delta^2$ with the magnitude of F_c.

An analysis of variance computed after the final refinement cycle gives an indication of the effectiveness of the weighting scheme. A resulting low value for the discrepancy factor index R (<10%) is indicative of a correctly refined structure.

Atomic radii used were those of Pauling,[144] while scattering factors for all atoms were from Cromer and Mann[145] with dispersion corrections from Cromer and Liberman.[146]

A programme written for the Apple computer was used to calculate geometrical parameters.[147] Molecular illustrations and projections were produced by the programme PLUTO.[148]

3.2 The X-Ray Crystal Structure of Dichlorododecacarbonyl -triosmium, $Os_3(CO)_{12}Cl_2$

3.2.1 Introduction

There are few linear homotrinuclear complexes known. Little structural information on chain cluster complexes of the type, $Os_3(CO)_{12}X_2$, is known since only three structures have been determined, i.e. for $Os_3(CO)_{12}X_2$ (X = $SiCl_3$,[38] I[40] or Me[49]). The most probable structures for an $Os_3(CO)_{12}X_2$ compound are shown in the diagram below (CO ligands are omitted for clarity):

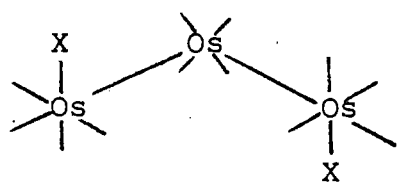

1)

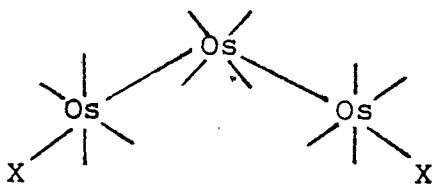

2)

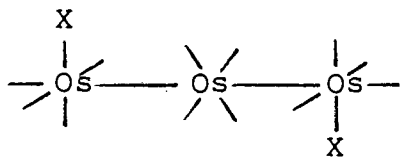

3)

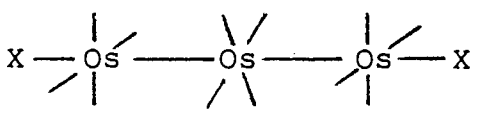

4)

IR spectroscopic evidence suggests that structure 3 is the one most commonly adopted. The X-Ray crystal structure determination of $Os_3(CO)_{12}I_2$[40] confirmed that the molecule comprises a linear chain of three osmium atoms, that the terminal iodide ligands occupy equatorial sites on the terminal osmium atoms and that the molecule adopts a conformation where the equatorial carbonyl groups on the central osmium atom are staggered with respect to those on the two terminal osmium atoms. However, the X-Ray crystal structure of $Os_3(CO)_{12}(SiCl_3)_2$[38] showed that this molecule also comprises a linear chain of three osmium atoms, but that the $SiCl_3$ groups are situated in axial positions on the terminal osmium atoms. The molecule also adopts a staggered conformation, i.e. the isomer depicted in structure 4.

IR spectroscopic evidence suggests[126] that the chloro complex, $Os_3(CO)_{12}Cl_2$ adopts a similar structure to $Os_3(CO)_{12}I_2$,[40] as do the complexes $Os_3(CO)_{12}X_2$ (X = Br,[126] H,[127] or Me[149]). Thus the X-Ray crystal structure of $Os_3(CO)_{12}Cl_2$ was determined to confirm this expectation and also to add to the structural information known about chain complexes of this type.

3.2.2 Experimental

$Os_3(CO)_{12}Cl_2$ was obtained from the reaction of $Os_3(CO)_{12}$ with chlorine gas, as described in the literature[119] and characterised by its IR spectrum in CH_2Cl_2 in the ν(CO) region, by its melting point and by the %C analysis. These data - see Experimental Section in Chapter 6 - were found to be in agreement with the literature values.[119] Single crystals of $Os_3(CO)_{12}Cl_2$ suitable for an X-Ray study were obtained by recrystallisation of the compound from dichloromethane/n-hexane.

3.2.3 Intensity Data Collection

Accurate cell parameters were obtained from a least-squares analysis of the setting angles of 24 reflections ($16° \leq \theta \leq 17°$) which were automatically located and centred on an Enraf-Nonius CAD4 diffractometer. The intensities of three reference reflections were checked every hour, to monitor crystal decay, and centering checked every 100 measured reflections. The data were Lp processed and an empirical absorption correction applied.[150] Crystal data and experimental details of the collection and final refinement are listed in Table 3.2.1.

Table 3.2.1 Crystal Data, Data Collection and Refinement Parameters for $Os_3(CO)_{12}Cl_2$

Crystal Data	
Molecular Formula	$C_{12}Cl_2O_{12}Os_3$
Molecular Weight/g mol^{-1}	977.62
Space Group	C2/m
a/Å	12.105(3)
b/Å	10.612(3)
c/Å	8.798(1)
β/°	117.02(2)
V/$Å^3$	1006.8
Z	2
$D_C Mgm^{-3}$	3.22
μ (MoK_α) mm^{-1}	18.4
F(000)	860
Data Collection	
Crystal Dimensions/mm	0.13 X 0.16 X 0.16
Scan Mode	ω - 2θ
Scan Width, ω/°	(0.54 + 0.35tanθ)
Aperture Width/mm	(1.12 + 1.05tanθ)
Aperture Length/mm	4
Crystal Decay/%	0.67
Range Scanned, θ/°	1-25
Radiation used, MoK_α,Å	0.7107

continued/...

Table 3.2.1 continued ...

Refinement	
Number of Reflections Collected	890
Number of Reflections Observed	821 (with $I_{rel} > 2\sigma I_{rel}$)
Number of Parameters	75
$R = \Sigma \| \|F_o\| - \|F_c\| \| / \Sigma \|F_o\|$	0.036
$R_w = \Sigma w^{\frac{1}{2}} \| \|F_o\| - \|F_c\| \| / \Sigma w^{\frac{1}{2}} \|F_o\|$	0.037
Weighting Scheme, w	$(\sigma^2 F)^{-1}$

3.2.4 Solution and Refinement of the Structure

Systematic absences identified in the data set were consistent with the space groups C2, Cm and C2/m. A three-dimensional Patterson map was computed in order to locate the positions of the osmium atoms, by comparison with the Patterson grid constructed using the symmetry elements of the first chosen space group, C2/m. Successful refinement in C2/m vindicates its choice as the correct space group. C2/m has eight general positions. However, since there were found to be two molecules per unit cell, it was required for all osmium atoms to be on special positions. One osmium atom was located on the 2/m site having occupancy 1/4 at (0,0,0), denoted by Wykoff as a. Another osmium atom was located on the mirror, occupancy ½, denoted by Wykoff as c, which is symmetry related to the

third osmium of the molecule. A subsequent difference Fourier synthesis revealed that the chlorine, one carbon and one oxygen atom were lying on general positions; that two carbon and two oxygen atoms were lying on special positions, occupancy ½, denoted by Wykoff as g, and that one carbon and one oxygen atom were also lying on special positions, occupancy ½, and on the mirror, denoted by Wykoff as i. The positions indicated that it was necessary to input the coordinates of only half the molecule, the other half being generated by the symmetry elements of the space group. However, the symmetry elements would generate four chlorine atoms per molecule, which was known to be incorrect, since $Os_3(CO)_{12}Cl_2$ had been characterised. Careful analysis of the isotropic temperature factors of the C, O and Cl atoms, showed an incongruity in that the value for Cl was $U = 0.1Å^2$, considerably higher than the values obtained for C and O, which were close to each other and averaged $0.05\ Å^2$. In addition, peaks of residual electron density were apparent in the vicinity of the Cl atom. We concluded, therefore, that what was observed, was due to a CO, Cl disorder and that the stoichiometric requirements, together with symmetry demands, dictated a site occupancy of ½ for this C, O and the Cl. Anisotropic temperature factors for all atoms lying on special positions were fixed according to the literature.[151] Six least-squares refinements, in which all atoms except the three disordered

Table 3.2.2 Analyses of Variance for $Os_3(CO)_{12}Cl_2$

a) By parity groups

Group	GGG	UGG	GUG	UUG	GGU	UGU	GUU	UUU	ALL
N	217	0	0	188	217	0	0	199	821
V	609	0	0	553	470	0	0	538	545

b) As a function of sinθ

sinθ	0.00	-.19	-.24	-.28	-.31	-.36	-.37	-.39	-.41	-.43
N	86	84	93	87	64	49	85	94	67	
V	1225	586	459	410	334	355	273	383	303	

c) As a function of (F/F_{max})

(F/F_{max})	0.00	-.27	-.31	-.35	-.41	-.46	-.51	-.56	-.61	-.69	-1.00
N	89	86	76	95	76	74	86	87	72	80	
V	330	423	458	363	458	386	435	448	444	1236	

d) As a function of | Miller Index |

|h|	0	1	2	3	4	5	6	7	8	9	10	11	12	13	REST
N	40	89	97	66	93	78	61	65	67	33	51	39	18	17	7
V	730	712	733	770	427	372	549	390	379	342	402	337	245	346	278

|k|	0	1	2	3	4	5	6	7	8	9	10	11	12	13	REST
N	95	95	90	92	84	75	70	64	56	43	31	18	8	0	0
V	708	711	555	589	558	472	436	378	379	381	384	429	314	0	0

|l|	0	1	2	3	4	5	6	7	8	9	10	11	12	13	REST
N	61	114	115	111	94	96	78	65	48	30	9	0	0	0	0
V	721	714	812	493	433	338	326	340	287	256	236	0	0	0	0

N = Number of reflections in the group.
V = $100\ [M \sum (\omega |F_O - F_C|^2)/N \sum \omega]$ where M = total number of reflections.

atoms were treated anisotropically, with the latter three treated isotropically, yielded a conventional R factor of 0.036. A weighting scheme of $(\sigma^2 F)^{-1}$ was employed, which produced an R_w factor of 0.037. The analyses of variance - see table 3.2.2 - computed after the final cycle indicated satisfactory convergence. The final difference Fourier map was smooth except close to the terminal osmium atom where the largest residual peaks were 1.4 $e\text{Å}^{-3}$ attributable to imperfect modelling of the thermal anisotropy. Table 3.2.3 lists the final fractional atomic coordinates and temperature factors for all atoms. The observed and calculated structure factors for $Os_3(CO)_{12}Cl_2$ can be found in Appendix I.

Table 3.2.3 Fractional Atomic Coordinates (X 10^4) and Temperature Factors (Å^2 X 10^3) with Estimated Standard Deviations in Parentheses

Atoms	x/a	y/b	z/c	U_{iso}
Os_2	0	0	0	*
Os_1	2195(1)	0	3263(1)	*
Cl_1	1306(11)	-1671(11)	4237(15)	43(3)
C_1	1238(35)	-1328(36)	4111(51)	36(10)
O_1	719(21)	-1929(22)	4312(29)	50(6)
C_{11}	2812(11)	1305(13)	2290(17)	*
O_{11}	3200(10)	2075(10)	1775(15)	*
C_{12}	3590(19)	0	5457(28)	*
O_{12}	4485(19)	0	6908(28)	*
C_{21}	0	1901(21)	0	*
O_{21}	0	2913(13)	0	*
C_{22}	1037(18)	0	-1237(27)	*
O_{22}	1631(15)	0	-1894(23)	*

continued/...

Table 3.2.3 continued ...

* Anisotropic Temperature Factors

Atoms	U_{11}	U_{22}	U_{33}	U_{23}	U_{13}	U_{12}
Os_2	22(1)	20(1)	16(1)	0	5(1)	0
Os_1	21(1)	23(1)	17(1)	0	5(1)	0
C_{11}	29(7)	33(8)	29(8)	-3(7)	7(6)	0(6)
O_{11}	57(7)	48(7)	54(8)	14(6)	28(6)	-16(6)
C_{12}	30(11)	59(15)	23(12)	0	-5(10)	0
O_{12}	83(17)	136(22)	60(16)	0	-42(14)	0
C_{21}	44(12)	45(14)	39(13)	0	29(11)	0
O_{21}	91(13)	17(7)	67(12)	0	46(10)	0
C_{22}	34(11)	31(11)	30(12)	0	9(10)	0
O_{22}	53(10)	52(10)	62(12)	0	43(10)	0

3.2.5 Description of the Structure and Discussion

The molecular structure of $Os_3(CO)_{12}Cl_2$ consists of a linear chain of three osmium atoms bonded to each other by osmium-osmium bonds. Taking cognisance of the chlorine/carbonyl disorder, there are effectively one terminal equatorial chlorine and four terminal carbonyl ligands bonded to each terminal osmium atom and four terminal carbonyl ligands bonded to the central osmium atom - see figure 3.1. The spine of the molecule comprises the almost linear sequence O-C-Os-Os-Os-C-O. The equatorial ligands on the terminal osmium atoms are staggered with respect to the four equatorial carbonyl ligands on the central osmium atom. This feature is illustrated in figure 3.2.

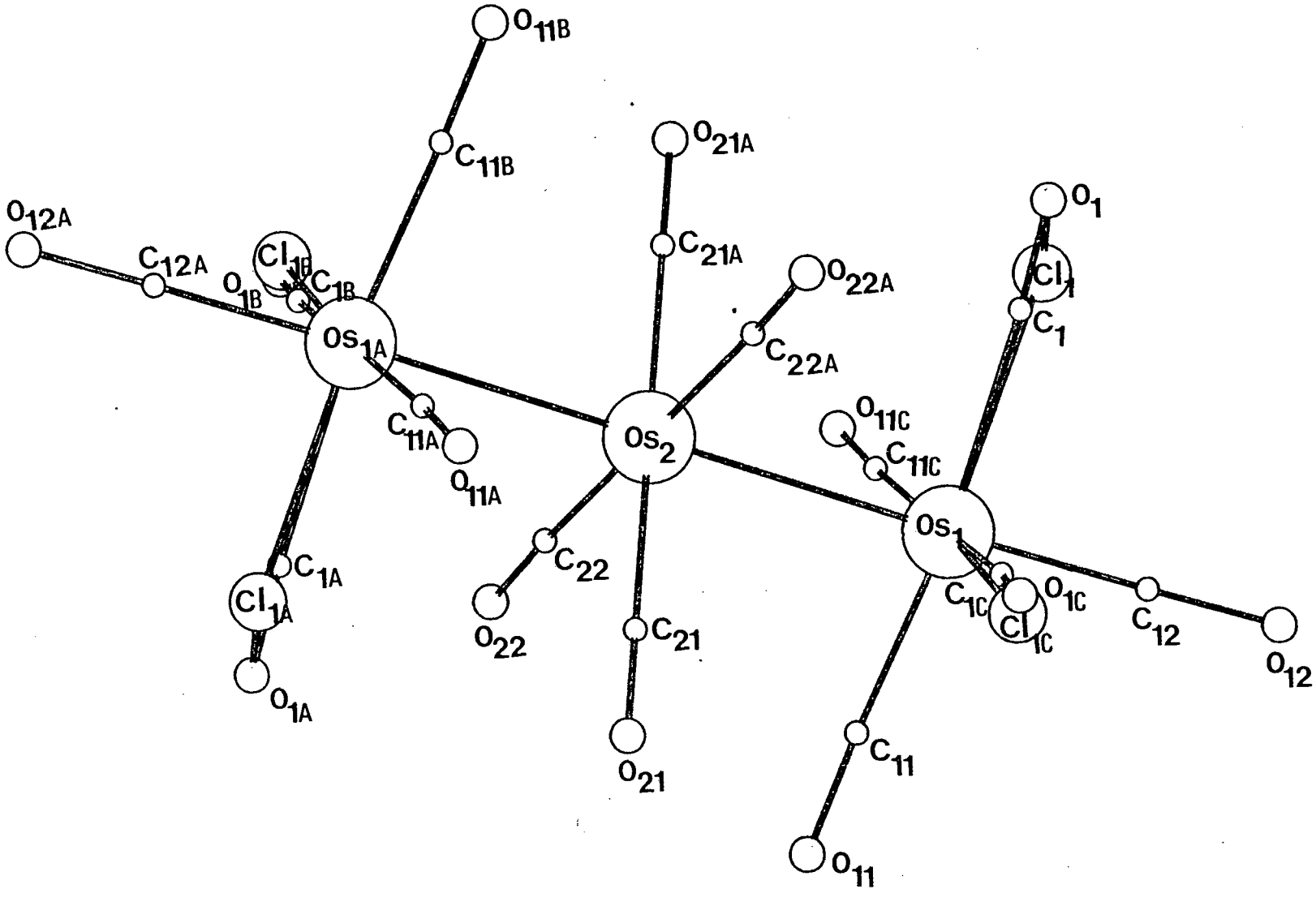

Figure 3.1 The molecular structure of $Os_3(CO)_{12}Cl_2$

symmetry-generated atoms denoted A, B and C

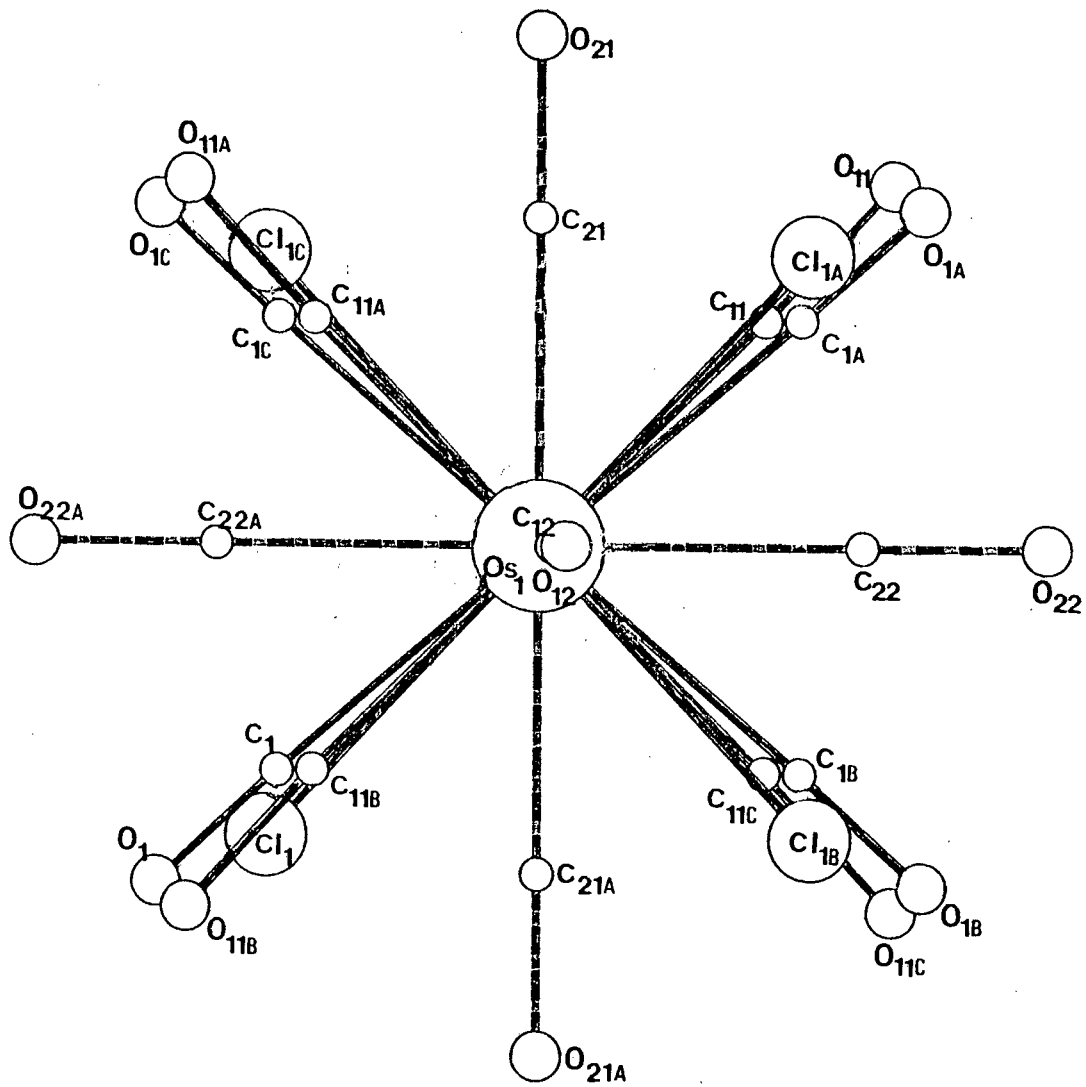

Figure 3.2 A view of $Os_3(CO)_{12}Cl_2$ along the molecular axis
symmetry-generated atoms denoted A, B and C

Owing to the problem of this disorder, it is not possible to determine the real orientation of the chloride ligands to each other, although it is expected that by analogy with $Os_3(CO)_{12}I_2$ that the chloride ligands would occupy positions as far away from each other as possible. Each osmium atom in the chain obeys the effective atomic number rule and displays pseudo-octahedral geometry. Tables 3.2.4 and 3.2.5 list the bond lengths and bond angles respectively for $Os_3(CO)_{12}Cl_2$.

The molecule $Os_3(CO)_{12}Cl_2$ may be isostructural with the complexes, $Os_3(CO)_{12}X_2$ (X = I[40] or Me[149]) but due to the crystal disorder, we cannot be certain. In the complexes, $Os_3(CO)_{12}X_2$ (X = Cl, I,[40] Me[149] or $SiCl_3$[38]), there is a linear triosmium chain and the equatorial ligands on the terminal osmium atom are staggered with respect to those on the central osmium atom as expected for molecules of this type, e.g. $[Mn_3(CO)_{14}]^-$[41] or dinuclear complexes of the type, $M_2(CO)_{10}$ (M = Mn,[152] Tc[153] or Re[152]). This has been attributed to bonding interactions between a metal atom and the equatorial carbonyl groups on the adjacent metal atom which lead these carbonyl groups to seek regions of high d-electron density.[41] In polynuclear and dinuclear complexes this would be the regions between the metal atoms. By adopting a staggered conformation, the molecule maximises the effect of such interactions for, otherwise, in an

eclipsed conformation, steric repulsions between opposite sets of equatorial carbonyl groups would prevent too much out-of-plane bending.[41] A staggered conformation is also expected to minimise repulsions between equatorial ligands.[154] In the $Os_3(CO)_{12}X_2$ (X = Cl, I[40] or Me[149]) complexes, the halogen ligands occupy equatorial sites on the terminal osmium atoms, i.e. structure 3, whereas in $Os_3(CO)_{12}(SiCl_3)_2$[38] the $SiCl_3$ groups occupy axial sites, i.e. structure 4. Most compounds of the type $M(CO)_4X_2$ (M = Fe, Ru, Os) exist as the more thermodynamically stable cis isomer, since this avoids as far as possible the strong π-acceptor carbonyl ligands competing for the same π-electron density on the central metal. In the complexes $Os_3(CO)_{12}X_2$ (X = Cl, I,[40] Me[149] or $SiCl_3$[38]), since the X group, when bonded to osmium, has π-acceptor properties weaker than CO, then on electronic grounds, a position cis to the osmium-osmium bond would be preferred, thus minimising the number of CO groups trans to each other. However, if the X group, when bonded to osmium has π-acceptor properties comparable to CO, or if X is very large, then neither geometry shown in structures 3 or 4, would be preferred on electronic grounds. In such a situation, steric factors could dictate the geometry. Cl, I and Me are poorer π-acceptors than CO. Therefore, a structure for $Os_3(CO)_{12}X_2$ with X cis to the osmium-osmium bond, would be favoured on electronic grounds. However, the

$SiCl_3$ group has been considered by some workers[38] to have π-acceptor properties comparable to CO and hence the steric factors would dictate the geometry adopted. Hence, the $SiCl_3$ groups might be expected to be situated **trans** to the osmium-osmium bond, since this configuration minimises the steric interactions between the bulkier trichlorosilyl substituents and the equatorial carbonyl groups on the central osmium atom. Indeed, workers have constructed models which show that there is a close approach of the chlorine atoms of the $SiCl_3$ ligand to the carbonyls on the central osmium atom if the silyl moieties are placed **cis** to the osmium-osmium bond.[38] The X-Ray crystal structures of the complexes $Os_3(CO)_{12}X_2$ (X = Cl, I,[40] Me[149] or $SiCl_3$[38]), can therefore be rationalised on either electronic or steric grounds. In the complexes $Os_3(CO)_{12}X_2$ (X = Cl, I,[40] or Me[149]) the halogen ligands might be expected to be situated **cis** to the osmium-osmium chain whereas in $Os_3(CO)_{12}(SiCl_3)_2$ the $SiCl_3$ groups might be expected to be situated in a **trans** position to the osmium-osmium bond, as was indeed found.

The osmium-osmium distance in $Os_3(CO)_{12}Cl_2$ of 2.893(1) Å agrees with that found for $Os_2(CO)_8Cl_2$ - section 3.4 - of 2.897(1) Å and for $Os_3(CO)_{12}$[39] of 2.877(13) Å, **i.e.** a normal osmium-osmium single bond distance. The osmium-osmium distance of $Os_3(CO)_{12}Cl_2$ is significantly shorter than that found for $Os_3(CO)_{12}(SiCl_3)_2$[38] of 2.912(1) Å, for

$Os_3(CO)_{12}I_2$[40] of 2.935(2) Å and for $Os_2(CO)_8I_2$ - section 3.5 - of 2.947(3) Å. It was observed in the structure of $Os_3(CO)_{12}(SiCl_3)_2$,[38] that some multiple bonding occurred between the osmium and silicon atoms, i.e. the Os-Si bond length of 2.377(3) Å is more than 0.2 Å shorter than a normal Os-Si single bond. This could result in a weakening of the osmium-osmium bonds and thus a lengthening from a normal osmium-osmium distance. Also, the $SiCl_3$ group is regarded as a strong σ-withdrawing ligand.[155] This would also have an effect on the osmium-osmium bond length in $Os_3(CO)_{12}(SiCl_3)_2$. The lengthening of the osmium-osmium distances in $Os_3(CO)_{12}I_2$[40] and $Os_2(CO)_8I_2$ - section 3.5 - from a normal osmium-osmium single bond distance may be attributed to a steric effect of the bulky iodide ligands in equatorial postions interacting with the equatorial carbonyl groups on the adjacent metal atom or to the fact that I^- is a better π-acceptor than Cl^-. The latter proposal could result in more osmium d-electron density being involved in the bonding with I^- than with Cl^-, resulting in the weakening and thus a lengthening of the osmium-osmium bond in the complexes, $Os_3(CO)_{12}I_2$[40] and $Os_2(CO)_8I_2$ -section 3.5.

The terminal osmium-chlorine distance in $Os_3(CO)_{12}Cl_2$ of 2.43(1) Å agrees with the two osmium-chlorine distances of 2.452(6) and 2.442(6) Å, found for $Os_2(CO)_8Cl_2$ - section

3.4. In both molecules, osmium is present in a +I oxidation state.

The osmium-carbon distances for $Os_3(CO)_{12}Cl_2$ were found to be in the range 1.90(2)-2.16(4) Å, while the carbon-oxygen distances were found to be in the range 0.97(4)-1.24(3) Å. The osmium-carbon and carbon-oxygen distances for $Os_3(CO)_{12}I_2$[40] were found to be in the ranges 1.91(3)-1.97(3) and 1.12(3)-1.15(3) Å, respectively. The wider ranges of respective distances for $Os_3(CO)_{12}Cl_2$ compared with $Os_3(CO)_{12}I_2$ can be attributed to the chlorine/carbonyl disorder, since the long osmium-carbon (2.16(4) Å) and short carbon-oxygen (0.97(4) Å) distances were for the disordered carbonyl groups. There are three types of Os-C bonds in $Os_3(CO)_{12}Cl_2$ and these are Os-C (i) **trans** to the osmium-osmium bond; (ii) **trans** to the chloride ligands, and (iii) **trans** to a carbonyl ligand. Due to the crystal disorder, it is not possible to ascertain the Os-C distance for carbonyl ligands **trans** to each other on the terminal osmium atoms. However, the Os-C distances for carbonyl ligands which are **trans** to each other on the central osmium atom are the longest Os-C distances found for $Os_3(CO)_{12}Cl_2$, these being 2.02(2) and 2.00(2) Å, respectively, with a mean of 2.01(2) Å. The Os-C distance for the osmium-carbon bond **trans** to the osmium-osmium bond, i.e. for the axial carbonyl ligand, is the shortest at 1.90(2) Å, while that for the

equatorial osmium-carbon bond, i.e. Os_1-C_{11}, is 1.95(1) Å. This sort of variation in osmium-carbon and carbon-oxygen distances was also observed in $Os_2(CO)_8Cl_2$ - section 3.4, $Os_2(CO)_8I_2$ - section 3.5, and [HOsRe(CO)$_8$Br]PPN - section 3.6, and can be explained in terms of availability and competition for osmium d-electrons for back-bonding.

In $Os_3(CO)_{12}I_2$,[40] the osmium-carbon distances did not differ significantly from one another, but any real differences may have been masked by large standard deviations. The shortest carbon-oxygen distance, i.e. C_1-O_1 in $Os_3(CO)_{12}Cl_2$ of 0.97(4) Å was found to correspond to the longest osmium-carbon distance, i.e. Os_1-C_1, of 2.16(4) Å, while the longest carbon-oxygen distance of 1.24(3) Å was found to correspond to the shortest osmium-carbon distance, i.e. Os_1-C_{12} of 1.90(2) Å. This is as expected because the more osmium d-electron density that is involved in back-bonding into the π^* orbitals of carbon monoxide, the more the C-O bond order is reduced, and vice versa.

In $Os_3(CO)_{12}Cl_2$, all Os_2-Os_1-C(equatorial) angles were found to be acute, ranging from 85.8(4)-87.0(10) Å. Similarly, in $Os_3(CO)_{12}I_2$,[40] the respective angles ranged from 85.1(7)-89.0(6) Å. This bending of equatorial carbonyl groups towards the molecular centre is a well-known phenomenon, and has been previously noticed in $[Mn_3(CO)_{14}]^-$,[41]

Table 3.2.4 Bond Lengths (Å) for $Os_3(CO)_{12}Cl_2$ with the Estimated Standard Deviations in Parentheses

Os_1-Os_2	2.893(1)
Os_1-Cl_1	2.43(1)
Os_1-C_1	2.16(4)
Os_1-C_{11}	1.95(1)
Os_1-C_{12}	1.90(2)
Os_2-C_{21}	2.02(2)
C_1-O_1	0.97(4)
$C_{11}-O_{11}$	1.14(2)
$C_{12}-O_{12}$	1.24(3)
$C_{21}-O_{21}$	1.08(2)
$C_{22}-O_{22}$	1.11(3)
Os_2-C_{22}	2.00(2)

Table 3.2.5 Bond Angles (°) for $Os_3(CO)_{12}Cl_2$ with the Estimated Standard Deviations in Parentheses

$Os_1-Os_2-C_{21}$	90.0
$Os_1-Os_2-C_{22}$	91.1(6)
$C_{22}-Os_2-C_{21}$	90.0
$Os_2-Os_1-Cl_1$	89.7(3)
$Os_2-Os_1-C_1$	87.0(10)
$Os_2-Os_1-C_{11}$	85.8(4)
$Cl_1-Os_1-C_{11}$	175.3(5)
$C_1-Os_1-C_{11}$	171.4(11)
$Os_2-Os_1-C_{12}$	177.4(7)
$Cl_1-Os_1-C_{12}$	88.5(6)
$C_1-Os_1-C_{12}$	91.0(12)
$C_{11}-Os_1-C_{12}$	96.0(6)
$Cl_1-Os_1-Cl_{1c}$	94.0(5)
$Os_1-C_1-O_1$	171.4(37)
$C_1-Os_1-C_{1c}$	81.4(21)
$Os_1-C_{11}-O_{11}$	177.8(12)
$C_{11}-Os_1-C_{11c}$	90.7(8)
$Os_1-C_{12}-O_{12}$	178.6(24)
$Os_2-C_{21}-O_{21}$	180.0
$C_{21}-Os_2-C_{21A}$	180.0
$Os_2-C_{22}-O_{22}$	178.7(19)
$C_{22}-Os_2-C_{22A}$	180.0

$Mn_2Fe(CO)_{14}$[156] as well as in many dinuclear complexes - see section 3.4. This bending has been attributed to bonding interactions between the filled d-orbitals on the central metal atom and the π^* orbitals of the equatorial carbonyl groups on the terminal metal atoms.[41] The Os-C-O bonds in $Os_3(CO)_{12}Cl_2$ were found to be almost linear, as in the related complexes $Os_3(CO)_{12}X_2$ (X = I,[40] Me[149] or $SiCl_3$[38]) and is generally found in metal complexes which contain a terminal carbonyl group.[157]

3.2.6 Conclusion

The molecular structure of $Os_3(CO)_{12}Cl_2$ has been determined by X-Ray crystallography and the solution and least-squares refinements led to a conventional weighted R factor of 0.038. This study has confirmed that $Os_3(CO)_{12}Cl_2$ adopts the structure with a linear triosmium chain and with the Cl ligands occupying equatorial sites on the terminal osmium atoms. Both features were also found for the complexes $Os_3(CO)_{12}X_2$ (X = I[40] or Me[149]).

3.3 The X-Ray Crystal Structure of Di-μ-iodohexacarbonyldiosmium(I), $Os_2(CO)_6I_2$

3.3.1 Experimental

$Os_2(CO)_6I_2$ was obtained by refluxing $Os_2(CO)_8I_2$ in n-heptane for forty minutes. Single crystals of $Os_2(CO)_6I_2$ were obtained by sublimation (60°C/0.01 mm Hg) of the compound and were identified by IR and mass spectral and melting point data. These data - see Experimental Section in Chapter 6 - were in agreement with the literature.[115] The crystals obtained were slightly large but attempts to cut them to more suitable dimensions were unsuccessful. Hence the crystal selected for the determination was the best available.

3.3.2 Preliminary X-Ray Analysis

Preliminary oscillation, zero and upper-layer Weissenberg photography using CuK_α radiation (λ = 1.5418 Å) indicated that the compound had crystallised in either of the two monoclinic space groups $P2_1$ or $P2_1/m$.

3.3.3 Intensity Data Collection

A suitable single crystal of $Os_2(CO)_6I_2$ was sent to the National Physical Research Laboratory (NPRL) at the Council for Scientific and Industrial Research (CSIR), Pretoria, for a diffractometer data collection. The relative intensities of the reflections were measured on a Philips PW 1100 computer-controlled four-circle diffractometer operating in the ω-2θ scan mode. Graphite-monochromated MoK_α, λ= 0.7107 Å, X-radiation was generated by a Philips 1140 generator operating at 20 mA and 50 kV. The data collection was carried out at room temperature. Lorentz-polarization corrections were applied to the data immediately after data collection. No absorption correction was applied.

The intensities of the reflections revealed systematic absences consistent with the space group being either $P2_1$ or $P2_1/m$. 1170 reflections were collected within the range $6° < 2\theta < 52°$ and of these 1048 reflections remained with $I_{rel} > 2\sigma I_{rel}$. The intensities of three reference reflections were examined after every 68 measured reflections to monitor the stability of the crystal, and these yielded a stability of 0.81%.

Accurate cell dimensions were obtained by least-squares analysis from the settings of 25 high order reflections

measured on the four-circle diffractometer. Crystal data and experimental details of the data collection and final refinement are listed in Table 3.3.1 below.

Table 3.3.1 Crystal Data, Data Collection and Refinement Parameters for $Os_2(CO)_6I_2$

Crystal Data	
Molecular Formula	$C_6I_2O_6Os_2$
Molecular Weight/g mol^{-1}	802.27
Space Group	$P2_1/m$
a/Å	6.453(3)
b/Å	14.017(7)
c/Å	7.328(4)
β/°	91.03(2)
V/$Å^3$	661
Z	2
$D_C Mgm^{-3}$	4.03
$\mu(MoK_\alpha)mm^{-1}$	22.85
F(000)	688
Radiation used, MoK. α, Å	0.7107
Data Collection	
Crystal Dimensions/mm	0.80 x 0.40 x 0.50
Scan Mode	ω - 2θ
Scan Width, /°θ	1.4
Range Scanned, θ/°	6-52
Stability of Standard Reflections/%	0.81
Scan Speed, /·θs^{-1}	

continued/...

Table 3.3.1 continued ...

Refinement	
Number of Reflections Collected	1170
Number of Reflections Observed	1048 ($I_{rel} > 2\sigma I_{rel}$)
Number of Parameters	46
$R = \Sigma \| \|F_o\| - \|F_c\| \| / \Sigma \|F_o\|$	0.079
$R_w = \Sigma w^{\frac{1}{2}} \| \|F_o\| - \|F_c\| \| / \Sigma w^{\frac{1}{2}} \|F_o\|$	0.086
Weighting Scheme, w	$(\sigma^2 F + 2 \times 10^{-3} F^2)^{-1}$

3.3.4 Solution and Refinment of the Structure

An examination of the E-statistics on data reduction, indicated a centrosymmetric space group; hence $P2_1/m$ was chosen and the structure was subsequently solved and refined in this space group. A Patterson map revealed the osmium atom lying on a general position and subsequent weighted difference Fourier syntheses revealed two independent iodines on special positions (Wykoff notation e) and the carbonyls on positions of general symmetry. The final full-matrix least-squares refinement was carried out with the osmium and iodine atoms treated anisotropically and the carbon and oxygen atoms, isotropically. The weighting scheme was chosen to give the smallest systematic variation of $w\Delta^2$ with the magnitude of F_o, as shown by analyses of variance - see table 3.3.2 - computed after the final

Table 3.3.2 Analyses of Variance for $Os_2(CO)_6I_2$

a) By parity groups

Group	GGG	UGG	GUG	UUG	GGU	UGU	GUU	UUU	ALL
N	146	127	116	125	129	150	126	129	1048
V	560	547	522	562	561	673	712	611	599

b) As a function of sin0

sin0	0.00	-.19	-.24	-.28	-.31	-.36	-.37	-.39	-.42	-.44
N	111	110	112	123	70	107	110	113	70	
V	714	561	548	594	641	563	553	635	561	

c) As a function of (F/F_{max})

(F/F_{max})	0.00	-.28	-.33	-.39	-.43	-.48	-.53	-.58	-.64	-.73	-1.00
N	107	114	113	107	106	99	94	103	106	99	
V	604	622	568	667	689	479	512	547	679	560	

d) As a function of | Miller Index |

| h |	0	1	2	3	4	5	6	7	8	9	10	11	12	13	REST
N	97	203	186	166	145	114	89	48	0	0	0	0	0	0	0
V	498	530	684	782	587	490	482	402	0	0	0	0	0	0	0

| k |	0	1	2	3	4	5	6	7	8	9	10	11	12	13	REST
N	90	91	84	77	85	89	84	70	58	63	61	51	44	29	72
V	475	574	506	433	478	535	577	629	568	640	764	813	753	729	691

| l |	0	1	2	3	4	5	6	7	8	9	10	11	12	13	REST
N	95	189	184	180	160	121	73	44	0	0	0	0	0	0	0
V	644	888	563	412	438	508	600	473	0	0	0	0	0	0	0

N = Number of reflections in the group.
V = 100 [M Σ (ω | F_O-F_C | ^{2})/N$\Sigma\omega$] where M = total number of reflections.

cycles. In the final cycle, the mean e.s.d. in the atomic parameters was more than 100 times the average parameter shift, while the final difference map was smooth, except close to the osmium atom where the largest residual peaks were 4 $e\text{Å}^{-3}$. Table 3.3.3 lists the final fractional atomic coordinates and temperature factors for all the atoms. The observed and calculated structure factors for $Os_2(CO)_6I_2$ can be found in Appendix II.

Table 3.3.3 Fractional Atomic Coordinates (x 10^4) and Temperature Factors (Å x 10^3) with Estimated Standard Deviations in Parentheses

Atoms	x/a	Y/b	z/c	U_{iso}
Os	2478(1)	1529(1)	2824(1)	*
I_1	5617(3)	2500	4605(3)	*
I_2	3892(4)	2500	-121(3)	*
C_1	1207(44)	1282(20)	5039(44)	37(6)
O_1	413(38)	1090(18)	6362(39)	60(6)
C_2	70(46)	1195(21)	1534(46)	41(7)
O_2	-1413(36)	974(17)	716(35)	57(6)
C_3	3894(41)	302(20)	2526(39)	35(6)
O_3	4648(35)	-402(17)	2465(34)	58(6)

* Anisotropic Temperature Factors

Atoms	U_{11}	U_{22}	U_{33}	U_{23}	U_{13}	U_{12}
Os	22(1)	27(1)	7(1)	1(1)	-2(1)	-1(1)
I_1	20(1)	44(1)	12(1)	0	-7(1)	0
I_2	44(1)	45(2)	3(1)	0	5(1)	0

3.3.5 Description of the Structure and Discussion

Figures 3.3. and 3.4 show perspective views of the molecule, $Os_2(CO)_6I_2$. Figure 3.3 also shows bond lengths and atomic labelling. Tables 3.3.4 and 3.3.5 list bond lengths and bond angles, respectively, for $Os_2(CO)_6I_2$.

The molecular structure of $Os_2(CO)_6I_2$ shows the two equivalent osmium atoms bonded together by an osmium-osmium bond, which is bridged by two iodine atoms, and with three terminal carbonyl ligands on each osmium atom - see figures 3.3 and 3.4. In this structure, which formally has a single bond between the two osmium atoms, the metal atoms obey the 18-electron rule. This type of structure had previously been proposed for the complexes, $Os_2(CO)_6I_2$ (X = Cl, Br or I), on the basis of IR and mass spectral data,[115,126] and has been found for a related ruthenium complex, $Ru_2Cl_2(CO)_4(P(t\text{-}Bu)_2(p\text{-}tolyl)_2$.[158] The geometry about the osmium atoms is distorted octahedral and is similar to that found for $Co_2(CO)_8$ in the solid state[159] and for $Fe_2(CO)_6X_2$ (X = SMe, S, NH_2 or NMe).[160] $Os_2(CO)_6I_2$ can be described as having a butterfly structure with iodine atoms at the apices of the wings - see figure 3.4.

The osmium-osmium distance of 2.722(2) Å is shorter than that found for $Os_3(CO)_{12}$[39] of 2.887(3) Å, for $Os_3(CO)_{12}Cl_2$

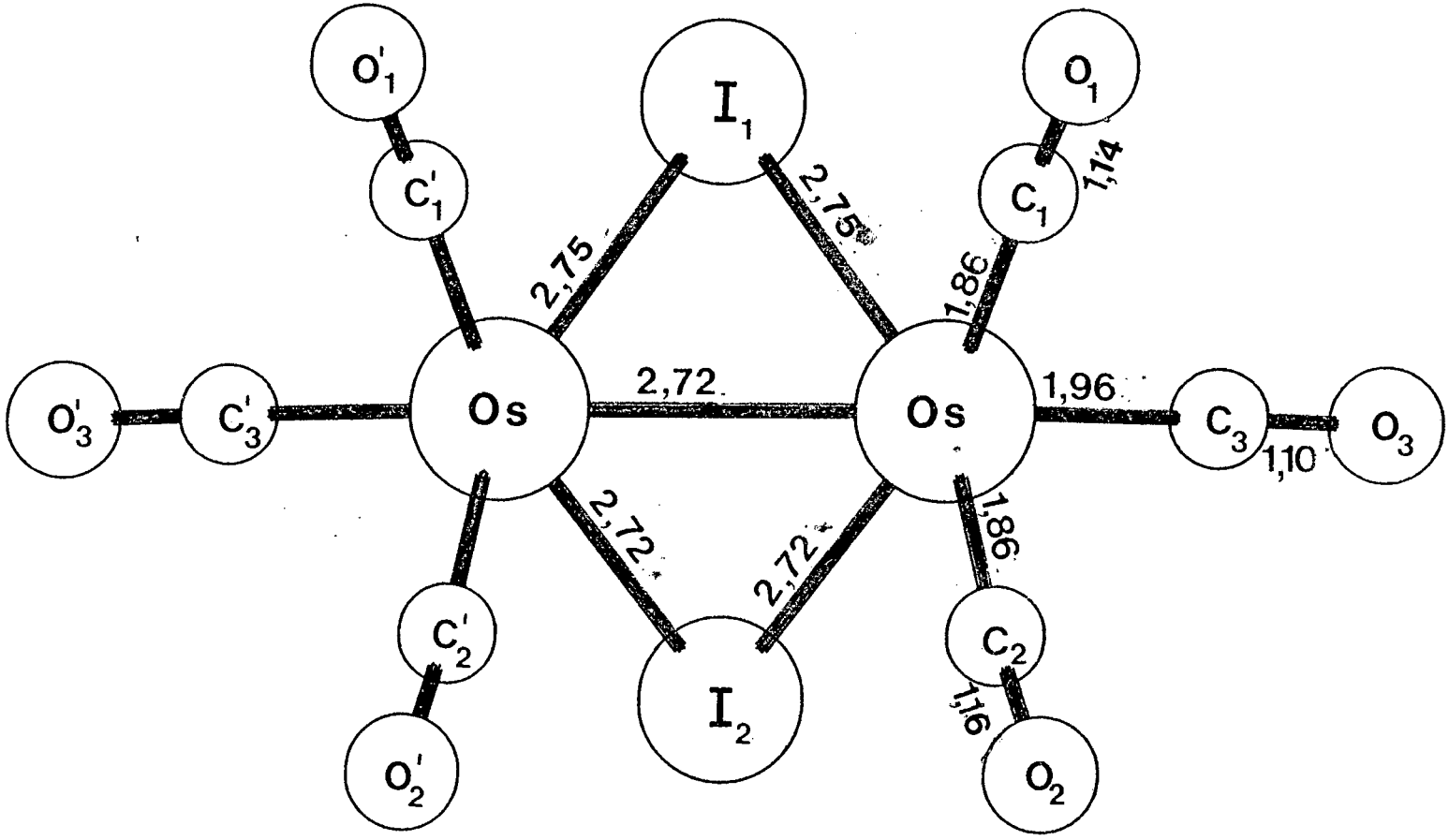

Figure 3.3 [100] projection of $Os_2(CO)_6I_2$ depicting atomic nomenclature and bond lengths (Å).

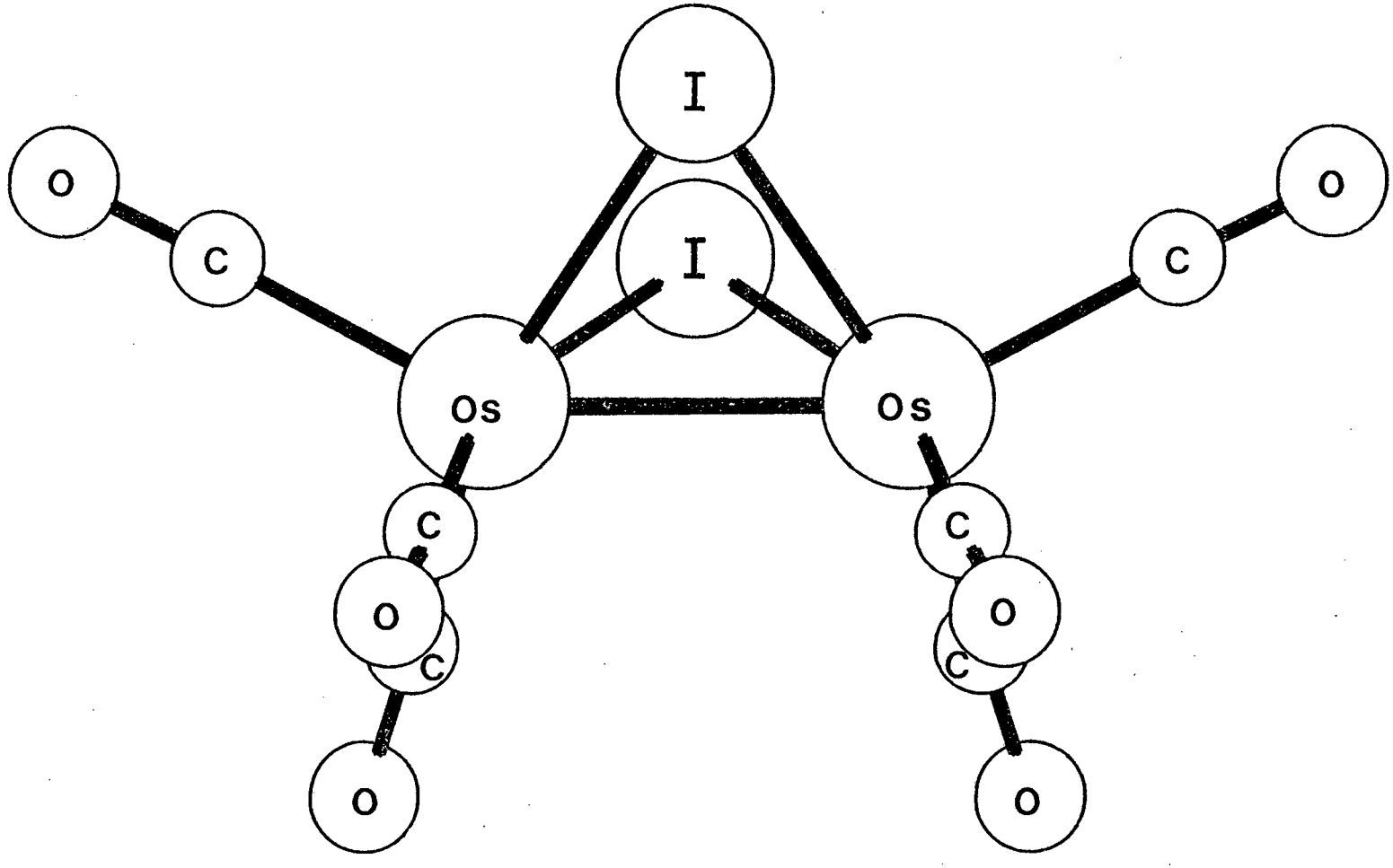

Figure 3.4 [001] projection of the molecule $Os_2(CO)_6I_2$

of 2.893(1) Å - section 3.2 - for $Os_3(CO)_{12}I_2$[40] of 2.935(2) Å, for $Os_2(CO)_8Cl_2$ of 2.947(3) Å - section 3.4 - and for $Os_2(CO)_8I_2$ of 2.897(1) Å - section 3.5. It is very slightly longer than that found in bulk osmium metal (2.70 Å)[161] but similar to that in $Os_2(CO)_6(CH_3COO)_2$[162] (2.731 Å) - figure 3.5. The latter molecule also has two ligands bridging the osmium-osmium bond.

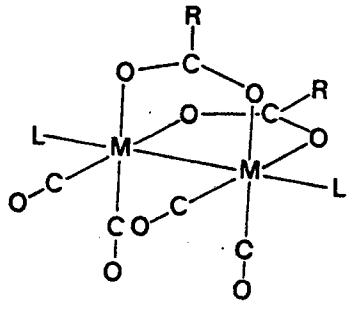

Figure 3.5 Diagrammatic representation of $Os_2(CO)_6(CH_3COO)_2$ where L = CO; R = CH_3.

The X-Ray crystal structure of $Os_2(CO)_6C_6H_8$[163] - see figure 3.6 - was determined and the osmium-osmium distance was found to be 2.74 Å which is close to that found for $Os_2(CO)_6I_2$ and for $Os_2(CO)_6(CH_3COO)_2$.[162] A possible explanation for this similarity in the osmium-osmium distance is that in $Os_2(CO)_6C_6H_8$,[163] there is a 2,3-dimethylbuta-1,3-diene ligand which exhibits bridging behaviour.

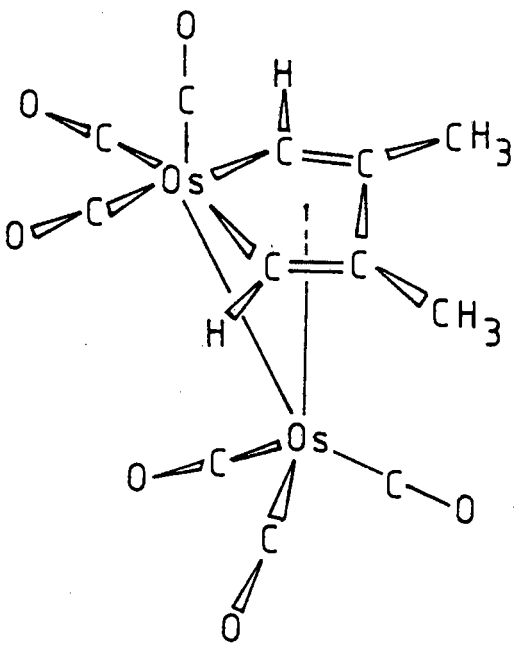

Figure 3.6 The structure of the complex, $Os_2(CO)_6C_6H_8$

In $Os_3(CO)_{10}H_2$,[164] which formally contains an osmium-osmium double bond bridged by hydride ligands, the osmium-osmium distance was found to be 2.681 Å. Thus, the osmium-osmium distances in $Os_2(CO)_6I_2$, $Os_2(CO)_6(CH_3COO)_2$[162] and $Os_2(CO)_6C_6H_8$[163] are apparently closer to a double distance than a single bond distance. The results suggest that these short osmium-osmium bonds result from the presence of bridging ligands.

The bridging osmium-iodine distances in $Os_2(CO)_6I_2$ are 2.722(2) and 2.746(2) Å, respectively, (mean 2.734 Å) which are shorter than the terminal osmium-iodine distance

of 2.767(3) Å in both $Os_3(CO)_{12}I_2$[40] and $Os_2(CO)_8I_2$ - section 3.5 - respectively. The distances in $Os_2(CO)_6I_2$ are similar to that found for $[Os_4(CO)_{12}H_2I]PPN$[165] of 2.732(2) Å where the iodide ligand was found to be terminally bonded to an osmium atom. This is somewhat surprising since in similar compounds, the terminal Os-I distance might be expected to be shorter than the bridging Os-I distance. Since, as has been found in some cases, terminal M-X bonds are usually shorter than bridging M-X bonds, for example, in $[OsCl_2(C_{10}H_{14})]_2$[166] - see figure 3.11 - and $Ru_2(CO)_6Br_4$.[117] However, the average Os-I distance of 2.734(2) Å in the present structure is not unreasonable for a bridging osmium-iodine distance, since for the compounds $[Os_{10}C(CO)_{24}I]^-$ and $Os_{10}C(CO)_{24}I_2$,[167] the bridging Os-I distances range from 2.717 - 2.746 Å. However, in these decaosmium complexes, there is no osmium-osmium bond connecting the osmium atoms bridged by the iodine atoms. In the structure of $Os_8(CO)_{22}HI$,[168] the two osmium-iodine distances were found to be 2.753(2) and 2.736(2) Å, respectively. In this latter molecule, the iodide ligand bridges two osmium atoms, which are at the apices of an osmium "butterfly" unit and which are not bonded to each other.

The osmium-carbon distances in $Os_2(CO)_6I_2$ range from 1.86(3)-1.96(3) Å. Similar variation is found in the

osmium-carbon distances in $Os_2(CO)_6(CH_3COO)_2$,[162] and in iron-carbon distances in $Fe_2(CO)_6X_2$ (X = SMe, S, NH_2 or NMe).[160] The carbon-oxygen distances in $Os_2(CO)_6I_2$ are in the range 1.10(3)-1.16(4) Å. These distances can be compared with the respective ranges found for $Os_2(CO)_8I_2$ of 1.05(5)-1.18(4) Å, - section 3.5 - and for $Os_3(CO)_{12}I_2$[40] of 1.12(3)-1.15(3) Å. All Os-C-O bond angles are close to linear, as was found for $Os_2(CO)_8I_2$ - section 3.5 - ranging from 177(3)-179(3)°.

Table 3.3.4 Bond Lengths (Å) for $Os_2(CO)_6I_2$ with the Estimated Standard Deviations in Parentheses

Os_1-Os_1'	2.722(2)
Os_1-I_1	2.746(2)
Os_1-I_2	2.722(2)
Os_1-C_1	1.86(3)
Os_1-C_2	1.86(3)
Os_1-C_3	1.96(3)
C_1-O_1	1.14(4)
C_2-O_2	1.16(4)
C_3-O_3	1.10(3)

Table 3.3.5 Bond Angles (°) for $Os_2(CO)_6I_2$ with the Estimated Standard Deviations in Parentheses

I_2-Os_1-I_1	82.9(1)
C_1-Os_1-I_1	90.5(9)
C_1-Os_1-I_2	160.4(9)
C_2-Os_1-I_1	164.8(9)
C_2-Os_1-I_2	91(1)
C_2-Os_1-C_1	91(1)
C_3-Os_1-I_1	98.5(8)
C_3-Os_1-I_2	100.8(8)
C_3-Os_1-C_1	98(1)
C_3-Os_1-C_2	96(1)
Os_1-I_1-Os_1'	59.4(1)
Os_1-I_2-Os_1'	60.0(1)
O_1-C_1-Os_1	177(3)
O_2-C_2-Os_1	179(3)
O_3-C_3-Os_1	176(3)

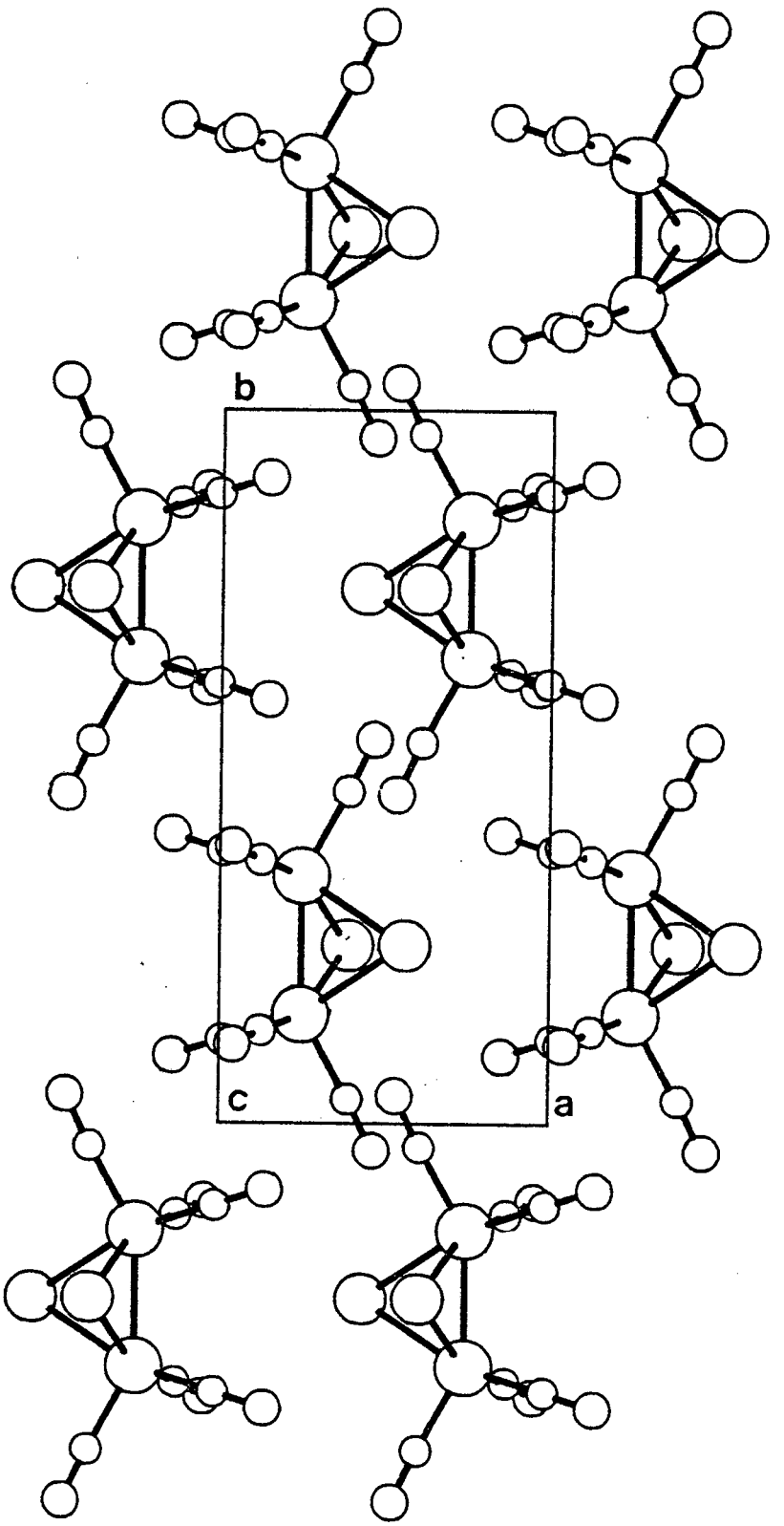

Figure 3.7 [001] projection of the molecular packing in the unit cell of $Os_2(CO)_6I_2$.

3.3.6 Molecular Packing

The [001] projection of the molecular packing in the unit cell is shown in figure 3.6. The compound packs in a zig-zag fashion, with alternate molecules pointing in the same direction. The Os-Os non-bonded distance is 6.251(2) Å. Therefore uni-dimensional conductor properties are unlikely for $Os_2(CO)_6I_2$.

3.3.7 Conclusion

The solution of the structure and least-squares refinement of the structural parameters led to a conventional R factor of 0.079. The modelling of this structure, as evidenced by a comparison of the standard deviations of the molecular parameters and the R value, is not as good as that of $Os_3(CO)_{12}Cl_2$ (R_w = 0.037) - section 3.2, $Os_2(CO)_8Cl_2$ (R_w = 0.038) - section 3.4, $Os_2(CO)_8I_2$ (R_w = 0.0424) - section 3.5, or [HOsRe(CO)$_8$Br]PPN (R_w = 0.0391) - section 3.6. We attribute this to the fact that no absorption correction was carried out. The problem was exacerbated by the somewhat large size of the crystal employed for the data collection.

This X-Ray determination has confirmed the structure previously proposed[115] on the basis of IR and other data.

The osmium-osmium distance of 2.722(2) Å is short compared with a normal single bond (e.g. in $Os_3(CO)_{12}$ of 2.88 Å) but is close to that found in bulk osmium metal (2.70 Å).[161] However, in $Os_2(CO)_6I_2$, the two osmium atoms are joined by what is formally considered to be a single osmium-osmium bond bridged by two iodide ligands. Similarly, the presence of bridging ligands in $Os_2(CO)_6(CH_3COO)_2$[162] and $Os_2(CO)_6C_6H_8$[163] also results in the shortening of the osmium-osmium bond. A further interesting feature in the structure of $Os_2(CO)_6I_2$ is the short mean bridging osmium-iodine distance of 2.734 Å.

3.4 The X-Ray Crystal Structure of Dichlorooctacarbonyldiosmium(I), $Os_2(CO)_8Cl_2$

3.4.1 Introduction

There are relatively few simple dinuclear complexes where a metal-metal single bond is unsupported by bridging ligands and particularly few known carbonyl halides with this type of structural arrangement. The main class of dinuclear compounds with a single metal-metal bond unsupported by bridging ligands is the Group VII complexes of the type $M_2(CO)_{10}$ (M = Mn,[152] Tc[153] or Re[152]) and their substitution products.[137] We have determined the structures of the complexes $Os_2(CO)_8X_2$ (X = Cl, I) - sections 3.4 and 3.5, respectively, to add to the structural information known on complexes of this type; to obtain data on osmium-osmium distances in dinuclear complexes; to confirm the equatorial site occupation of the halide ligands, as has been suggested from IR spectroscopic evidence,[126] and to compare the structures with those of the triosmium homologues, $[Os(CO)_4]_3X_2$ (X = Cl or I). The structure of $Os_2(CO)_8Cl_2$ has previously been determined,[169] although the details were never published.

3.4.2 Experimental

$Os_2(CO)_8Cl_2$ was prepared from $Os_2(CO)_8H_2$ by reaction with CCl_4, as described in the literature.[126] Crystals of $Os_2(CO)_8Cl_2$, suitable for an X-Ray crystallographic analysis, were obtained on recrystallisation of the compound from dichloromethane/n-hexane. The compound was identified by its IR spectrum in n-hexane in the υ(CO) region, its mass spectrum and its melting point. The data - see Experimental Section in Chapter 6 - were in agreement with those reported in the literature.[126]

3.4.3 Intensity Data Collection

Accurate cell parameters were determined by a least-squares analysis of the setting angles of 24 reflections ($16° \leq \theta \leq 17°$) which were automatically located and centred on an Enraf-Nonius CAD4 diffractometer. The intensities of 3 reference reflections were checked every hour to monitor crystal decay and centering checked every 100 measured reflections. The data set was Lp processed and an empirical absorption correction applied.[150] Crystal data and experimental details of the data collection and final refinements are listed in table 3.4.1.

Table 3.4.1 Crystal Data, Data Collection and Refinement Parameters for $Os_2(CO)_8Cl_2$

Crystal Data	
Molecular Formula	$C_8Cl_2O_8Os_2$
Molecular Weight/g mol^{-1}	675.39
Space Group	$P2_12_12_1$
a/Å	9.3599(9)
b/Å	9.879(2)
c/Å	16.014(3)
V/$Å^3$	1480.7
Z	4
$D_c Mgm^{-3}$	3.03
μ (MoK_α)mm^{-1}	16.8
F(000)	1192
Data Collection	
Crystal Dimensions/mm	0.13 X 0.16 X 0.19
Scan Mode	ω - 2θ
Scan Width, ω/°	(0.64 + 0.35tanθ)
Aperture Width/mm	(1.11 + 1.05tanθ)
Aperture Length/mm	4
Crystal Decay/%	1.24
Range Scanned, θ/°	1-25
Radiation used, MoK_α,Å	0.7107

continued/...

Table 3.4.1 continued ...

Refinement	
Number of Reflections Collected	1416
Number of Reflections Observed	1270 (with $I_{rel} > 2\sigma I_{rel}$)
Number of Parameters	141
$R = \Sigma \| \|F_o\| - \|F_c\| \| / \Sigma \|F_o\|$	0.038
$R_w = \Sigma w^{\frac{1}{2}} \| \|F_o\| - \|F_c\| \| / \Sigma w^{\frac{1}{2}} \|F_o\|$	0.038
Weighting Scheme, w	$(\sigma^2 F)^{-1}$

3.4.4 Solution and Refinement of the Structure

Systematic absences identified in the data set were consistent with the space group $P2_12_12_1$. The atomic coordinates of two independent osmium atoms were obtained from a three-dimensional Patterson map by comparison with the Patterson grid constructed, using the symmetry elements of the non-centrosymmetric space group $P2_12_12_1$, corresponding to four general positions. Subsequent difference Fourier syntheses yielded the positions of two chlorine, eight carbon and eight oxygen atoms. Having determined the correct absolute structure - see section 3.4.5 - six least-squares refinements in which the two osmium, two chlorine and eight oxygen atoms were treated anisotropically and the carbon atoms isotropically, yielded a conventional R factor

Table 3.4.2 Analyses of Variance for $Os_2(CO)_8Cl_2$

a) By parity groups

Group	GGG	UGG	GUG	UUG	GGU	UGU	GUU	UUU	ALL
N	195	156	160	155	165	148	152	139	1270
V	544	333	400	328	320	310	307	308	372

b) As a function of sinθ

sinθ	0.00	-.18	-.24	-.27	-.30	-.32	-.35	-.37	-.39	-.41	-.43
N	127	159	114	132	105	167	128	125	138	75	
V	690	354	350	365	300	301	293	302	284	283	

c) As a function of (F/F_{max})

(F/F_{max})	0.00	-.27	-.31	-.35	-.41	-.46	-.51	-.56	-.61	-.69	-1.00
N	142	126	138	111	144	110	136	130	116	117	
V	267	286	274	328	325	314	352	355	372	702	

d) As a function of | Miller Index |

|h|	0	1	2	3	4	5	6	7	8	9	10	11	12	13	REST
N	141	167	152	152	145	129	122	100	82	45	30	5	0	0	0
V	637	332	336	350	369	338	287	246	307	262	293	266	0	0	0

|k|	0	1	2	3	4	5	6	7	8	9	10	11	12	13	REST
N	133	147	144	146	144	133	119	102	83	65	41	13	0	0	0
V	382	551	551	387	405	320	313	250	261	233	221	202	0	0	0

|l|	0	1	2	3	4	5	6	7	8	9	10	11	12	13	REST
N	76	102	105	99	98	96	94	85	88	71	71	61	56	43	125
V	702	283	406	323	338	300	323	315	344	383	371	304	354	255	383

N = Number of reflections in the group.
V = $100\,[M \sum (\omega |F_O-F_C|^2)/N\sum\omega]$ where M = total number of reflections.

of 0.0381 and R_w of 0.0375, employing a weighting scheme of $(\sigma^2 F)^{-1}$. The analyses of variance - see table 3.4.2 - computed after the final cycle were satisfactory. A final difference Fourier synthesis showed residual electron density of <2 $e\text{Å}^{-3}$, attributable to the inadequate modelling of the thermal anisotropy of the osmium atoms. Table 3.4.3 lists the final fractional atomic coordinates and thermal parameters with estimated standard deviations in parentheses. The observed and calculated structure factors for $Os_2(CO)_8Cl_2$ can be found in Appendix III.

3.4.5 Determination of the Absolute Structure of $Os_2(CO)_8Cl_2$.

Since $P2_12_12_1$ is a non-centrosymmetric space group, either set of coordinates x, y, z or -x, -y, -z will solve the structure. In order to determine the absolute structure, the following procedure was carried out. The initially found coordinate set $+x_j$ was refined to convergence with all atoms treated isotropically and $\Delta f'' = 0.0$ for all atoms. Two sets of structure factors, F_c, were then calculated without any further refinement, one with all $\Delta f''$ positive and one with all $\Delta f''$ negative. Both sets used the same isotropic thermal parameters and scale factor. Two different residuals were obtained, $R_G^+ = 0.0645$ and $R_G^- = 0.0609$ where R_G is the generalised R factor. Using Hamilton's test,[170] the

hypothesis that the structure giving the higher residual (corresponding to the positive $\Delta f''$ values) is a better model of the measured intensities, can be rejected at a significance level of 0.005. Hence, using the usual positive $\Delta f''$ values, it is the inverse of the structure originally determined which is correct. The atomic coordinates reported in this work are those of the correct absolute structure, using the positive imaginary part of the scattering factors $\Delta f''$ for all atoms.

Table 3.4.3 Fractional Atomic Coordinates (X 10^4) and Temperature Factors ($Å^2$ X 10^3) with Estimated Standard Deviations in Parentheses

Atoms	x/a	y/b	z/c	U_{iso}
Os_1	5311(1)	-238(1)	6367(1)	*
Os_2	8135(1)	-59(1)	5635(1)	*
Cl_1	5091(7)	2235(6)	6337(5)	*
Cl_2	7527(7)	-1926(6)	4700(4)	*
C_{11}	3382(27)	-404(29)	6839(17)	60(7)
O_{11}	2228(20)	-422(50)	7058(17)	*
C_{12}	6240(23)	-108(31)	7461(16)	55(6)
O_{12}	6846(21)	34(31)	8061(11)	*
C_{13}	4637(24)	-266(24)	5172(14)	48(6)
O_{13}	4251(16)	-247(31)	4533(11)	*
C_{14}	5594(24)	-2148(23)	6423(17)	40(6)
O_{14}	5771(19)	-3242(17)	6464(11)	*
C_{21}	8728(30)	-1500(29)	6445(20)	55(7)
O_{21}	9038(27)	-2293(24)	6900(16)	*
C_{22}	10000(23)	102(29)	5142(14)	54(6)
O_{22}	11162(17)	249(27)	4903(14)	*
C_{23}	8490(35)	1501(32)	6401(23)	70(8)
O_{23}	8793(26)	2247(26)	6837(16)	*
C_{24}	7216(22)	1252(21)	4841(15)	36(5)
O_{24}	6759(21)	1926(18)	4366(12)	*

continued/...

Table 3.4.3 continued ...

* Anisotropic Temperature Factors

Atoms	U_{11}	U_{22}	U_{33}	U_{23}	U_{13}	U_{12}
Os_1	39(1)	46(1)	34(1)	1(1)	5(1)	-2(1)
Os_2	33(1)	40(1)	44(1)	-2(1)	-1(1)	1(1)
Cl_1	57(4)	48(3)	62(4)	1(3)	1(4)	17(3)
Cl_2	54(3)	42(3)	43(4)	-5(3)	12(3)	1(3)
O_{11}	46(11)	404(58)	130(23)	100(36)	39(13)	7(26)
O_{12}	108(15)	157(22)	36(10)	20(16)	-25(10)	-20(27)
O_{13}	49(10)	188(27)	46(10)	32(17)	-22(8)	-14(15)
O_{14}	74(12)	48(11)	53(12)	6(9)	10(10)	3(9)
O_{21}	101(17)	91(17)	86(18)	27(14)	-31(15)	30(15)
O_{22}	50(10)	109(19)	113(17)	10(18)	12(11)	1(13)
O_{23}	104(19)	104(19)	96(20)	-68(16)	-31(17)	-5(15)
O_{24}	87(14)	60(11)	62(13)	23(10)	4(12)	33(11)

3.4.6 Description of the Structure and Discussion

The molecular structure of $Os_2(CO)_8Cl_2$ can be seen in figure 3.8. The molecular $Os_2(CO)_8Cl_2$ has two formally equivalent halves, joined by an osmium-osmium bond. There are four terminal carbonyl ligands and one terminal equatorial chloride ligand bonded to each osmium atom. The two halves of the molecule exist in a staggered conformation with respect to one another, as can be seen in figure 3.9. With this structure, each osmium atom obeys the effective atomic number rule. The coordination about each osmium atom is approximately octahedral. Tables 3.4.5 and 3.4.6 list bond lengths and bond angles, respectively, for $Os_2(CO)_8Cl_2$.

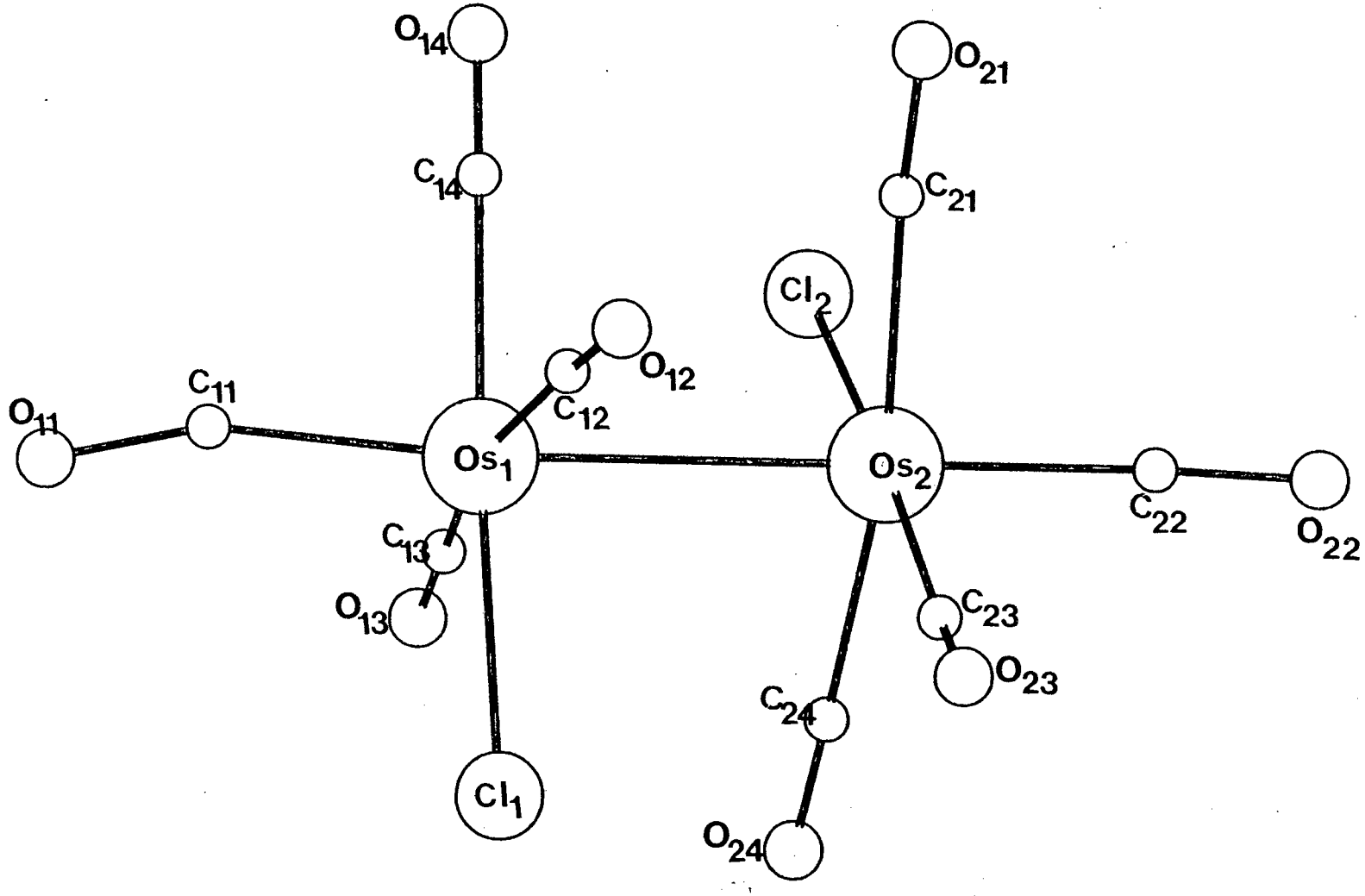

Figure 3.8 The molecular structure of $Os_2(CO)_8Cl_2$

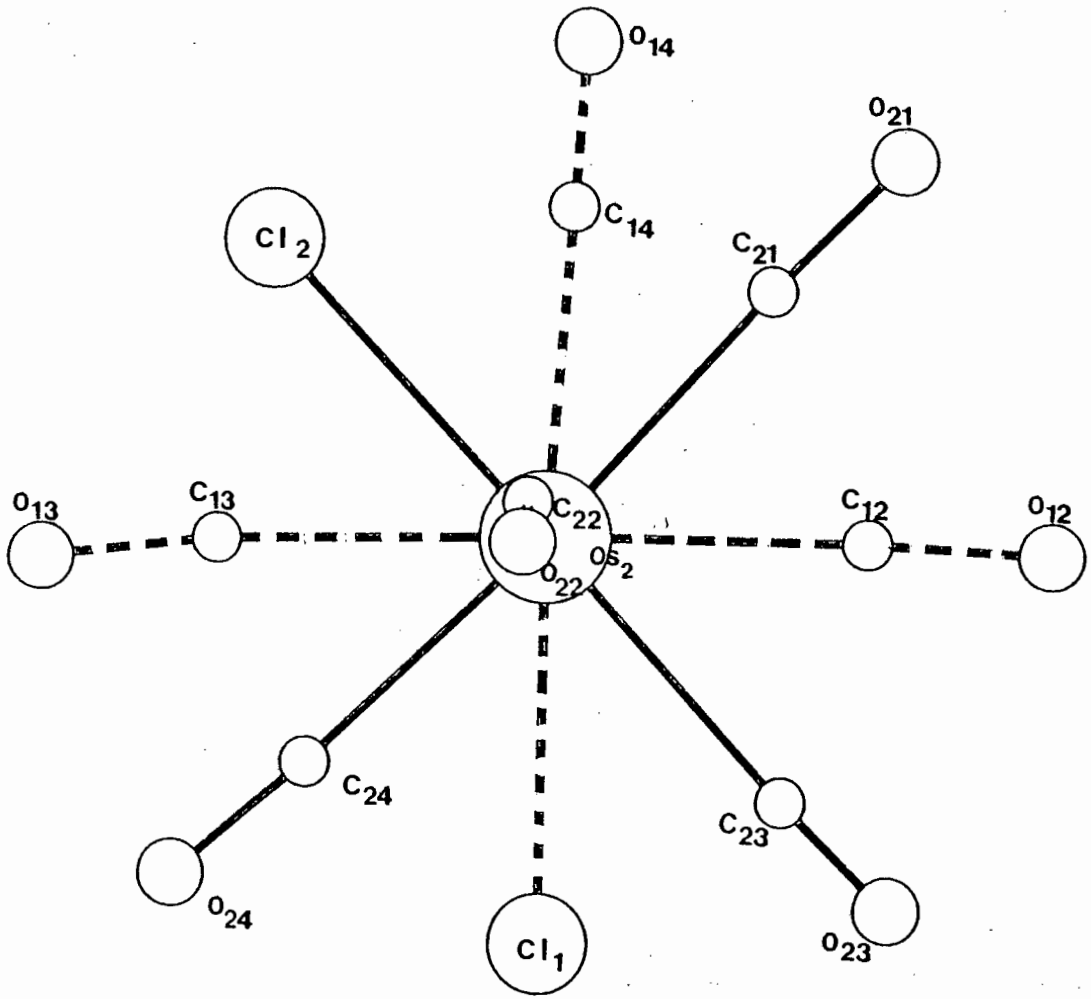

Figure 3.9 A view of $Os_2(CO)_8Cl_2$ along the molecular axis

The molecule, $Os_2(CO)_8Cl_2$, is isostructural with $Os_2(CO)_8I_2$, the X-Ray crystal structure of which has also been determined in this study - section 3.5. The equatorial site occupation of the halide ligands in $Os_2(CO)_8X_2$ (X = Cl or I) is the preferred configuration on electronic grounds, since CO groups prefer to adopt positions cis to each other, as far as possible. Interestingly, in the structure of $Ru_2(CO)_8(SnMe_3)_2$[80] the two $SnMe_3$ ligands adopt axial sites. Presumably, this is the preferred orientation of these bulky ligands on steric grounds. Reasons for the occurrence of the staggered conformation of the two molecular halves with respect to each other have been discussed previously[41] - see section 3.2.4. The molecular structures of $Os_2(CO)_8X_2$ (X = Cl or I) both closely resemble those of $M_2(CO)_{10}$ (M = Mn[152] or Tc[153]) or isoelectronic $Re_2(CO)_{10}$[152]. In these molecules, $M_2(CO)_{10}$ (M = Mn,[152] Tc[153] or Re[152]), there are two $M(CO)_5$ units joined by a single metal-metal bond - see figure 3.10. The molecules also exist in a staggered conformation, having approximate D_{4d} symmetry.

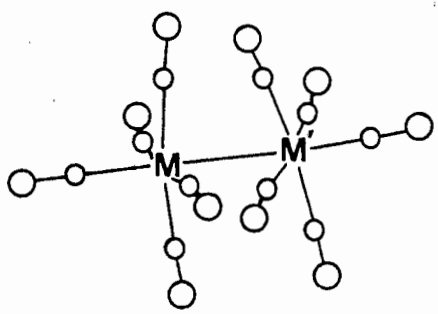

Figure 3.10 Diagrammatic representation of $M_2(CO)_{10}$ where M = Mn, Tc or Re.

The osmium-osmium bond length of 2.897(1) Å in $Os_2(CO)_8Cl_2$ agrees with that found for $Os_3(CO)_{12}Cl_2$ of 2.893(1) Å - section 3.2 - and for $Os_3(CO)_{12}$[39] of 2.877(3) Å, i.e. a normal osmium-osmium single bond. The osmium-osmium bond in $Os_2(CO)_8Cl_2$ is significantly shorter than that found for $Os_2(CO)_8I_2$ of 2.947(3) Å - section 3.5 - and for $Os_3(CO)_{12}I_2$[40] of 2.935(2) Å, as has been discussed in section 3.2.5 above. $Os_2(CO)_8Cl_2$ and $Os_3(CO)_{12}Cl_2$ can be regarded as part of the homologous series, $Os_n(CO)_{4n}Cl_2$ (n = 1-3). It is interesting to note that the osmium-osmium distance does not significantly alter from n = 2 to n = 3, i.e. when the number of metal atoms increases by one.

The terminal osmium-chlorine distances of 2.452(6) and 2.442(6) Å, respectively, agree with the osmium-chlorine of 2.43(1) Å found for $Os_3(CO)_{12}Cl_2$ - section 3.2. Table 3.4.4 lists some osmium-chlorine distances.

Table 3.4.4 Table of Some Terminal Osmium-Chlorine Distances (Å)

$Os_2(CO)_8Cl_2$	2.452(6)	2.442(6)
$Os_3(CO)_{12}Cl_2$	2.43(1)	
$Os_2(hp)_4Cl_2$[171]	2.496(7)	2.47(1)
$Os(CR)Cl(CO)(PPh_3)$[172] (R = C_7H_8)	2.506(4)	
$[OsCl_2(C_{10}H_{14})]_2$[166]	2.389(2)	
$[OsCl_2(\mu\text{-}CO)_2(\mu\text{-dppm})_2RhBr]$[173]	2.443(8)	2.447(9)

The terminal ósmium-chlorine distances found for the compound $Os_2(hp)_4Cl_2$[171] - see figure 3.11 - are 2.496(7) and 2.47(1) Å, respectively - see table 3.4.4 - which are longer than those found for $Os_2(CO)_8Cl_2$. The chloride ligands in $Os_2(hp)_4Cl_2$[171] are situated in axial positions to the osmium-osmium bond and this may have some bearing on the osmium-chlorine distance.

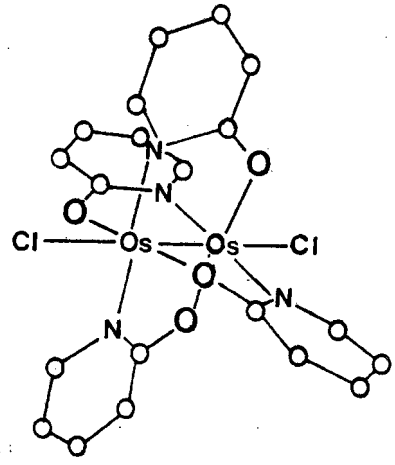

Figure 3.11 The structure of $Os_2(hp)_4Cl_2$

The osmium-chlorine distance for the compound $Os_2(CR)Cl(CO)(PPh_3)_2$ (R = C_7H_8)[172] - see figure 3.1 - a carbyne complex in which osmium is in the +I oxidation state, was found to be 2.506(4) Å - see table 3.4.4. This is slightly longer than the value obtained for $Os_2(CO)_8Cl_2$ but agrees with the one osmium-chlorine distance obtained for $Os_2(hp)_4Cl_2$[171] above.

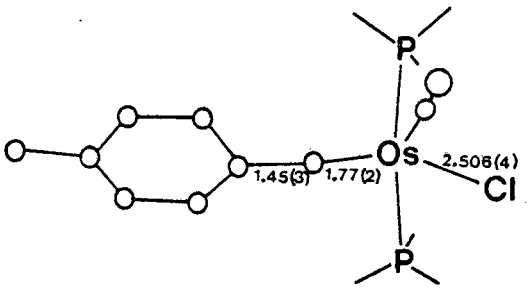

Figure 3.12 Diagrammatic representation of $Os(CR)Cl(CO)(PPh_3)_2$ where R = C_7H_8

In $[OsCl_2(C_{10}H_{14})]_2$[166] - see figure 3.13 - the mean terminal osmium-chlorine distance was reported as 2.389(2) Å - see table 3.4.4. This distance is slightly shorter than that found for $Os_2(CO)_8Cl_2$. In $[OsCl_2(C_{10}H_{14})]_2$,[166] the osmium atoms are both in a +II oxidation state which would also be expected to have a bearing on the osmium-chlorine distance.

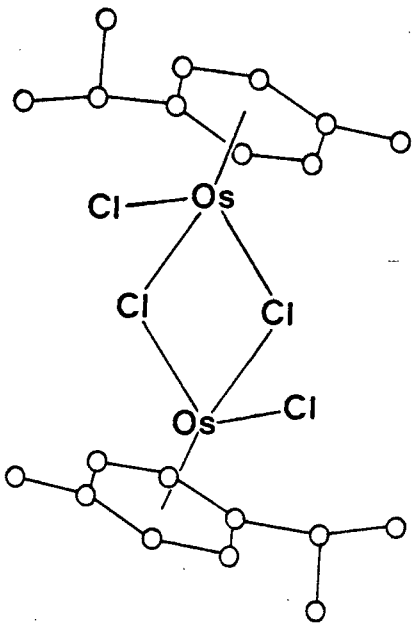

Figure 3.13 The structure of $[OsCl_2(C_{10}H_{14})]_2$

In $[OsCl_2[\mu\text{-}CO)_2(\mu\text{-}dppm)_2RhBr]$[173] where the terminal chloride ligands are situated **trans** to bridging carbonyl ligands, the two osmium-chlorine distances were found to be 2.443(8) and 2.447(9) Å, respectively - see table 3.4.4. These distances are very similar to those found for $Os_2(CO)_8Cl_2$ and this can partly be attributed to the presence of the carbonyl groups **trans** to the chloride ligands in $[OsCl_2[\mu\text{-}CO)_2(\mu\text{-}dppm)_2RhBr]$,[173] among other factors.

The osmium-carbon distances for $Os_2(CO)_8Cl_2$ were found to be in the range 1.91(2)-2.02(2) Å, while the carbon-oxygen distances were found to be in the range 1.05(4)-1.16(3) Å. These distances are in the expected ranges for Os-C and C-O distances and can be compared with the respective ranges of osmium-carbon and carbon-oxygen distances found for $Os_3(CO)_{12}Cl_2$ of 1.90(2)-2.16(4) and 0.97(4)-1.24(3) Å - section 3.2; for $Os_3(CO)_{12}I_2$[40] of 1.91(3)-1.97(3) and 1.12(3)-1.15(3) Å and for $Os_2(CO)_8I_2$ of 1.86(4)-2.16(4) and 1.05(5)-1.18(4) Å - section 3.5. There are three types of osmium-carbon bonds in the molecule $Os_2(CO)_8X_2$ (X = Cl, I) as was found previously for $Os_3(CO)_{12}Cl_2$ - see section 3.2.4. The mean osmium-carbon distance for the two axial carbonyl ligands in $Os_2(CO)_8Cl_2$ is 1.94(3) Å. In $Os_2(CO)_8I_2$, this mean was found to be 1.86(4) Å. I^- is known to be a better π-bonding ligand than Cl^-, therefore

it would be expected that more π-electron density would be concentrated in the Os-I bond than in the Os-Cl bond. This would result in there being less π-electron density between the two osmium atoms in $Os_2(CO)_8I_2$ than in $Os_2(CO)_8Cl_2$, resulting in a longer osmium-osmium bond for the iodo complex. Consequently, there would be more π-electron density between each osmium atom and the axial carbonyl ligands in $Os_2(CO)_8I_2$, resulting in a shorter Os-C_{ax} bond. This lengthening of the osmium-osmium bond could also be attributed to the steric effect of the bulky iodide ligands in equatorial positions interacting with the equatorial carbonyl ligands on the adjacent metal atom. The osmium-carbon distances for osmium-carbon bonds trans to halogen were found to be 1.91(2) and 2.00(3) Å, respectively, and averaging 1.96(3) Å for $Os_2(CO)_8Cl_2$, while for $Os_2(CO)_8I_2$ - section 3.5 - this distance was found to be 1.99(4) Å. These distances are longer than the axial osmium-carbon distances in the two structures, respectively, suggesting that I^- is a better π-acceptor than the $Os(CO)_4I$ group. The mean osmium-carbon distances for osmium-carbon bonds trans to carbonyl ligands were found to be 2.00(3) Å for $Os_2(CO)_8Cl_2$ and 2.08(4) Å for $Os_2(CO)_8I_2$ - section 3.5. These distances were significantly the longest Os-C distances as expected, since CO is the strongest π-acceptor of all the groups trans to the osmium-carbon bonds, in both structures. Similarly, in the structures $M_2(CO)_{10}$

(M = Mn,[152] Tc[153] and Re[152]) the axial metal-carbon distances were also found to be shorter than the average equatorial metal-carbon distances. In these latter complexes there are only two types of metal-carbon bonds, i.e. **trans** to the metal-metal bond and **trans** to carbonyl ligands. This variation in metal-carbon distances was also observed for $Os_3(CO)_{12}Cl_2$ - section 3.2.4. The shortest carbon-oxygen bond in $Os_2(CO)_8Cl_2$, i.e. C_{13}-O_{13}, of 1.09(3) Å, was found to correspond with the longest osmium-carbon bond, i.e. Os_1-C_{13} of 2.02(3) Å, while the longest carbon-oxygen bond, i.e. C_{22}-O_{22} of 1.16(3) Å was found to correspond to the shortest osmium-carbon bond, i.e. Os_2-C_{22}, of 1.92(2) Å. This is as expected because the more osmium d-electron density that is involved in back-bonding into the π^* orbitals of carbon monoxide, the more the C-O bond order is reduced, and vice versa.

The Os_1-Os_2-C(equatorial) and Os_2-Os_1-C(equatorial) angles in $Os_2(CO)_8Cl_2$ are all acute, ranging from 84.4(6)-87.3(7)° and averaging 86.3°. These bond angles can be compared with the range of Os_1'-Os_1-C(equatorial) angles found for $Os_2(CO)_8I_2$ of 86(1)-88(1)° and averaging 87(1)°. This inward tilting of equatorial carbonyl groups towards the molecular centre was also observed for the equatorial carbonyl groups attached to the terminal osmium atoms in $Os_3(CO)_{12}Cl_2$ - section 3.2 - and in $Os_3(CO)_{12}I_2$[40] where the

respective ranges were found to be 85.8(4)-87.0(10)° and 85.1(7)-89.0(6)°. The M'-M-C(equatorial) angles in $Mn_2(CO)_{10}$[152] are also all acute, ranging from 84.21(7)-89.71(17)° and averaging 86.38°. Likewise, in $Re_2(CO)_{10}$[152] the M'-M-C(equatorial) angles range from 84.21(17)-89.71(17)° and average 86.38°. This bending of equatorial carbonyl groups has been attributed to a bonding interaction between the π^* orbitals of the carbonyl groups and the filled d-orbitals on the adjacent metal atom,[41] as discussed previously - section 3.2.4. All Os-C-O bond angles in $Os_2(CO)_8Cl_2$ were found to be close to linear, as was found for $Os_2(CO)_8I_2$ - section 3.5 - ranging from 172.3(35)-178.9(29)° and averaging 175.6(32)° and is found generally for M-C-O bond angles.[157]

Table 3.4.5 Bond Lengths (Å) for $Os_2(CO)_8Cl_2$ with the Estimated Standard Deviations in Parentheses

Os_1-Os_2	2.897(1)
Os_1-Cl_1	2.452(6)
Os_2-Cl_2	2.442(6)
Os_1-C_{11}	1.96(3)
Os_1-C_{12}	1.96(3)
Os_1-C_{13}	2.02(2)
Os_1-C_{14}	1.91(2)
Os_2-C_{21}	2.01(3)
Os_2-C_{22}	1.92(2)
Os_2-C_{23}	2.00(3)
Os_2-C_{24}	2.01(2)
C_{11}-O_{11}	1.14(3)
C_{12}-O_{12}	1.12(3)
C_{13}-O_{13}	1.09(3)
C_{14}-O_{14}	1.10(3)
C_{21}-O_{21}	1.11(3)
C_{22}-O_{22}	1.16(3)
C_{23}-O_{23}	1.05(4)
C_{24}-O_{24}	1.10(3)

Table 3.4.6 Bond Angles (°) for $Os_2(CO)_8Cl_2$ with the Estimated Standard Deviations in Parentheses

Os_2-Os_1-Cl_1	90.4(2)
Os_2-Os_1-C_{11}	178.3(8)
Cl_1-Os_1-C_{11}	90.8(9)
Os_2-Os_1-C_{12}	87.3(6)
Cl_1-Os_1-C_{12}	89.4(9)
C_{11}-Os_1-C_{12}	94.0(10)
Os_2-Os_1-C_{13}	84.4(6)
Cl_1-Os_1-C_{13}	88.2(7)
C_{11}-Os_1-C_{13}	94.4(10)
C_{12}-Os_1-C_{13}	171.3(9)
Os_2-Os_1-C_{14}	87.3(7)
Cl_1-Os_1-C_{14}	176.5(7)
C_{11}-Os_1-C_{14}	91.5(11)
C_{12}-Os_1-C_{14}	87.8(12)
C_{13}-Os_1-C_{14}	94.3(10)
Os_1-Os_2-Cl_2	89.4(1)
Os_1-Os_2-C_{21}	87.0(8)
Cl_2-Os_2-C_{21}	85.7(9)
Os_1-Os_2-C_{22}	178.7(8)
Cl_2-Os_2-C_{22}	91.3(8)
C_{21}-Os_2-C_{22}	94.2(11)
Os_1-Os_2-C_{23}	87.2(9)
Cl_2-Os_2-C_{23}	176.1(9)
C_{21}-Os_2-C_{23}	96.0(11)
C_{22}-Os_2-C_{23}	92.1(12)
Os_1-Os_2-C_{24}	84.5(6)
Cl_2-Os_2-C_{24}	90.0(6)
C_{21}-Os_2-C_{24}	170.5(10)
C_{22}-Os_2-C_{24}	94.4(10)
C_{23}-Os_2-C_{24}	87.9(12)
Os_1-C_{11}-O_{11}	173.9(31)
Os_1-C_{12}-O_{12}	174.6(25)
Os_1-C_{13}-O_{13}	177.9(25)
Os_1-C_{14}-O_{14}	178.9(24)
Os_2-C_{21}-O_{21}	178.9(29)
Os_2-C_{22}-O_{22}	174.5(24)
Os_2-C_{23}-O_{23}	172.3(35)
Os_2-C_{24}-O_{24}	175.4(22)

3.4.7 Conclusion

The structure of $Os_2(CO)_8Cl_2$ has been determined by X-Ray crystallography and the solution and least-squares refinements led to a conventional weighted R factor of 0.0375. The molecule, $Os_2(CO)_8Cl_2$, adopts a structure with an osmium-osmium single bond and with the chloride ligands occupying equatorial sites i.e. the molecule is isostructural with $Os_2(CO)_8I_2$ - section 3.5.

3.5 The X-Ray Crystal Structure of Diiodooctacarbonyl-diosmium(I), $Os_2(CO)_8I_2$

3.5.1 Experimental

$Os_2(CO)_8I_2$ was obtained from the reaction of $Os_3(CO)_{12}$ with iodine in the presence of sunlight, as described in the Experimental Section in Chapter 6, and characterised by IR and mass spectroscopic and melting point data. All data - see Experimental Section in Chapter 6 - were found to be in agreement with those reported in the literature.[115] Single crystals of $Os_2(CO)_8I_2$, suitable for X-Ray analysis were obtained after several recrystallisations of the compound from n-hexane. Preliminary photography (Oscillation and Weissenberg, CuK_α λ = 1.5418 Å) established the space group $I4_1cd$.

3.5.2 Intensity Data Collection

Accurate cell parameters were determined by a least-squares analysis of the setting angles of 24 reflections ($16° \leq \theta \leq 17°$) which were automatically located and centred on an Enraf-Nonius CAD4 diffractometer. A total of 1637 reflections were collected out to θ=25°. The data were Lp processed and an empirical absorption correction applied.[150] Crystal data and experimental details of the data collection and final refinement are listed in table 3.5.1.

Table 3.5.1 Crystal Data, Data Collection and Refinement Parameters for $Os_2(CO)_8I_2$

Crystal Data	
Molecular Formula	$C_8I_2O_8Os_2$
Molecular Weight/g mol^{-1}	858.3
Space Group	$I4_1cd$
a/Å	11.791(2)
c/Å	23.583(4)
V/$Å^3$	3278.6(1)
Z	8
$D_C Mgm^{-3}$	3.48
μ (MoK_α) mm^{-1}	18.44
F(000)	2960
Data Collection	
Crystal Dimensions/mm	0.10 x 0.10 x 0.20
Scan Mode	$\omega - 2\theta$
Scan Width, ω/°	(1.04 + 0.35tanθ)
Aperture Width/mm	(1.57 + 1.05tanθ)
Aperture Length/mm	4
Crystal Decay/%	<1
Range Scanned, θ/°	1-25
Radiation Used, MoK_α, Å	0.7107
Refinements	
Number of Reflections Collected	1637
Number of Reflections Observed	578 (with $I_{rel} > 2\sigma I_{rel}$)
Number of Parameters	50
$R = \Sigma \| F_o \| - \| F_c \| / \Sigma \| F_o \|$	0.0477
$R_w = \Sigma w^{\frac{1}{2}} \| F_o \| - \| F_c \| / \Sigma w^{\frac{1}{2}} \| F_o \|$	0.0424
Weighting Scheme, w	$(\sigma^2 F)^{-1}$

3.5.3 Solution and Refinement of the Structure

The atomic coordinates of the osmium atom were obtained from a three-dimensional Patterson map by comparison with the Patterson grid constructed using the symmetry elements of the space group $I4_1cd$, corresponding to sixteen general positions. Since Z = 8, this implies that the asymmetric unit comprises one half the molecule. The remaining iodine, four carbon and four oxygen atoms were revealed in subsequent difference Fourier syntheses. In the final refinements, the osmium and iodine atoms were treated anisotropically and all other atoms, isotropically. Unit weights were employed, reducing the systematic variation of $w\Delta^2$ with the magnitude of F_o, as shown by the analyses of variance, computed after the final cycle - see table 3.5.2. In the last cycle of refinement, the average estimated standard deviation was greater than 50 times the average shift, which indicated satisfactory convergence. In the final difference map, maximum and minimum electron density was 1.75 and -1.76 $e\text{Å}^{-3}$, respectively. Table 3.5.3 lists the final fractional atomic coordinates and thermal parameters with estimated standard deviations in parentheses. The observed and calculated structure factors for $Os_2(CO)_8I_2$ can be found in Appendix IV.

Table 3.5.2 Analyses of Variance for $Os_2(CO)_8I_2$

a) By parity groups

Group	GGG	UGG	GUG	UUG	GGU	UGU	GUU	UUU	ALL
N	181	0	0	138	0	151	108	0	578
V	1327	0	0	1116	0	1007	1007	0	1154

b) As a function of sinθ

sinθ	0.00	-.18	-.23	-.27	-.30	-.32	-.35	-.37	-.39	-.40	-.43
N	59	59	68	61	44	80	56	59	35	57	
V	2181	1181	1093	1004	842	987	950	856	803	822	

c) As a function of (F/F_{max})

(F/F_{max})	0.00	-.27	-.31	-.35	-.41	-.46	-.51	-.56	-.61	-.69	-1.00
N	68	49	56	59	59	67	47	55	58	57	
V	698	946	712	1040	1040	962	1178	1156	1465	2010	

d) As a function of | Miller Index |

|h|	0	1	2	3	4	5	6	7	8	9	10	11	12	13	REST
N	72	114	105	82	59	60	43	28	10	6	0	0	0	0	0
V	1709	1180	1149	1062	1031	934	766	762	882	1015	0	0	0	0	0

|k|	0	1	2	3	4	5	6	7	8	9	10	11	12	13	REST
N	7	7	30	27	52	45	68	58	78	57	54	39	42	13	0
V	3009	1917	1854	1625	1370	1061	968	1076	897	893	856	659	962	1264	0

|l|	0	1	2	3	4	5	6	7	8	9	10	11	12	13	REST
N	32	30	35	30	37	29	29	30	29	29	31	26	29	22	160
V	1301	1202	1492	1221	1679	1341	1134	1333	1302	733	936	793	992	878	964

N = Number of reflections in the group.
V = $100\ [M \sum (\omega \mid F_o - F_c \mid^2)/N \sum \omega]$ where M = total number of reflections.

Table 3.5.3 Fractional Atomic Coordinates (x 10^4) and Temperature Factors ($Å^2$ x 10^3) with Estimated Standard Deviations in Parentheses

Atoms	x/a	y/b	z/c	U_{iso}
Os_1	5919(1)	1235(1)	0	*
I_1	7322(2)	1049(2)	-482(2)	*
C_1	5428(29)	2796(30)	-37(18)	57(10)
O_1	5478(22)	3797(25)	-12(20)	85(9)
C_2	4524(36)	1203(37)	-851(18)	67(13)
O_2	4128(33)	1097(33)	-1246(16)	107(12)
C_3	5992(34)	1047(35)	740(17)	63(12)
O_3	6363(26)	909(28)	1160(14)	77(9)
C_4	3684(33)	1386(33)	374(16)	61(12)
O_4	2871(28)	1521(28)	610(14)	36(9)

* Anisotropic Temperature Factors

Atoms	U_{11}	U_{22}	U_{33}	U_{23}	U_{13}	U_{12}
Os_1	38(1)	35(1)	43(1)	-3(1)	1(1)	2(1)
I_1	54(2)	62(2)	94(2)	-2(2)	29(2)	-2(2)

3.5.4 Description of the Structure and Discussion

An overall view of the molecular structure of $Os_2(CO)_8I_2$ can be seen in figure 3.14, while figure 3.15 shows a projection of the molecule viewed down the osmium-osmium bond. The molecule is similar with $Os_2(CO)_8Cl_2$ - section 3.4 - and both bear a very close resemblance to the structures of $M_2(CO)_{10}$ (M = Mn,[152] Tc[153]) and isoelectronic $Re_2(CO)_{10}$.[152] The molecule has two formally equivalent halves joined by an osmium-osmium bond. There are four terminal carbonyl

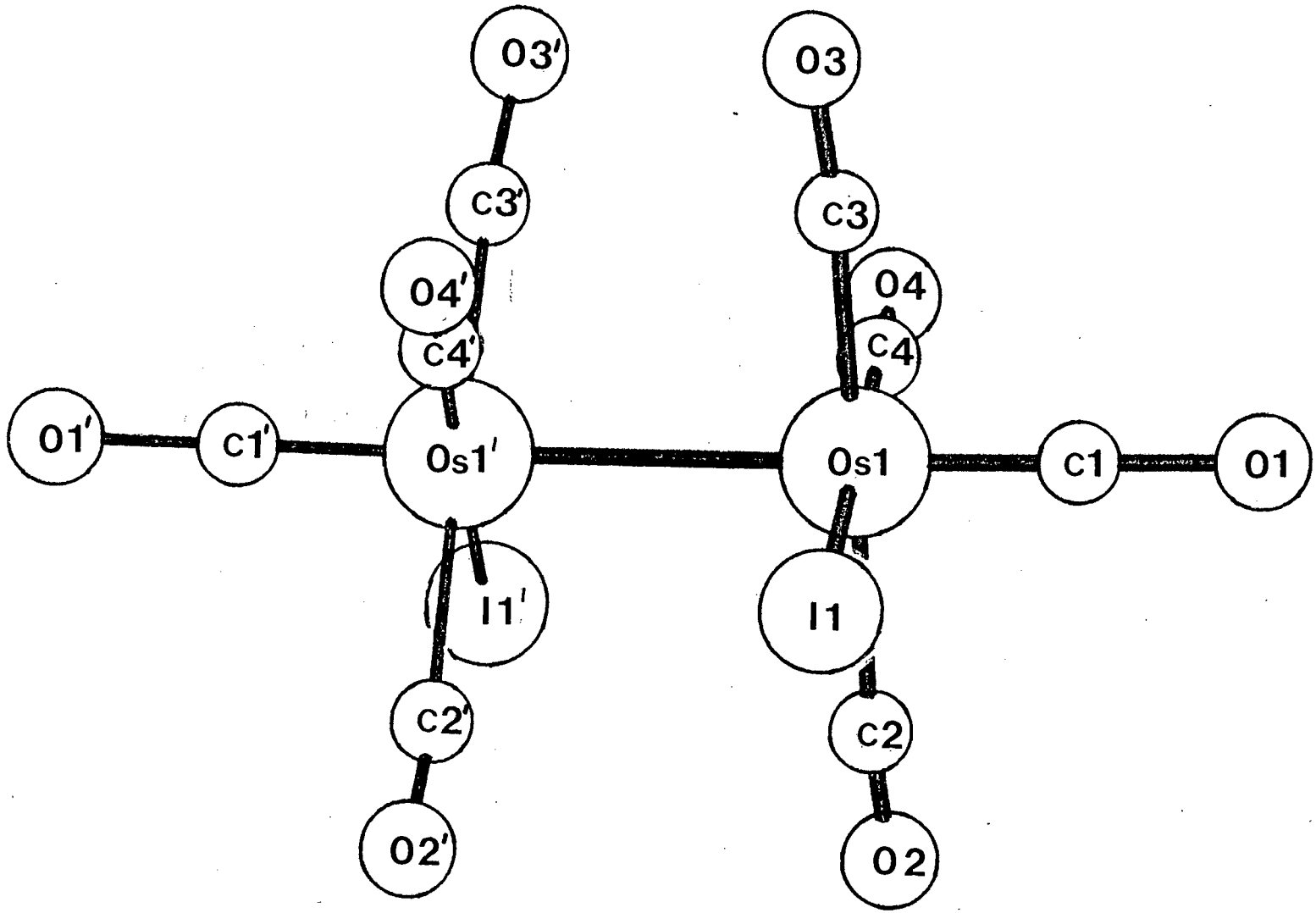

Figure 3.14 The molecular structure of $Os_2(CO)_8I_2$

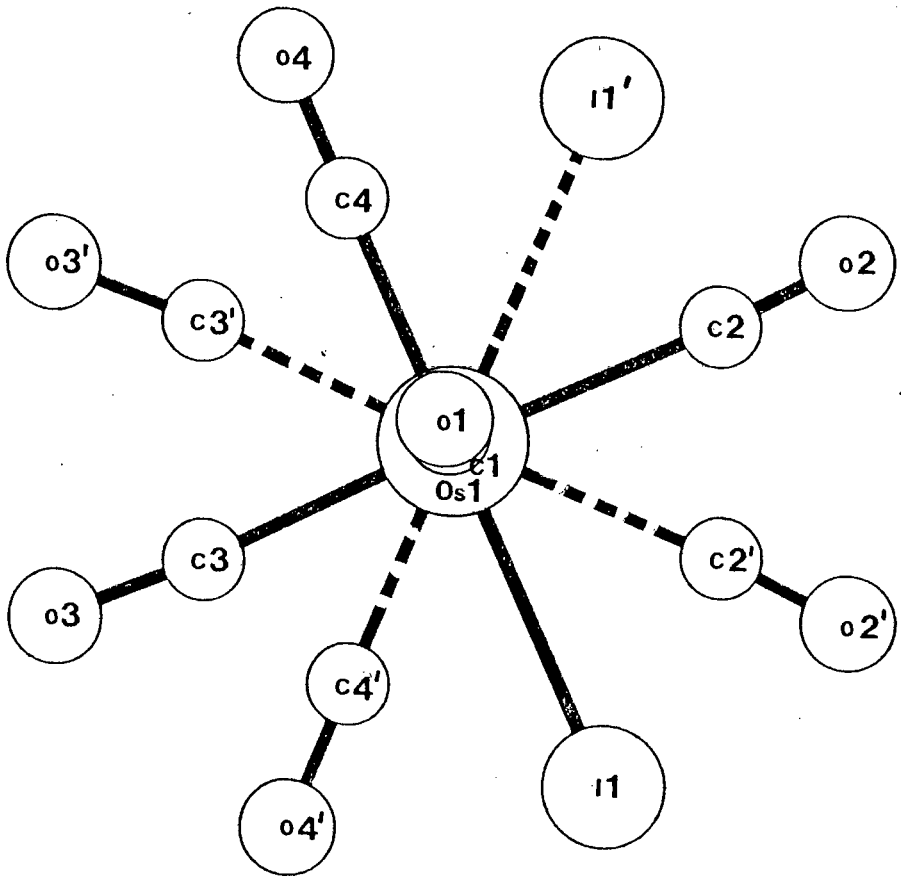

Figure 3.15 A view of $Os_2(CO)_8I_2$ along the molecular axis

ligands and one terminal equatorial iodide ligand bonded to each osmium atom which is six-coordinate and which adopts an approximately octahedral configuration. The two halves of the molecule exist in a staggered conformation, as can be seen in figure 3.15. The staggered conformation is typical for molecules of this type and has previously also been found for $M_2(CO)_{10}$ (M = Mn,[152] Tc[153] or Re[152]), $Os_2(CO)_8Cl_2$ - section 3.4, $Os_3(CO)_{12}Cl_2$ - section 3.2, $Os_3(CO)_{12}I_2$,[40] $Os_3(CO)_{12}(SiCl_3)_2$[38] and $[Mn_3(CO)_{14}]^-$[41]. Reasons for the molecule adopting a staggered, rather than an eclipsed, conformation have been discussed previously,[38,41] and see section 3.2.4. Tables 3.5.4 and 3.5.5 list the bond lengths and bond angles, respectively, for $Os_2(CO)_8I_2$.

The osmium-osmium distance in $Os_2(CO)_8I_2$ of 2.947(3) Å is significantly longer than that found for $Os_3(CO)_{12}I_2$[40] of 2.935(2) Å. These distances are both significantly longer than those found for $Os_2(CO)_8Cl_2$ - section 3.4 - and $Os_3(CO)_{12}Cl_2$ - section 3.2 - of 2.897(1) and 2.893(1) Å, respectively i.e. longer than a normal osmium-osmium single bond. This lengthening of the osmium-osmium bond in the iodo analogues can possibly be attributed to the steric repulsions between the equatorial iodide ligands and the equatorial carbonyl ligands on the adjacent metal atom, as has been discussed above - sections 3.2.5 and 3.4.5. Another contributing factor could be that I^- is a better π-bonding

ligand than Cl^- resulting in less π-electron density between the osmium atoms in the iodo complexes than in their chloro analogues. Both factors would result in a lengthening of the osmium-osmium bonds in the complexes, $Os_2(CO)_8I_2$ and $Os_3(CO)_{12}I_2$, as is found experimentally.

The osmium-iodine distance for $Os_2(CO)_8I_2$ of 2.767(3) Å is identical to the corresponding distance found for $Os_3(CO)_{12}I_2$.[40] The X-Ray crystal structure of the compound $[Os_5(CO)_{15}I]PPN$[174] was found to have a terminal osmium-iodine distance of 2.740(5) Å - see figure 3.16. $[Os_5(CO)_{15}I]PPN$[174] is an anionic complex and this may affect the osmium-iodine distance. These workers[174] compared the osmium-iodine distance with that found for $Os_4(CO)_{12}H_3I$ of 2.749(5) Å, where the iodide ligand was found to be bridging two osmium atoms.[175] The osmium-iodine distance of $[H_2Os_4(CO)_{12}I]PPN$[165] was found to be 2.732(2) Å which is shorter than the osmium-iodine distance found for $Os_2(CO)_8I_2$. The osmium-iodine distance for $Os_2(CO)_8I_2$ was found to be longer than the mean bridging osmium-iodine distance of 2.734(2) Å in $Os_2(CO)_6I_2$ - section 3.3.

The osmium-iodine distance in $Os_2(CO)_8I_2$ and $Os_3(CO)_{12}I_2$, respectively, therefore appears to be longer than both terminal and bridging Os-I distances reported for the anionic complexes, as mentioned above. This could be

attributed to the greater electron density surrounding the metal atoms. The more osmium π-electron density there is for back-bonding into the empty outer d-orbitals of the iodide ligands, the shorter the osmium-iodine distance.

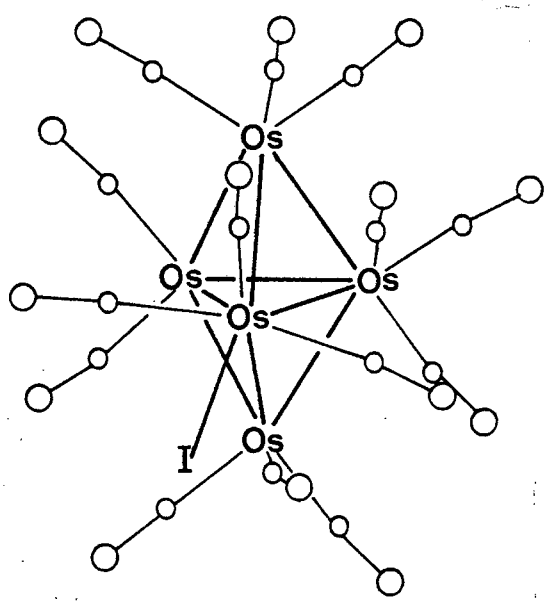

Figure 3.16 The structure of $[Os_5(CO)_{15}I]PPN$

$Os_2(CO)_8I_2$ and $Os_3(CO)_{12}I_2$ are part of the homologous series $Os_n(CO)_{4n}I_2$. It is interesting to note that on increasing the number of metal atoms in the complex, i.e. going from n = 2 to n = 3, the osmium-osmium distances are only just significantly shortened and the osmium-iodine distance remains unaffected. Similarly, for the complexes $Os_2(CO)_8Cl_2$ and $Os_3(CO)_{12}Cl_2$ - see section 3.4.5 - neither the osmium-osmium nor the osmium-chlorine distances, respectively, were significantly altered.

The osmium-carbon distances for $Os_2(CO)_8I_2$ were found to be in the range 1.86(4)-2.16(4) Å, while the carbon-oxygen distances were found to be in the range 1.05(5)-1.18(4) Å. The variation in the osmium-carbon distances has been discussed previously - see section 3.4.5. The longest carbon-oxygen distance of 1.18(4) Å was found for C_1-O_1 which corresponds to the shortest osmium-carbon bond, i.e. Os_1-C_1 with a distance of 1.86(4) Å. The shortest carbon-oxygen distance of 1.05(5) Å was found for C_2-O_2, which corresponds with the longest osmium-carbon distance, i.e. Os_1-C_2 of 2.16(4) Å. This is as expected since the more osmium d-electron density that is involved in back-bonding into the π^* orbitals of carbon monoxide, the more the C-O bond order is reduced and vice versa.

The Os_1'-Os_1-C(equatorial) angles in $Os_2(CO)_8I_2$ were found to lie in the range 86(1)-88(1)° and average 87(1)°. These have previously been compared with the corresponding angles in $Os_2(CO)_8Cl_2$ - see section 3.4.5. All Os-C-O angles in $Os_2(CO)_8I_2$ were found to be close to linear, ranging from 172(4)-175(4)° and averaging 174(4)°. This was also found for $Os_2(CO)_8Cl_2$ and is generally found for M-C-O bond angles.[157]

One close intermolecular oxygen-oxygen contact of 2.69(6) Å was found between O_2 at x,y,z and O_4 at y,0,5-x,0,25-z.

Table 3.5.4 Bond Lengths (Å) for $Os_2(CO)_8I_2$ with the Estimated Standard Deviations in Parentheses

Os_1-Os_1'[a]	2.947(3)
Os_1-I	2.767(3)
Os_1-C_1	1.86(4)
Os_1-C_2	2.16(4)
Os_1-C_3	2.00(4)
Os_1-C_4	1.99(4)
C_1-O_1	1.18(4)
C_2-O_2	1.05(5)
C_3-O_3	1.10(4)
C_4-O_4	1.12(5)

[a] Translated by symmetry element -x + 1, -y, z

Table 3.5.5 Bond Angles (°) for $Os_2(CO)_8I_2$ with the Estimated Standard Deviations in Parentheses

C_1-Os_1-I	86(1)
C_2-Os_1-I	87(1)
$C_2-Os_1-C_1$	92(2)
C_3-Os_1-I	86(1)
$C_3-Os_1-C_1$	95(2)
$C_3-Os_1-C_2$	170(2)
C_4-Os_1-I	178(1)
$C_4-Os_1-C_1$	94(2)
$C_4-Os_1-C_2$	95(2)
$C_4-Os_1-C_3$	93(2)
$Os_1-C_1-O_1$	172(4)
$Os_1-C_2-O_2$	172(5)
$Os_1-C_3-O_3$	175(4)
$Os_1-C_4-O_4$	175(4)

This is closer than the sum of the van der Waal's radii[176] for two oxygen atoms of 3.0 Å. A short intermolecular contact between two oxygen atoms of 2.98 Å was also found in the structure of $Os_3(CO)_{12}I_2$.[40]

3.5.5 Molecular Packing

Figure 3.17 shows the [001] projection of the molecular packing in the unit cell. The molecules pack in alternate layers, with the molecules in one layer lying perpendicular to those in the adjacent layer. No close osmium non-bonded interactions were observed, thus making it unlikely that $Os_2(CO)_8I_2$ would function as a uni-dimensional conductor.

3.5.6 Conclusion

The structure of $Os_2(CO)_8I_2$ has been determined by X-Ray crystallography and the solution and least-squares refinements led to a conventional weighted R factor of 0.0424. The molecule, $Os_2(CO)_8I_2$, adopts a structure with an osmium-osmium single bond, with the terminal iodide ligands in equatorial positions and with the two equivalent halves in a staggered conformation with respect to each other. Since the structures of $Os_3(CO)_{12}I_2$[40] and $Os_2(CO)_6I_2$[134] had already been determined, and as part of our study on dinuclear osmium carbonyl halide complexes, the structural determination of $Os_2(CO)_8I_2$ was carried out. These three structures together provide data on osmium-iodine distances where the iodide ligand is both in a terminal and a bridging environment and where the only other ligand is the carbonyl group. As has been previously

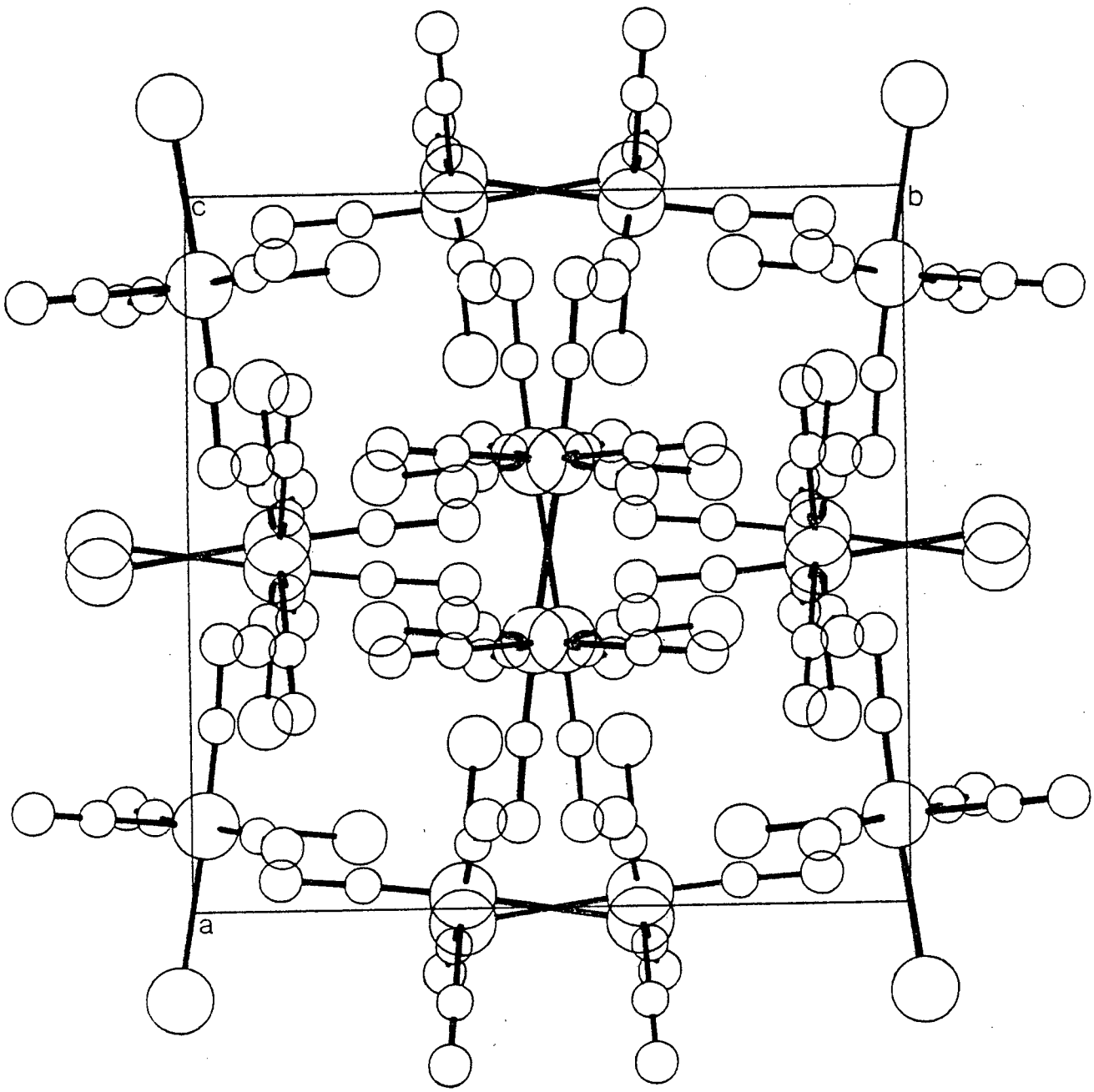

Figure 3.17 [001] projection of the molecular packing in the unit cell of $Os_2(CO)_8I_2$.

mentioned - section 3.4 - there are very few dinuclear carbonyl halide complexes known, where the metal-metal bond is unsupported by bridging ligands. Thus the structures of $Os_2(CO)_8I_2$ and $Os_2(CO)_8Cl_2$ are important in that they provide data on osmium-osmium bond lengths in dinuclear osmium complexes, and also confirm the expected equatorial site occupation of the halide ligands.

3.6 The X-Ray Crystal Structure of Hydridotetracarbonylosmiumbromotetracarbonylrheniumbis(triphenylphosphine)iminium, [HOsRe(CO)$_8$Br]PPN

3.6.1 Experimental

[HOsRe(CO)$_8$Br]PPN was obtained from the reaction of [HOs(CO)$_4$]PPN with Re(CO)$_5$Br and characterised by IR, ^{1}H nmr spectroscopy and elemental analysis as described in the Experimental Section in Chapter 6. Single crystals suitable for an X-Ray determination were obtained by recrystallisation of the compound from methanol/water.

3.6.2 Intensity Data Collection

Accurate cell parameters were determined by a least-squares analysis of the setting angles of 24 reflections ($14° \leq \theta \leq 15°$) which were automatically located and centred on an Enraf-Nonius CAD4 diffractometer. The intensities of 3 reference reflections were checked every hour to monitor crystal decay and centering checked every 100 measured reflections. The data set was Lp processed and an empirical absorption correction applied.[150] Crystal data and experimental details of the data collection and final refinement are listed in Table 3.6.1.

Table 3.6.1 Crystal Data, Data Collection and Refinement Parameters for [$HOsRe(CO)_8Br$]PPN

Crystal Data	
Molecular Formula	$C_{44}BrH_{31}NO_8OsP_2Re$
Molecular Weight/g mol^{-1}	1219.99
Space Group	$P\bar{1}$
a/Å	11.762(2)
b/Å	14.206(2)
c/Å	14.333(2)
α/°	117.75(1)
β/°	92.68(1)
γ/°	95.55(1)
V/$Å^3$	2097.9
Z	2
$D_c Mgm^{-3}$	1.93
μ (MoK_α)mm^{-1}	6.7
F(000)	1164
Data Collection	
Crystal Dimensions/mm	0.06 x 0.13 x 0.13
Scan Mode	ω - 2θ
Scan Width, ω/°	(0.79 + 0.35tanθ)
Aperture Width/mm	(1.16 + 1.05tanθ)
Aperture Length/mm	4
Crystal Decay/%	1.32
Range Scanned, θ/°	1-23
Radiation used, MoK_α, Å	0.7107

continued/...

Table 3.6.1 continued ...

Refinement	
Number of Reflections Collected	4574
Number of Reflections Observed	3072 (with $I_{rel} > 2\sigma I_{rel}$)
Number of Parameters	309
$R = \Sigma \| \|F_o\| - \|F_c\| \| / \Sigma \|F_o\|$	0.043
$R_w = \Sigma w^{\frac{1}{2}} \| \|F_o\| - \|F_c\| \| / \Sigma w^{\frac{1}{2}} \|F_o\|$	0.039
Weighting Scheme, w	$(\sigma^2 F)^{-1}$

3.6.3 Solution and Refinement of the Structure

The atomic coordinates of the osmium and rhenium atoms were obtained from a three-dimensional Patterson map by comparison with the Patterson grid constructed, using the symmetry elements of the centrosymmetric space group, $P\bar{1}$, corresponding to two general positions. Four subsequent difference Fourier syntheses yielded the positions of the bromine, carbon and oxygen atoms of the anion, as well as the two phosphorus, nitrogen and carbon atoms of the PPN cation. The hydride ligand was located at a distance of 1.66 Å from the osmium atom, a distance which concurs with osmium-hydrogen(terminal) distances previously obtained from neutron diffraction data.[177] This hydrogen was inserted and subsequently constrained to ride at a distance of 1.66(1) Å from the osmium atom. The hydrogen atoms on the

Table 3.6.2 Analyses of Variance for $[HOsRe(CO)_8Br]PPN$

a) By parity groups

Group	GGG	UGG	GUG	UUG	GGU	UGU	GUU	UUU	ALL
N	392	406	372	383	379	369	378	393	3072
V	380	371	543	396	525	382	390	380	425

b) As a function of sin0

sin0	0.00	-.16	-.20	-.24	-.26	-.29	-.31	-.33	-.35	-.37	-.40
N	342	281	392	249	391	279	283	295	268	292	
V	785	421	328	335	332	353	348	362	367	355	

c) As a function of (F/F_{max})

(F/F_{max})	0.00	-.33	-.36	-.39	-.41	-.44	-.47	-.50	-.55	-.63	-1.00
N	366	285	373	242	358	309	239	297	307	296	
V	387	531	518	357	377	371	377	398	368	495	

d) As a function of | Miller Index |

| h |	0	1	2	3	4	5	6	7	8	9	10	11	12	13	REST
N	178	393	419	366	298	320	311	257	155	154	134	61	26	0	0
V	882	433	407	397	354	364	347	320	319	359	393	319	593	0	0

| k |	0	1	2	3	4	5	6	7	8	9	10	11	12	13	REST
N	167	325	335	324	296	284	261	234	213	177	150	114	87	57	48
V	734	591	378	387	387	377	365	385	326	356	355	383	293	311	365

| l |	0	1	2	3	4	5	6	7	8	9	10	11	12	13	REST
N	179	307	322	317	289	282	256	215	204	191	157	118	105	72	58
V	741	599	407	414	375	359	352	350	324	352	332	335	380	316	289

N = Number of reflections in the group.
V = $100\,[M \sum (\omega\,|F_O-F_C|^2)/N\sum\omega]$ where M = total number of reflections.

Table 3.6.3 Fractional Atomic Coordinates ($X10^4$) and Temperature Factors ($Å^2 \times 10^3$) with Estimated Standard Deviations in Parentheses

Atoms	x/a	y/b	z/c	U_{iso}
Os	3710(1)	2888(1)	3397(1)	*
Re	5040(1)	2108(1)	1504(1)	*
Br	6914(2)	3304(2)	2745(2)	*
P_1	8752(4)	2665(3)	-2534(3)	*
P_2	10787(3)	1699(3)	-2075(3)	*
N	9923(11)	2257(10)	-2420(9)	*
O_1	2253(12)	3758(11)	5233(11)	*
O_2	2312(11)	642(10)	2170(10)	*
O_3	4818(12)	5072(11)	3743(10)	*
O_4	5669(10)	2335(10)	4494(11)	*
O_5	2873(11)	739(10)	104(9)	*
O_6	6387(14)	1276(12)	-464(12)	*
O_7	4400(12)	4015(12)	1261(11)	*
O_8	5726(11)	340(11)	2019(10)	*
H_1	2636(57)	2789(77)	2549(58)	16(30)
C_1	2795(18)	3370(16)	4498(17)	69(6)
C_2	2868(16)	1432(15)	2619(14)	55(5)
C_3	4428(16)	4201(16)	3612(14)	59(5)
C_4	4965(16)	2551(14)	4097(14)	55(5)
C_5	3719(17)	1273(15)	642(15)	61(6)
C_6	5908(17)	1604(16)	282(17)	62(6)
C_7	4624(17)	3336(17)	1338(15)	62(6)
C_8	5454(15)	973(14)	1813(13)	46(5)
C_{111}	8162(12)	3381(12)	-1313(11)	32(4)
C_{112}	8354(16)	3119(15)	-502(15)	68(6)
H_{112}	8810(16)	2527(15)	-598(15)	92(11)
C_{113}	7893(16)	3722(15)	473(16)	70(6)
H_{113}	8095(16)	3598(15)	1089(16)	92(11)
C_{114}	7190(15)	4439(14)	583(14)	57(5)
H_{114}	6818(15)	4803(14)	-1252(14)	92(11)
C_{115}	6965(16)	4686(15)	-200(15)	68(6)
H_{115}	6460(16)	5244(15)	-108(15)	92(11)
C_{116}	7449(15)	4164(14)	-1138(15)	60(6)
H_{116}	7275(15)	4348(14)	-1719(15)	92(11)
C_{121}	7679(13)	1579(11)	-3367(11)	34(4)
C_{122}	7720(13)	1068(12)	-4463(12)	39(4)
H_{122}	8283(13)	1378(12)	-4781(12)	92(11)
C_{123}	6994(14)	141(13)	-5118(14)	52(5)
H_{123}	7049(14)	-228(13)	-5899(14)	92(11)
C_{124}	6202(15)	-293(14)	-4691(14)	57(5)
H_{124}	5641(15)	-940(14)	-5164(14)	92(11)

continued/....

Table 3.6.3 continued ...

Atoms	x/a	y/b	z/c	U_{iso}
C_{125}	6175(15)	201(14)	-3597(14)	57(5)
H_{125}	5643(15)	-133(14)	-3278(14)	92(11)
C_{126}	6894(14)	1120(13)	-2957(13)	49(5)
H_{126}	6834(14)	1475(13)	-2176(13)	92(11)
C_{131}	8940(13)	3541(12)	-3109(11)	33(4)
C_{132}	9971(14)	4191(13)	-2887(13)	49(5)
H_{132}	10613(14)	4145(13)	-2433(13)	92(11)
C_{133}	10146(16)	4922(15)	-3300(14)	60(5)
H_{133}	10895(16)	5390(15)	-3145(14)	92(11)
C_{134}	9264(14)	4969(14)	-3916(13)	53(5)
H_{134}	9372(14)	5488(14)	-4203(13)	92(11)
C_{135}	8213(15)	4316(14)	-4162(14)	58(5)
H_{135}	7583(15)	4371(14)	-4621(14)	92(11)
C_{136}	8053(14)	3593(13)	-3762(12)	47(5)
H_{136}	7306(14)	3116(13)	-3941(12)	92(11)
C_{211}	10707(12)	1912(12)	-745(11)	34(4)
C_{212}	11252(14)	2879(13)	86(13)	45(5)
H_{212}	11728(14)	3408(13)	-61(13)	92(11)
C_{213}	11087(15)	3093(15)	1118(14)	58(5)
H_{213}	11471(15)	3781(15)	1723(14)	92(11)
C_{214}	10405(15)	2385(14)	1301(15)	61(5)
H_{214}	10333(15)	2551(14)	2053(15)	92(11)
C_{215}	9848(16)	1446(15)	492(15)	68(6)
H_{215}	9324(16)	956(15)	655(15)	92(11)
C_{216}	10022(14)	1193(14)	-556(13)	50(5)
H_{216}	9640(14)	499(14)	-1155(13)	92(11)
C_{221}	10569(13)	270(12)	-2868(11)	34(4)
C_{222}	11273(14)	-346(13)	-2644(12)	43(4)
H_{222}	11914(14)	-1(13)	-2058(12)	92(11)
C_{223}	11071(15)	-1452(14)	-3242(14)	59(5)
H_{223}	11574(15)	-1898(14)	-3082(14)	92(11)
C_{224}	10228(15)	-1931(15)	-4039(14)	55(5)
H_{224}	10091(15)	-2732(15)	-4450(14)	92(11)
C_{225}	9547(16)	-1332(14)	-4288(14)	59(5)
H_{225}	8913(16)	-1688(14)	-4880(14)	92(11)
C_{226}	9748(14)	-209(13)	-3688(12)	47(5)
H_{226}	9271(14)	231(13)	-3883(12)	92(11)
C_{231}	12213(12)	2163(11)	-2162(11)	32(4)
C_{232}	12393(14)	2654(12)	-2822(12)	40(4)
H_{232}	11719(14)	2749(12)	-3208(12)	92(11)
C_{233}	13494(15)	2988(14)	-2943(14)	58(5)
H_{233}	13616(15)	3315(14)	-3422(14)	92(11)

continued/....

Table 3.6.3 continued ....

Atoms	x/a	y/b	z/c	U_{iso}
C_{234}	14424(17)	2891(14)	-2372(14)	68(6)
H_{234}	15219(17)	3168(14)	-2428(14)	92(11)
C_{235}	14257(16)	2380(14)	-1767(14)	60(5)
H_{235}	14932(16)	2271(14)	-1395(14)	92(11)
C_{236}	13189(15)	2063(13)	-1650(13)	51(5)
H_{236}	13091(15)	1718(13)	-1185(13)	92(11)

* Anisotropic Temperature Factors ($Å^2 \times 10^3$)

Atoms	U_{11}	U_{22}	U_{33}	U_{23}	U_{13}	U_{12}
Os	42(1)	45(1)	39(1)	17(1)	1(1)	6(1)
Re	47(1)	44(1)	37(1)	19(1)	4(1)	6(1)
Br	64(2)	88(2)	70(2)	39(1)	1(1)	-3(1)
P_1	34(3)	33(3)	37(3)	18(2)	4(2)	6(2)
P_2	30(3)	38(3)	35(3)	18(2)	5(2)	8(2)
N	36(8)	57(9)	33(8)	25(7)	9(6)	11(7)
O_1	79(10)	72(10)	75(10)	26(9)	20(9)	27(8)
O_2	73(10)	69(9)	58(9)	22(7)	5(7)	-25(8)
O_3	91(11)	58(9)	68(10)	11(8)	11(8)	-5(8)
O_4	49(8)	84(10)	104(11)	54(9)	-24(8)	-10(7)
O_5	71(10)	71(9)	55(9)	25(8)	-3(8)	8(8)
O_6	107(13)	107(13)	77(11)	34(11)	42(10)	19(11)
O_7	104(12)	90(11)	88(11)	60(10)	18(9)	27(10)
O_8	73(10)	73(10)	76(10)	41(8)	16(8)	29(8)

phenyl rings were placed in calculated positions. Eight least-squares refinements in which the osmium, rhenium, bromine, two phosphorus, nitrogen and eight oxygen atoms were treated anisotropically and the hydrogens and all carbon atoms were treated isotropically, yielded a conventional R factor of 0.043. A weighting scheme $(\sigma^2 F)^{-1}$,

gave R_w = 0.039. The analyses of variance - see table 3.6.2 - computed after the final least-squares refinement were satisfactory. A final difference Fourier synthesis revealed maximum residual electron density <1 $e\text{Å}^{-3}$, near the osmium and rhenium atoms resulting from inadequate modelling of their thermal anisotropy. Table 3.6.3 lists the final fractional atomic coordinates and thermal parameters with estimated standard deviations in parentheses. The observed and calculated structure factors for [$HOsRe(CO)_8Br$]PPN can be found in Appendix V.

3.6.4 Description of the Structure and Discussion

The structure of [$HOsRe(CO)_8Br$]PPN can be seen in figure 3.18. The structure of the anion shown in figure 3.19 consists of the osmium and rhenium atoms bonded together by a metal-metal bond. There are four terminal carbonyl ligands and one terminal hydride ligand bonded to the osmium atom and four terminal carbonyl ligands and one terminal bromide ligand bonded to the rhenium atom. Both the hydride and bromide ligands occupy equatorial positions since the CO groups prefer to adopt cis positions as far as possible, as was found for the complexes $Os_2(CO)_8X_2$ (X = Cl or I) - sections 3.4 and 3.5. The geometry about both metal atoms is distorted octahedral with greater distortion at osmium.

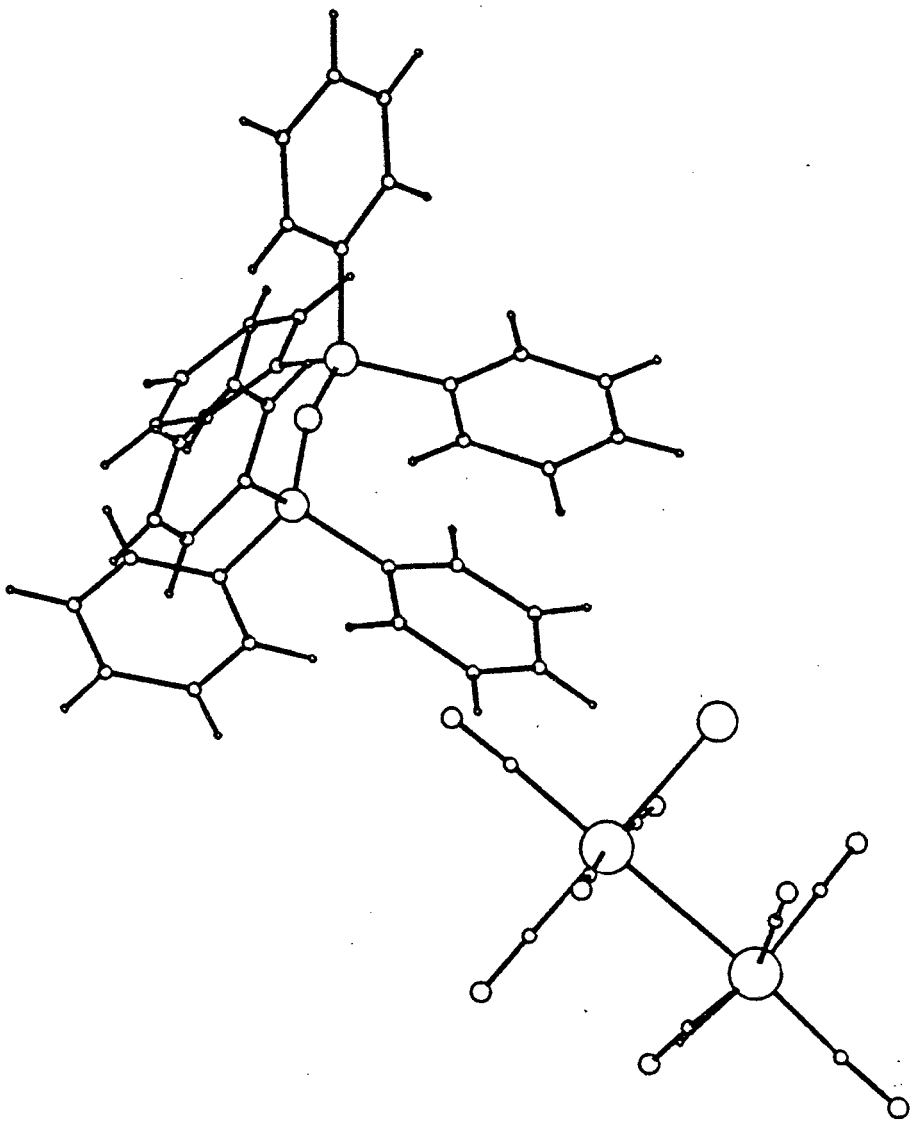

Figure 3.18 The structure of [HOsRe(CO)$_8$Br]PPN

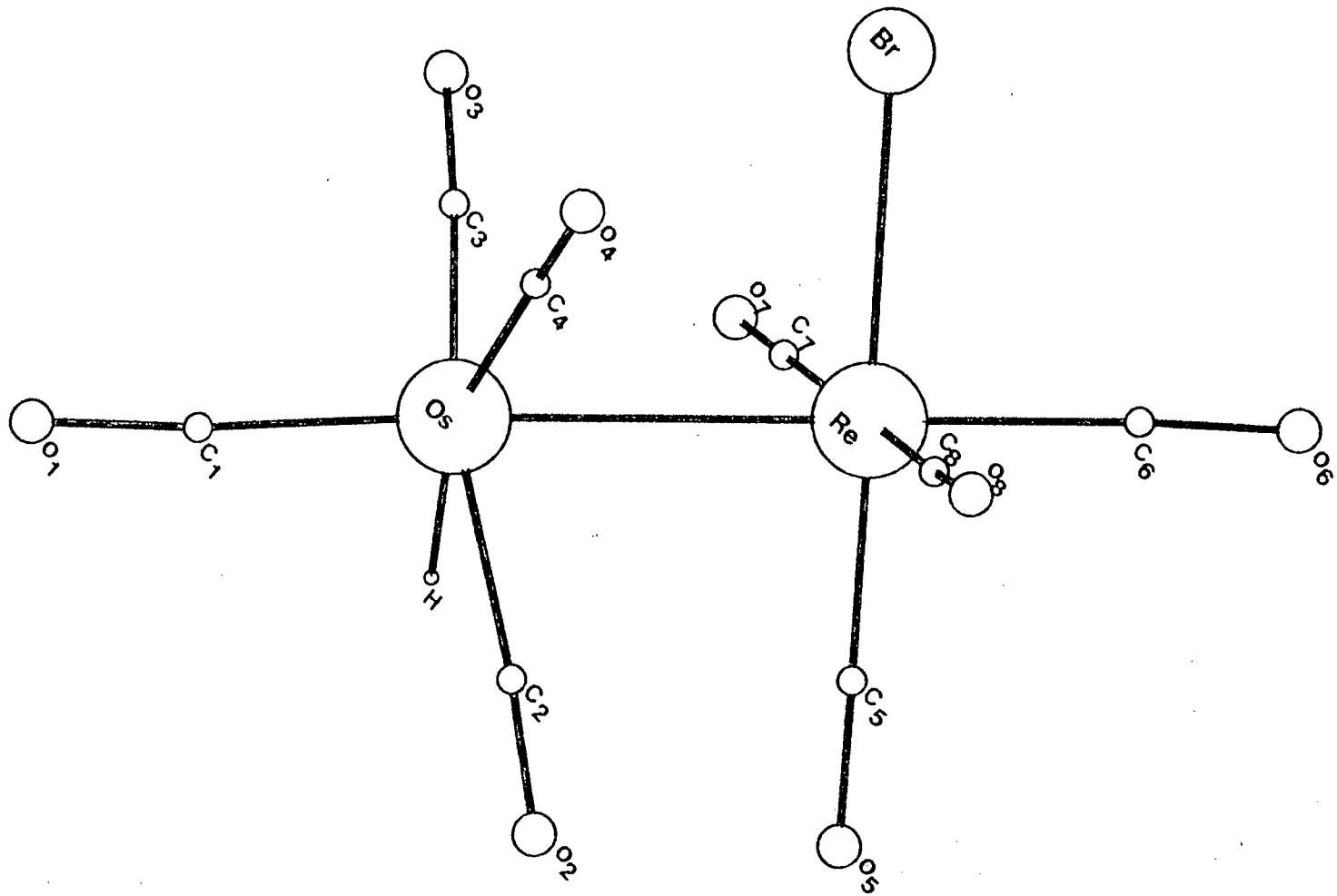

Figure 3.19 The structure of the $[HOsRe(CO)_8Br]$ anion

Figure 3.20 shows a view of the [$HOsRe(CO)_8Br$] anion along the molecular axis. The two parts of the anion exist in a staggered conformation, as might be expected.[41,152] Thus the molecules, $Os_2(CO)_8Cl_2$ - section 3.4, $Os_2(CO)_8I_2$ - section 3.5, $Os_3(CO)_{12}Cl_2$ - section 3.2, $Os_3(CO)_{12}I_2$[40] and the anions, $[HRe_2(CO)_9]^-$[178], $[Re_2(CO)_9(COOMe)]^-$[178] and $[Re_2(CO)_9I]^-$[179] as well as many complexes of this type were also found to exist in staggered conformations. Since PPN is a useful counterion from which to crystallise anions, it has been used extensively for this purpose and many X-Ray crystallographic determinations have been carried out on salts of which it is the cation.[165,168] It will, therefore, not be discussed in any crystallographic detail in this report. Tables 3.6.4 and 3.6.5 list the bond lengths and bond angles, respectively, for [$HOsRe(CO)_8Br$]PPN.

The osmium-rhenium distance in [$HOsRe(CO)_8Br$]PPN was found to be 2.995(1) Å. Since no other dinuclear osmium- rhenium complexes have been structurally characterised, no such direct comparison for an osmium-rhenium distance is available. The osmium-rhenium distance in [$HOsRe(CO)_8Br$]PPN is longer than that found in the polynuclear complexes, $HOs_3Re(CO)_{15}$[180] and (μ-H)$Os_3Re(CO)_{15}(NCCH_3)$,[181] which were found to be 2.957(1) and 2.959(1) Å, respectively. These were both considered to be normal osmium-rhenium single σ bonds.

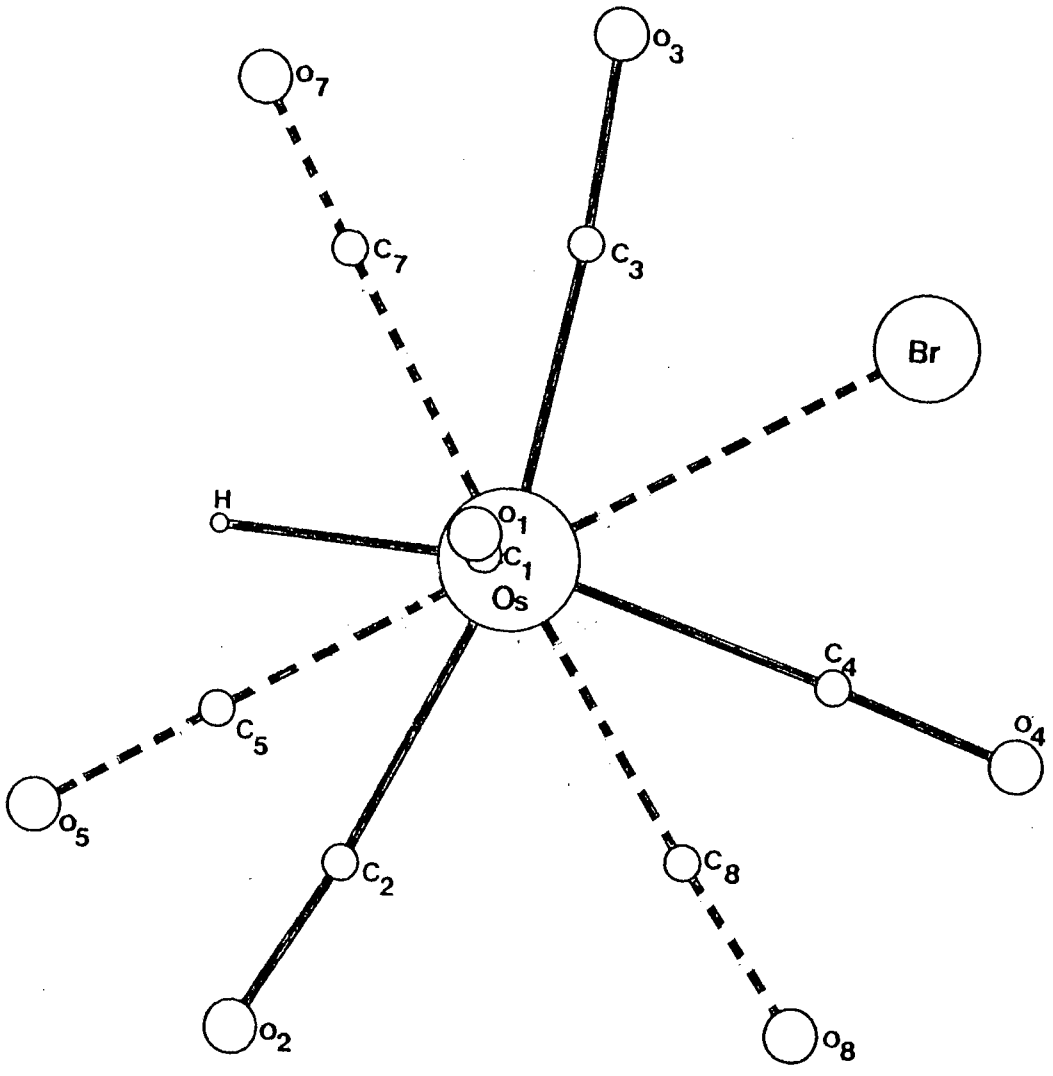

Table 3.20 A view of the [HOsRe(CO)$_8$Br] anion along the molecular axis

Since the average osmium-osmium distance in $Os_3(CO)_{12}$[39] is 2.877 Å and the average rhenium-rhenium distance in $[Re_4(CO)_{16}]^{2-}$[182] is 2.989 Å, therefore the predicted osmium distance is 2.933 Å.[180] The rhenium-rhenium distances in the dinuclear anionic complexes,[178] $[HRe_2(CO)_9]^-$ and $[Re_2(CO)_9(COOMe)]^-$ of 3.041 and 3.05 Å, respectively, and $[Re_2(CO)_9I]^-$[179] of 3.052(4) Å are longer than the average rhenium-rhenium distance in $[Re_4(CO)_{16}]^{2-}$[182] of 2.989 Å. The osmium-osmium distance in the diosmium anionic complex, $[Os_2(CO)_8]^{2-}$,[183] was found to be 2.992(1) Å which is longer than the average osmium-osmium distance in $Os_3(CO)_{12}$[39] of 2.877 Å, i.e. a normal osmium-osmium single bond, but almost identical to the osmium-rhenium distance of 2.995(1) Å found for $[HOsRe(CO)_8Br]PPN$.

The osmium-hydrogen(terminal) distance of 1.66(8) Å found for $[HOsRe(CO)_8Br]PPN$ is shorter than the Os-H(bridging) distances determined by neutron-diffraction studies. For example, the average Os-H(bridging) distance in $Os_3(CO)_{10}(\mu\text{-}H)_2$[184] is 1.845(3) Å. The osmium-hydrogen distance in $[HOsRe(CO)_8Br]PPN$ agrees very well, however, with the average osmium-hydrogen distance of 1.659 Å found in the neutron-diffraction study of $Os(PMe_2Ph)_3H_4$.[177] The latter complex contains an osmium atom formally in the +IV oxidation state, whereas in $[HOsRe(CO)_8Br]PPN$, osmium exists in the +I oxidation state. This difference in oxidation

state might have been expected to have affected the osmium-hydrogen distance. However, this is obviously not so in these two complexes.

The rhenium-bromine distance of 2.646(2) Å in $[HOsRe(CO)_8Br]PPN$ agrees with that found in $Re(CO)_5Br$[185] of 2.62(1) Å.

The metal-carbon distances for $[HOsRe(CO)_8Br]PPN$ were found to be in the range 1.85(2)-1.97(2) Å, while the carbon-oxygen distances were found to be in the range 1.08(3)-1.20(2) Å. These are all within the expected ranges. As discussed previously for $Os_2(CO)_8Cl_2$ - section 3.4, $Os_2(CO)_8I_2$ - section 3.5, $Os_3(CO)_{12}Cl_2$ - section 3.2 and $Os_3(CO)_{12}I_2$,[40] there are three types of metal-carbon bonds for both the osmium and the rhenium atoms in $[HOsRe(CO)_8Br]PPN$. For carbonyls bonded to the osmium atom in $[HOsRe(CO)_8Br]PPN$, the shortest osmium-carbon distances - see table 3.6.4(a) and figure 3.19 - were for the two carbonyl ligands trans to the osmium-rhenium bond, i.e. the axial carbonyl ligand, $Os-C_1$, and for one carbonyl ligand trans to another carbonyl ligand, i.e. $Os-C_3$. For carbonyls bonded to the rhenium atom in $[HOsRe(CO)_8Br]PPN$, the shortest rhenium-carbon distance was found for the carbonyl ligand trans to the bromide ligand and not for the axial rhenium-carbon bond - see table 3.6.4(a) and figure 3.19.

The two longest Re-C distances were found for two carbonyl ligands trans to one another, i.e. Re-C_7 and Re-C_8, which is as expected since CO is the strongest π-acceptor ligand and, therefore, competition between two trans CO ligands for metal d-π-electron density is greatest. The longest C-O bond in [HOsRe(CO)$_8$Br]PPN, i.e. C_3-O_3 of 1.20(2) Å was found to correspond with the shortest metal-carbon distance, i.e. Os-C_3 of 1.85(2) Å, while the shortest C-O bond, i.e. C_7-O_7 of 1.08(3) Å was found to correspond with the longest metal-carbon distance, i.e. Re-C_7 of 1.97(2) Å. This is as expected since as the extent of back donation from M to CO increases, the M-C bond becomes stronger and the C≡O bond becomes weaker.

The M'-M-C(equatorial) angles in [HOsRe(CO)$_8$Br]PPN were found to be in the range 81.4(6)-90.1(6)° and averaging 86.0(5)° and were all found to be acute, except for C_5-Re-Os, which was found to be 90.1(6)°. The bending of equatorial carbonyl ligands towards the molecular centre has been attributed to a bonding interaction between the π^* orbitals of the carbonyl groups and the filled d-orbitals on the adjacent metal atom[41] and has been observed for many complexes of this type. The Re-Os-C(equatorial) angles were found to be more acute, ranging from 81.4(6)-86.4(6)° than the Os-Re-C(equatorial) angles which were found to be in the range 86.8(6)-90.1(6)°.

This can possibly be explained by the short osmium-hydrogen distance of 1.66(8) Å, compared to the osmium-carbon(equatorial) distances which were found to be in the range 1.85(2)-1.96(2) Å. This would allow for more spacial distortion of the equatorial carbonyl ligands from octahedral positions on the osmium atom, than is found around the osmium atoms in the neutral compounds, $Os_2(CO)_8X_2$ (X = Cl or I). One very acute angle of 67.2(37)° was found for C_2-Os-H.

In the complex, $Os_4Br(CO)_{13}H_3$,[186] which contains an $Os(CO)_4H$ "spike" bonded to an $Os_3Br(CO)_9H_2$ fragment - see figure 3.21 - the Os_1-Os_4-C(equatorial) angles were found to be in the range 84.8(5)-87.4(4)°. These angles are not quite as acute as was found in [HOsRe(CO)$_8$Br]PPN, i.e. a similar distortion from the expected octahedral geometry around the $Os(CO)_4H$ osmium atom in $Os_4Br(CO)_{13}H_3$ was not observed.

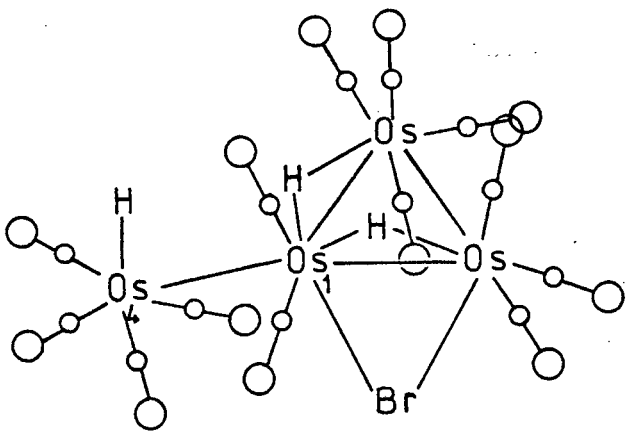

Figure 3.21 The molecular structure of $Os_4Br(CO)_{13}H_3$

A possible explanation for the greater distortion from octahedral geometry found around the osmium atom in $[HOsRe(CO)_8Br]PPN$ than around Os_4 in $Os_4Br(CO)_{13}H_3$[186] above - see figure 3.21 - is that in $[HOsRe(CO)_8Br]PPN$, the rhenium atom is formally negatively charged according to the 18-electron rule. The bonding interaction between the π^* orbitals of the equatorial carbonyl groups on the osmium atom and the filled d-orbitals on the rhenium atom would therefore be stronger, causing the carbonyl groups to bend more inwards towards the molecular centre, than in e.g. $Os_4Br(CO)_{13}H_3$,[186] where the adjacent atom, i.e. Os_1 - see figure 3.21 - is neutral. This bonding interaction in $[HOsRe(CO)_8Br]PPN$ could enable the negative charge to be delocalised over the whole structure, which might also explain the difficulty encountered in the attempted chemical removal of Br^- from $[HOsRe(CO)_8Br]PPN$.

Table 3.6.4(a) Bond Lengths (Å) for the $[HOsRe(CO)_8Br]$ Anion with the Estimated Standard Deviations in Parentheses

Os-Re	2.995(1)
Re-Br	2.646(2)
Os-H_1	1.66(8)
Os-C_1	1.85(2)
Os-C_2	1.96(2)
Os-C_3	1.85(2)
Os-C_4	1.96(2)
Re-C_5	1.86(2)
Re-C_6	1.94(2)
Re-C_7	1.97(3)
Re-C_8	1.96(2)
C_1-O_1	1.19(3)
C_2-O_2	1.12(2)
C_3-O_3	1.20(3)
C_4-O_4	1.13(3)
C_5-O_5	1.18(2)
C_6-O_6	1.15(3)
C_7-O_7	1.08(3)
C_8-O_8	1.14(3)

Table 3.6.4(b) Bond Lengths (Å) for the PPN cation with the Estimated Standard Deviations in Parentheses

P_1-N	1.58(2)
P_2-N	1.54(2)
P_1-C_{111}	1.78(2)
P_1-C_{121}	1.78(1)
P_1-C_{131}	1.79(2)
P_2-C_{211}	1.79(2)
P_2-C_{221}	1.79(1)
P_2-C_{231}	1.77(2)
C_{ring}-C_{ring} in the range	1.33(3)-1.43(3)

Table 3.6.5(a) Bond Angles (°) for the $[HOsRe(CO)_8Br]$ Anion with the Estimated Standard Deviations in Parentheses

H_1-Os-Re	84.4(25)
C_1-Os-Re	175.5(7)
C_1-Os-H_1	91.1(26)
C_2-Os-Re	82.7(6)
C_2-Os-H_1	67.2(37)
C_2-Os-C_1	95.8(8)
C_3-Os-Re	81.4(6)
C_3-Os-H_1	96.0(38)
C_3-Os-C_1	98.8(9)
C_3-Os-C_2	157.9(9)
C_4-Os-Re	86.4(6)
C_4-Os-H_1	163.0(32)
C_4-Os-C_1	98.1(10)
C_4-Os-C_2	97.5(8)
C_4-Os-C_3	96.8(9)
Br-Re-Os	89.5(1)
C_5-Re-Os	90.1(6)
C_5-Re-Br	179.6(5)
C_6-Re-Os	179.7(3)
C_6-Re-Br	90.2(5)
C_6-Re-C_5	90.2(8)
C_7-Re-Os	86.8(6)
C_7-Re-Br	90.3(5)
C_7-Re-C_5	89.7(9)
C_7-Re-C_6	93.4(10)
C_8-Re-Os	88.7(5)
C_8-Re-Br	86.9(4)
C_8-Re-C_5	93.1(9)
C_8-Re-C_6	91.2(9)
C_8-Re-C_7	174.6(7)
O_1-C_1-Os	174.9(18)
O_2-C_2-Os	174.3(19)
O_3-C_3-Os	175.4(18)
O_4-C_4-Os	178.3(17)
O_5-C_5-Re	179.2(21)
O_6-C_6-Re	177.3(15)
O_7-C_7-Re	179.1(16)
O_8-C_8-Re	177.5(13)

Table 3.6.5(b) Bond Angles (°) for the PPN cation with the Estimated Standard Deviations in Parentheses

P_1-N-P_2	158.3(12)
C_{111}-P_1-N	114.1(8)
C_{121}-P_1-N	111.4(7)
C_{121}-P_1-C_{111}	106.0(7)
C_{131}-P_1-N	110.2(8)
C_{131}-P_1-C_{111}	107.2(8)
C_{131}-P_1-C_{121}	107.7(8)
C_{211}-P_2-N	113.7(7)
C_{221}-P_2-N	112.9(7)
C_{221}-P_2-C_{211}	104.2(8)
C_{231}-P_2-N	110.4(9)
C_{231}-P_2-C_{211}	107.5(7)
C_{231}-P_2-C_{221}	107.7(7)
C_{ring}-C_{ring}-C_{ring} in the range	116.5(15)-123.4(21)
C_{ring}-C_{ring}-P in the range	118.1(4)-124.8(15)

3.6.5 Conclusion

The structure of $[HOsRe(CO)_8Br]PPN$ has been determined by X-Ray crystallography and the solution and least-squares refinements led to a conventional weighted R factor of 0.039. The anion, $[HOsRe(CO)_8Br]$, adopts a structure with an osmium-rhenium single bond, and with the terminal hydride and bromide ligands occupying equatorial sites on the osmium and rhenium atoms, respectively. The two parts of the anion exist in a staggered conformation with respect to each other. The structural determination of $[HOsRe(CO)_8Br]PPN$ has provided previously unknown data on osmium-rhenium distances in dinuclear complexes.

CHAPTER 4

HETERO DI- AND TRI-NUCLEAR CARBONYL COMPLEXES CONTAINING OSMIUM

4.1 Introduction

The design and synthesis of coordination compounds which contain two different metal ions are priority goals of contemporary inorganic chemistry.[187-190] A large number of heteronuclear metal-metal bonded compounds have been prepared and characterised but relatively few have had their chemistry explored and even fewer have shown catalytic activity.[191-193] This is surprising in view of the unique reactivity features which may accrue to these systems as a result of adjacent metals possessing differing chemical properties. The lack of catalytic activity appears to be partly due to the absence of open coordination sites or easily dissociable ligands in the complexes examined.[194] Another problem inherent with low-valent metal-metal bonded complexes is their susceptibility to cleavage of the metal-metal bond during reaction.[195,12]

The low symmetry which mixed-metal clusters inherently possess can allow a differentiation of specific sites of reactivity and can, therefore, provide important insight into reaction mechanisms.[7] Mixed-metal clusters are also ideally suited for studies of fluxional processes in which the carbonyls, hydrides and even the metals themselves, undergo rearrangement. In such clusters, the majority of ligands are in chemically non-equivalent environments and are thus distinguishable by nmr spectroscopy.

Many mixed-metal clusters have been prepared by nongeneral, serendipitous methods and often their yields have been quite low.[192] Procedures in which potential constituents are mixed and caused to react randomly, are generally unattractive because separation is usually difficult and inefficient, even by chromatographic techniques. However, these have been the type of reactions by which many mixed-metal carbonyl complexes are currently only obtainable.[196]

The most widely applicable basis for rational synthesis depends on the reaction of carbonylate anions with metal carbonyl halides causing elimination of halide ion.[196] The general reaction may be represented by:

$$[M_n(CO)_x]^- + XM'(CO)_y \xrightarrow{\pm z\ CO} M_nM'(CO)_{x+y\pm Z} + X^-$$

The synthetic approach is so designed that, like metal atoms cannot react with each other.[196] Examples of this type of approach are:

$$[Mn(CO)_5]^- + Re(CO)_5Br \longrightarrow (OC)_5MnRe(CO)_5 + Br^-$$

$$2[Co(CO)_4]^- + \text{trans-}PtCl_2py_2 \longrightarrow (OC)_4Co\text{-}Pt(Py)_2\text{-}Co(CO)_4 + 2Cl^-$$

The carbonylate anions can be obtained in a number of ways - by treating metal carbonyls with aqueous or alcoholic alkali hydroxide or with amines, sulfoxides or other Lewis bases, by cleaving metal-metal bonds with sodium or, in special cases, by refluxing carbonyls with salts in an ether medium.[196] A sodium-potassium alloy has also been efficiently utilised for the production of metal carbonyl anions.[197]

The nucleophilicities of anionic metal carbonyl derivatives vary enormously. For this reason, there are major differences between the chemistries of different metal carbonyl anions. The preparative applications of metal carbonyl anions depend on their reactivity as nucleophiles toward electrophilic reagents.[198]

Many carbonyl anions are known within the iron triad. Two mononuclear carbonyl anions of osmium were obtained from the action of sodium in liquid ammonia on $Os_3(CO)_{12}$.[199] A saturated solution of the product in THF showed ν(CO) bands in the IR spectrum which could be attributed to both $[Os(CO)_4]^{2-}$ and $[Os(CO)_4H]^-$. The monoanion had been obtained previously through the action of sodium sand on $Os(CO)_4H_2$.[200] Reaction of the anionic mixture of $[Os(CO)_4]^{2-}$ and $[Os(CO)_4H]^-$ with 2 equivalents of various halide compounds per g-atom of osmium employed gave $Os(CO)_4X_2$ (X = Me, H_3Ge, Ph_3Sn, Me_3Pb and $AuPPh_3$) as well as, on occasion, the formation of minor products

of $Os(CO)_4HX$ (X = Me and H_3Ge).[199] The preparation and chemistry of $[Os(CO)_4]^{2-}$ and its ruthenium analogue $[Ru(CO)_4]^{2-}$ have been reviewed.[201]

Effective syntheses for $[M(CO)_4H]PPN$ (M = Ru or Os; PPN = bis(triphenylphosphine)iminium) have recently been reported.[202] Treatment of the appropriate $[M(CO)_4]Na_2$ salt in methanol with [PPN]Cl at -78°C afforded the product in 60% yield. At 25°C, in methanol, rapid decomposition of $[Ru(CO)_4H]^-$ led to the formation of $[Ru_3(CO)_{11}H]^-$. It was proposed[203] that this decomposition proceeds via protonation of $[Ru(CO)_4H]^-$ to afford $Ru(CO)_4H_2$ which then further reacts to give $[Ru_3(CO)_{11}H]^-$ as a final product. The lability of $Ru(CO)_4H_2$ was suggested to be due to rapid, reversible hydride migration to form the unsaturated formyl complex, $Ru(CHO)(CO)_3H$. Another possible explanation for the lability of $Ru(CO)_4H_2$ is that the hydride ligands labilise the molecule toward CO dissociation.[203,204]

Trinuclear anions, $[Fe_3(CO)_{11}H]^-$ [205] and $[Os_3(CO)_{11}H]^-$ [206] are also known. Stoichiometric reduction of $Os_3(CO)_{12}$ and $Ru_3(CO)_{12}$ with benzophenone-potassium, respectively, yielded two new cluster dianions $[Os_3(CO)_{11}]^{2-}$ and $[Ru_3(CO)_{11}]^{2-}$ which have been isolated and characterised.[207] Both these dianions reacted with one equivalent of HCl to form the hydrido monoanions, respectively.

The interest in linear polymetallic chains and their possible significance in the search for unidimensional conductors has been outlined in chapter 1. The heteroatomic pentanuclear linear compounds,[82] $Cl(OC)_4Os\text{-}Os(CO)_4\text{-}Os(CO)_4\text{-}SnCl_2\text{-}M(CO)_nL$, ($M(CO)_nL$ = $W(CO)_3(\eta\text{-}C_5H_5)$, $Re(CO)_5$ and $Fe(CO)_2(\eta\text{-}C_5H_5)$, were obtained by reaction of the osmium carbonyl species, $ClOs_3(CO)_{12}SnCl_3$,[83] with the corresponding carbonylmetalate species. In these reactions, the presence of readily replaceable halogen ligands on the tin moiety allowed for chain extension. The exciting potential illustrated by these reactions prompted the synthetic study presented in this thesis.

The mononuclear dianion, $[Os(CO)_4]^{2-}$, has the capacity to coordinate two one-electron acceptors. For example, it can coordinate two protons to form $Os(CO)_4H_2$. In terms of the abovementioned chain extension reactions, $[Os(CO)_4]^{2-}$ could coordinate two metal carbonyl groups to produce a polynuclear species. The hydrido monoanion, $[Os(CO)_4H]^-$, could coordinate a one-electron acceptor to produce, e.g. $Os(CO)_4H_2$ or $HOs(CO)_4M$ (M = metal carbonyl species). The hydride ligand could be replaced by a halide ligand which, in turn, is readily replaceable by a further carbonylmetalate species.

Careful selection of the metal carbonyl species for employment in reaction with the osmium species, could result in the reaction process being repeated many times to produce

an ever-increasing chain length of covalently-bound metal atoms. The important criterion for the success of this scheme, however, would hypothetically be to ensure that the replaceable hydride or halide ligand was always situated coaxial with the metal-metal bond. If this is not the case, and isomerization did not occur, the chain would be more likely to double back on itself and thus inhibit chain extension. The termination step of the reaction sequence would be reaction with a carbonyl-metalate which does not contain a terminal hydride ligand, e.g. $[M(CO)_5]^-$. With the belief in the rationale of the above synthetic scheme, the present study was undertaken.

4.2 Results and Discussion

4.2.1 Synthesis of Heteronuclear Derivatives of Osmium containing Rhenium

4.2.1.1 Reaction between $[Os(CO)_4]Na_2$ and $Re(CO)_5Br$ in a 1:2 Molar Ratio

Reaction of $[Os(CO)_4]Na_2$[199] with two equivalents of $Re(CO)_5Br$, at room temperature and with typical reaction times of 20 hours, resulted in a mixture of products being obtained. Removal of the solvent and extraction of the oily residue with n-hexane, gave a clear yellow solution and an orange, hexane insoluble solid. The hexane solution was found to contain $HOsRe(CO)_9$, $Re_2(CO)_{10}$ and

$Re_2Os(CO)_{14}$. $HOsRe(CO)_9$ and $Re_2(CO)_{10}$ were separated from $Re_2Os(CO)_{14}$ by sublimation (30°C/0.01 mm Hg). $HOsRe(CO)_9$ and $Re_2(CO)_{10}$ were more difficult to separate. Both compounds were found to sublime at similar temperatures, to have similar solubilities and $HOsRe(CO)_9$ was found to be difficult to recover from chromatographic separation methods. Pure $HOsRe(CO)_9$ was obtained by repeated sublimation, but in a much reduced yield. A ^1H nmr spectrum run on a sample of pure $HOsRe(CO)_9$, showed a high field singlet at 20.37τ in d_6-benzene and after several days of standing in solution showed an additional peak at 20.11τ in the position expected for $Os_2(CO)_8H_2$. This might suggest that $HOsRe(CO)_9$ possibly decomposes to $Os_2(CO)_8H_2$ and $Re_2(CO)_{10}$ and could explain the difficulty experienced in attempts to separate $HOsRe(CO)_9$ from $Re_2(CO)_{10}$. However, a solution of $HOsRe(CO)_9$ in n-hexane on standing for several days did not show additional ν(CO) bands of $Re_2(CO)_{10}$ in the IR spectrum. $HOsRe(CO)_9$ was identified by the ν(CO) bands in the IR spectrum, by a molecular ion at m/e 629 corresponding to $[HOsRe(CO)_9]^+$ with sequential loss of nine carbonyl groups and by a high field singlet at 20.37τ in the ^1H nmr spectrum; all data were found to be in agreement with the literature.[126,208] $Re_2Os(CO)_{14}$, a yellow microcrystalline compound, which was recrystallised from acetone, was identified by comparison of the ν(CO) bands in the IR spectrum with those reported in

the literature.[37] The mass spectrum of this compound revealed a molecular ion at m/e 958, corresponding to $[Re_2Os(CO)_{14}]^+$ with sequential loss of fourteen carbonyl groups, all peaks displaying the correct polyisotopic patterns. $Re_2Os(CO)_{14}$ was previously obtained from the reaction of $Re_2(CO)_{10}$ with $Os_3(CO)_{12}$.[37]

The hexane insoluble product, after removal of $HOsRe(CO)_9$, $Re_2(CO)_{10}$ and $Re_2Os(CO)_{14}$, showed ν(CO) bands in the IR spectrum in THF at 2089(sh) 2077(w) 2040(w) 2004(sh) 1995(s) 1970(m) 1909(sh) 1877(vs) cm^{-1}. The low frequency ν(CO) band at 1877(vs) cm^{-1} suggested that this product might be anionic. An IR spectrum of the solution reported to contain the sodium salt of the dinuclear dianion, $[Os_2(CO)_8]^{2-}$, showed a strong ν(CO) band at 1878 cm^{-1}; the IR spectrum of $[Os_2(CO)_8H]^-$ in CH_3CN[209] gave a strong low frequency ν(CO) band at 1882 cm^{-1}. The dinuclear anion $[FeMn(CO)_9]^-$ also displayed a low frequency band at 1870 cm^{-1} in its IR spectrum run as a Nujol mull.[210] By comparison, it would appear likely that the hexane insoluble product of this reaction contains the sodium salt of an anion. Treatment of a THF solution of this salt with acetic acid resulted in the formation of a hexane soluble compound, some of the ν(CO) bands in the IR spectrum of which could be assigned to $HOsRe(CO)_9$. This suggested that the hexane insoluble product might contain $[OsRe(CO)_9]Na$.

In a separate experiment, protonation of the hexane insoluble product resulted in four hydride signals being observed in the ^{1}H nmr spectrum of the hexane soluble protonated product, one of which could possibly be assigned to $HOsRe(CO)_9$. A chromatographic separation of this protonated product revealed the presence of four species, as four separate bands were observed. These compounds could not be identified due to small amounts of material available. This presence of four protonated species indicated that either the hexane insoluble product was a mixture of components or that cleavage of the molecule had occurred on protonation, possibly leading to the formation of mononuclear hydride species. The anionic product was not further characterised. Isolated as the sodium salt, the compound could possibly have been unstable and could have decomposed in solution, thus making its purification difficult.

4.2.1.2 Reaction between $[Os(CO)_4]Na_2$ and $Re(CO)_5Br$ in a 1:1 Molar Ratio

Reaction of $[Os(CO)_4]Na_2$[199] with one equivalent of $Re(CO)_5Br$ in THF at room temperature and typical reaction times of 20 hours, also resulted in a mixture of products being obtained. Removal of the solvent and extraction of the oily residue with n-hexane gave a clear yellow solution and an orange hexane insoluble solid. $HOsRe(CO)_9$ and

$Re_2(CO)_{10}$ were found to be present in the hexane solution and were separated with difficulty and with loss of product yield by repeated sublimations (30°C/0.01 mm Hg) as mentioned above. The proportion of $Re_2(CO)_{10}$ which collected on the cold finger was found to decrease with successive sublimations. The hexane insoluble solid was dissolved in methanol and treated with [PPN]Cl. Separation by fractional crystallisation yielded two pure anionic products. Elemental analyses showed these products to be $[HOsRe(CO)_8Br]PPN$ and $[OsRe(CO)_9]PPN$, respectively. A high field singlet at 20.50τ was observed in the ^1H nmr spectrum in d_6-benzene of $[HOsRe(CO)_8Br]PPN$. The $\nu(CO)$ bands in the IR spectrum of the hexane insoluble solid were identical with those observed for the hexane insoluble solid mixture obtained in the reaction of $[Os(CO)_4]Na_2$ with 2 equivalents of $Re(CO)_5Br$. This possibly indicated that $[HOsRe(CO)_8Br]PPN$ and $[OsRe(CO)_9]PPN$ were also components of the anionic product obtained in the reaction 4.2.1.1 above. The $\nu(CO)$ bands in the IR spectrum in THF of $[HOsRe(CO)_8Br]PPN$ occurred at 2091(w) 2043(s) 2019(m) 1990(vs) 1979(sh) 1955(s) 1948(s) 1895(s) cm^{-1}. The IR spectrum of $[OsRe(CO)_9]PPN$ in THF displayed $\nu(CO)$ bands at 2042(w) 2022(sh) 2005(sh) 1998(vs) 1955(sh) 1945(sh) 1925(m) 1880(sh) 1876(vs) cm^{-1}.

Protonation of the anionic mixture, using CF_3COOH in CH_3CN, (a reagent employed by Norton[209] as a more efficient

protonation system), yielded $HOsRe(CO)_9$, after 2 hours, in low yield, as a hexane-soluble product. This hexane insoluble product showed almost identical $\nu(CO)$ bands in the IR spectrum in THF as the starting anionic mixture of this reaction. This result indicated that either the reaction time was insufficient or that the anionic mixture contained a very stable anion which resisted protonation, under the conditions employed.

A mixed-metal anionic complex, $[FeMn(CO)_9]PPN$, analagous to the latter anionic product, $[OsRe(CO)_9]PPN$, has been prepared by the reaction between $Fe(CO)_5$ and $[Mn(CO)_5]PPN$ in THF.[210] The IR spectrum of this product in CH_2Cl_2 displayed $\nu(CO)$ bands at 2066(w) 2024(w) 1968(vs) 1937(m,sh) 1870(m) cm^{-1}.

If a simple metal-metal bond exists in the $[OsRe(CO)_9]^-$ anion, then the rhenium would be expected to be in an octahedral environment. The coordination around the osmium would be in the form of either a tetragonal pyramid or a trigonal pyramid, as shown in figure 4.1.

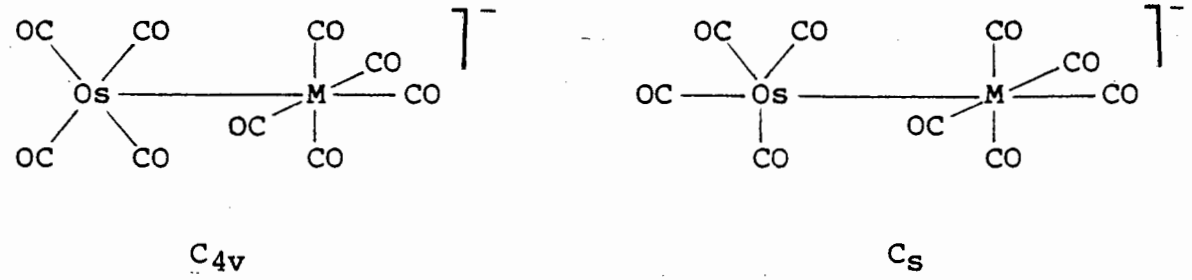

Figure 4.1 Proposed structures for the $[OsM(CO)_9]^-$ anion.

The former configuration would result in an overall symmetry for the ion of C_{4v}, while the latter would result in C_s symmetry. This would lead to the expectation of five (3A and 2E) or nine (6A' and 3A") IR ν(CO) stretching frequencies, respectively, assuming that coupling of the carbonyl vibrations occurs across the metal-metal bond.[210] Since eight ν(CO) bands, including clearly defined shoulders, are observed in the spectra of these compounds, it would appear that the structure with C_s symmetry is the favoured one for these ions.

The reactions of $[Os(CO)_4]Na_2$ with $Re(CO)_5Br$ can be summarised as follows:

1. $[Os(CO)_4]Na_2 + 2Re(CO)_5Br \xrightarrow[R\ T]{THF}$

(hexane-soluble)	+	(hexane-insoluble)
1) $HOsRe(CO)_9$		anionic product (I)
2) $Re_2(CO)_{10}$		+ 2NaBr
3) $Re_2Os(CO)_{14}$		

[I] $\xrightarrow[THF]{CH_3COOH}$ $HOsRe(CO)_9$ + anionic product (II)

2. $[Os(CO)_4]Na_2 + Re(CO)_5Br \xrightarrow[R\ T]{THF}$

(hexane-soluble)	+	(hexane-insoluble)
1) $HOsRe(CO)_9$		1) $[OsRe(CO)_9]Na$(I)
2) $Re_2(CO)_{10}$		2) $[HOsRe(CO)_8Br]Na$(II)
		3) NaBr

[I] + [II] $\xrightarrow[MeOH]{[PPN]Cl}$ $[OsRe(CO)_9]PPN + [HOsRe(CO)_8Br]PPN$

The use of [PPN] cations in the isolation of many metal carbonyl anions has proved fruitful.[210] The [PPN] cation was, in this study, found to impart stability to these carbonyl anions, at least in the solid state.

The presence of $HOsRe(CO)_9$ and $[HOsRe(CO)_8Br]PPN$ as products of the above two reactions concurred with the findings of George et al.[199] It would appear that $[Os(CO)_4H]Na$ had been present as a contaminant in $[Os(CO)_4]Na_2$ and had reacted with $Re(CO)_5Br$. Thus, the reaction of $[Os(CO)_4H]PPN$ with one equivalent of $Re(CO)_5Br$ was investigated.

4.2.1.3 Reaction between $[Os(CO)_4H]PPN$ and $Re(CO)_5Br$ in a 1:1 Molar Ratio

Reaction of $[Os(CO)_4H]PPN$ with one equivalent of $Re(CO)_5Br$ resulted in the formation of a number of products. The major products isolated were $HOsRe(CO)_9$ and the new anionic compound, $[HOsRe(CO)_8Br]PPN$. The formation of $[OsRe(CO)_9]PPN$ and $Re_2Os(CO)_{14}$ obtained in very low yields, could be explained by a small amount of $[Os(CO)_4]^{2-}$ being present as an impurity in $[Os(CO)_4H]PPN$, possibly resulting from an incomplete protonation reaction.

After typical reaction times of 20 hours for the reaction of $[Os(CO)_4H]PPN$ with $Re(CO)_5Br$, the solvent was removed

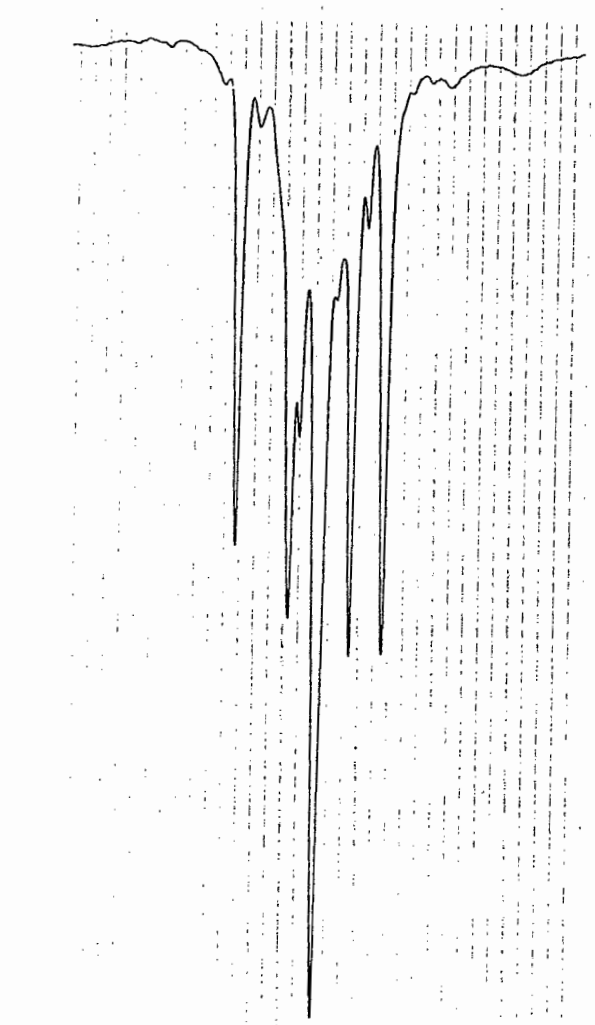

a)

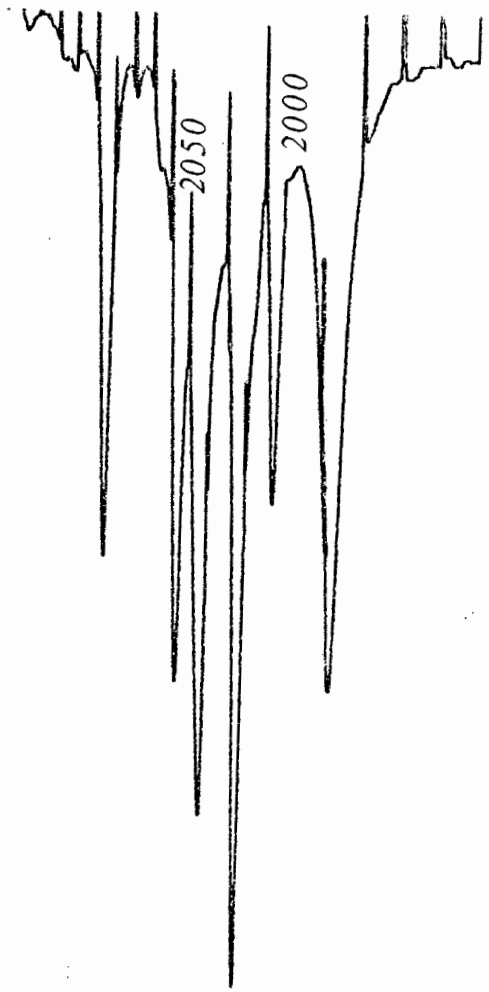

b)

Figure 4.2 IR spectra of a) $HOsRe(CO)_9$, and b) $BrOsRe(CO)_9$ in n-hexane.

and the oily, yellow residue extracted with n-hexane to yield a pale yellow solution and a yellow-orange, hexane insoluble solid. An IR spectrum of the hexane extract showed that $HOsRe(CO)_9$ had been obtained pure, uncontaminated by $Re_2(CO)_{10}$, in this reaction. An IR spectrum run on a very concentrated solution of $HOsRe(CO)_9$ showed a weak band at 1942 cm^{-1} which we tentatively assign to ν(Os-H). $HOsRe(CO)_9$ has previously only been reported to be obtained as a component of a mixture.[126,208] The ν(CO) bands in n-hexane are here reported as occurring at: 2092(w) 2081(s) 2068(w) 2046(s) 2040(m) 2028(vs) 2005(s) 1997(w) 1984(s) cm^{-1} - see figure 4.2(a). A high field singlet at 20.37 τ was observed in the ^1H nmr spectrum in d_6-benzene in agreement with the literature[126,208] An osmium-hydrogen coupling constant, ^1J (^{187}Os-^1H) = 37.5 Hz, was measured - see section 5.3.2. A correlation between the calculated and observed polyisotopic pattern for the parent ion $[HOsRe(CO)_9]^+$ can be seen in figure 4.3.

The hexane-insoluble product was recrystallized from a methanol/ether solvent system to give a yellow, crystalline compound. An IR spectrum in THF displayed ν(CO) bands at 2091(w) 2043(s) 2019(m) 1990(vs) 1979(sh) 1955(s) 1948(s) 1895(s) cm^{-1} - see figure 4.4(a). A Far IR spectrum as a Nujol mull showed a strong band at 179 cm^{-1}, which we tentatively assign to ν(Re-Br) in comparison with ν(Re-Br) in $Re(CO)_5Br$[184] at 203 cm^{-1}.

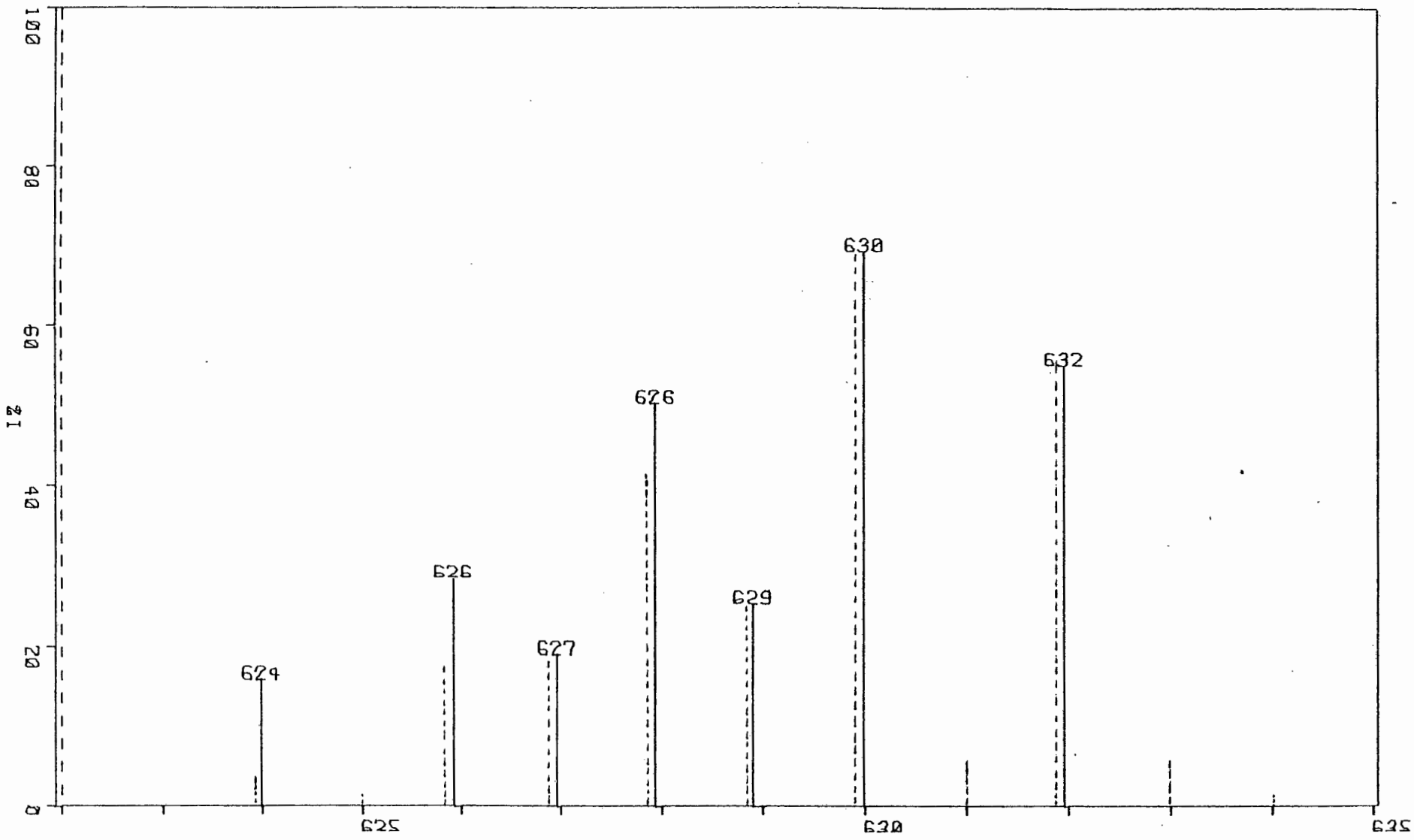

Figure 4.3 Comparison of observed (-) and calculated (---) polyisotopic distribution of the parent ion, $[HOsRe(CO)_9]^+$.

A ^{1}H nmr spectrum in CD_3CN showed a high field singlet at 20.5τ . An osmium-hydrogen coupling constant $^{1}J(^{187}Os-^{1}H)$ = 40.5 Hz was measured - see section 5.3.2. A minor peak at 20.65τ was also observed in the spectrum and was assigned to an impurity present in solution - see section 5.3.2. Elemental analysis indicated the compound to be of molecular formulation $[HOsRe(CO)_8Br]PPN$. That the anion was present as a PPN salt was evident from the addition of $NaBPh_4$ to a methanol solution of the compound which resulted in the formation of a white precipitate (mpt 270°-275°C). An identical precipitate of $[PPN]BPh_4$ was obtained on the addition of a methanol solution of $NaBPh_4$ to a methanol solution of [PPN]Cl. The compound was further characterised by protonation with CF_3COOH in CH_3CN.[209] The products of this reaction were identified as $Os(CO)_4H_2$ (a volatile product trapped at -196°C) and $[Re(CO)_4Br]_2$. Pure samples of these latter compounds were synthesised[200,122] and their ^{1}H nmr and/or IR spectra determined in CH_3CN. The ^{1}H nmr spectrum of $Os(CO)_4H_2$ showed a high field singlet at 19.07τ , while the ν(CO) bands in the IR spectrum appeared at 2144(vw) 2070(sh) 2055(sh) 2048(s) cm^{-1}. $[Re(CO)_4Br]_2$ gave ν(CO) bands in its IR spectrum in CH_3CN at 2120(w) 2021(vs) 2000(m) 1948(s) cm^{-1}. The dropwise addition of one equivalent of the halide abstractor, $AgBF_4$, as a solution in acetone, to an acetone solution of $[HOsRe(CO)_8Br]PPN$ was shown to produce a white precipitate after standing without

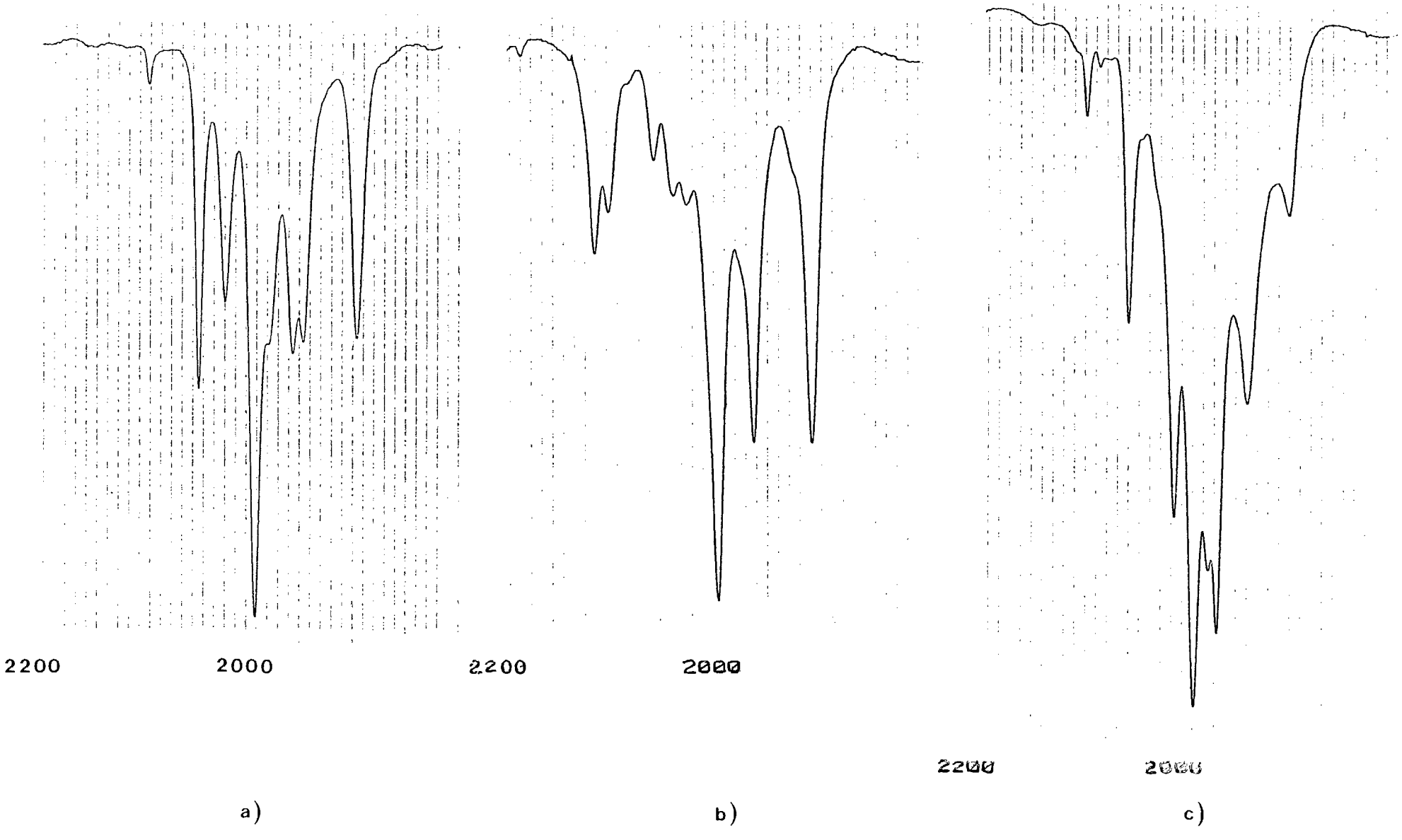

Figure 4.4 IR spectra of a) $[HOsRe(CO)_8Br]PPN$, b) $[BrOsRe(CO)_8Br]PPN$, and c) $[HOsMn(CO)_8Br]PPN$ in THF.

stirring for several days. The supernatant liquid was syringed off and the solvent removed under reduced pressure. An IR spectrum revealed that reaction had occurred. However, the reaction was conducted on such a minute scale that identification of this product was not attempted, although it was believed that the bromide ligand has been removed by precipitation as AgBr.

The dirhenium hydrido anionic complex, $[Re_2(CO)_9H]NEt_4$,[212] is known. The IR spectrum of this anion showed ν(CO) bands in THF at 2078(vw) 2028(m) 1972(s) 1924(m) 1888(m) cm^{-1}. The low frequency of the ν(CO) band at 1888 cm^{-1} was indicative that the compound was of an anionic nature. The diosmium hydrido anion, $[Os_2(CO)_8H]^-$ recently reported by Norton,[209] showed ν(CO) bands in its IR spectrum in CH_3CN at 2085(w) 2077(sh) 2026(m) 1996(vs) 1935(m) 1905(sh) 1882(vs) cm^{-1} and a high field singlet at 20.65τ in the ^1H nmr spectrum run in CD_3CN. Since these data are similar to those obtained for $[HOsRe(CO)_8Br]PPN$, it is possible that the hydride ligand is in a similar electronic environment in the two compounds. The structure proposed[183] for the diosmium anion can be seen in figure 4.5. On the basis of the number of ν(CO) bands observed in the IR spectrum, it could be predicted that an unsymmetrical structure analagous to those determined in this thesis for diosmium octacarbonyl dihalides, e.g. $Os_2(CO)_8X_2$ (X = Cl or I) might be adopted by the osmium-rhenium anion.

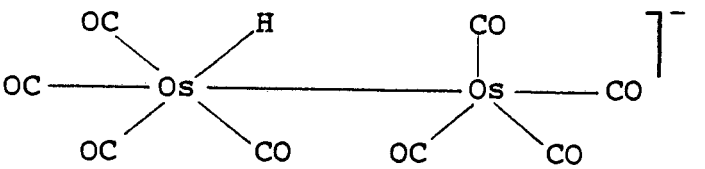

Figure 4.5 Proposed structure for the $[Os_2(CO)_8H]$ anion

Thus equatorial positioning of the hydride and bromide ligands with the molecule adopting a staggered conformation might be expected for $[HOsRe(CO)_8Br]PPN$ - as shown in figure 4.6. This was indeed the structure found for $[HOsRe(CO)_8Br]PPN$ as determined by X-Ray crystallography - see section 3.6.

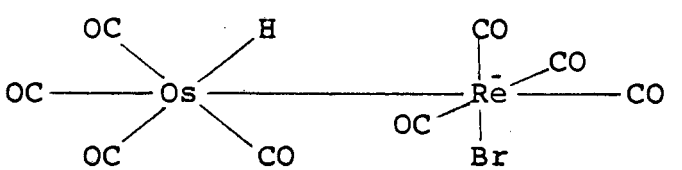

Figure 4.6 Proposed structure for the $[HOsRe(CO)_8Br]$ anion

Similar to that proposed for $[Os_2(CO)_8H]^{-}$[182] the IR spectrum in the $\nu(CO)$ region of $[HOsRe(CO)_8Br]PPN$ has a range of 200 cm^{-1}, which is more consistent with a

formally neutral [$Os(CO)_4H$] unit and a formally negatively charged [$Re(CO)_4Br$] unit, than with the charge being completely delocalised over the structure. Interestingly, though, it is apparent from the products obtained from the protonation reaction, that it is the [$Os(CO)_4H$] unit which undergoes protonation and not the [$Re(CO)_4Br$] unit, as might be expected. Attempts to further characterise the anion were also carried out. Reaction of [$HOsRe(CO)_8Br$]PPN with CH_3I in THF for 1.5 days, at room temperature, with subsequent removal of the solvent and recrystallization of the product from a methanol/ether solvent system, yielded white needles. The product was obtained in too low a yield to enable characterisation by microanalysis. However, the product was believed to be [$IOsRe(CO)_8Br$]PPN, by a comparison of the pattern of the ν(CO) bands in the IR spectrum in THF with those of the product, believed to be [$BrOsRe(CO)_8Br$]PPN obtained from the reaction of [$HOsRe(CO)_8Br$]PPN with CBr_4 - see table 4.2. Both [$IOsRe(CO)_8Br$]PPN and [$BrOsRe(CO)_8Br$]PPN revealed no high field singlet in their respective ^1H nmr spectra, indicative that the hydride ligand had been replaced and neither reaction produced volatile products, indicative that cleavage of the metal-metal bond had not occurred. The ν(CO) bands in the IR spectrum of both products occurred at similar positions and displayed intensities similar to those observed for the hydrido anion and thus analagous structures could be proposed for these halo derivatives.

The reaction of $[Os(CO)_4H]PPN$ with $Re(CO)_5Br$ can be summarised as follows:

$$[Os(CO)_4H]PPN + Re(CO)_5Br \xrightarrow[R\ T]{THF}$$

(hexane-soluble) + (hexane-insoluble)

$HOsRe(CO)_9$ + $[HOsRe(CO)_8Br]PPN$ + $[PPN]Br$

The distribution of product yield percentages was believed to critically depend on the purity of $[Os(CO)_4H]PPN$, employed as the starting material in this reaction. The yield of $HOsRe(CO)_9$, which was obtained pure in this reaction, uncontaminated by $Re_2(CO)_{10}$, was believed to be dependent on the amount of $[Os(CO)_4]PPN_2$ present as an impurity in $[Os(CO)_4H]PPN$. Any $[Os(CO)_4]PPN_2$ present would have also reacted with $Re(CO)_5Br$ to produce $[OsRe(CO)_9]PPN$. This anionic product could have then abstracted a proton from the solvent to produce $HOsRe(CO)_9$.

4.2.1.4 Reaction between $[Os(CO)_4H]PPN$ and $Re(CO)_5I$ in a 1:1 Molar Ratio

Reaction of $[Os(CO)_4H]PPN$ with an equivalent of $Re(CO)_5I$ resulted in the formation of three products which were

identified as $Re_2(CO)_{10}$, $IOsRe(CO)_9$ and $[HOsRe(CO)_8I]PPN$. After a reaction time of 4 hours, the solvent was removed and the oily, orange residue extracted with n-hexane to yield a pale yellow-orange solution and a yellow-orange hexane insoluble solid. An IR spectrum of the hexane extract showed $\upsilon(CO)$ bands of unreacted $Re(CO)_5I$, $Re_2(CO)_{10}$ and $IOsRe(CO)_9$. Unreacted $Re(CO)_5I$ was removed by fractional sublimation (60°C/0.01 mm Hg). Attempts to separate $Re_2(CO)_{10}$ and $IOsRe(CO)_9$ by fractional sublimation were unsuccessful and yields of the products were too low to risk loss of product by a chromatographic separation. In the mass spectrum of the hexane extract, initial scans showed peaks corresponding to both $Re_2(CO)_{10}$ and $IOsRe(CO)_9$ which confirmed that the product was a mixture. However, in later scans, peaks corresponding to $IOsRe(CO)_9$ were more prominent, showing a parent ion at $^m/_e$ 758 with subsequent losses of nine carbonyl groups to give a peak at $^m/_e$ 504 corresponding to the positive ion $[IOsRe]^+$. The $\upsilon(CO)$ bands in the IR spectrum of the mixture were identified as being those of $Re_2(CO)_{10}$[187] and $IOsRe(CO)_9$, the latter by comparison with the IR spectrum in the $\upsilon(CO)$ region of the product of the reaction of $HOsRe(CO)_9$ with CH_3I, believed to be $IOsRe(CO)_9$ - see section 4.2.4.1. The hexane soluble product, $HOsRe(CO)_9$ is believed to have formed initially by nucleophilic attack of $[Os(CO)_4H]PPN$ on $Re(CO)_5I$ with loss of I^- rather than CO. Further reaction of $Re(CO)_5I$ with

$HOsRe(CO)_9$ could lead to the formation of $IOsRe(CO)_9$.

The hexane insoluble product was recrystallised from a methanol/water solvent system to give a yellow crystalline compound in 81% yield. An IR spectrum of the compound in THF displayed υ(CO) bands at 2090(w) 2042(s) 2020(m) 1990(vs) 1980(sh) 1954(m) 1949(m) 1898(m) cm^{-1}. The ^1H nmr spectrum in CD_3CN showed a high field singlet at 20.5 τ. The pattern of the υ(CO) bands was identical to that observed for $[HOsRe(CO)_8Br]PPN$. Elemental analysis indicated the compound to be of molecular formulation, $[HOsRe(CO)_8I]PPN$. The two analogues are proposed to have similar structures - see section 3.6.

4.2.2 Synthesis of Heteronuclear Derivatives of Osmium Containing Manganese

4.2.2.1 Reaction between $[Os(CO)_4]Na_2$ and $Mn(CO)_5Br$ in a 1:2 Molar Ratio

Reaction of $[Os(CO)_4]Na_2$[199] with two equivalents of $Mn(CO)_5Br$, at room temperature and with typical reaction

times of 20 hours, resulted in a mixture of products being formed, as was found for the analagous rhenium reaction. Removal of the solvent and extraction of the oily residue with n-hexane, gave a clear yellow solution and an orange, hexane insoluble solid. The hexane solution was found to contain $HOsMn(CO)_9$, $Mn_2(CO)_{10}$ and $Mn_2Os(CO)_{14}$. Attempts to separate $HOsMn(CO)_9$ from $Mn_2(CO)_{10}$ by sublimation, column chromatography and on the basis of solubility differences, proved to be unsuccessful. IR and mass spectroscopy indicated that the products of these attempted separations were still present as mixtures of the two components. These two products were separated from $Mn_2Os(CO)_{14}$ by sublimation (50°C/0.1 mm Hg). The presence of $HOsMn(CO)_9$ was indicated by a high field singlet in the ^1H nmr spectrum of a C_6D_6 solution of the sublimate at 19.80 τ. A parent ion at m/e 499, corresponding to $[HOsMn(CO)_9]^+$ in the mass spectrum was observed with sequential loss of nine carbonyl groups, the peaks of which were clearly distinguishable from those corresponding to $Mn_2(CO)_{10}$. The IR spectrum of the material which collected on the cold finger in n-hexane showed ν(CO) bands corresponding to $Mn_2(CO)_{10}$ at 2046(s) 2014(vs) 1984(s) cm^{-1} and, in addition, ν(CO) bands at 2091(vw) 2067(w) 2055(m) 2037(s) 1993(w) cm^{-1}. By analogy with the corresponding rhenium reaction, these latter bands were attributed to $HOsMn(CO)_9$ being present as a component of the mixture. $Mn_2Os(CO)_{14}$, a pale yellow crystalline compound, was recrystallised from acetone by

cooling and was identified by comparison of the ν(CO) bands in the IR spectrum with those values reported in the literature[37] of 2068(s) 2020(vs) 1987(m) cm^{-1}. An additional band at 2036(m) cm^{-1} was observed in the IR spectrum of $Mn_2Os(CO)_{14}$ in the present work, which might have been obscured in previously observed spectra. A further possibility is that a different isomer of $Mn_2Os(CO)_{14}$ may have formed in this reaction. The analagous compound, $Re_2Fe(CO)_{14}$, has been reported[213] to display four ν(CO) bands in its IR spectrum at 2097(m) 2034(m) 2022(s) 1982(m) cm^{-1} and, therefore, the observation of four ν(CO) bands for $Mn_2Os(CO)_{14}$ is not unreasonable. A molecular ion at m/e 694 displaying the correct polyisotopic pattern corresponding to $[Mn_2Os(CO)_{14}]^+$ was observed in the mass spectrum with sequential loss of fourteen carbonyl groups. Figure 4.7 shows the correlation between the computed and the actual polyisotopic patterns obtained for the parent ion $[Mn_2Os(CO)_{14}]^+$. $Mn_2Os(CO)_{14}$ was previously reported to be obtained from the reaction between $Mn_2(CO)_{10}$ and $Os_3(CO)_{12}$[37] and was characterised only by IR spectroscopy.

The hexane insoluble product showed ν(CO) bands in the IR spectrum in THF at 2083(vw) 2068(w) 2042(m) 2009(vs) 1997(sh) 1982(m) 1920(s) cm^{-1}. The appearance of the strong ν(CO) band at 1920 cm^{-1} in the IR spectrum, suggested that the compound might be anionic. Protonation of this product with acetic acid in THF with stirring for

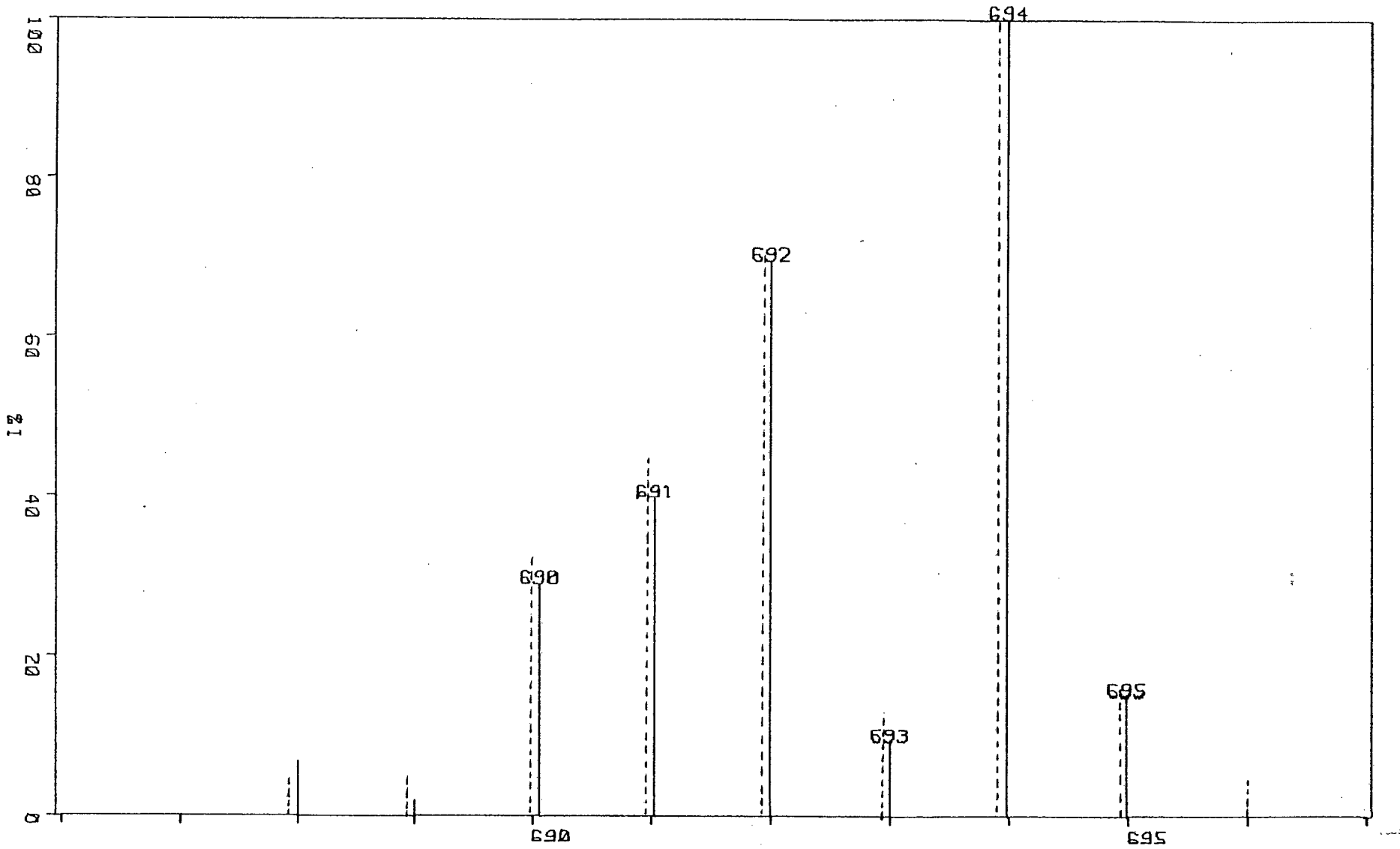

Figure 4.7 Comparison of observed (-) and calculated (---) polyisotopic distribution of the parent ion, $[Mn_2Os(CO)_{14}]^+$.

1 hour showed from an IR spectrum of the hexane extract, after removal of solvent, that $Mn_2(CO)_{10}$ and $HOsMn(CO)_9$ had been produced. This suggested that $[OsMn(CO)_9]^-$ might have been present as a component of the hexane-insoluble product. The remaining unprotonated hexane-insoluble solid displayed ν(CO) bands in its IR spectrum, very similar to those displayed in the IR spectrum of the initial hexane insoluble product. This suggested that either protonation had not proceeded to completion or an anion of very similar structure, which does not undergo facile protonation, was also present. Further characterisation was not attempted as the compound, isolated as the sodium salt, was found to be unstable and to decompose in solution.

4.2.2.2 Reaction between $[Os(CO)_4]Na_2$ and $Mn(CO)_5Br$ in a 1:1 Molar Ratio

Reaction of $[Os(CO)_4]Na_2$[199] with one equivalent of $Mn(CO)_5Br$ in THF at room temperature for 22 hours reaction time, also resulted in a mixture of products being obtained. Removal of the solvent and extraction of the orange, oily residue with n-hexane gave a clear orange solution and an orange, hexane insoluble solid. $Mn_2(CO)_{10}$, identified by IR and mass spectroscopy, was found to be present in the hexane extract. The hexane insoluble solid was recrystallised from a methanol/

ether solvent system and decomposed without melting at 130°-170°C. The IR spectrum of this anion in THF showed ν(CO) bands at similar wavenumbers to those observed for the hexane insoluble solid obtained from the reaction of $[Os(CO)_4]Na_2$ with 2 equivalents of $Mn(CO)_5Br$, in 4.2.2.1 above. Protonation of the product also yielded a mixture of $Mn_2(CO)_{10}$ and $HOsMn(CO)_9$ in low yield. Analytical data indicated that the compound was not of the formulation, $[OsMn(CO)_9]Na$, as might have been suggested from the products of the protonation reaction. The anionic nature of the product was suggested by the low frequency ν(CO) bands observed in the IR spectrum. Further characterisation of the product, believed to be present as the sodium salt, was hampered in that the compound was unstable and appeared to be decomposing, possibly to give the parent carbonyl complexes, $Mn_2(CO)_{10}$ and $Os_3(CO)_{12}$.

The reactions of $[Os(CO)_4]Na_2$ with $Mn(CO)_5Br$ can be summarised as follows:

1. $[Os(CO)_4]Na_2 + 2Mn(CO)_5Br \xrightarrow[R\ T]{THF}$

(hexane soluble)	+	(hexane insoluble)
1. $HOsMn(CO)_9$		anionic products (I)
2. $Mn_2(CO)_{10}$		+ 2NaBr
3. $Mn_2Os(CO)_{14}$		

[I] $\xrightarrow[THF]{CH_3COOH}$ $HOsMn(CO)_9 + Mn_2(CO)_{10}$
+ anionic product (uncharacterised)

2. $[Os(CO)_4]Na_2 + Mn(CO)_5Br \xrightarrow[R\ T]{THF}$

(hexane soluble) + (hexane insoluble)

1. $Mn_2(CO)_{10}$ anionic product (I)

+ NaBr

The presence of $HOsMn(CO)_9$ as a product of Reaction 1 and not of Reaction 2 appears to indicate the amount of $[Os(CO)_4H]Na$ present as an impurity in $[Os(CO)_4]Na_2$. It is believed that a small amount of $[Os(CO)_4H]Na$ present in $[Os(CO)_4]Na_2$,[199] reacted with $Mn(CO)_5Br$ to produce $HOsMn(CO)_9$ or that the anion $[OsMn(CO)_9]Na$ may have abstracted a proton from the solvent to produce the neutral hydride. The anionic products were not fully characterised since difficulty was experienced in their purification. Isolated as sodium salts, the products were unstable and decomposed during the purification and characterisation process. The reaction of $[Os(CO)_4H]PPN$ with one equivalent of $Mn(CO)_5Br$ was also investigated.

4.2.2.3 Reaction between $[Os(CO)_4H]PPN$ and $Mn(CO)_5Br$ in a 1:1 Molar Ratio

$Mn(CO)_5Br$ as a solution in THF was added dropwise to a THF solution of $[Os(CO)_4H]PPN$ with stirring. Typical reaction times of 18 hours, with subsequent removal of the solvent and extraction of the orange residue with n-hexane yielded an orange solution and an orange, hexane insoluble solid.

The hexane extract showed υ(CO) bands at 2120(w) 2069(m) 2055(m) 2042(m) 2034(s) 2013(vs) 2002(m) 1995(w) 1985(w) cm^{-1}. A ^1H nmr spectrum of the pale yellow oily product, remaining after evaporation of n-hexane, as a solution in d_6-benzene exhibited a high field singlet at 19.80 τ, while a mass spectrum revealed a molecular ion at m/e 499 with sequential loss of nine carbonyl groups. These data provided evidence for the formation of the neutral hydride, $HOsMn(CO)_9$, analagous to the reaction of $[Os(CO)_4H]PPN$ with $Re(CO)_5Br$. No $Mn_2(CO)_{10}$ was produced in this reaction, as evidenced by IR and mass spectroscopy. The red dinuclear dihydride, $Mn_2(CO)_9H_2$, was reported to be obtained upon acidification of a mixture of anions formed from $Mn_2(CO)_{10}$ and $NaBH_4$, but no ^1H nmr spectral data was reported.[214]

The hexane insoluble product was recrystallised from a methanol/ether solvent system which yielded an orange, microcrystalline product, while a second yellow powder was obtained from the mother liquors on addition of water, and by cooling. The orange, microcrystalline product, melting point 126°-133°C, displayed υ(CO) bands in its IR spectrum in THF at 2087(w) 2075(vw) 2048(w) 2005(m) 1987(vs) 1975(m) 1966(s) 1938(m) 1899(w) cm^{-1} - see figure 4.4(c). The appearance of υ(CO) bands at lower frequency would seem to indicate that the compound was anionic in nature. This belief was further supported by elemental analysis which indicated that the compound was a [PPN] salt. A high field singlet at 19.52 τ, as well as a complex multiplet at 2.42 τ for the phenyl protons

of the [PPN] cation, were observed in the ^1H nmr spectrum of the compound run as a solution in d_4-methanol. A Far IR spectrum of the product run as a Nujol mull showed a medium, broad band at 192 cm^{-1}. Since for $Mn(CO)_5Br$[211] a medium band is observed at 218 cm^{-1}, this band at 192 cm^{-1} has been tentatively assigned to the υ(Mn-Br) vibration.

The available evidence suggested that the compound was of the formulation, $[HOsMn(CO)_8Br]PPN$, analagous to $[HOsRe(CO)_8Br]PPN$ obtained in the corresponding rhenium reaction. Elemental analysis did not yield data corresponding to a compound of this formulation. However, solvent inclusion may have occurred and evidence for this was apparent from the ^1H nmr spectrum, where peaks due to solvent were observed. Further evidence to support the belief that the hydride ligand is coordinated to the osmium atom and not to the manganese atom, is that the compound $Mn(CO)_5H$, as a solution in ether, displays a high field singlet in the ^1H nmr spectrum at 17.73 τ.[215] Hieber et al presented evidence for a dinuclear manganese carbonyl hydrido-anionic complex, $[Mn_2(CO)_9H]^-$, formed by hydrolysis of $Mn(CO)_5H$. However, ^1H nmr spectral data for the compound was not reported.[216] Several osmium-manganese neutral complexes, among them, $HMnOs_2(CO)_{12}$, $HMnOs_3(CO)_{16}$, $H_3MnOs_3(CO)_{13}$ and the anionic $[MnOs_2(CO)_{12}]NMe_4$, have been

prepared and characterised.[217] However, the hydride derivatives were reported to be insufficiently soluble to enable detection of the hydride ligand by ^1H nmr spectroscopy. A perusal of the literature[191,218] revealed that no heteronuclear hydrido anionic complexes of this type and, in particular, where the hydride ligand is coordinated to the osmium atom, have previously been reported.

The loss of CO rather than bromide ligand from the metal carbonyl halide, $Mn(CO)_5Br$, on reaction with carbonyl-metalates has previously been observed,[219] although under different conditions to those employed in the present study. The dinuclear anion, $[Mn(CO)_5Mn(CO)_4Br]^-$, was isolated in high yield as the quaternary ammonium salt in a series of phase transfer catalytic reactions involving $Mn(CO)_5Br$ and $[OH]^-$, according to the scheme below:

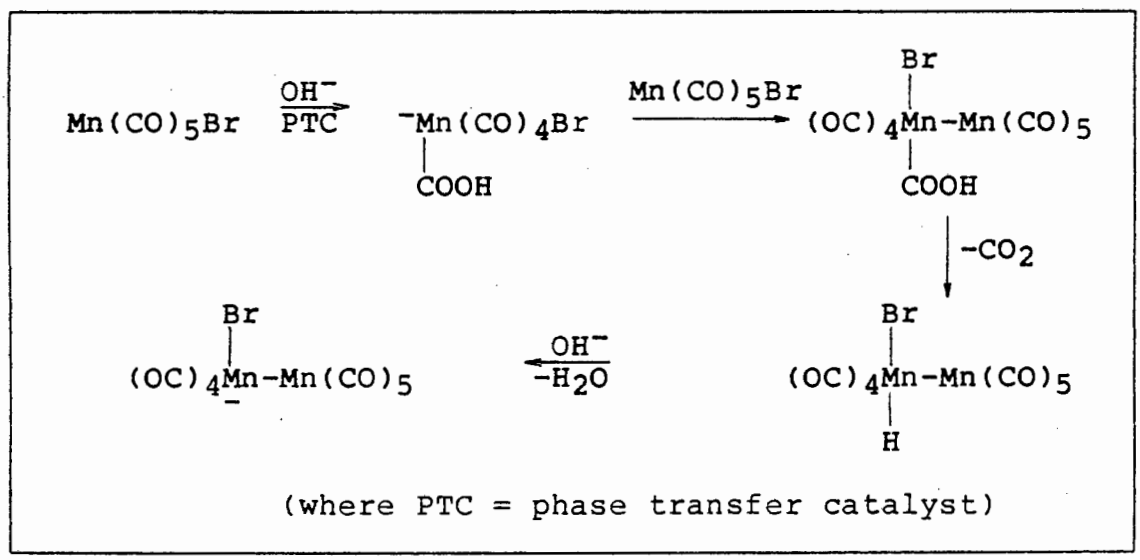

(where PTC = phase transfer catalyst)

The second yellow product, isolated in the reaction of $[Os(CO)_4H]PPN$ with $Mn(CO)_5Br$, and recrystallised from the mother liquors, melted at 190°-200°C with decomposition occurring at 130°C. The product displayed υ(CO) bands in its IR spectrum in THF at 2088(vw) 2044(m) 2022(sh) 2008(vs) 1987(m) 1966(sh) 1925(s) 1915(sh) 1683(m) cm^{-1}. The υ(CO) bands at 1925 and 1683 cm^{-1} suggested that the product was anionic and that it possibly contained a bridging carbonyl group. This latter suggestion was prompted by the fact that the dianion, $[Os_3(CO)_{11}]^{2-}$ isolated as the potassium salt, was found to display a υ(CO) band at 1625 cm^{-1} in its IR spectrum in THF, which was assigned to a bridging carbonyl group.[207] The initial yellow solution of the second yellow product was seen to rapidly change colour to give an orange solution, the υ(CO) bands in the IR spectrum of which occurred at 2088(vw) 2050(sh) 2020(sh) 2008(vs) 1987(m) 1965(w) 1927(vs) 1778(m) 1726(w) 1683(m) cm^{-1}. This change in the IR spectrum of the compound in solution could either indicate that an isomerisation or decomposition occurred.

Thus the reaction of $[Os(CO)_4H]PPN$ with $Mn(CO)_5Br$ can be summarised as shown below, on the basis of the products isolated. The products obtained in the reaction can be rationalised as discussed in the conclusion.

$$[Os(CO)_4H]PPN + Mn(CO)_5Br \xrightarrow[R\ T]{THF}$$

hexane soluble	+	(hexane insoluble)
$HOsMn(CO)_9$		anionic product (I) possibly $[HOsMn(CO)_8Br]PPN$ + anionic product (II) (unstable)

4.2.3 Reactions of the neutral hydride complex, $HOsRe(CO)_9$

The neutral hydride complex, $HOsRe(CO)_9$ obtained from the reaction of $[Os(CO)_4H]PPN$ with $Re(CO)_5Br$, and purified by sublimation (30 °C/0.01 mm Hg) as discussed above, was dissolved in n-hexane and ten-fold excesses of various reagents added, respectively. Although the products were obtained in insufficient yield for elemental analysis, they were identified by the molecular ions in their corresponding mass spectra and further characterised by IR spectroscopy and melting points, respectively. The absence of a high field singlet in the ^1H nmr spectra of a solution of the products provided further evidence that reaction had occurred.

4.2.3.1 Reaction between $HOsRe(CO)_9$ and CH_3I

To a THF solution of $HOsRe(CO)_9$ at 0 °C, CH_3I was added in a ten-fold excess with stirring and the reaction mixture allowed to warm up to room temperature. Stirring was

continued overnight, whereupon the solvent was removed and the residue extracted with n-hexane. The product was recrystallised from CH_2Cl_2/petroleum ether (bp 30°-40°C) ν(CO) peaks at 2092(m) 2055(m) 2052(sh) 2041(s) 2024(vs) 2015(sh) 2005(m) 1988(s) cm^{-1} - see table 4.1 - were observed in the IR spectrum of the recrystallised product which sublimed at 60°-75°C and melted at 100°C. A mass spectrum gave a peak at $^m/_e$ 758, consistent with the parent ion $[IOsRe(CO)_9]^+$ with loss of nine carbonyl groups to give a peak at $^m/_e$ 504, corresponding to the positive ion $[IOsRe]^+$. The yield of product obtained was too low to enable identification by microanalysis. This is another example of the reaction of a transition metal hydride with an organic halide to produce a transition metal halide, as was also demonstrated in the reactions of $Os_2(CO)_8H_2$ with CCl_4 and CBr_4 to produce the complexes, $Os_2(CO)_8X_2$ (X = Cl or Br).[126]

4.2.3.2 Reaction between $HOsRe(CO)_9$ and CBr_4

A ten-fold excess of CBr_4 was added to a n-hexane solution of $HOsRe(CO)_9$ at room temperature and the reaction mixture stirred for 30 minutes. The solvent was removed and the residue extracted with n-hexane. Removal of the solvent and recrystallisation from a CH_2Cl_2/petroleum ether (bp 30°-40°C) solvent system yielded white needles which

melted at 105°-110°C. An IR spectrum in n-hexane in the ν(CO) region showed bands at 2111(vw) 2094(m) 2055(m) 2042(s) 2032(sh) 2023(vs) 2015(sh) 2005(m) 1988(s) cm^{-1} - see figure 4.2 b) and table 4.1. A mass spectrum of the product showed a peak at m/e 708, consistent with the parent ion, $[BrOsRe(CO)_9]^+$, with sequential loss of nine carbonyl groups to exhibit a peak at m/e 456, corresponding to the positive ion, $[BrOsRe]^+$. The wavenumbers and intensities of the ν(CO) bands in the IR spectra of the bromo-complex were found to be very similar to those observed for the product obtained in 4.2.3.1 above.

4.2.3.3 Reaction between $HOsRe(CO)_9$ and CCl_4

Although the corresponding chloro-complex, $ClOsRe(CO)_9$, had previously been reported,[126] it was only identified mass spectrometrically. The stirring of a CCl_4 solution of $HOsRe(CO)_9$ over a 40 minute period with subsequent removal of solvent and dissolution of the colourless residue in n-hexane, yielded ν(CO) bands in the IR spectrum at 2095(w) 2081(vw) 2069(vw,sh), 2056(m) 2044(vs) 2024(vs) 2016(sh) 2004(m) 1986(s) cm^{-1} - see table 4.1. The compound was recrystallised from a CH_2Cl_2/petroleum ether (bp 30°-40°C) solvent system to yield white needles which melted at 100°-105°C. A mass spectrum of the product showed a molecular ion at m/e 664 corresponding to $[ClOsRe(CO)_9]^+$ and displaying the correct

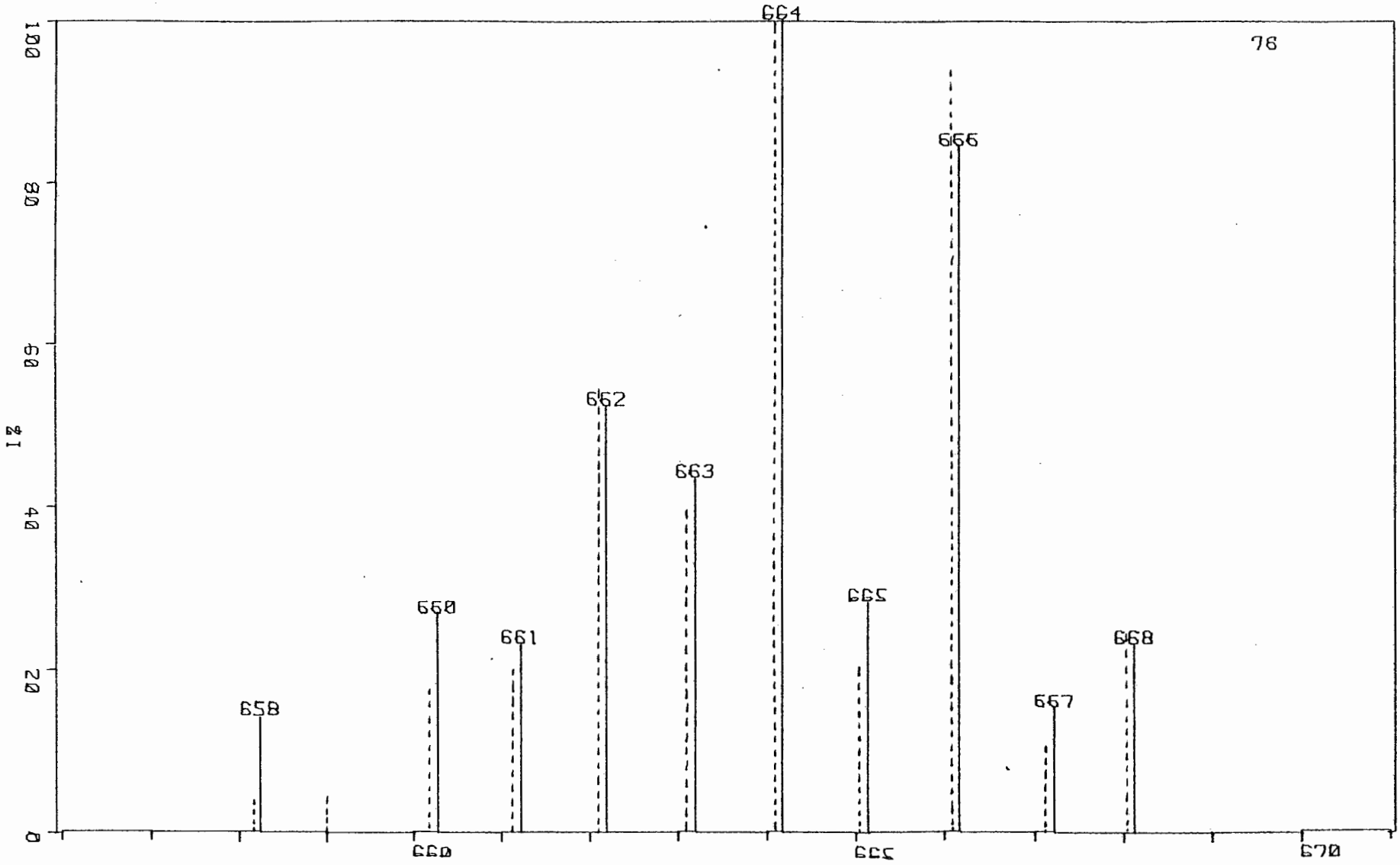

Figure 4.8 Comparison of observed (-) and calculated (---) polyisotopic distribution of the parent ion, $[ClOsRe(CO)_9]^+$.

polyisotopic pattern, which can be seen in figure 4.8, with sequential loss of nine carbonyl groups to exhibit a peak at m/e 415, corresponding to $[ClOsRe]^+$.

The wavenumbers and intensities of the ν(CO) bands in the IR spectrum of $ClOsRe(CO)_9$ were found to be very similar to the hydrido, iodo and bromo derivatives - see table 4.1. This evidence was indicative of all four compounds having similar structures. The compounds formulated as $XOsRe(CO)_9$ (X = H, Cl, Br or I) could exist in two possible structural forms shown in figure 4.9 below:

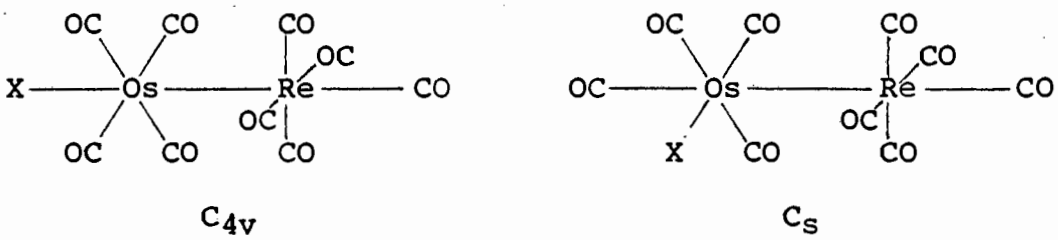

Figure 4.9 Proposed structures for the series of complexes $[XOsRe(CO)_9]$ where X = H, Cl, Br or I.

For the structure where X is trans to the $[Re(CO)_5]$ fragment, on local symmetry arguments, the compound should exhibit 5 IR ν(CO) stretching frequencies corresponding to (3A + 2E) modes. For the structure where X is cis to the $[Re(CO)_5]$ fragement, based on local symmetry arguments, the overall symmetry belongs to the C_s point group. The compound would be expected to exhibit nine IR active modes (6A' + 3A"). Since eight ν(CO) bands are observed for X = Br or I and nine ν(CO) bands are actually observed in

Table 4.1 IR Carbonyl Stretching Vibrations (cm^{-1})[a,b] for the Series of Complexes $XOsRe(CO)_9$ (X = H, Cl, Br or I)

$HOsRe(CO)_9$	2092(w) 2081(s) 2068(w) 2046(s) 2040(m) 2028(vs) 2005(s) 1997(w) 1984(s)
$ClOsRe(CO)_9$	2095(w) 2081(vw) 2068(vw,sh) 2056(m) 2044(s) 2023(vs) 2015(sh) 2004(m) 1986(s)
$BrOsRe(CO)_9$	2094(m) 2055(m) 2042(s) 2032(sh) 2023(vs) 2015(sh) 2005(m) 1988(s)
$IOsRe(CO)_9$	2092(m) 2055(m) 2052(sh) 2041(s) 2024(vs) 2015(sh) 2005(m) 1988(s)

Table 4.2 IR Carbonyl Stretching Vibrations (cm^{-1})[a,b] for the Series of Complexes $[XOsRe(CO)_8Br]PPN$ (X = H, Br or I)

$[HOsRe(CO)_8Br]PPN$	2091(vw) 2044(s) 2019(m) 1991(vs) 1979(sh) 1955(m) 1946(m) 1895(m)
$[BrOsRe(CO)_8Br]PPN$	2180(vw) 2109(m) 2097(m) 2055(w) 2022(m) 1995(vs) 1961(s) 1908(s)
$[IOsRe(CO)_8Br]PPN$	2093(vw) 2062(w) 2054(w) 2018(sh) 2005(sh) 1993(vs) 1963(s) 1910(s)

[a] Key: sh, shoulder; w, weak; m, medium; s, strong; v, very

[b] All spectra were run in n-hexane

the spectra for X = H or Cl, in the series of complexes $XOsRe(CO)_9$, the more likely structure which these complexes would be expected to adopt is that where the X group is situated cis to the $[Re(CO)_5]$ fragment and not coaxial with the osmium-rhenium bond. This suggestion is in agreement with the structures determined for the complexes, $Os_2(CO)_8X_2$ (X = Cl or I). These halogenation reactions of $HOsRe(CO)_9$ can be summarised as shown below:

$$HOsRe(CO)_9 \xrightarrow[\text{n-hexane}]{CH_3I,\ CBr_4 \text{ or } CCl_4} XOsRe(CO)_9 \quad (X = Cl, Br \text{ or } I)$$

4.2.3.4 Reaction between $HOsRe(CO)_9$ and I_2

Reaction of $HOsRe(CO)_9$, as a hexane solution, with a ten-fold excess of iodine, resulted in metal-metal bond cleavage, and conversion of the hydrido osmium moiety to an iodo osmium moiety. An IR spectrum of the reaction solution in the $\upsilon(CO)$ region clearly showed peaks of cis-$Os(CO)_4I_2$ and $Re(CO)_5I$, respectively. The observed $\upsilon(CO)$ bands were compared with $\upsilon(CO)$ bands of authentic samples of cis-$Os(CO)_4I_2$ - see section 2.2.1.3 - and $Re(CO)_5I$ prepared by reacting $Re_2(CO)_{10}$ with I_2.[220] Metal-metal bond cleavage by halogens has been demonstrated previously[119] and also in this thesis - see chapter 2.

4.2.4 Reactions of the mixed-metal anionic complex [HOsRe(CO)$_8$Br]PPN

Attempts to convert the mixed-metal anionic complex, [HOsRe(CO)$_8$Br]PPN into a neutral mixed-metal complex, which might have facilitated characterisation by mass spectroscopy, were unsuccessful. On protonation, carbonylmetalate anions generally yield hydroacids or metal hydrides.[201] However, as mentioned above, protonation of [HOsRe(CO)$_8$Br]PPN with CF_3COOH in CH_3CN did not yield a neutral mixed-metal hydride complex, but rather $Os(CO)_4H_2$ and $Re_2(CO)_8Br_2$. Protonation of the anion may well have occurred to give an unstable neutral species, [$H_2Os(CO)_4$-$Re(CO)_4Br$], which then fragmented to give the observed products, $Os(CO)_4H_2$ and $[Re(CO)_4Br]_2$. This reaction lends support to the formulation of $[HOs(CO)_4Re(CO)_4Br]^-$ for the anion.

4.2.4.1 Reaction between [HOsRe(CO)$_8$Br]PPN and CH_3I.

The addition of CH_3I to [HOsRe(CO)$_8$Br]PPN in THF at room temperature in an equimolar ratio was undertaken on a small scale and it was found that no reaction had taken place after 20 hours. Excess CH_3I was then added and the reaction mixture stirred for a further 36 hours at room temperature, whereupon reaction was judged to be complete by the disappearance of υ(CO) bands of the starting material in the

IR spectrum. The solvent and any possible volatile products were collected in a trap at -196°C. No carbonyl-containing products were observed in this volatile portion. The remaining solid product was recrystallised from a methanol/ether solvent system to produce white needles which melted at 110°-120°C (decomp). After recrystallisation the amount of product was too small to enable an elemental analysis to be performed. An IR spectrum of the product in THF showed υ(CO) bands at 2093(vw) 2062(vw) 2054(w) 2018(sh) 2005(sh) 1993(vs) 1963(s) 1910(m) cm^{-1} - see table 4.2. The low frequency υ(CO) bands indicated that the product was still of an anionic nature. The possible splitting of the osmium-rhenium bond with the resultant formation of $Os(CO)_4H(CH_3)$ and possibly $[Re(CO)_4BrI]PPN$ was ruled out on the basis that the osmium moiety would have been detected as a volatile product. This metal-metal bond fission by CH_3I has been previously observed for other mixed-metal compounds, e.g. reaction of $(PEt_3)_2(CO)Rh\text{-}Co(CO)_4$ with CH_3I led to the formation of **trans**-$RhI(CO)(PEt_3)_2$ and $CH_3Co(CO)_4$.[194] Since this metal-metal bond fission was not found to take place, a second possibility analagous to the reaction of $HOsRe(CO)_9$ with CH_3I - see 4.2.3.1 above - may have occurred, i.e. reaction of a hydride with an organic halide, with the resultant formation of an anion of the formulation, $[IOsRe(CO)_8Br]PPN$. Similarly, treatment of $Os_2(CO)_8H_2$ with CH_3I led to the formation of $Os_2(CO)_8I_2$.[109] However, since

insufficient evidence was available for positive identification of the compound, reaction of [HOsRe(CO)$_8$Br]PPN with CBr_4 was attempted.

4.2.4.2 Reaction between [HOsRe(CO)$_8$Br]PPN and CBr_4

A ten-fold excess of CBr_4 was added in the solid state to a THF solution of [HOsRe(CO)$_8$Br]PPN with stirring. The reaction mixture was stirred for 45 minutes during which time a colour change of the solution from yellow to yellow-orange was observed. Removal of the solvent and trituration of the orange-brown, oily residue produced a brown solid which was recrystallised from a methanol/ether solvent system to yield pale orange-red crystals which decomposed at 80°-90°C to give a brown product which melted at 130°-150°C. An IR spectrum in the ν(CO) region gave bands at 2180(vw) 2109(m) 2097(m) 2055(w) 2022(m) 1995(vs) 1961(s) 1908(s) cm^{-1} - see figure 4.4 b) and table 4.2. These low frequency ν(CO) bands suggested that the product was of an anionic nature. The similarity between this IR spectrum in the ν(CO) region with that obtained for the product of the reaction discussed in 4.2.4.1. above, suggests that the two products have similar structures. Since CBr_4 is a reagent commonly employed for bromide replacement of hydride ligand,[126,129] it would be reasonable to suggest a complex of formulation, [BrOsRe(CO)$_8$Br]PPN, as a possible product of this reaction. Moreover, the strong ν(CO) bands in the IR

spectra of the proposed bromo and iodo analogues closely resemble those displayed in the IR spectrum of the hydrido anionic complex, $[HOsRe(CO)_8Br]PPN$ - see table 4.2. Elemental analysis for the orange, crystalline product was consistent with the compound being of the formulation, $[BrOsRe(CO)_8Br]PPN$.

These halogenation reactions of $[HOsRe(CO)_8Br]PPN$ can be summarised as follows:

$$[HOsRe(CO)_8Br]PPN \xrightarrow[\text{THF}]{CH_3I \text{ or } CBr_4} [XOsRe(CO)_8Br]PPN \quad (X = I \text{ or } Br)$$

In the IR spectrum of $[HOsRe(CO)_8Br]PPN$ discussed above, these lower frequency $\nu(CO)$ bands are assigned to the rhenium half of the molecule, which bears the negative charge. If the hydride ligand on the osmium atom has been replaced by bromide or iodide ligands, respectively in 4.2.4.1 and 4.2.4.2 as discussed above, then the carbonyl stretching vibrations of the carbonyl ligands bonded to the rhenium atom in the molecules should not be significantly affected. This is indeed found to be the case with all three complexes exhibiting their most intense $\nu(CO)$ band at 1991 (X = H), 1995 (X = Br) and 1993 (X = I) cm^{-1}.

4.2.4.3 Reaction between [HOsRe(CO)$_8$Br]PPN and AuPPh$_3$Cl

[HOsRe(CO)$_8$Br]PPN as a solution in THF was reacted with one and two moles of AuPPh$_3$Cl. The additions of AuPPh$_3$Cl were carried out at room temperature and the reactions monitored by IR spectroscopy. After 53 hours the reactions were judged to be complete, by the disappearance of the strong, low frequency υ(CO) band of the starting anionic material, in the IR spectrum of the reaction mixtures. The IR spectra of the two reaction mixtures were identical, indicative of the same main product having been formed, irrespective of whether one or two moles of the gold-halide complex were employed. Removal of solvent and extraction of the oily, brown residue with n-hexane produced a clear solution and a purple-brown solid. No carbonyl-containing product was observed in the hexane soluble extract. The hexane insoluble, purple-brown solid was recrystallised by slow evaporation of an ether/n-hexane solvent system. A brown microcrystalline solid precipitated from solution first and then, after several days of slow evaporation of the mother liquors, a purple-black crystalline product formed. The first product gave υ(CO) bands in the IR spectrum in THF at 2013(s) 1993(m) 1959(m) 1906(vs) 1871(m) cm^{-1} - see figure 4.10 a). Elemental analysis was most closely consistent with the formula [OsRe(CO)$_8$(AuPPh$_3$)Cl]PPN.2C$_4$H$_{10}$O. The ^{1}H nmr

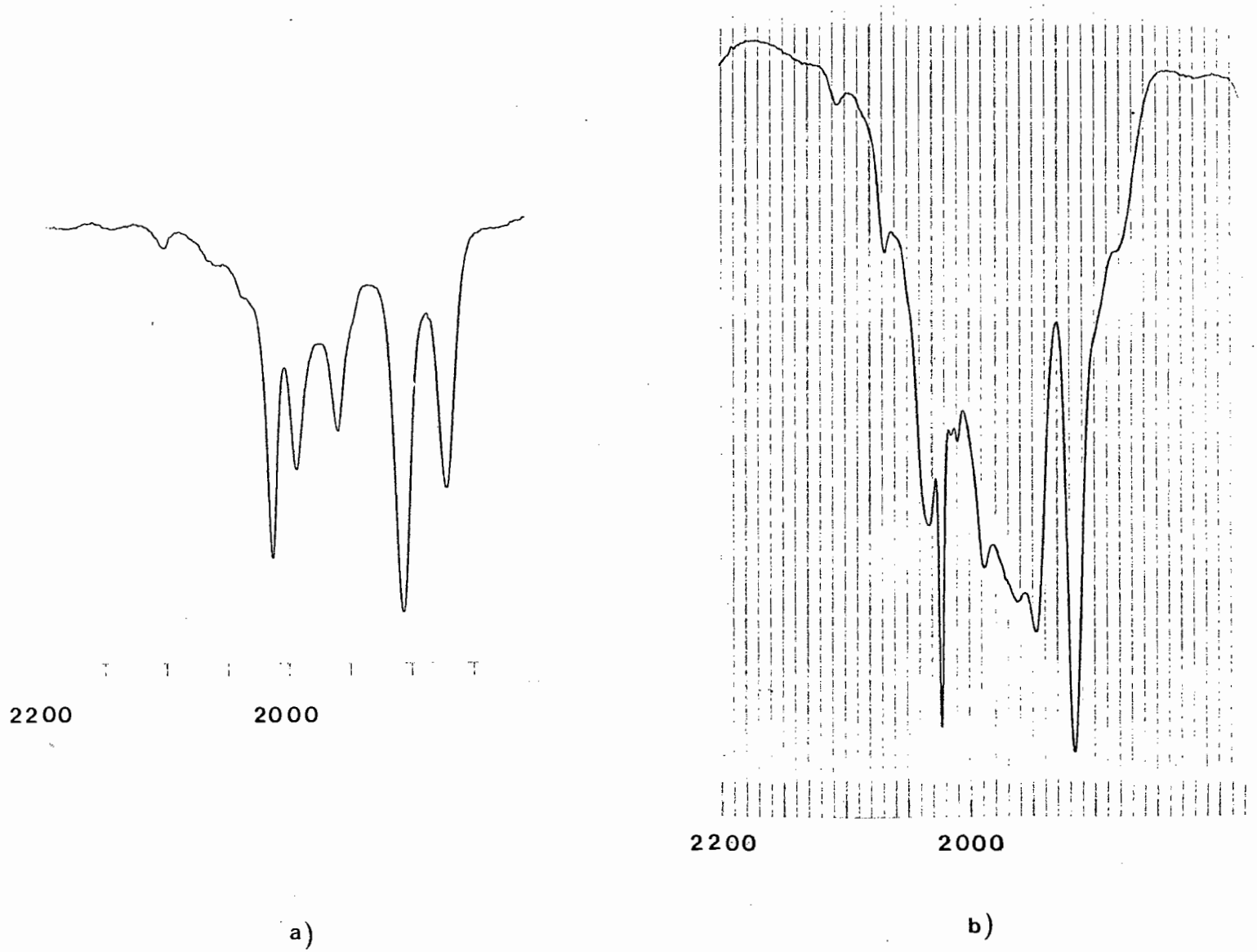

Figure 4.10 IR Spectra of possible products of the reaction of $[HOs(CO)_4Re(CO)_4Br]PPN$ and $AuPPh_3Cl$
a) $[Os(CO)_4(AuPPh_3)(Cl)Re(CO)_4]PPN$, and
b) $[Os_2Re_2(AuPPh_3)_2(CO)_{12}]PPN$ in THF.

spectrum confirmed the presence of $C_4H_{10}O$. In addition, this spectrum confirmed the presence of additional phenyl groups due to the presence of the $AuPPh_3$ ligand, the solution employed in the determination was too dilute for positive confirmation of the loss of the hydride ligand. The available evidence, however, is insufficient to enable a structure to be predicted for the product. The pattern of the υ(CO) bands resembles, although is not identical to, that observed in the IR spectrum of $Os_3(CO)_{10}(AuPPh_3)Cl$, where the $AuPPh_3$ and Cl ligands were found to bridge an osmium-osmium bond.[221] It is possible therefore, that the first product, in the above reaction, adopts a structure with bridging $AuPPh_3$ and Cl ligands. It has been suggested that ligands without sufficient lone pairs for bridging (e.g. H and $AuPPh_3$) do not sufficiently hold the molecule together. Instead, stability would be imparted to the molecule either by a strong metal-metal bond as in $Os_3(CO)_{10}(\mu\text{-H})(\mu\text{-}AuPPh_3)$ or by a strong metal-metal bond and a bridging halogen atom as in $Os_3(CO)_{10}(\mu\text{-Cl})(\mu\text{-}AuPPh_3)$.[222] In metal cluster chemistry, the group $AuPR_3$ is similar to a hydrogen atom or a methyl group in being a source of one electron and one orbital for skeletal bonding.[222,223]

The second anionic, hexane-insoluble product which was obtained from the mother liquors by slow evaporation, displayed the following υ(CO) bands in its IR spectrum in THF: 2105(vw) 2069(w) 2031(s) 2020(s) 2010(m,sh) 1989(m) 1960(sh) 1944(m) 1913(vs) 1880(sh) cm^{-1} - see figure 4.10 b). It was found to have a much higher melting point than the first product, 200°C (decomp) and elemental analysis revealed 39.3%C; 3.4%H; 0.6%N. These data were most consistent with a molecular formula of higher nuclearity and possibly of $[Os_2Re_2(CO)_{12}(AuPPh_3)_2]PPN$ for which calculated elemental percentages are 39.6%C; 2.4%H; 0.6%N. The low frequency of the υ(CO) bands are in the region expected for an anionic compound. A ^1H nmr spectrum of the compound indicated a multiplet at 2.54 τ, in the region expected for all the phenyl protons and more complex than the multiplet corresponding to the phenyl protons in the ^1H nmr spectrum of $[HOsRe(CO)_8Br]PPN$. The crystal structure of a tetraosmium complex, $Os_4(CO)_{12}(AuPPh_3)_2H_2$, containing a direct gold-gold interaction (Au-Au = 2.793(4) Å) has recently been determined by X-Ray crystallography.[224] It is, therefore, not unreasonable to suggest that the second product isolated in the above reaction might be of a tetranuclear nature of possible formulation, $[Os_2Re_2(CO)_{12}(AuPPh_3)_2]PPN$. However, since only an X-Ray structure determination could unequivocally

characterise the compound, it would be premature to suggest a possible structure for it, at this stage.

A direct gold-gold interaction has been observed[224] in $Os_3(CO)_{11}(AuPPh_3)_2$ (Au-Au = 2.845(1) Å). Osmium-gold complexes have been shown to possess high stability.[225] The reaction of a carbonylmetalate with a phosphine-substituted gold halide is the standard method employed in the preparation of gold-metal complexes. George et al[199] prepared $Os(CO)_4(AuPPh_3)_2$ by reaction of $[Os(CO)_4]Na_2$ with 2 moles of $AuPPh_3Cl$. Lewis and Johnson[226] have utilised this standard reaction for a wide variety of polynuclear osmium anions and have isolated many stable gold-substituted cluster complexes.

4.2.4.4 Substitution Reactions of [HOsRe(CO)$_8$Br]PPN

Since ligand substitution reactions are known to occur for metal carbonyl complexes, including anions, e.g. the photolysis of $[Mn(CO)_5]^-$ in the presence of PPh_3 gave $[Mn(CO)_4PPh_3]^-$,[227] and reaction of $Re(CO)_5X$ with L (L = PPh_3, py) gave $Re(CO)_4XL$,[228] it was decided to investigate the reactivity of [HOsRe(CO)$_8$Br]PPN with the neutral ligands, PPh_3, pyridine and CO.

4.2.4.4.1 Reaction of [HOsRe(CO)$_8$Br]PPN with PPh$_3$

The reaction of [HOsRe(CO)$_8$Br]PPN in THF with an equimolar amount of PPh$_3$ did not proceed at room temperature, even after stirring for 4 days, as judged by IR spectra of the reaction solution at regular intervals. The reaction temperature was raised to 60 °C and only after 3 days at that temperature was the reaction judged to be complete by the disappearance of the υ(CO) bands of [HOsRe(CO)$_8$Br]PPN. The solvent was removed to yield an oily, brown product. Trituration with n-hexane yielded a pale yellow solid which melted at 65 °-75 °C. Attempts to recrystallise the compound resulted in it reverting to an oily product. An IR spectrum in THF in the υ(CO) region gave peaks at 2078(w) 2043(m) 2018(sh) 2005(s) 1992(vs) 1955(m) 1946(m) 1887(vs) cm^{-1}. The low frequency of the very strong band at 1887 cm^{-1} was indicative of the anionic nature of the product. A ^{1}H nmr spectrum in d_4-methanol showed a multiplet at 2.54 τ corresponding to the phenyl protons and of a more complex pattern than that observed for [HOsRe(CO)$_8$Br]PPN, indicative of the presence of extra phenyl protons other than those of the [PPN] cation. A high field doublet centred at 18.12 τ was observed with a separation of 14 Hz. The magnitude of this coupling constant which we assign to phosphorus-hydrogen coupling, suggested that the PPh$_3$ ligand was situated cis to the hydride ligand as is found in

$Os_2(CO)_6(PPh_3)_2H_2$.[126,129] Analytical data for the compound suggested that although slightly impure, PPh_3 substitution of CO had occurred on the evidence presented by the ^1H nmr spectral data. Found: 50.0%C; 3.8%H; 0.9%N. Calculated for $[Os(CO)_3(PPh_3)(H)Re(CO)_4Br]PPN$: 50.31%C; 3.18%H; 0.96%N.

4.2.4.4.2 Reaction of $[HOsRe(CO)_8Br]PPN$ with pyridine

A similar reaction to 4.2.4.4.1 above was carried out, except that an equimolar amount of pyridine was used in place of PPh_3 in reaction with $[HOsRe(CO)_8Br]PPN$. A reaction temperature of 60°C with a reaction time of 3 days in THF was required for reaction to proceed to completion, as judged by the υ(CO) bands in the IR spectrum of the reaction mixture. A brown, oily product remaining after removal of the solvent was triturated with n-hexane to yield a brown, microcrystalline product which melted at 78°-88°C. As with the PPh_3 reaction product above, difficulty was experienced in the recrystallisation of the product. Analytical data were not entirely consistent with pyridine substitution of CO. However, this could possibly be due to solvent inclusion. Found: 44.9%C; 3.5%H; 2.3%N. Calculated for $[Os(CO)_3(py)(H)Re(CO)_4Br]PPN$: 45.3%C; 2.9%H; 2.2%N. The IR spectrum in THF gave υ(CO) bands at 2043(w) 2011(sh) 1996(s) 1959(w) 1940(sh) 1924(m) 1895(sh) 1870(vs) cm^{-1}.

The intensities and wavenumbers of these bands appeared to be very similar to those obtained for the product in 4.2.4.4.1 above, suggestive of similar structures for the two products. A ^1H nmr spectrum in d_4-methanol showed a complex multiplet centred at 2.42 τ corresponding to the phenyl protons of the [PPN] cation and smaller multiplets centred at 1.34 τ and 1.13 τ which are in the region expected for the pyridine protons. The amount of sample available for identification purposes did not allow detection of a high field singlet.

By comparison of the IR spectra of the products obtained in the reactions of $[HOsRe(CO)_8Br]PPN$ with PPh_3 and pyridine, respectively, similar structures can be proposed for both compounds, $[HOs(CO)_3(PPh_3)Re(CO)_4Br]PPN$ and $[HOs(CO)_3(py)Re(CO)_4Br]PPN$. Two possible structures proposed are shown in figure 4.11, where L = PPh_3 or py.

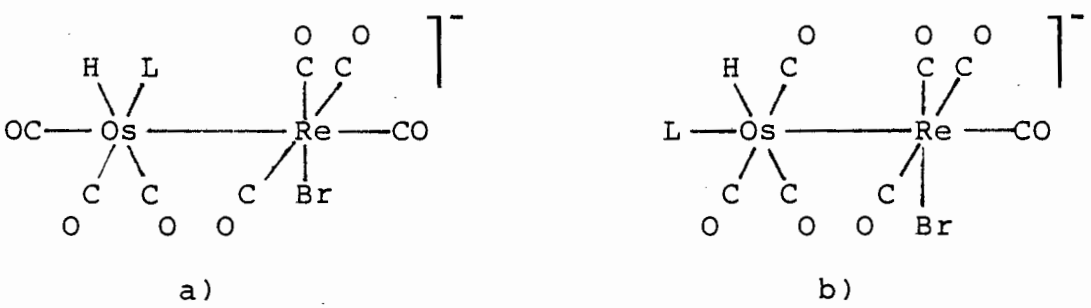

Figure 4.11 Two possible structures for the complexes $[HOs(CO)_3LRe(CO)_4Br]PPN$ where L = PPh_3 or py

The nucleophilic ligands would be expected to preferentially coordinate to the osmium atom than the electron-rich rhenium atom. The ligands, L, as dictated by the phosphorus-hydrogen coupling constant in the ^1H nmr spectrum of $[HOs(CO)_3(PPh_3)Re(CO)_4Br]PPN$ are situated **cis** to the hydride ligand.These substitution reactions can be summarised as follows:

$$[HOsRe(CO)_8Br]PPN \xrightarrow[\text{THF}\\ 60\,^\circ C]{L} [HOs(CO)_3LRe(CO)_4Br]PPN \quad (L = PPh_3 \text{ or py})$$

4.2.4.4.3 Reaction of $[HOsRe(CO)_8Br]PPN$ with CO

Since transition metal cluster compounds are currently being examined as catalysts for a variety of reactions involving carbon monoxide,[229,230] it is essential that the basic reactivity patterns of clusters with CO be understood.[7] Most mixed-metal clusters of the type, $H_2FeRu_3(CO)_{13}$, have been found to fragment in the presence of CO, under rather mild conditions (1 atm of CO, 25°-50°C), generally to produce monomeric and trimeric products.[7] However, the metal composition of the cluster was found to have a substantial effect on its reactivity. Clusters with increasing third row metal content were found to become more resistant to fragmentation,[7] presumably because of the

greater strength of the metal-metal bonds which involve third-row metals.[231] Since the dinuclear anion, $[HOsRe(CO)_8Br]PPN$ contains only third-row transition metals and since it was believed that the neutral hydride complex, $HOsRe(CO)_9$, might have arisen from the anion, $[HOsRe(CO)_8Br]PPN$ by a disproportionation reaction, it was decided to investigate the reaction of CO with this latter anionic complex. A THF solution of $[HOsRe(CO)_8Br]PPN$ was subjected to a stream of CO which was bubbled through the solution for 10 minutes. The reaction mixture was left to stir for 3 days at room temperature, after which period no reaction was observed to have occurred. This result was indicative of the high stability of the anion and provided good evidence that the neutral hydride, $HOsRe(CO)_9$ was not obtained from $[HOsRe(CO)_8Br]PPN$.

4.3 Conclusion.

The most important factor to emerge from the present investigation is the difference in the reactivity pathway of the reaction between $[Os(CO)_4]Na_2$ and $M(CO)_5Br$ (M = Mn or Re), compared with that between $[Os(CO)_4H]PPN$ and $M(CO)_5Br$ (M = Mn or Re) - see reaction scheme below:

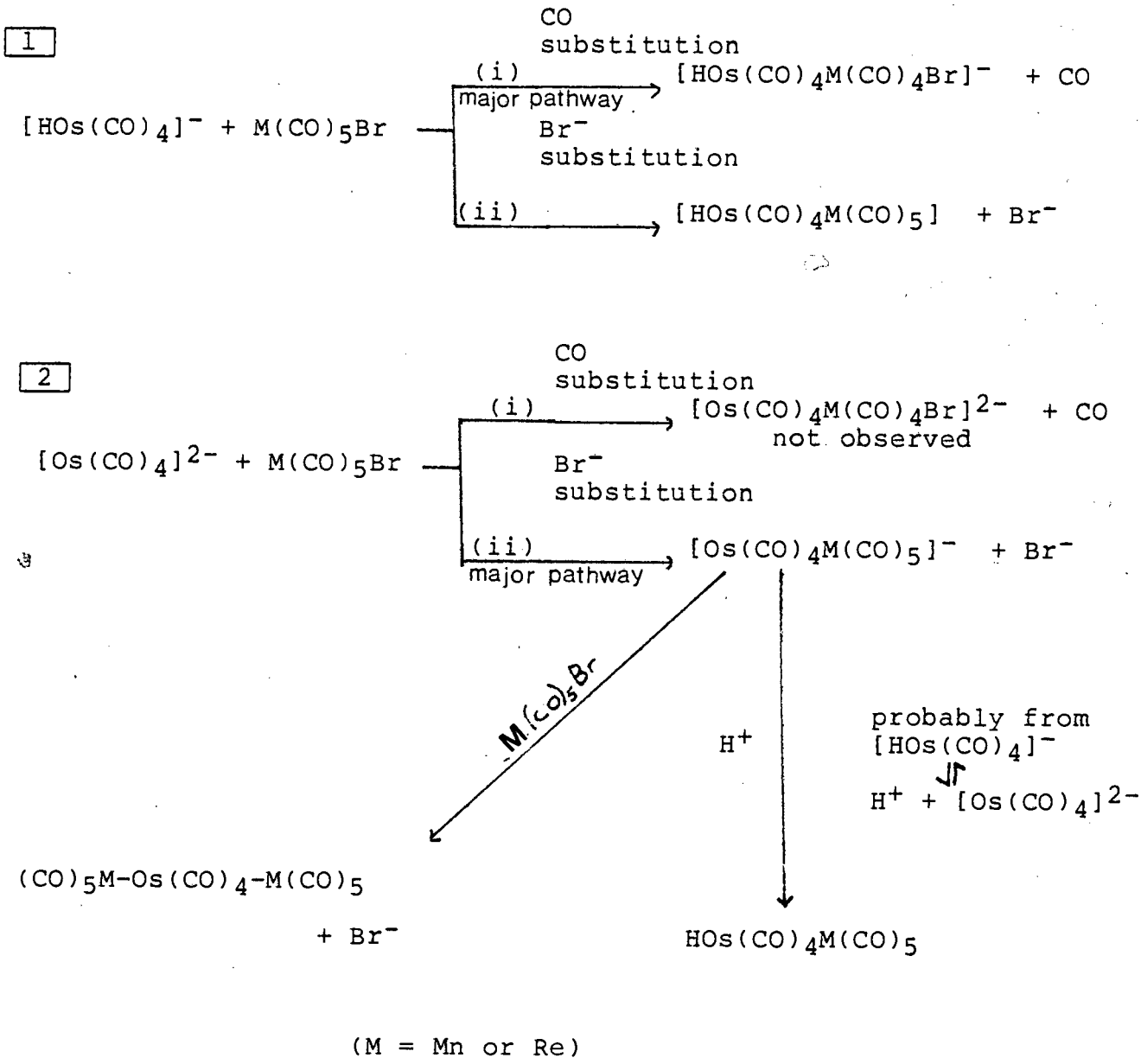

(M = Mn or Re)

The rate constants for the CO dissociation pathway for the reaction of $Re(CO)_5X$ with tertiary phosphines have previously been found to change with the nature of the halogen in the order Cl > Br > I.[228] Thus it was decided to investigate whether altering the halide on the metal

carbonyl reactant, i.e. employing $Re(CO)_5I$ instead of $Re(CO)_5Br$ in reaction with $[HOsRe(CO)_8Br]PPN$, would result in the formation of different products. It was hoped that yields of $HOsRe(CO)_9$ from this reaction might be increased, since I^- is a better leaving group than Br^-, i.e. that reaction 1(i), outlined in the reaction scheme above, would be the preferred pathway. However, it was found that in the reaction of $[HOsRe(CO)_8Br]PPN$ with $Re(CO)_5I$, CO dissociation from $Re(CO)_5I$ was still the favoured pathway, resulting in the formation of $[HOsRe(CO)_8I]PPN$.

Impurities of $[Os(CO)_4H]^-$ in $[Os(CO)_4]^{2-}$ and vice versa can easily explain products isolated from the reactions outlined in Chapter 4 above. Also, although the same products were probably formed in the reactions outlined in the scheme above for M = Mn, these products would be expected to be less stable than their rhenium analogues and therefore could not be isolated. This has previously been found to be the case and, for example, the heteronuclear complex, $HReOs_3(CO)_{15}$ is more stable than $HMnOs_3(CO)_{15}$, which was unable to be isolated.[217] The relative stability of these two tetranuclear clusters was reported to be as likely due to kinetic as to thermodynamic factors. If control was indeed kinetic, then since the greatest range of complexes obtained

contained two third-row metals, the activation-energy barriers for consecutive reactions appeared to be highest in this case. However, as mentioned above, it is a well established fact[231] that there is a greater inherent strength associated with metal-metal bonds involving two third-row metals as opposed to one third-row and one first-row metal. Thus, the reactivity study concentrated more on $HOsRe(CO)_9$ and $[HOsRe(CO)_8Br]PPN$.

Other reported anionic reactions[232] have been found to be critically dependent on reaction conditions such as reaction time, temperature and the mode of addition of reagents. This might suggest that the employment of different reaction conditions for all the reactions carried out in this study might lead to entirely different products being obtained.

The study of carbonylmetalate reactions of osmium was initially instigated with the hope that chains of metal atoms could be built up. Osmium was chosen as a starting material since it has the potential to form a dianion to which two one-electron donors can be coordinated. The hydrido anion, $[Os(CO)_4H]PPN$ was also considered to be an excellent choice of starting material, since it incorporated a readily replaceable ligand. Reaction of the anionic complex, $[Os(CO)_4H]PPN$ with Re(CO)Br produced

either a neutral or an anionic mixed-metal compound, $HOsRe(CO)_9$ or $[HOsRe(CO)_8Br]PPN$, which still both incorporated a readily replaceable ligand. Halogenation of these derivatives produced mixed-metal halide complexes, $XOsRe(CO)_9$ or $[XOsRe(CO)_8Br]PPN$, which could be further reacted with carbonylmetalate or metal carbonyl halide species, respectively, and hopefully so produce chain extension. This latter step was not attempted in this study, due to the small amounts of products of the type $XOsRe(CO)_9$ obtained and due to the high kinetic stability, under the conditions employed, of $[HOsRe(CO)_8Br]PPN$.

CHAPTER 5

HIGH RESOLUTION ^{1}H NUCLEAR MAGNETIC RESONANCE SPECTROSCOPIC STUDIES OF SOME HOMO- AND HETERONUCLEAR OSMIUM CARBONYL HYDRIDE COMPLEXES

5.1 Introduction

The unstable hydridocarbonyls, $Fe(CO)_4H_2$ and $Co(CO)_4H$ followed by the hydride complexes, $Re(\eta\text{-}C_5H_5)H$ and $M(\eta\text{-}C_5H_5)(CO)_3H$ (M = Cr or Mo) are the forerunners of the now vast array of transition metal hydride complexes.[218] These complexes have played an important role in the development of organometallic chemistry, have been found to be useful in numerous synthetic transformations and are of critical importance in many transition metal reaction mechanisms.[233] They have been recognised for some time as intermediates or catalysts in reactions such as hydroformylation, hydrogenation, olefin isomerisation and hydrogen exchange.[233]

Single crystals have not been obtained for the homologous series of osmium carbonyl hydride complexes, $[Os(CO)_4]_nH_2$ (n = 1, 2 or 3) and hence their X-Ray crystal structures have not been determined. However, they are believed from IR, ^1H nmr and mass spectral data as well as their reactivity, to all contain two terminal hydride ligands. $Os(CO)_4H_2$, being a volatile liquid at room temperature and $Os_2(CO)_8H_2$, being an oil, would require X-Ray studies to be carried out at low temperatures should single crystals be obtained. $Os_3(CO)_{12}H_2$, on the other hand, is a microcrystalline solid but cannot be obtained in a suitable crystalline form for an X-Ray study, although

studies are being conducted to obtain further structural information about the compound. EXAFS[234] and electron microscopy[235] studies are presently being independently conducted using pure $Os_3(CO)_{12}H_2$ supplied by the author. Extended X-Ray absorption fine structure (EXAFS) studies have been widely used to probe local geometries at metal centres,[236] but attempts to establish metal skeletons in discrete cluster compounds have been limited.[237,238] Recently, EXAFS studies have been carried out on $Os_3(CO)_{12}$ and several other higher nuclearity species and non-bonded osmium-osmium distances have been identified.[239]

Although the above homologous series of complexes have been reported and their ^1H nmr spectra documented,[129,127,240,241] osmium-187 satellites centred around the proton resonances were never observed. It is only since the advent of Fourier Transform ^1H nmr instruments that these very weak satellites have been observed.[242] The present study involved recording the ^1H nmr spectra of the above three members of the homologous series, $[Os(CO)_4]_nH_2$ (n = 1, 2 or 3) and, in addition, the ^1H nmr spectra of the three heterodinuclear osmium hydride complexes, $HOsRe(CO)_9$ and $[HOsRe(CO)_8X]PPN$ (X = Br or I), with the aims: (i) to observe ^{187}Os-^1H satellites and assign coupling constants and (ii) to see if useful structural information could be obtained.

Only one osmium-hydrogen coupling constant, for complexes of the homologous series, $[Os(CO)_4]_nH_2$ (n = 1, 2 or 3) has previously been reported[243] i.e. for n = 1 - see later. It has been suggested that valuable structural information can be obtained from both the chemical shift and the coupling constant determinations.[244] Osmium, itself, has received scant attention from nmr spectroscopists. Osmium-187 has spin $I = {}^1/_2$, has a natural abundance of 1.64% and lacking a quadrupole moment, its relaxation results from a magnetic dipole-dipole mechanism. Osmium-189, on the other hand, has spin $I = {}^3/_2$, has a natural abundance of 16.1%, has a natural detection sensitivity relative to ^{13}C of 2, and has a quadrupole moment of 0.8 barns.[242] The presence of the quadrupole moment in ^{189}Os causes shorter relaxation times and broad lines, since linewidths are proportional to Q^2, in its spectra and hence rendering it less useful for nmr purposes than ^{187}Os.

A large number of osmium hydride complexes have been studied by ^1H nmr spectroscopy from which chemical shift data have been obtained. However, in relatively few cases have the osmium-hydrogen coupling constants $^1J(^{187}Os-^1H)$ been measured.

The first reports[245] of osmium-hydrogen coupling were for the mononuclear tertiary phosphine and tertiary arsine polyhydride complexes $Os(PEt_2Ph)_3H_4$, $Os(AsEt_2Ph)_3H_4$ and a compound formulated as $Os(AsEt_2Ph)_2H_6$. These complexes displayed proton resonances at 21.84, 20.42 and 19.6 τ, respectively, while the measured coupling constants $^1J(^{187}Os-^1H)$ were found to be 30.8, 34.0 and 33.0 Hz, respectively.

Vancea and Graham[243] reported the first osmium-hydrogen coupling constant for an osmium carbonyl hydride complex, namely, the mononuclear hydride, $Os(CO)_4H_2$. They found the chemical shift of the proton resonance to be 18.7 τ in d_8-toluene (lit. value 18.73 τ in heptane)[129] and reported the coupling constant as $^1J(^{189}Os-^1H) = 40.5$ Hz.

Recently, a number of higher nuclearity osmium carbonyl hydrides have been studied and their osmium-hydrogen coupling constants reported.[244] The X-Ray crystal structures of all the compounds studied by these workers had previously been determined. ^1H nmr spectroscopy and the coupling constants obtained therefrom were thus used as confirmatory structural evidence. Satellites arising from coupling to spin I = $^1/2$ metal nuclei have become

increasingly recognised as valuable aids in the diagnosis of structures of organometallic complexes.[242]

For example, high resolution ^{1}H nmr spectroscopy confirmed the structures of $Os_3(CO)_{10}HCl$ and $Os_3(CO)_{11}HCl$.[244] For the decacarbonyl complex, only one set of satellites giving rise to a measured coupling constant $^{1}J(^{187}Os-^{1}H)$ = 36.6 Hz, was observed. For the undecacarbonyl complex, on the other hand, two sets of osmium satellites were observed in the ^{1}H nmr spectrum, centred around the hydride peak at 16.1 τ , giving rise to two osmium-hydrogen coupling constants of 38.1 and 27.3 Hz, respectively. This evidence is in agreement with the X-Ray crystal structures where in the former complex, the hydrido and chloro ligands are symmetrically bridging one osmium-osmium edge - see figure 5.1 a) - while in the latter complex, the hydride ligand bridges two non-equivalent osmium atoms in the molecule - see figure 5.1 b):

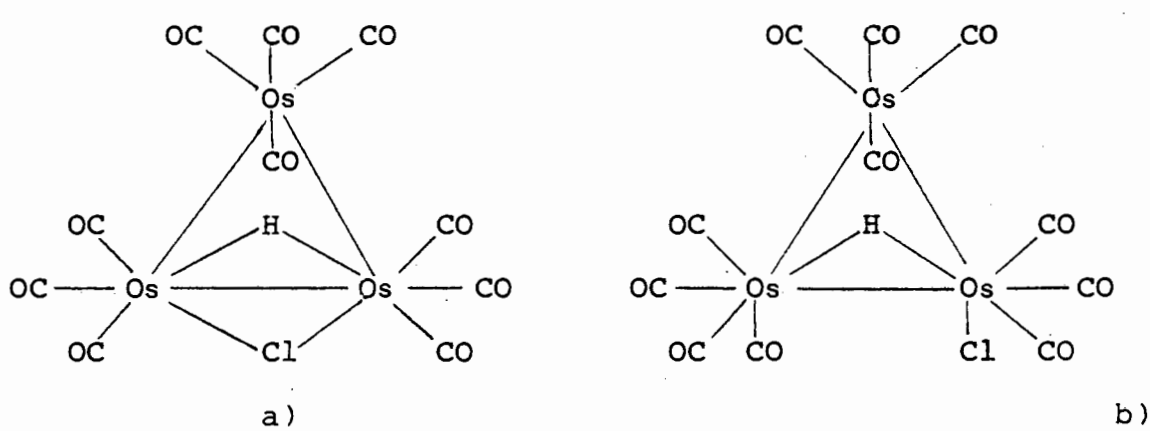

Figure 5.1 Diagrammatic representation of a) $Os_3(CO)_{10}HCl$ and b) $Os_3(CO)_{11}HCl$

^{1}H nmr spectroscopy further served as a tool for confirming the existence of two isomeric forms for the anion $[Os_4(CO)_{12}H_3]^-$.[244] Evidence for the presence of a tetrahedral interstitial hydride in $[Os_{10}C(CO)_{24}H]^-$ was presented as a result of the coupling constants and the satellite intensities observed in the ^{1}H nmr spectrum of the anion. Although the X-Ray structure of the decaosmium anion had been determined previously,[246] the hydride ligand was not located in the solid state. The intensities of the two sets of osmium satellites centred around the proton resonance at 15.3τ were found to be in a 3:1 ratio. Two coupling constants of 26.6 and 15.9 Hz, respectively were measured and were both assigned to $^{1}J(^{187}Os - ^{1}H)$. These workers postulated that the 1:3 intensity ratio - see figure 5.2 - provided evidence for the hydride ligand being in a tetrahedral environment.[244] That the hydride ligand occupied a tetrahedral interstitial site was proposed on the basis of the carbonyl packing and the osmium-osmium bond lengths obtained in the solid state structure.[246]

The possibility of smaller couplings (^{1}H-^{13}C) in either the carbide or carbonyls was eliminated by recording the spectrum of an ca 16% ^{13}C enriched sample. No change in the satellite positions or their relative intensities was observed. The largest observed coupling of ^{1}H to ^{13}C for the compound $[Os_{10}C(CO)_{24}H]^-$ was found to be ca 2Hz.[244] ^{1}H nmr spectroscopy and the measurement of osmium-hydrogen

coupling constants obtained for osmium hydride complexes, carried out at variable temperature, has also shed some light on the fluxional processes occurring in the molecule $Os_4(CO)_{12}H_4$.[247]

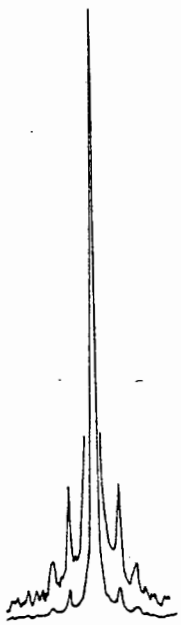

Figure 5.2 ^1H nmr spectrum of $[Os_{10}C(CO)_{24}H]^-$ showing two sets of satellites.[244]

5.2 Experimental

The mononuclear hydride, $Os(CO)_4H_2$, was prepared from $[Os(CO)_4]Na_2$ by protonation as described previously[199] and was condensed directly onto d_8-toluene at -196°C, warmed up to room temperature and a ^1H nmr spectrum obtained from this solution. $Os_2(CO)_8H_2$ and $Os_3(CO)_{12}H_2$ were obtained by reduction of the corresponding iodo-complexes - see Experimental Section - as described previously but in that work the corresponding bromo

complexes were used as starting materials.[127] The compounds were characterised by IR and ^1H spectral data which were in agreement with the literature[129,127] and by melting point in the case of $Os_3(CO)_{12}H_2$,[127] $HOsRe(CO)_9$ and $[HOsRe(CO)_8X]PPN$ (X = Br or I) were obtained from the reaction of $[Os(CO)_4H]PPN$ with $Re(CO)_5X$ (X = Br or I) - see section 4.2.1.3. The ^1H nmr spectra were obtained at 90 MHz on a Brucker WH-90 D/S Fourier Transform spectrometer at room temperature using solvents, d_8-toluene for $Os(CO)_4H_2$ and C_6D_6 for $Os_2(CO)_8H_2$, $Os_3(CO)_{12}H_2$ and $HOsRe(CO)_9$ and CD_3CN for $[HOsRe(CO)_8X]PPN$ (X = Br or I). Chemical shifts reported are relative to tetramethylsilane (τ 10.00) used as an internal reference. Between 3000 and 9000 scans each were employed for the data collections with typical accumulation times being 2-3 hours, and subjected to Fourier Transform analysis. Data collections at two spin rates were employed for each sample, in order to enable differentiation between satellites and spinning sidebands.

5.3 Results and Discussion

5.3.1 ^1H NMR Spectra of Homonuclear Osmium Hydride Complexes of the Form $[Os(CO)_4]_nH_2$ (n = 1, 2 or 3)

Since the structures of the complexes, $[Os(CO)_4]_nH_2$ (n = 1, 2 or 3), have not been determined and since Johnson et al[124] had illustrated that structural information

could be obtained from osmium-hydrogen coupling constants, the present high resolution ^{1}H nmr study was initiated.

The chemical shift of the proton resonance in $Os(CO)_4H_2$ has been twice previously reported.[129,243] In the latter report,[243] an osmium-hydrogen coupling constant of 40.5 Hz was also measured which these workers assigned to $^{1}J(^{189}Os-^{1}H)$. Since, as discussed in the introduction to this chapter, ^{189}Os satellites would be expected to be so broad as to render them indistinguishable from background noise, and further, since no other reports of ^{189}Os couplings have appeared in the literature, the ^{1}H nmr spectrum of $Os(CO)_4H_2$ was reinvestigated. The chemical shift of the proton resonance was found to be 18.70 τ in d_8-toluene (lit values 18.73 τ in heptane,[129] 18.70 τ in d_8-toluene).[243] We have now measured an osmium-hydrogen coupling constant of 41.0 Hz and this we assign to $^{1}J(^{187}Os-^{1}H)$ - see figure 5.3.

The high resolution ^{1}H nmr spectrum of the colourless oil $Os_2(CO)_8H_2$ which gave a pale yellow solution in d_6-benzene displayed a proton resonance at 20.11 τ, which is in agreement with the literature value.[127] Two sets of satellites were observed around the proton resonance, and these were found to correspond to coupling constants of 38.0 and 16.0 Hz, respectively - see figure 5.4. The

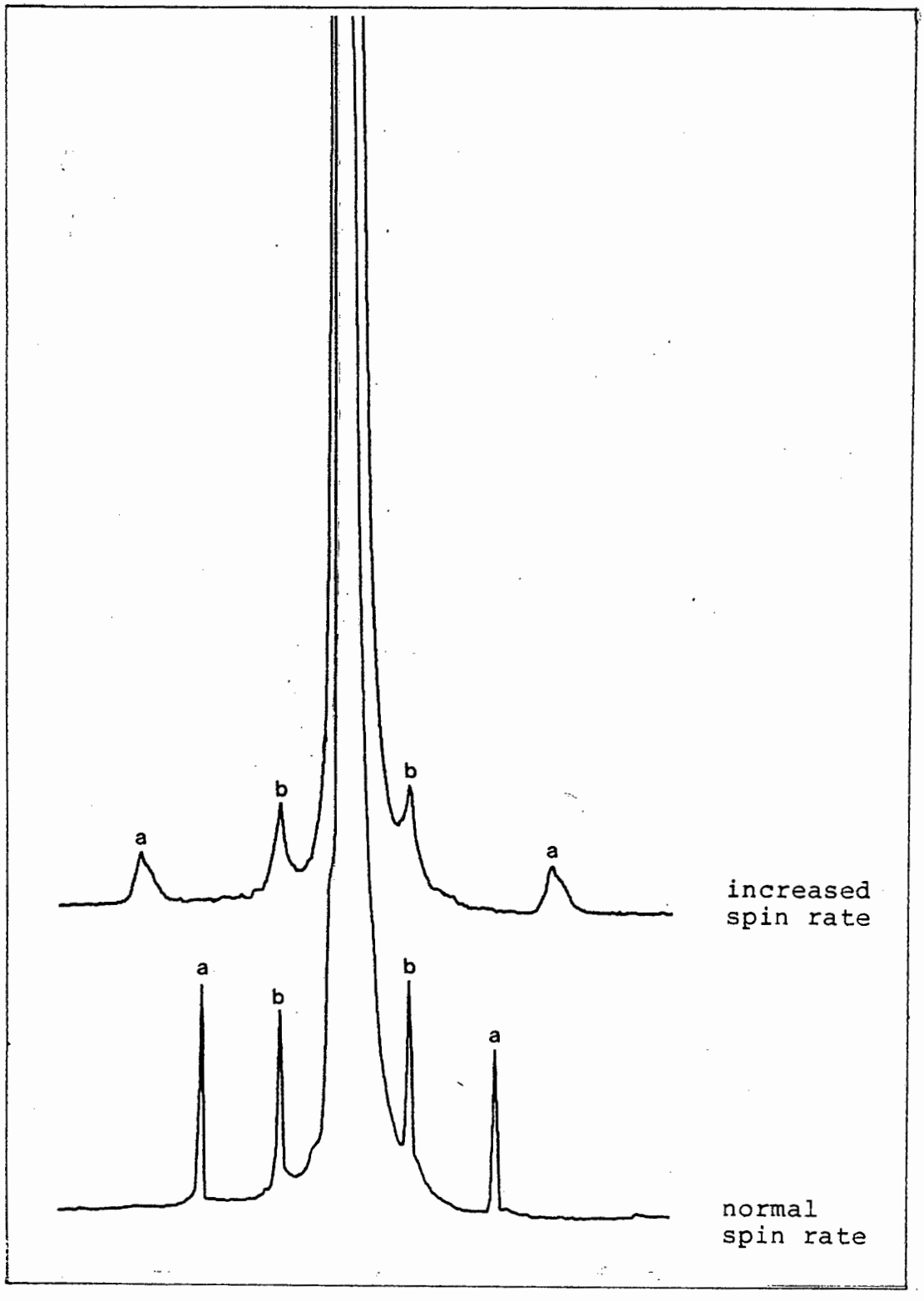

Figure 5.3 High resolution ^{1}H nmr spectrum of $Os(CO)_4H_2$ in d_8-toluene.
Key: a = spinning sidebands;
b = $^{1}J(^{187}Os-^{1}H)$ = 41.0 Hz.

former value was assigned to the 'primary' osmium-hydrogen coupling constant $^{1}J(^{187}Os-^{1}H)$, while the latter was assigned to the 'secondary' osmium-hydrogen coupling constant, $^{2}J(^{187}Os-^{1}H)$. See later in the discussion. Similarly, the high resolution ^{1}H nmr spectrum run on the pale yellow d_6-benzene solution of $Os_3(CO)_{12}H_2$, yielded a high field singlet at 19.88 τ, in close agreement with the literature value of 19.85 τ.[241] Two sets of satellites were observed from which two coupling constants of 37.5 and 16.0 Hz were obtained - see figure 5.5. These were similarly assigned as for $Os_2(CO)_8H_2$ above. See later for a discussion of these assignments.

Table 5.1 lists experimental results obtained for the homologous series of complexes.

Table 5.1 ^{1}H NMR Spectral Data for the Series of Homonuclear Hydride Complexes, $[Os(CO)_4]_nH_2$ (n = 1, 2 or 3)

Compound	Solvent	Chemical Shift (τ)	Coupling Constant[a] $^{1}J(^{187}Os-^{1}H)$	$^{2}J(^{187}Os-^{1}H)$
$Os(CO)_4H_2$	d_8-toluene	18.70 (s)	41.0	-
$Os_2(CO)_8H_2$	d_6-benzene	20.11 (s)	38.0	16.0
$Os_3(CO)_{12}H_2$	d_6-benzene	19.88 (s)	37.5	16.0

Key: a) The signs of the coupling constants were not measured but are assumed to be positive in comparison with values reported in the literature.[243,244,245]

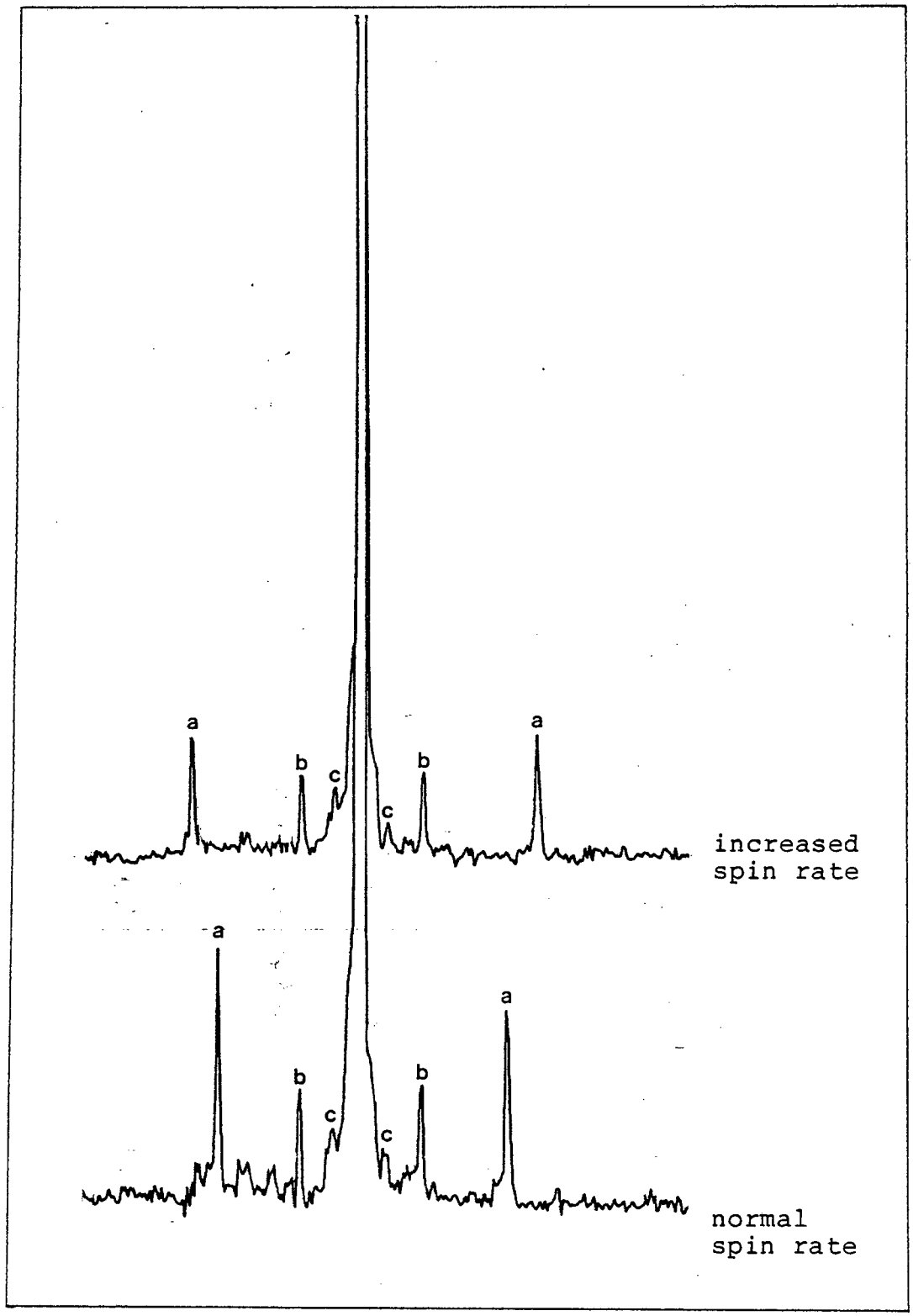

Figure 5.4 High Resolution ^{1}H nmr spectrum of $Os_2(CO)_8H_2$ in C_6D_6.
Key: a = spinning sidebands;
b = $^{1}J(^{187}Os-^{1}H)$ = 38.0 Hz;
c = $^{2}J(^{187}Os-^{1}H)$ = 16.0 Hz.

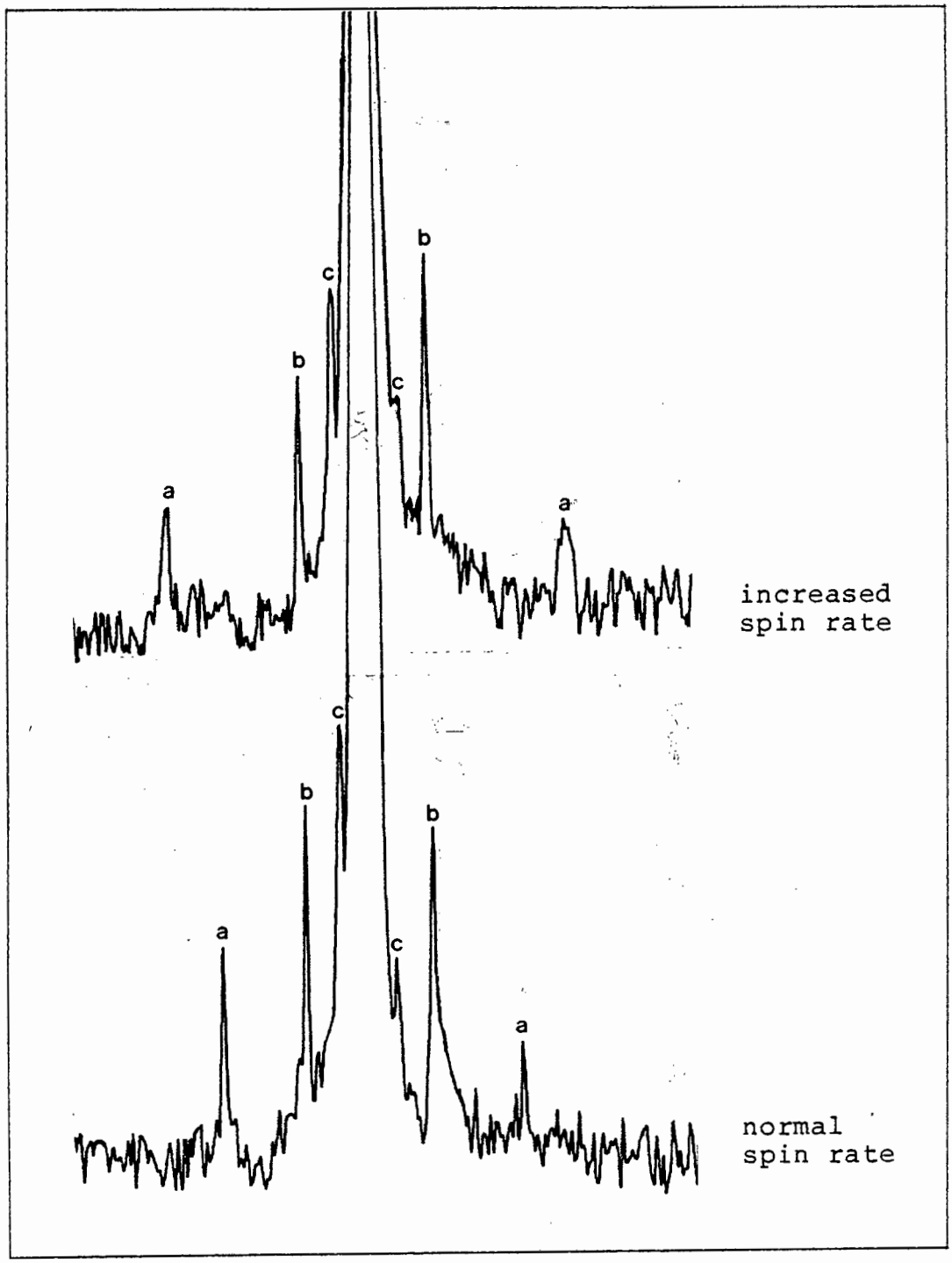

Figure 5.5 High resolution ^{1}H nmr spectrum of $Os_3(CO)_{12}H_2$ in C_6D_6.
Key: a = spinning sidebands;
b = $^{1}J(^{187}Os-^{1}H)$ = 37.5 Hz;
c = $^{2}J(^{187}Os-^{1}H)$ = 16.0 Hz.

5.3.2 ^{1}H NMR Spectra of Heterodinuclear Osmium Hydride Complexes

The neutral compound $HOsRe(CO)_9$ has previously been obtained from two separate reactions[126,208] and the chemical shift of the proton resonance was reported as 20.37 τ in C_6H_6 and 20.40 τ in CH_2Cl_2, respectively. In the first report the compound was obtained, contaminated with $Os_2(CO)_8H_2$, as a product of the reaction between $Os_3(CO)_{12}H_2$ and $Re(CO)_5H$,[126] while in the second report it was obtained, in a pure form, from $Os(CO)_4(CH_3)H$ and $Re(CO)_5H$.[208] In this present study, $HOsRe(CO)_9$ was obtained in a pure form, prior to the reported synthesis in 1982.[208] A pale yellow d_6-benzene solution of the mixed-metal hydride oil, yielded a sharp singlet at 20.37 τ, in close agreement with the literature,[126,208] with one set of satellites centred around it, from which the $^{1}J(^{187}Os-^{1}H)$ coupling constant of 37.5 Hz was measured - see figure 5.6.

The anionic derivative, $[HOsRe(CO)_8Br]PPN$ - see section 4.2.1.3 - showed a high field singlet at 20.5 τ in its ^{1}H nmr spectrum run in CD_3CN, with one set of satellites, from which the $^{1}J(^{187}Os-^{1}H)$ coupling constant of 40.5 Hz was measured - see figure 5.7. A very weak high field singlet at 20.65 τ was also observed. This may be due to another species which we believe is $[Os_2(CO)_8H]^-$.[208] The chemical shift of $[Os_2(CO)_8H]TMGH$[208] (TMGH = tetramethylguanidine) was reported in CD_3CN to occur at 20.65 τ. An IR spectrum

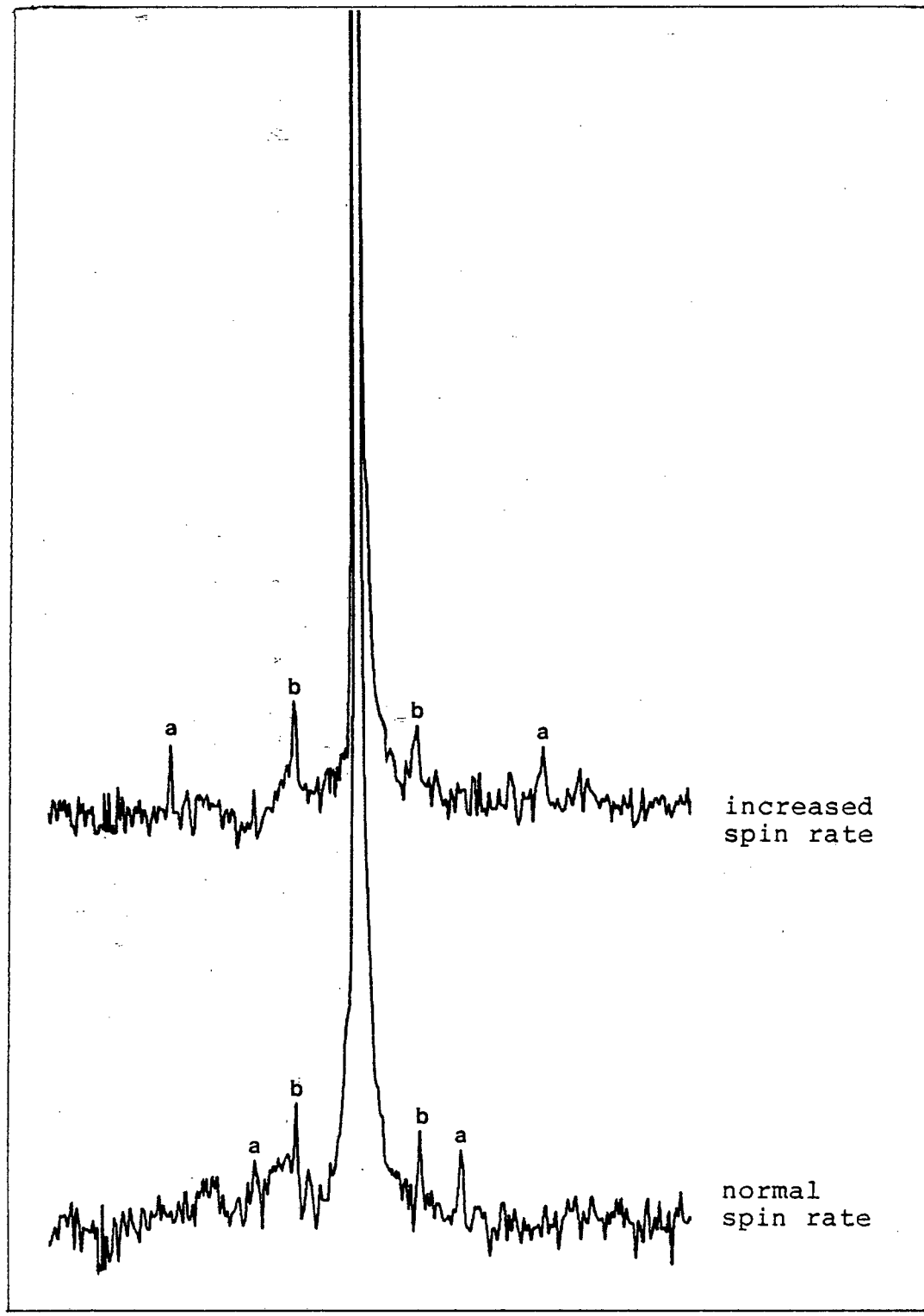

Figure 5.6 High resolution ^{1}H nmr spectrum of $HOsRe(CO)_9$ in C_6D_6.
Key: a = spinning sidebands;
b = $^{1}J(^{187}Os-^{1}H)$ = 37.5 Hz.

run on the nmr sample showed no extraneous υ(CO) bands other than corresponding to [HOsRe(CO)$_8$Br]PPN. The iodo derivative, [HOsRe(CO)$_8$I]PPN, showed a high field singlet at 20.50 τ in its IR spectrum in CD_3CN, with satellites [$^1J(^{187}Os-^1H)$ = 39.0 Hz] - see figure 5.8. The environment of the hydride ligand in the complexes, $[Os_2(CO)_8H]^-$ and [HOsRe(CO)$_8$X]$^-$ (X = Br or I), is believed to be quite similar and hence it would be expected for the proton resonances in all three complexes to have similar chemical shift values. Table 5.2 lists experimental results obtained for these heterodinuclear hydride complexes.

Table 5.2 ^{1}H NMR Spectral Data for the Heterodinuclear Hydride Complexes

COMPOUND	SOLVENT	CHEMICAL SHIFT (τ)	COUPLING CONSTANT (Hz)[a] $^1J(^{187}Os-^1H)$
HOsRe(CO)$_9$	C_6D_6	20.37(s)	37.5
[HOsRe(CO)$_8$Br]PPN	CD_3CN	20.50(s)	40.5
		2.54(m)[b]	
[HOsRe(CO)$_8$I]PPN	CD_3CN	20.50(s)	39.0
		2.54(m)[b]	

a) The signs of the coupling constants were not measured but are assumed to be positive in comparison with values reported in the literature.[245]

b) peaks due to PPh_3 protons.

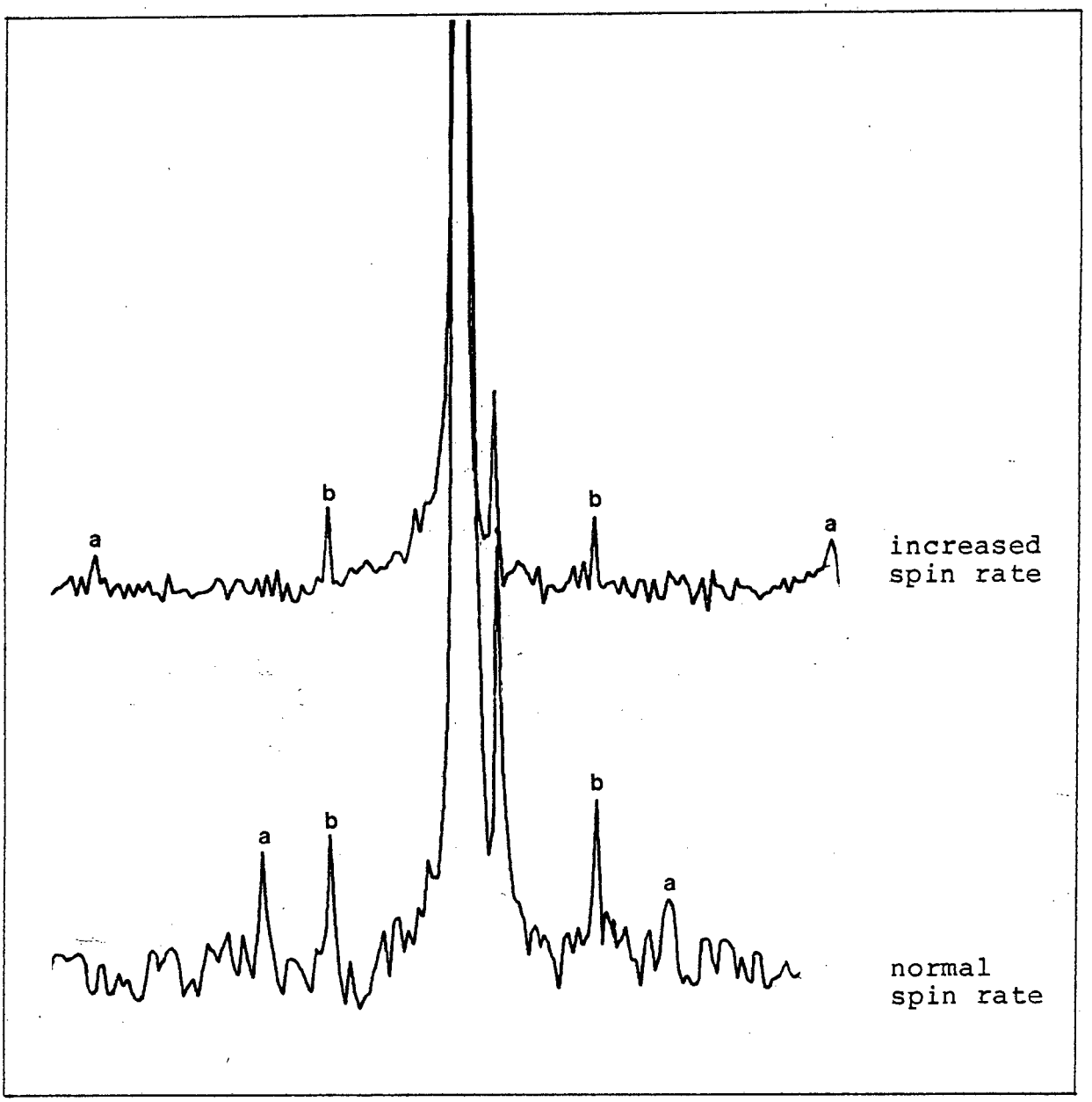

Figure 5.7 High resolution ^{1}H nmr spectrum of $[HOsRe(CO)_8Br]PPN$ in CD_3CN.
Key: a = spinning sidebands;
b = $^{1}J(^{187}Os-^{1}H)$ = 40.5 Hz;

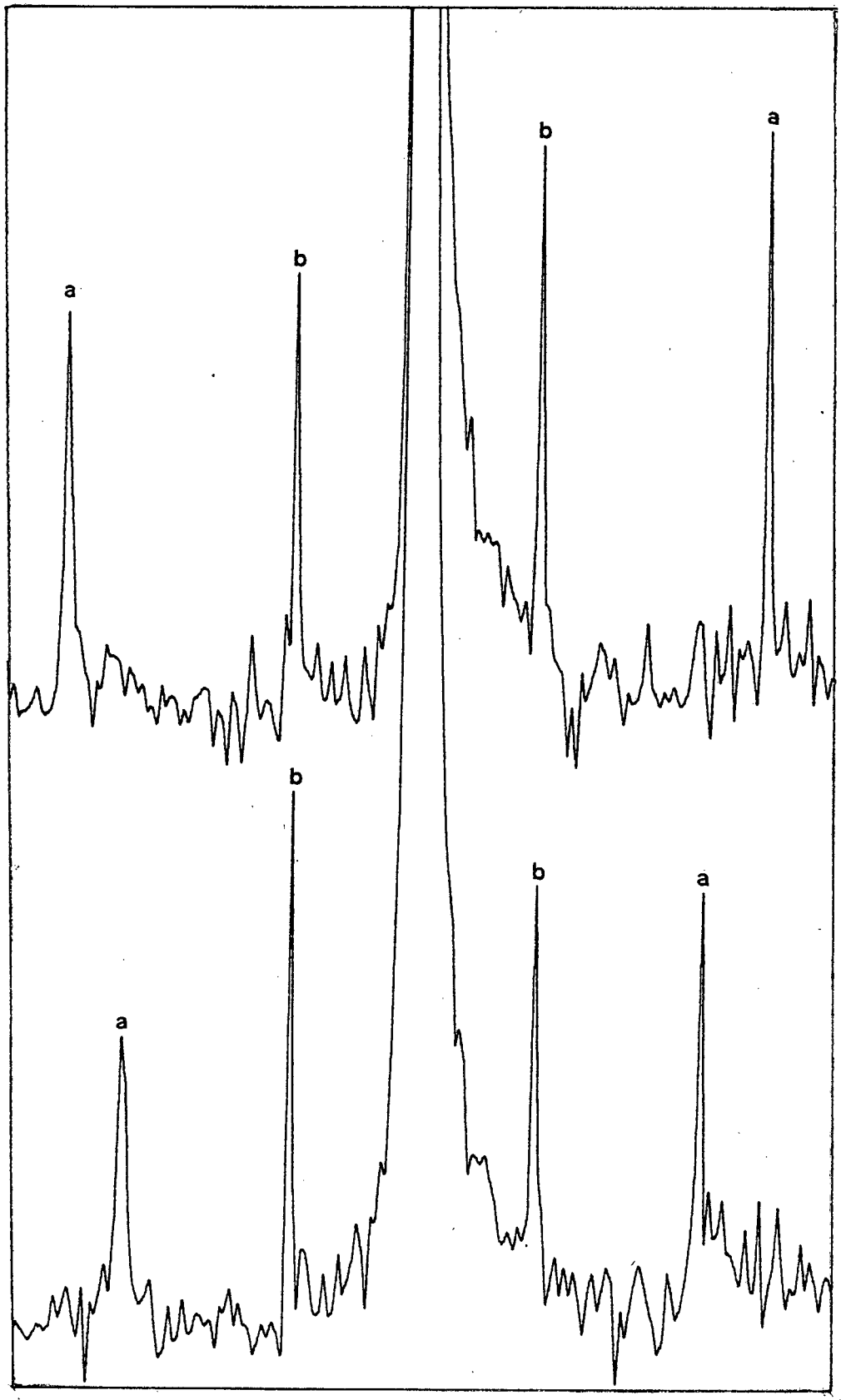

Figure 5.8 High Resolution ^{1}H nmr spectrum of $[HOsRe(CO)_8I]PPN$ in CD_3CN
Key: a = spinning sidebands
b = $^{1}J(^{187}Os-^{1}H)$ = 39.0 Hz

Chemical shifts and coupling constants may provide information about chemical structure.[242] Since each complex studied by ^1H nmr spectroscopy in this section contains the fragment $[Os(CO)_4H]$, one can consider that the general formula for these complexes be $Os(CO)_4LH$ (where L = H in $\{Os(CO)_4H_2\}$, $Os(CO)_4H$ in $\{Os_2(CO)_8H_2\}$, $Os_2(CO)_8H$ in $\{Os_3(CO)_{12}H_2\}$, $Re(CO)_5$ in $\{HOsRe(CO)_9\}$ and $Re(CO)_5X$ in $\{[HOsRe(CO)_8X]PPN\}$). The chemical shifts obtained for these proton resonances in each complex, in the above series, were 18.70, 20.11, 19.88, 20.37 and 20.50 τ, respectively. The diamagnetic screening of the proton by the electrons in the osmium atom results in substantial low frequency shift of the proton resonances. This is peculiar to metal hydrides where the hydrogen atom, due to its small size, is enveloped within the electron cloud of the metal atom. Small differences in these chemical shifts can be attributed to changes in the electron density on the osmium, directly bonded to the hydrogen atom. For a series of structurally related molecules in which the average excitation energy, ΔE and the bond order, Q_{AB} terms are reasonably constant, which is the case for the series of molecules considered in this discussion, a simple proportionality exists between nuclear shielding differences and atomic charge densities.[248] The anion, $[HOsRe(CO)_8I]^-$ PPN, contains the highest electron density of all the complexes in the series under discussion. The proton in this anion would, therefore, be expected to be the most

shielded and hence its resonance would be expected to occur at lower frequency than in any of the other complexes. In $Os(CO)_4H_2$, the least electron density would be expected in the environment of the protons since it contains only one metal atom, whereas all the other complexes are bimetallic. Therefore the protons would be the most deshielded and hence the proton resonance would be expected to be found at the highest frequency. This is found to be the case with the chemical shift of the proton in the anion being 20.50τ, while that for the mononuclear hydride was found to be 18.70τ. Thus, the chemical shift, as measured experimentally, is determined by the sum of all the magnetic fields about the nucleus, not only those of the bonding electrons in the immediate vicinity but the anisotropic effects of magnetic fields arising from atoms which may be several bonds away.[250]

The variation in the osmium-hydrogen coupling constants could be discussed in terms of the amount of the Os (6s) orbital involved in the osmium-hydrogen bond, as has been discussed previously for other complexes.[251,252] The primary effect of a drift of electron density away from the metal-hydrogen bond, to preferentially be involved in metal-metal bonding, is to cause a decrease in the s-character of the bond. From the values obtained for the coupling constants, for the series of complexes under

discussion, it can be suggested that there is more s-character in the osmium-hydrogen bond in the two limiting cases discussed above of $Os(CO)_4H_2$ and [$HOsRe(CO)_8X$]PPN (X = Br or I) which display coupling constants $^1J(^{187}Os-^1H)$ of 41.0, 40.5 and 39.0 Hz, respectively. The other members of the series $Os_2(CO)_8H_2$, $Os_3(CO)_{12}H_2$ and $HOsRe(CO)_9$, display very similar $^1J(^{187}Os-^1H)$ values of 38.0, 37.5 and 37.5 Hz, respectively. In the general formula $Os(CO)_4LH$, L for the latter three complexes could be thought of as withdrawing electron density away from the osmium-hydrogen bond to form metal-metal bonds and, in all three cases, the $[Os(CO)_4H]$ fragment has the osmium atom in a +I oxidation state. The coupling constant was found to decrease from 40.5 to 39.0 Hz in going from the bromo complex to its iodo analogue. The mononuclear complex, $Os(CO)_4H_2$, has no electron-withdrawing substituents attached to the osmium nucleus and therefore contains the largest amount of s-character in the osmium-hydrogen bond, resulting in the largest $^1J(^{187}Os-^1H)$ value.

The ^1H nmr spectra of $Os_2(CO)_8H_2$ and $Os_3(CO)_{12}H_2$ displayed a second set of satellites from which 'secondary' coupling constants were measured. The ^1H nmr spectrum of the complex $(\eta\text{-}C_5H_5)_2WH_2W(CO)_5$ was reported to display two sets of satellites around the proton resonance from which two sets

of coupling constants of 63.0 and 19.2 Hz, respectively, were obtained[253] - see figure 5.9.

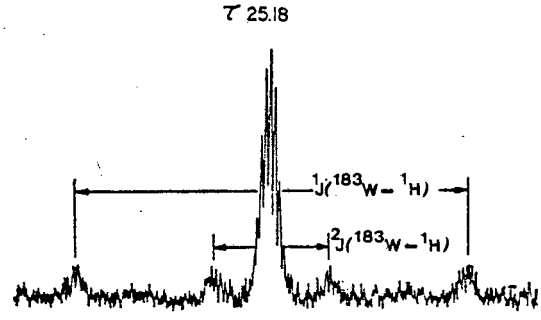

Figure 5.9 ^1H nmr spectrum of $(\eta\text{-}C_5H_5)WH_2W(CO)_5$ in THF showing two sets of satellites.[253]
Key: $^1J(^{183}W-^1H) = 63.0$ Hz.
$^2J(^{183}W-^1H) = 19.2$ Hz.

The larger coupling was assigned to $^1J(^{183}W-^1H)$ while the smaller coupling was assigned to $^2J(^{183}W-^1H)$. In the derivatives of $(\eta\text{-}C_5H_5)_2MH_2.M'(CO)_5$ (where M = W; M' = Cr or Mo), only large coupling constants were obtained while for M = Mo and M' = W, only small coupling constants were measured. Because the large coupling constant was found to be close to the value observed in $W(\eta\text{-}C_5H_5)_2H_2$ of 73.2 Hz, these workers took their observation to favour a static structure - see figure 5.10:

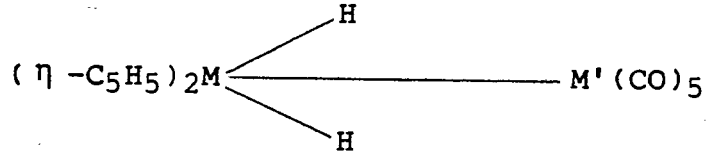

Figure 5.10 Proposed static structure for $W(\eta\text{-}C_5H_5)_2H_2$

This figure structure would appear to be more likely rather than the tautomeric species, as outlined below, in view of the large coupling constant measured.

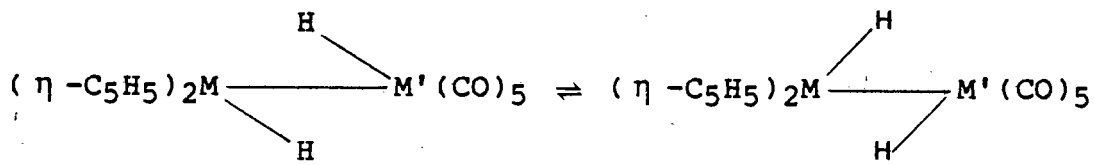

Thus the protons were believed to couple not only to the metal atoms to which they were directly bonded but also to the adjacent tungsten atom two bonds away. These two coupling constants are also consistent with the hydride ligands bridging the two tungsten atoms.

This coupling was also observed in the ^{29}Si nmr spectra of methyl silane derivatives.[254] A ^{29}Si atom in $[Me_2Si]_n$, a polymeric silicon compound - see figure 5.11 - was observed to be coupled to protons both on attached methyl groups and on methyl groups bonded to adjacent silicon atoms.

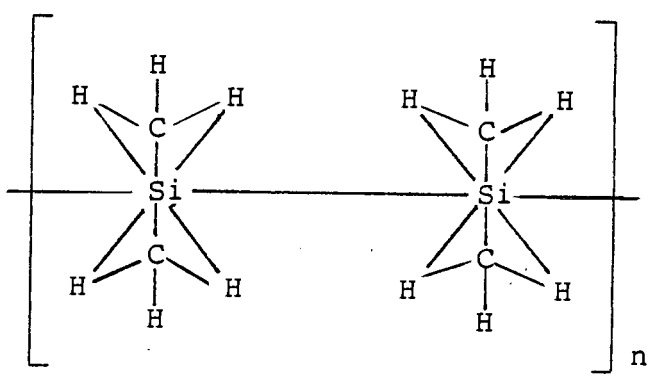

Figure 5.11 Diagrammatic representation of $[Me_2Si]_n$

This long range coupling has also been observed for some polynuclear platinum hydride complexes. The low temperature (-80 °C) ^{1}H nmr spectrum of the complex $Pt_3H_6(PBu^t_3)_3$ [255] - see figure 5.12 - showed two sets of hydride signals of equal intensity at 14.0 τ [d with ^{195}Pt satellites, $H_{bridging}$, $^{1}J(^{195}Pt-^{1}H)$ = 565 Hz and $^{2}J(^{195}Pt_2-^{1}H)$ = 405 Hz] and at 17.54 τ [d with ^{195}Pt satellites, $H_{terminal}$, $^{1}J(^{195}Pt-^{1}H)$ = 822 Hz and $^{2}J(^{195}Pt_2-^{1}H)$ = 100 Hz). As the temperature was raised, the terminal and bridging hydride ligands were found to exchange and move around the cluster. Thus the proton was found to couple equally with both the platinum and phosphorus nuclei.

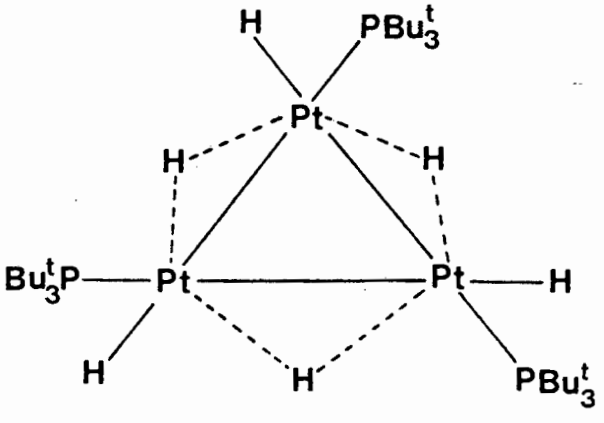

Figure 5.12 Diagrammatic representation of $Pt_3H_6(PBu^t_3)_3$

The proton resonance in the complex, $Pt_2HL(\mu\text{-dppm})_2PF_6$,[256] contained satellites around it, which were attributed to coupling to the directly bound platinum atom,

$^{1}J(^{195}Pt\text{-}^{1}H)$ = 936 Hz and to the other platinum atom, $^{2}J(^{195}Pt\text{-}^{1}H)$ = 76 Hz - see figure 5.13.

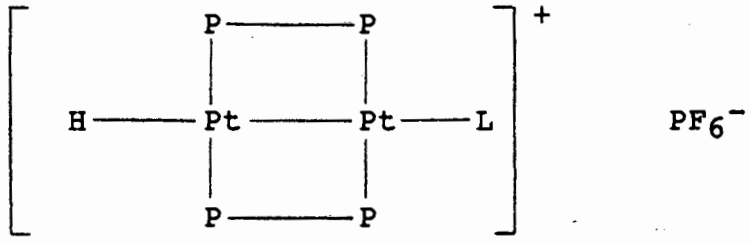

Figure 5.13 Diagrammatic representation of $[Pt_2HL(\mu\text{-dppm})_2]PF_6$

The only naturally occurring isotope of platinum with non-zero nuclear spin, ^{195}Pt has I = ½ and reasonable abundance and sensitivity. As coupling constants to ^{195}Pt are quite large and ligand exchange generally is slow, ^{195}Pt satellites are clearly visible.

Based on the above coupling assignments and on the fact that Johnson et al[244] assigned a secondary coupling constant of magnitude 15.9 Hz to osmium-hydrogen coupling for the compound, $[Os_{10}C(CO)_{24}H]^-$, it is tentatively proposed that the coupling constant of 16.0 Hz, observed in the spectra of $Os_2(CO)_8H_2$ and $Os_3(CO)_{12}H_2$, respectively, arises from the hydrogen atoms coupling to the osmium atom two bonds away, respectively. If the peaks which we have observed are due to $^{2}J(^{187}Os\text{-}^{1}H)$, then it would be expected that such couplings would also be observed in such complexes as $[Os_2(CO)_8H]^-$.

5.4 Conclusion

'Primary' coupling constants, $^{1}J(^{187}Os-^{1}H)$, have been determined for the complexes, $[Os(CO)_4]_nH_2$ (n = 1, 2 or 3), $HOsRe(CO)_9$ and $[HOsRe(CO)_8X]PPN$ (X = Br or I). It has been proposed in this study that 'secondary' coupling in an $H-Os_1-Os_2$ system is observable. It was hoped that the determination of the coupling constants might provide some structural information about the complexes under discussion. It has previously been suggested that the chemical shift of the proton resonance can provide evidence for the hydride ligand being in either a bridging or a terminal environment.[14] However, although this is true in most cases, the complex, $Os_3(CO)_{10}H_2$[119], which contains two bridging hydride ligands, displays a proton resonance at 21.6 τ in the ^{1}H nmr spectrum and not in the region of 30 τ expected for bridging hydride ligands. Therefore, the range of chemical shift of the proton resonances of 19.88 τ -20.50 τ obtained in this study cannot provide unequivocal evidence as to the environment of the hydride ligands in these complexes. Although no unequivocal structural information could be obtained from the values of the coupling constants determined in this study, it is interesting to note, that $^{1}J(^{187}Os-^{1}H)$ for the compound $Os_3(CO)_{11}HCl$, which contains an unsymmetrically bridging hydride ligand - see figure 5.1b), was found to be 38.1 Hz[257]. This value is similar to that determined for $Os_2(CO)_8H_2$, in this study.

CHAPTER 6

EXPERIMENTAL

A. Physical Methods

1. Infrared Spectra

The infrared spectra were determined on Nujol mulls (4000-400 cm^{-1}) between potassium bromide plates. Solution spectra in the carbonyl region (2200-1600 cm^{-1}) were determined between potassium bromide plates using 0,1 mm spacings. These solid state and solution spectra were determined on Perkin-Elmer 180 and Perkin-Elmer 983 spectrophotometers. Far infrared spectra were obtained on Nujol mulls between polyethylene plates on a Digilab FTS 16B/D interferometer (500-50 cm^{-1}). The quoted wavenumber accuracy of the Perkin-Elmer spectrophotometers is better than 1 cm^{-1} and their repeatibility better than 0.30 cm^{-1}. The Digilab interferometer behaves similarly.

2. Mass Spectra

Mass spectra on solid samples were measured on a VG Micromass 16F instrument operating in the electron impact mode, with electron beam energy 70eV and ion accelerating voltages 2kV and 4kV and with ion source temperatures in the range 100°-200°C. All positive ions containing osmium exhibited the most abundant peak for osmium existing as the ^{192}Os isotope. Mass spectra were interpreted with the aid of a computer program which calculated exact masses and isotope combination patterns.[258]

3. Melting Points

Melting points were obtained on a Kofler hot-stage microscope and are uncorrected.

4. Microanalyses

Microanalyses were performed by Mr W R T Hemsted, of the microanalytical laboratory of the University of Cape Town, or by F and E Pascher, Bonn, West Germany.

5. Computation

All computations were performed at the Computer Centre of the University of Cape Town, on a Sperry 1100/81 computer, unless otherwise stated.

6. Solvents

Where necessary, solvents were dried prior to use. Benzene was dried by distillation over anhydrous $CaCl_2$. Tetrahydrofuran was dried by distillation over $LiAlH_4$. Methanol was dried and purified by standard techniques.[259] Heptane and hexane were dried over sodium wire. Acetonitrile was dried over P_2O_5. All dried solvents were saturated with nitrogen prior to use.

7. Metal Salts, Ligands and Reagents

The following complexes were prepared by literature methods: $Os_3(CO)_{12}Br_2$,[119] $Os_3(CO)_{12}I_2$,[119] $Re(CO)_5Br$,[260] $Re(CO)_5I$,[261] $Mn(CO)_5Br$[215], $[Os(CO)_4]Na_2$[199], $[HOs(CO)_4]PPN$[202]. OsO_4 was obtained from Johnson Matthey Co Ltd and converted to $Os_3(CO)_{12}$ by Dr A J Deeming of University College, London, England, or purchased from Strem Chemicals. $AuPPh_3Cl$ was obtained from Dr T V Ashworth, CSIR, Pretoria, South Africa.

8. Column Chromatography

Column chromatography was carried out using Kieselgel 60 (35-70 mesh) (Merck) or Silica Gel (40-60 mesh) (BDH) as packing for column lengths, 10 cm and 40 cm and internal diameters, 2.2 cm and 2.5 cm, respectively, where short and long columns were necessary. For thin layer chromatography, employed for test purposes, DC-alufolien Kieselgel 60 F_{254} Merck TLC aluminium sheets were used.

9. Other

All reactions were carried out under an atmosphere of high-purity nitrogen. The $h\upsilon$ reactions were carried out in a 1 litre Hanovia photochemical reactor. The sunlight reactions were carried out in glass vessels. By "direct, bright sunlight" we mean that the reactions were carried out outside the laboratory.

B. Dinuclear Osmium Carbonyl Halide Complexes

1. Reaction between $Os_3(CO)_{12}$ and Chlorine

(a) $Os_3(CO)_{12}$ (0.22 g, 0.25 mmol) was refluxed in benzene (200 cm^3) until dissolved. Chlorine (0.87 mmol) (19.65 cm^3 of a 1 x 10^{-3} M solution in benzene) was added to the hot solution immediately after it had been removed from heating under reflux. The yellow colour of the solution was seen to pale. The reaction mixture was allowed to stand in direct, bright sunlight for 3 minutes at temperatures of (26°-30°C) whereupon the yellow colour of the solution deepened. Removal of the solvent under reduced pressure gave a yellow residue which was dissolved in a minimum of CH_2Cl_2 (10 cm^3) and passed through a silica gel column (8 cm long). Elution with CH_2Cl_2 (50 cm^3) gave a pale yellow solution, while a green band attributed to decomposition products, remained at the top of the column. The eluant was taken down to dryness to give a pale yellow solid. Extraction with n-hexane (3 x 20 cm^3) and subsequent filtration afforded a pale yellow solid (0.07 g) which was found by the υ(CO) bands in the IR spectrum[126] to be a mixture of $Os_2(CO)_8Cl_2$ and $Os_2(CO)_6Cl_2$. The pale yellow hexane insoluble solid was shown by its IR spectrum[126] in

CH_2Cl_2 to be $Os_3(CO)_{12}Cl_2$ (0.12 g, 49%) mpt 168°-172°C (decomp) lit[126] 164°-170°C (decomp).

(b) $Os_3(CO)_{12}$ (0.23 g, 0.25 mmol) was refluxed in benzene (200 cm^3) until dissolved. Chlorine (0.88 mmol) was added to the hot solution at 80°C. The reaction solution was transferred to a Hanovia photochemical reactor and irradiated for 2 minutes with stirring. The temperature of the reaction solution after this duration was 46°C. The reaction was monitored by IR spectroscopy and was stopped when υ(CO) bands, other than those corresponding to $Os_3(CO)_{12}Cl_2$ were observed in the IR spectrum of the reaction solution, indicating that $Os_3(CO)_{12}Cl_2$ was no longer the major species present in solution. A pale yellow precipitate which was filtered off was identified as $Os_3(CO)_{12}Cl_2$ (0.11 g, 45%) mpt 168°-172°C (decomp) lit[126] 164°-170°C (decomp) by comparison of the υ(CO) bands in its IR spectrum with those reported in the literature.[119] The filtrate was evaporated to dryness under reduced pressure and extracted with n-hexane (3 x 20 cm^3) to yield a pale yellow solution and a hexane insoluble solid (0.10 g). The solid was filtered off and identified as being a mixture of cis- $Os(CO)_4Cl_2$[129] and $Os_3(CO)_{12}Cl_2$[119] by the υ(CO) bands in the IR spectrum which were in agreement with the literature. $Os_3(CO)_{12}Cl_2$[119] by the υ(CO) bands in the IR spectrum which The hexane extract was found to contain $Os_2(CO)_8Cl_2$ and $Os_2(CO)_6Cl_2$.[126] Attempts to separate this mixture by column chromatography were not successful.

2. Preparation of $Os_2(CO)_8Br_2$ and $Os(CO)_4Br_2$ from $Os_3(CO)_{12}$

(a) $Os_3(CO)_{12}$ (0.22 g, 0.24 mmol) was dissolved in benzene by heating under reflux. Bromine (0.04 cm^3, 0.85 mmol) was added to the hot solution at 80°C and the reaction mixture placed in direct, bright sunlight, at ambient temperature, for 5 minutes. A colour change from orange-red to pale yellow was used as an indication that all the bromine was consumed. The solvent was removed in vacuo and the residue dissolved in a minimum of CH_2Cl_2 (ca 10 cm^3) and passed through a short silica gel column (made up with CH_2Cl_2) and then eluting with CH_2Cl_2 (60 cm^{-3}). The eluant was evaportated to dryness to give a yellow solid. Extraction with n-hexane (3 x 20 cm^3) and filtration, gave a yellow solution and an insoluble off-white solid. The hexane solution was evaporated to dryness to yield a yellow microcrystalline product identified as $Os_2(CO)_8Br_2$, by IR and mass spectroscopic and melting point data, in agreement with the literature.[126] (Crude yields ranged from 56-92% depending on the reaction conditions employed) mpt 126°-132°C, lit[126] 121°-126°C. The hexane insoluble yellow solid was identified as cis-$Os(CO)_4Br_2$ by comparison with the IR spectral data and melting point, reported in the literature[120] (0.09 g, 27%) mpt 275°-290°C, lit[129] 320°C. The mass spectrum of the product, cis- $Os(CO)_4Br_2$ showed a molecular ion at m/e 462 corresponding to $[Os(CO)_4Br_2]^+$ with loss of four carbonyl groups, followed by sequential loss of two bromide ligands. Far IR (Nujol): (Os-Br) 209(br) cm^{-1}, in agreement with the literature.[262]

(b) $Os_3(CO)_{12}$ (0.23 g, 0.25 mmol) was dissolved in benzene (200 cm^3) by heating under reflux. Bromine (0.88 mmol) (2.3 cm^3 of a 1.3 x 10^{-1}M solution in benzene) was added to the hot solution at 80°C. The orange-red reaction solution was transferred to a Hanovia photochemical reactor and irradiated for 7 minutes, with stirring. The temperature of the solution after this time was 33°C. The colour of the solution was pale yellow, indicative of the consumption of bromine. The reaction was monitored by IR spectroscopy and after an irradiation time of 7 minutes, additional υ(CO) bands, other than those corresponding to $Os_3(CO)_{12}Br_2$, were observed in the IR spectrum of the reaction solution. The solvent was removed under reduced pressure and the black residue (probably due to the presence of traces of osmium metal) extracted with n-hexane (3 x 30 cm^3) to give a white solid, contaminated with osmium metal, and a yellow solution. The hexane insoluble solid was dissolved in a minimum of CH_2Cl_2 and passed through a short silica gel column (made up as a slurry in CH_2Cl_2) with CH_2Cl_2. A colourless solution was collected and evaporated to dryness to yield an off-white solid, identified as cis-$Os(CO)_4Br_2$ (0.04 g, 12%) mpt 275°-290°C, lit[129] 320°C, by its mass spectrum, by its IR spectrum and melting point all data of which were in agreement with those reported in the literature.[129] Far IR (Nujol): υ(Os-Br) 209(br) cm^{-1}.[262] The column was further eluted with methanol to yield an oily yellow product,

identified as $Os_2(CO)_6Br_4$ (0.04 g, 18%) by its mass spectrum, which showed a molecular ion at m/e 870, corresponding to $[Os_2(CO)_6Br_4]^+$ with sequential loss of six carbonyl groups to give a positive ion at m/e 702 corresponding to $[Os_2Br_4]^+$. It was further identified by its IR spectrum which showed two strong ν(CO) bands at 2120 and 2032 cm^{-1}. We assign these two bands to $Os(CO)_3Br_2(MeOH)$ formed in solution by the interaction of $Os_2(CO)_6Br_4$ with methanol used as the eluent. Black osmium metal decomposition remained on the column. The hexane soluble portion was evaporated to dryness under reduced pressure and the yellow solid dissolved in a minimum of CH_2Cl_2 and chromatographed on a long silica gel column (made up as a slurry in CH_2Cl_2) with a 30% CH_2Cl_2/n-hexane solution. The first yellow band to be eluted was collected and evaporated to dryness to yield a yellow solid identified as $Os_2(CO)_6Br_2$[126] (<0.01 g, 3%). The column was further eluted with CH_2Cl_2 and the eluted solution evaporated to dryness to yield a pale yellow solid. Recrystallisation of this solid from n-hexane gave pure $Os_2(CO)_8Br_2$ (0.09 g, 46%) mpt 126°-132°C lit[126] 121°-126°C, identified by IR and mass spectroscopic data, all of which were in agreement with the literature.[126]

3. Preparation of $Os_2(CO)_8Br_2$ and $Os(CO)_4Br_2$ from $Os_3(CO)_{12}Br_2$

$Os_3(CO)_{12}Br_2$ (0.17 g, 0.16 mmol) was dissolved in CH_2Cl_2 with warming. Bromine (0.08 cm^3, 0.16 mmol) was added to the solution and the reaction mixture left to stand at ambient temperature under laboratory light conditions for 3 hours. Removal of the solvent in **vacuo** afforded a yellow solid. Extraction with n-hexane (3 x 20 cm^3) gave a yellow solution and an off-white insoluble solid. The solvent was removed from the hexane solution to yield a yellow microcrystalline solid shown to be $Os_2(CO)_8Br_2$ by IR and mass spectroscopy and by melting point, all data found to be in agreement with the literature[126] (0.09 g, 72%) mpt 126°-132°C lit[126] 121°-126°C. The hexane-insoluble solid was shown to be **cis**-$Os(CO)_4Br_2$ by IR and mass spectral and melting point data in agreement with the literature[129] (0.07 g, 30%) mpt 275°-295°C lit[129] 310°C.

4. Preparation of $Os_2(CO)_8I_2$ and $Os(CO)_4I_2$ from $Os_3(CO)_{12}$

(a) $Os_3(CO)_{12}$ (0.23 g, 0.25 mmol) was heated in benzene (250 cm^3) under reflux until dissolved. Iodine (0.22 g, 0.89 mmol) was added to the hot solution at 80°C. The red reaction mixture was placed in direct, bright sunlight for 20 minutes at ambient temperature with intermittent

swirling. The solvent was removed in vacuo to leave a brown-yellow solid which was dissolved in a minimum of CH_2Cl_2 (ca 10 cm^3) and passed through a long silica gel column (made up as a slurry in 20% CH_2Cl_2/n-hexane). Elution with a 30% CH_2Cl_2/n-hexane solution caused a red and a yellow band to separate on the column. The eluant ahead of the red band was collected and evaporated to dryness to yield trans-$Os(CO)_4I_2$ in very low yield. IR (n-hexane): ν(CO) 2071 cm^{-1}, in agreement with the literature.[130] It was further characterised by a molecular ion in the mass spectrum at m/e 462 corresponding to $[Os(CO)_4I_2]^+$ with sequential loss of four carbonyl groups and by its melting point, 130°-150°C (sublimed). The red band (indicative of excess of iodine which was removed at low pressure) was collected and evaporated to dryness, to yield a bright yellow microcrystalline solid identified by comparison of the ν(CO) bands in the IR spectrum and of the mass spectrum with those reported in the literature[115] to be $Os_2(CO)_8I_2$ (0.11 g, 51%) mpt 137°-140°C lit[115] 138°C. Far IR (Nujol): ν(Os-I) 162 cm^{-1}. The yellow band, on evaporation of the solvent, was shown to consist of cis-$Os(CO)_4I_2$ (0.24 g, 56%) mpt 320°-330°C, by IR and mass spectroscopy with a molecular ion at m/e 462 with sequential loss of four carbonyl groups. Far IR (Nujol): ν(Os-I) 164 cm^{-1}.

(b) $Os_3(CO)_{12}$ (0.23 g, 0.25 mmol) was heated in benzene (200 cm^3) under reflux until dissolved. Iodine (0.22 g dissolved in benzene (10 cm^3), 0.88 mmol) was added to the hot solution at 80°C. The red reaction solution was transferred to a Hanovia photochemical reactor and irradiated for 15 minutes, with stirring. The temperature of the reaction solution after this duration was 31°C. The reaction was monitored by IR spectroscopy and after the irradiation time of 15 minutes, new υ(CO) bands other than those corresponding to $Os_3(CO)_{12}I_2$ were observed, indicating that $Os_3(CO)_{12}I_2$ was no longer the major species present in solution. Removal of the solvent under reduced pressure left a yellow-brown solid which was dissolved in a minimum of CH_2Cl_2 and chromatographed on a long silica gel column (made up as a slurry in 30% CH_2Cl_2/n-hexane) with a 30% CH_2Cl_2/n-hexane solution. As for 4.(a) above, the compounds were separated by column chromatography. Trans-$Os(CO)_4I_2$, obtained in low yield, was eluted first and identified as in 4.(a) above.[130] A yellow band, which separated on the column, was shown to consist of mostly $Os_2(CO)_8I_2$[115] and some cis-$Os(CO)_4I_2$.[129] These latter two compounds were

separated by fractional crystallisation, the monomeric compound being more soluble in n-hexane than the dimeric complex. $Os_2(CO)_8I_2$ crystallised from solution first and the mother liquors were then further purified by recrystallisation to yield pure $Os_2(CO)_8I_2$ (0.09, 41%) mpt 137°-140°C lit[115] 138°C. Far IR (Nujol): ν(Os-I) 162 cm^{-1}. The ν(CO) bands in the IR spectrum and its mass spectrum were in agreement with the literature.[115] Cis-$Os(CO)_4I_2$ (0.02 g, 5%) mpt 320°-330°C was identified by comparison of the ν(CO) bands in the IR spectrum with those reported in the literature.[129] Far IR (Nujol): ν(Os-I) 164 cm^{-1}. The mass spectrum showed a molecular ion at m/e 462 with sequential loss of four carbonyl groups. A yellow band remaining on the column was eluted with methanol to give a yellow microcrystalline compound identified as $Os(CO)_3I_2$-(MeOH), formed by the interaction of $Os_2(CO)_6I_4$ with methanol (0.06 g, 23%) mpt 225°-232°C by its mass spectrum which gave a molecular ion at m/e 1058 corresponding to $[Os_2(CO)_6I_4]^+$. Sequential loss of six carbonyl groups gave a positive ion at m/e 890 corresponding to $[Os_2I_4]^+$. IR (CH_2Cl_2): ν(CO) 2119(s) 2050(s) cm^{-1} in agreement with the literature.[114]

The mass spectrum of cis-$Os(CO)_4I_2$

m/e 558 (100%-$[Os(CO)_4I_2]^+$), 530 (40%-$[Os(CO)_3I_2])^+$),
502 (20%-$[Os(CO)_2I_2]^+$, 474 (43%)-$[Os(CO)I_2]^+$),
446 (53%-$[OsI_2]^+$), 431 (10%-$[Os(CO)_4I]^+$),
403 (24%-$[Os(CO)_3I]^+$), 375 (17%-$[Os(CO)_2I]^+$),
347 (17%-$[Os(CO)I]^+$), 319 (57%-$[OsI]^+$),
246 (4%-$[Os(CO)_2]^+$), 218 (6%-$[Os(CO)]^+$),
192 (31%)-$[Os]^+$), 127 (56%-$[I]^+$).

5. Preparation of $Os_2(CO)_6I_2$ from $Os_2(CO)_8I_2$

A solution of $Os_2(CO)_8I_2$ (0.11 g, 0.13 mmol) in n-heptane (12 cm^3) was heated under reflux for 40 minutes. During this time, the solution became a brighter yellow. Evaporation of the solvent yielded a bright yellow solid, identified[115] by IR and mass spectroscopy and by melting point to be $Os_2(CO)_6I_2$ (0.089 g, 80%) mpt 82°-87°C lit[115] 87°C. The compound was purified by sublimation (60°C/ 0.01 mm Hg). Far IR (Nujol): ν(Os-I) 160(br) cm^{-1}.

6. Reaction between $Os_2(CO)_6I_2$ with $2PPh_3$

PPh_3 (0.05 g, 0.17 mmol) dissolved in n-hexane (5 cm) was added to a solution of $Os_2(CO)_6I_2$ (0.07 g, 0.08 mmol) in n-hexane (15 cm^3) with stirring. An immediate reaction took place with the precipitation of a yellow solid.

After 10 minutes, stirring was discontinued and the reaction mixture left to stand for 30 minutes. The supernatant liquid was syringed off, leaving a bright yellow microcrystalline product which was washed with n-hexane (2 x 10 cm^3) and dried **in vacuo** (0.05 g, 40%) **mpt** 105°-112°C identified as hexacarbonyldiiodobis(triphenylphosphine)-diosmium, $[Os_2(CO)_6(PPh_3)_2I_2]$ (Found: C, 38.2; H, 2.4; I, 19.4; mol wt (benzene) 1300. $C_{42}H_{30}I_2O_6Os_2P_2$ requires: C, 38.03; H, 2.28; I, 19.13; mol wt 1325 IR (CH_2Cl_2): ν(CO) 2114(w) 2086(m) 2052(s) 2016(vs) 2001(s,sh) 1990(s,sh) 1978(m,sh) cm^{-1}. IR (Nujol): ν(CO) 2111(vw) 2082(w) 2046(m) 2010(vs) 1982(s) 1935(sh) 1889(w) cm^{-1}. NMR: ^1H ($CDCl_3$) 2.48(m) τ.

7. **The reaction between $Os_2(CO)_6I_2$ and $2PMe_2Ph$**

PMe_2Ph (0.04 cm^3, 0.03 g, 0.21 mmol) was added to a solution of $Os_2(CO)_6I_2$ (0.08 g, 0.11 mmol) in n-hexane (15 cm^3) with stirring. The immediate precipitation of a yellow solid was observed. Stirring was continued for 3 minutes and the reaction mixture thereafter allowed to stand for a further 15 minutes without stirring. The supernatant liquid was syringed off, and the oily, yellow residue triturated with n-hexane (2 x 10 cm^3) and dried in vacuo to yield a fine yellow solid (0.04 g, 35%) mpt 68°-75°C, identified as hexacarbonyldiiodobis(dimethylphenylphosphine)diosmium, $[Os_2(CO)_6(PMe_2Ph)_2I_2]$. (Found: C,25.8; H, 2.5.

$C_{22}H_{22}I_2O_6Os_2P_2$ requires: C, 24.5; H, 2.1). IR (CH_2Cl_2): υ(CO) 2113(w) 2050(m,sh) 2036(s) 2014(vs) 1996(m) 1965(s) cm^{-1}. Far IR (Nujol): 159 cm^{-1}, which we assign to υ(Os-I). NMR: ^1H (CD_3Cl) 2.49(m) τ (phenyl protons); 8.25(d) τ (methyl protons), [$J(^{31}P-^1H)$ = 13 Hz].

8. Reaction between $Os_2(CO)_6I_2$ and I_2

Iodine (0.004 g, 0.034 mmol) dissolved in n-hexane was added to a soution of $Os_2(CO)_6I_2$ (0.027 g, 0.034 mmol) in n-hexane (10 cm^3) with stirring. The almost immediate precipitation of a yellow precipitate was observed. This precipitate was washed with n-hexane and recrystallised from benzene to give a bright yellow solid (0.02 g, 49%) mpt 225°C. IR (CCl_4): υ(CO) 2115(s) 2025(vs) cm^{-1} lit[114] 2119(s) 2051(s) cm^{-1}. (We believe the bands at 2119 and 2051 cm^{-1} [114] are due to a monomeric species present in solution, possibly $Os(CO)_3I_2(H_2O)$, formed by the interaction of $Os_2(CO)_6I_4$ with an impurity, possibly H_2O, in the CCl_4 solvent). Mass spectrum: molecular ion observed for $[Os_2(CO)_6I_4]^+$ at m/e 1058, with sequential loss of 6 carbonyl groups, to give a positive ion at m/e 890, corresponding to $[Os_2I_4]^+$.

9. Reaction of $Os_2(CO)_6I_2$ with CO

CO was bubbled through a solution of $Os_2(CO)_6I_2$ (0.05 g, 0.06 mmol) in n-hexane (15 cm^3) at room temperature and the solution then allowed to stir, in a closed Schlenk tube,

under an atmosphere of CO for 2 days. The bright yellow colour of the solution had paled over this period. An IR spectrum in n-hexane of a portion of the reaction solution showed υ(CO) bands of both $Os_2(CO)_6I_2$ and $Os_2(CO)_8I_2$. Complete conversion to $Os_2(CO)_8I_2$ was not observed under the conditions employed.

10. Reaction of $Os_2(CO)_6I_2$ with H_2 and with C_2H_4, respectively

H_2 and C_2H_4 were bubbled through two separate saturated solutions of $Os_2(CO)_6I_2$ in n-hexane for 20 minutes, at room temperature. Stirring was continued, at room temperature, in closed Schlenk tubes, under an atmosphere of H_2 or C_2H_4, for 12 hours. Evaporation of the solvent yielded a yellow product in both cases, which was shown to be pure $Os_2(CO)_6I_2$ by the υ(CO) bands in the IR spectra indicating that no reaction had occurred under the conditions employed.

11. Preparation of $Os_2(CO)_6Cl_4$ from cis-$Os(CO)_4Cl_2$

A solution of cis-$Os(CO)_4Cl_2$ (0.13 g, 0.34 mmol) in n-hexane (10 cm^3) was heated under reflux for 3 hours. During this time, a white solid (0.1 g, 82%) precipitated from the solution. IR(CH_2Cl_2): υ(CO) 2133(s) 2125(m) 2061(vs) 2035(s) cm^{-1}. (It was previously believed[115] that both the α- and β-isomers of $Os_2(CO)_6Cl_4$ were present but it has since been shown that these additional bands are due to an interaction

of $Os_2(CO)_6Cl_4$ with an impurity, possibly H_2O, present in the solvent, forming $Os(CO)_3Cl_2(H_2O)$ in solution).

A mass spectrum of the solid revealed a molecular ion at m/e 689, displaying the correct isotope pattern, with sequential loss of six carbonyl ligands, followed by the loss of chlorine ligands.

Mass Spectrum of $Os_2(CO)_6Cl_4$

m/e 689 (100%-$[Os_2(CO)_6Cl_4]^+$), 659 (96%-$[Os_2(CO)_5Cl_4]^+$),
630 (67%-$[Os_2(CO)_4Cl_4]^+$), 604 (100%-$[Os_2(CO)_3Cl_4]^+$),
577 (64%-$[Os_2(CO)_2Cl_4]^+$), 549 (75%-$[Os_2(CO)Cl_4]^+$),
522 (81%-$[Os_2Cl_4]^+$), 445 (60%-$[Os_2(CO)Cl]^+$),
384 (40%-$[Os_2]^+$), 299 (26%-$[OsCl_3]^+$),
285 (30%-$[Os(CO)_2Cl]^+$), 271 (58%-$[Os(CO)_3]^+$),
192 (54%-$[Os]^+$).

12. Preparation of $Os_2(CO)_6Br_4$ from cis-$Os(CO)_4Br_2$

A solution of cis-$Os(CO)_4Br_2$ (0.13 g 0.28 mmol) in light petroleum ether (bp 100°-120°C) (30 cm^3) was heated under reflux for 4 hours. During this time, a white solid precipitated from the solution which was shown by IR spectroscopy to be $Os_2(CO)_6Br_4$, the ν(CO) bands being consistent with those reported in the literature.[105] (0.11 g, 91%) mpt 210°-215°C. IR (CCl_4): ν(CO) 2120(s) 2050(s) cm^{-1}; (CH_2Cl_2): 2129(s) 2119(sh) 2055(vs) 2025(sh) cm^{-1}; lit[105] (CH_2Cl_2) 2125 2052 cm^{-1}. A mass

spectrum of the solid revealed a molecular ion at m/e 870 providing further evidence for the compound being of the molecular formulation $Os_2(CO)_8Br_4$.

Mass Spectrum of $Os_2(CO)_6Br_4$

m/e 870 (50%-$[Os_2(CO)_6Br_4]^+$), 842 (7%-$[Os_2(CO)_5Br_4]^+$), 814 (16%-$[Os_2(CO)_4Br_4]^+$), 786 (100%-$[Os_2(CO)_3Br_4]^+$), 758 (62%-$[Os_2(CO)_2Br_4]^+$), 730 (45%-$[Os_3(CO)Br_4]^+$), 702 (75%-$[Os_2Br_4]^+$), 679 (9%-$[Os_2(CO)_3Br_3]^+$), 651 (9%-$[Os_2(CO)Br_3]^+$), 622 (74%-$[Os_2Br_3]^+$), 550 (10%-$[Os_2(CO)_6]^+$), 542 (41%-$[Os_2Br_2]^+$), 492 (3%-$[Os_2(CO)_4]^+$), 462 (24%-$[Os_2Br]^+$), 434 (4%-$[Os(CO)_2Br_2]^+$), 408 (10%-$[Os_2(CO)]^+$), 384 (18%-$[Os_2]^+$), 354 (43%-$[Os(CO)_3Br]^+$), 274 (26%-$[Os(CO)_3]^+$), 192 (17%-$[Os]^+$).

13. Preparation of $Os_2(CO)_6I_4$ from cis-$Os(CO)_4I_2$

A solution of cis-$Os(CO)_4I_2$ (0.16 g, 0.28 mmol) in light petroleum ether (bp 100°-120°C) (20 cm^3) was heated under reflux for 4 hours. A yellow product crystallised out of the solution on cooling. Removal of the solvent yielded a bright microcrystalline solid believed to be $Os_2(CO)_6I_4$ (0.08 g, 54%) mpt 225°-235°C which was washed with n-hexane (2 x 10 cm^3) and recrystallised from benzene.

IR (CCl_4): ν(CO) 2119(s) 2116(sh) 2049(s) 2025(sh) cm^{-1}. After a 2 hour period, the IR spectrum showed only two ν(CO) bands at 2119(s) 2049(s) cm^{-1}; lit[114] 2119(s) 2151(s) cm^{-1}. We believe these latter ν(CO) bands are due to the interaction of $Os_2(CO)_6I_4$ with an impurity, possibly H_2O, present in the CCl_4 solvent. Far IR (Nujol): 159 and 139 cm^{-1}, which we assign to ν(Os-I). The mass spectrum of this yellow solid revealed a molecular ion at m/e 1058, providing further evidence for the compound being of the formulation $Os_2(CO)_6I_4$.

Mass Spectrum of $Os_2(CO)_6I_4$

m/e 1058 (70%-$[Os_2(CO)_6I_4]^+$), 1030 (68%-$[Os_2(CO)_5I_4]^+$), 1002 (39%-$[Os_2(CO)_4I_4]^+$), 974 (43%-$[Os_2(CO)_3I_4]^+$), 946 (79%-$[Os_2(CO)_2I_4]^+$), 931 (100%)-$[Os_2(CO)_6I_3]^+$), 918 (59%-$[Os_2(CO)I_4]^+$), 903 (88%)-$[Os_2(CO)_5I_3]^+$), 890 (79%-$[Os_2I_4]^+$), 875 (34%-$[Os_2(CO)_4I_3]^+$), 847 (36%-$[Os_2(CO)_3I_3]^+$), 817 (21%-$[Os_2(CO)_2I_3]^+$), 789 (16%-$[Os_2(CO)I_3]^+$), 776 (7%-$[Os_2(CO)_5I_3]^+$), 763 (96%-$[Os_2I_3]^+$), 748 (4%-$[Os_2(CO)_4I_2]^+$), 720 (5%-$[Os_2(CO)_3I_2]^+$), 649 (6%-$[Os_2(CO)_5I]^+$), 636 (52%-$[Os_2I_2]^+$), 621 (4%-$[Os_2(CO)_4I]^+$), 593 (7%-$[Os_2(CO)_3I]^+$), 565 (5%-$[Os_2(CO)_2I]^+$), 535 (9%-$[Os_2(CO)I]^+$), 530 (38%-$[Os(CO)_3I_2]^+$), 507 (32%-$[Os_2I]^+$), 474 (38%-$[Os(CO)I_2]^+$), 384 (46%-$[Os_2]^+$), 319 (33%-$[OsI]^+$), 272 (55%-$[Os(CO)_3]^+$), 192 (27%-$[Os]^+$).

14. Preparation of $Os_2(CO)_8H_2$ from $Os_2(CO)_8I_2$

$Os_2(CO)_8I_2$ (0.10 g, 0.12 mmol), zinc dust (0.13 g, 1.99 mmol), glacial acetic acid (0.15 cm^3) in methanol (7 cm^3) were refluxed for 10 minutes. Removal of the solvent and extraction of the residue with n-hexane (3 x 20 cm^3; 3 x 10 cm^3) with subsequent filtration and removal of solvent yielded a colourless oil (0.03 g, 40%) which was identified as $Os_2(CO)_8H_2$ by IR and ^1H nmr spectroscopy, the data found to be in agreement with the literature.[127] The oil was purified by sublimation (30°C/0.01 mm Hg) and used for a high resolution ^1H nmr study. NMR: $^1H(C_6D_6)$ 20.11 (s)τ, $\left[{}^1J(^{187}Os-^1H)=37.5\ Hz\right]$ and a possible assignment, $\left[{}^2J(^{187}Os-^1H)=16.0\ Hz\right]$.

C. Homo-trinuclear Osmium Carbonyl Complexes

15. Preparation of $Os_3(CO)_{12}Cl_2$ from $Os_3(CO)_{12}$

This was prepared as described in the literature.[119] $Os_3(CO)_{12}$ (0.30 g, 0.33 mmol) was refluxed in benzene (250 cm^3) until dissolved. Chlorine gas was bubbled through

the solution for 15 seconds. The solution was cooled quickly under the cold tap and the solution then evaporated to dryness under reduced pressure. Methanol was added and the pale yellow solid was brought to the filter and dried. The solid was recrystallised from CH_2Cl_2/n-hexane and identified as $Os_3(CO)_{12}Cl_2$ (0.28 g, 87%) mpt 165°-171°C (decomp) lit[126] 164°-170°C (decomp). (Found: C, 14.75; $C_{12}Cl_2O_{12}Os_3$ requires: C, 14.74). The mass spectrum revealed a molecular ion at m/e 980 corresponding to $[Os_3(CO)_{12}Cl_2]^+$ with sequential loss of twelve carbonyl groups. IR (CH_2Cl_2): ν(CO) 2150 (w) 2120 (s) 2085(w,sh) 2063(vs) 2030(s) 2001(m) cm^{-1} in agreement with the literature.[119,126]

16. Preparation of $Os_3(CO)_{12}H_2$ from $Os_3(CO)_{12}I_2$

The following preparation is an adapation of that reported in the literature.[127] $Os_3(CO)_{12}I_2$ (0.25 g, 0.21 mmol), zinc dust (0.63 g, 9.67 mmol), glacial acetic acid (0.15 cm^3) in methanol (15 cm^3) were refluxed for 25 minutes. Removal of the solvent and extraction of the residue with n-hexane (3 x 20 cm^3; 4 x 10 cm^3) with subsequent filtra-

tion and removal of solvent, yielded a pale yellow solid (0.16 g, 85%) mpt 94°-104°C lit[127] 95°-98°C, identified as $Os_3(CO)_{12}H_2$ by IR spectroscopy, the ν(CO) bands in agreement with these reported in the literature.[127] NMR: ^1H (C_6D_6) 19.88(s)τ, [$^1J(^{187}Os-^1H)$ = 37.5 Hz]; [$^2J(^{187}Os-^1H)$ = 16 Hz] lit[127] 19.85(s) τ.

D. Heteronuclear Carbonyl Complexes Containing Osmium

17. Preparation of $[Os(CO)_4H]PPN$ from $[Os(CO)_4]Na_2$

The following preparation is a more specific, detailed description of a procedure outlined in the literature.[202] $[Os(CO)_4]Na_2$ was prepared from $Os_3(CO)_{12}$ (0.25 mmol) as described in the literature[199] and the white solid dried on the vacuum for 4 hours to ensure complete removal of excess ammonia. Methanol (7 cm^3) was condensed onto the white solid at -196°C. The solution was warmed up to -78°C under nitrogen and allowed to stir until all the solid was seen to have dissolved. [PPN]Cl (0.21 g, 0.36 mmol) in methanol (5 cm^3) was added dropwise to the solution at -78°C with stirring. The reaction mixture was then removed from the -78°C bath and allowed to warm up to room temperature until a white precipitate was seen to form. The reaction vessel was immediately returned to the

-78°C bath for precipitation to be completed. The white solid (0.06 g, 59.3%) was collected on a dry ice-chilled frit, pumped dry on the vacuum line and recrystallised from a THF/hexane solvent system. IR (THF): ν(CO) 2010(m) 1947(m) 1881(s) cm^{-1} in agreement with the literature.[202]

18. Reaction between $[Os(CO)_4]Na_2$ and 2 moles $Re(CO)_5Br$

$[Os(CO)_4]Na_2$ (0.23 g, 0.76 mmol) was suspended in THF (30 cm^3). $Re(CO)_5Br$ (0.62 g, 1.52 mmol) dissolved in THF (15 cm^3) was added dropwise over a period of 5 minutes to the anion solution at room temperature, with stirring. Stirring of the yellow reaction mixture was continued for 20 hours, after which time the solvent was removed under reduced pressure and the yellow solid dried in vacuo. The yellow solid was extracted with n-hexane (5 x 20 cm^3), filtered and the filtrate evaporated to dryness to yield an oily, yellow product (0.07 g) which was shown by IR and ^1H nmr spectroscopy to contain $HOsRe(CO)_9$, $Re_2(CO)_{10}$ and $Re_2Os(CO)_{14}$. Separation of $HOsRe(CO)_9$ from $Re_2(CO)_{10}$ and $Re_2Os(CO)_{14}$ was attempted by column chromatography (no separation and possible decomposition), sublimation (30°C/0.01 mm Hg) (separation with reduced yields of components) and tlc from which $HOsRe(CO)_9$ could not be easily recovered and appeared to decompose. $Re_2Os(CO)_{14}$ was separated from $Re_2(CO)_{10}$ and $HOsRe(CO)_9$, in that the trinuclear compound was sparingly soluble in n-hexane whereas both $Re_2(CO)_{10}$ and $HOsRe(CO)_9$ are readily soluble

in n-hexane, and by means of a fractional sublimation ($\leq$60°C/.01 mm Hg), which separated the dinuclear complexes from $Re_2Os(CO)_{14}$. This latter compound was obtained pure by repeated recrystallisation from acetone with considerable loss of product yield. The compound was obtained pure (< 5 mg) mpt 192°-202°C (decomp) in too small a yield to enable an elemental analysis to be performed. Mass spectrum: parent ion at m/e 958 corresponding to $[Re_2Os(CO)_{14}]^+$ with loss of fourteen carbonyl groups to give a positive ion at m/e 566 of correct polyisotope pattern for $[Re_2Os]^+$. IR (cyclohexane): ν(CO) 2092(m) 2019(vs) 1981(s) cm^{-1} in agreement with the literature.[37] The hexane-insoluble yellow solid (0.14 g), IR (THF): ν(CO) 2089(sh) 2077(w) 2040(w) 2004(sh) 1995(s) 1970(m) 1909(sh) 1877(vs) cm^{-1}, was treated with acetic acid (2 cm^3) in THF (5 cm^3) with stirring for 2 hours. Removal of solvent and extraction with n-hexane (5 x 20 cm^3) yielded a pale yellow solution. IR (n-hexane): ν(CO) 2081(m) 2045(s) 2040(sh) 2028(vs) 2015(sh) 2005(s) 1984(s) cm^{-1} corresponding to $HOsRe(CO)_9$.[126,208] NMR: ^1H (C_6D_6) 20.37 τ in agreement with the literature for $HOsRe(CO)_9$.[126,208]

19. Reaction between $[Os(CO)_4]Na_2$ and 1 mole $Re(CO)_5Br$

$[Os(CO)_4]Na_2$ (0.35 g, 0.99 mmol) was suspended in THF (20 cm^3) at room temperature and solid $Re(CO)_5Br$ (0.40 g, 0.99 mmol) added in one quantity. The yellow reaction

mixture was stirred for 20 hours at room temperature after which time the solvent was removed to yield an oily yellow residue. Extraction of the residue with n-hexane (5 x 20 cm^3), with subsequent filtration, yielded a pale yellow solution and a yellow hexane insoluble solid. The hexane extract was found to contain $HOsRe(CO)_9$ and $Re_2(CO)_{10}$ as evidenced by IR and ^1H nmr spectroscopy and which were separated with difficulty and loss of product yield by sublimation, as described in reaction 18. above. The hexane insoluble product was dissolved in methanol (5 cm^3) and [PPN]Cl (0.57 g, 0.99 mmol) dissolved in methanol (4 cm^3) added to the solution dropwise with stirring. The reaction mixture was kept at 0°C after which time a white, water-soluble precipitate, presumably NaBr, was filtered off and the supernatant evaporated to dryness to yield an orange, oily residue. This residue was extracted with n-hexane to yield no carbonyl-containing hexane soluble product and an orange hexane insoluble powder. Recrystallization of the orange powder from a methanol/H_2O solvent system yielded two products. A yellow-orange compound (0.07 g, 5.5%) mpt 65°-75°C, identified as $[HOsRe(CO)_8Br]PPN$ - see reaction 20. below for full characterisation - precipitated from solution first (Found: C,42.3; H,2.7; N,1.1. $C_{44}H_{31}BrNO_8OsP_2Re$ requires: C,43.3; H,2.6; N,1.2). IR (THF): ν(CO) 2091(vw) 2043(s) 2019(m) 1991(vs) 1980(sh) 1956(m) 1946(m) 1895(m) cm^{-1}. A yellow compound was obtained from the mother liquors by dropwise addition of water. Attempts to

recrystallise the compound (0.35 g, 31 %) mpt 110°-120°C, believed to be [OsRe(CO)$_9$]PPN, from THF/hexane or methanol/H_2O solvent systems, resulted in an oil. (Found: C,46.2; H,3.3; N,1.5. $C_{45}H_{30}NO_9OsPRe$ requires: C,46.3; H,2.6; N,1.2). IR (THF): ν(CO) 2089(sh) 2077(w) 2040(w) 2004(sh) 1995(s) 1970(m) 1909(sh) 1877(vs) cm^{-1}. NMR: ^{1}H (CD_3CN) 2.54(m)τ (phenyl protons).

20. Reaction between [Os(CO)$_4$H]PPN and 1 mole of Re(CO)$_5$Br

[Os(CO)$_4$H]PPN (0.44 g, 0.52 mmol) was dissolved in THF (20 cm^3). Re(CO)$_5$Br (0.21 g, 0.52 mmol) dissolved in THF (5 cm^3) was added dropwise over a period of 5 minutes with stirring at room temperature to the anion solution. After 1 hour a portion of the reaction mixture was removed, the solvent removed and the residue extracted with n-hexane to yield a pale yellow solution, the IR spectrum of which showed ν(CO) bands of pure HOsRe(CO)$_9$.[126,208] The hexane insoluble material of this portion still showed ν(CO) bands of both starting materials. Stirring was continued for 23 hours, after which time the solvent was removed under reduced pressure. The oily, orange residue was extracted with n-hexane (5 x 20 cm^3) and filtered to yield a pale yellow solution and a hexane insoluble solid. Evaporation to dryness of the hexane extract yielded a colourless oil which was identified as HOsRe(CO)$_9$ (0.06 g, 18 %). IR (n-hexane): ν(CO) 2091(vw) 2081(s) 2068(w) 2046(s) 2040(m) 2028(vs)

2005(s) 1997(w) 1984(s) cm^{-1}. NMR: ^1H (C_6D_6) 20.37(s)τ . A mass spectrum of the oil showed a molecular ion at m/e 629, corresponding to $[HOsRe(CO)_9]^+$, with sequential loss of nine carbonyl groups to give a positive ion at m/e 378, corresponding to $[OsRe]^+$. The hexane insoluble solid was recrystallised from methanol/ether to give yellow crystals (0.50 g, 79%) mpt 115°-125°C and identified as $[HOsRe(CO)_8Br]PPN$. (Found: C,43.5; H,2.7; N,1.3; Br,6.3; Os,18.6; Re,15.8. $C_{44}BrH_{31}NO_8OsP_2Re$ requires: C,43.3; H,2.6; N,1.2; Br,6.6; Os,15.6; Re,15.3.) IR (THF): ν(CO) 2091(w) 2043(s) 2019(m) 1991(vs) 1980(sh) 1956(m) 1946(m) 1895(m) cm^{-1}. Far IR (Nujol): ν(Re-Br) 179(s) cm^{-1}. NMR: ^1H (CD_3CN) 20.50(s)τ [$^1J(^{187}Os-^1H)$ = 40.5 Hz]; 2.54(m)τ (phenyl protons).

21. Reaction between $[Os(CO)_4H]PPN$ and 1 mole $Re(CO)_5I$

$[Os(CO)_4H]PPN$ (0.50 g, 0.59 mmol) was dissolved in THF (20 cm^3). $Re(CO)_5I$ (0.27 g, 0.59 mmol) dissolved in THF (5 cm^3) was added dropwise over a period of 5 minutes with stirring at room temperature to the anion solution. After 4 hours a portion of the yellow-orange reaction solution was extracted and an IR spectrum of it showed that the low

frequency ν(CO) band of [Os(CO)$_4$H]PPN had disappeared, indicating that reaction was complete. The solvent was removed under reduced pressure. The oily, orange residue was extracted with n-hexane (10 x 20 cm^3) and filtered to yield a pale yellow-orange solution and yellow-orange hexane insoluble solid. Evaporation to dryness of the hexane extract yielded an oily product (0.06 g) which showed ν(CO) bands in the IR spectrum indicating it to be a mixture of unreacted Re(CO)$_5$I, Re$_2$(CO)$_{10}$ and IOsRe(CO)$_9$. Re(CO)$_5$I was removed by fractional sublimation (60°C/0.01 mm Hg). Attempts to separate Re$_2$(CO)$_{10}$ and IOsRe(CO)$_9$ were unsuccessful. In the mass spectrum of the hexane extract, initial scans showed peaks corresponding to both Re$_2$(CO)$_{10}$ and IOsRe(CO)$_9$, confirming that the product was a mixture. However, in later scans, peaks corresponding to IOsRe(CO)$_9$ were more prominent, showing a molecular ion at m/e 758 corresponding to [IOsRe(CO)$_9$]$^+$ with sequential loss of nine carbonyl groups to give a positive ion at m/e 504 corresponding to [IOsRe]$^+$. ν(CO) bands of the IOsRe(CO)$_9$ component, in the IR spectrum of the mixture, were identified by comparison with the IR spectrum of an authentic sample of IOsRe(CO)$_9$ obtained from the reaction of HOsRe(CO)$_9$ with CH$_3$I. The hexane insoluble solid was recrystallised from methanol/water to give yellow crystals (0.61 g, 81%) mpt 103°-107°C and identified as [HOsRe(CO)$_8$I]PPN. (Found: C,41,8; H,2.5; N,1.2; I,11.76;

$C_{44}H_{31}IO_8OsP_2Re$ requires: C,42.2; H,2.5; N,1.1; I,10.1). IR (THF): ν(CO) 2090(w) 2042(s) 2020(m) 1990(vs) 1980(sh) 1954(m) 1949(m) 1898(m) cm^{-1}. NMR: ^1H (CD_3CN) 20.5(s) τ [$^1J(^{187}Os-^1H)$ = 39.0 Hz]; 2.54(m) τ (phenyl protons).

22. Reaction between $[Os(CO)_4]Na_2$ and 2 moles $Mn(CO)_5Br$

$[Os(CO)_4]Na_2$ (0.35 g, 0.99 mmol) was suspended in THF (20 cm^3). $Mn(CO)_5Br$ (0.55 g, 1.98 mmol) as a solution in THF (10 cm^3) was added dropwise with stirring to the anion solution over a period of 5 minutes at room temperature. The reaction was monitored by IR spectroscopy and after 20 hours the reaction was judged to be complete. Removal of solvent yielded an orange, oily residue which was extracted with n-hexane (5 x 20 cm^3) and filtered, to yield an orange solution and an orange insoluble solid. The hexane extract was evaporated to dryness to yield a yellow solid product (0.07 g). IR (n-hexane): ν(CO) bands of $Mn_2(CO)_{10}$ plus additional bands at 2120(vw) 2069(m)

2034(s) 1995(w) cm^{-1}. NMR: ^1H (C_6D_6) 19.80(s)τ. A mass spectrum of the product showed positive ions consistent with the presence of $[HOsMn(CO)_9]^+$ at m/e 499 and $[Mn_2(CO)_{10}]^+$ at m/e 390, respectively, with sequential losses of the respective carbonyl groups for both components of the mixture. Attempts to separate the two components by sublimation (20°-50°C/0.01 mm Hg) were only partly successful and it was believed that possible decomposition of the hydride to $Mn_2(CO)_{10}$ was taking place. The orange hexane insoluble solid was extracted with CH_2Cl_2 (5 x 20 cm^3) and the extract filtered with subsequent removal of solvent to yield a yellow residue (0.02 g). This residue was subjected to sublimation (60°C/0.01 mm Hg) to yield $Mn_2Os(CO)_{14}$, which was recrystallised from acetone, by cooling. (8 mg) mpt 165°-185°C (decomp). IR (n-hexane): ν(CO) 2066(s) 2037(m) 2021(vs) 1987(m) cm^{-1} lit[37] 2067(s) 2020(s) 1987(m) cm^{-1}. A parent ion at m/e 692 with the expected polyisotopic pattern corresponding to $[Mn_2Os(CO)_{14}]^+$ was observed in the mass spectrum with positive ions corresponding to sequential loss of fourteen carbonyl group to give a peak corresponding to the positive ion, $[Mn_2Os]^+$. The yield of product after identification was too low to enable an elemental analysis to be performed. The unsublimed product was recrystallised from methanol/ ether to yield an orange solid (0.07 g) mpt 130°-170°C (decomposed without melting). IR (THF): ν(CO) 2090(w) 2043(sh) 2018(s) 1990(sh) 1917(vs) cm^{-1}. Elemental

analyses of the product were inconsistent with any of the possible products of this reaction and thus positive identification of the product was impossible.

23. Reaction between $[Os(CO)_4]Na_2$ and 1 mole $Mn(CO)_5Br$

To a suspension of $[Os(CO)_4]Na_2$ (0.35 g, 0.99 mmol) in THF (20 cm^3), $Mn(CO)_5Br$ (0.27 g, 0.99 mmol) was added at room temperature in the solid state. The reaction was monitored by IR spectroscopy, by extracting portions of the reaction mixture at various time intervals, and was judged to be complete after 22 hours of stirring. The reaction mixture was filtered and the solvent removed under reduced pressure, to yield a yellow, oily product. Extraction of this oil with n-hexane, filtration of the extract and evaporation of the filtrate to dryness under reduced pressure yielded a yellow solid product. As in reaction 22. above, this solid was shown to contain $HOsMn(CO)_9$ and $Mn_2(CO)_{10}$ which were found to be difficult to separate. The hexane insoluble red-brown powder was recrystallised from methanol/ether, to give a red-orange, microcrystalline product (0.13 g) mpt 130°-170°C (decomposed without melting). IR (THF): ν(CO) 2083(vw) 2068(w) 2042(m) 2009(vs) 1997(sh) 1982(m) 1920(s) cm^{-1}. Elemental analysis indicated that the product was impure. A small portion of the product was protonated with acetic acid (1 cm^3) in THF (4 cm^3) with stirring for 1 hour. Removal of solvent under reduced pressure yielded an oily, yellow product which was extracted with n-hexane (3 x 20 cm^3).

The yellow hexane extract was evaporated to dryness and sublimed (25°-65°C/0.01 mm Hg). A yellow product collected on the cold finger, which was shown to be a mixture of $HOsMn(CO)_9$ and $Mn_2(CO)_{10}$. The hexane insoluble product was shown to have ν(CO) bands at similar wavenumbers to the original product which was subjected to protonation, indicative either that a mixture of products was originally present, all of which were not protonated, or that the reaction time was insufficient.

24. Reaction between $[Os(CO)_4H]PPN$ and 1 mole $Mn(CO)_5Br$

$[Os(CO)_4H]PPN$ (0.44 g, 0.52 mmol) was dissolved in THF (20 cm^3) and $Mn(CO)_5Br$ (0.15 g, 0.52 mmol) as a solution in THF (5 cm^3) added dropwise, over a period of 5 minutes, with stirring at room temperature. The reaction mixture was stirred for 18 hours, at which stage reaction was judged to be complete. Removal of the solvent under reduced pressure and extraction of the orange, oily residue with n-hexane (5 x 20 cm^3) with subsequent filatration, gave a yellow solution and an orange hexane insoluble solid. The hexane extract was evaporated to dryness under reduced pressure to yield a pale yellow, oily product (0.06 g). IR (n-hexane): ν(CO) 2120(w) 2069(m) 2042(m) 2034(s) 2013(vs) 2002(m) 1995(w) 1985(w) cm^{-1}. NMR: ^1H (C_6D_6) 19.80(s) τ. A mass spectrum showed a molecular ion at m/e 499, corresponding to $[HOsMn(CO)_9]^+$, with peaks corresponding to sequential loss of nine carbonyl groups and a peak at m/e 248 corresponding

to $[OsMn]^+$. No $Mn_2(CO)_{10}$ was found to be present in the hexane extract, as shown by IR and mass spectroscopy. The hexane insoluble product recrystallised to yield two products. The first product to crystallise from solution on cooling was an orange powder, believed to be $[HOsMn(CO)_8Br]PPN$ (0.13 g, 23%) mpt 126°- 133°C. (Found: C,46.0; H,2.8; N,1.4. $C_{44}H_{31}BrMnNO_8OsP_2$ requires C,48.5; H,2.9; N,1.3). IR (THF): ν(CO) 2087(w) 2075(vw) 2048(w) 2005(m) 1987(vs) 1975(m) 1966(s) 1938(m) 1899(w) cm^{-1}. Far IR (Nujol): ν(Mn-Br) 192(m) cm^{-1}. NMR: ^1H (CD_3OD) 19.52(s)τ. A second, air-sensitive yellow product was obtained from the mother liquors by the addition of H_2O and cooling (0.02 g) mpt 190°-200°C. (Found: C,36.3; H,2.7; N,1.6). These values indicated either that the compound was still impure or that a much higher nuclearity compound had been formed. IR (THF): ν(CO) 2088(vw) 2044(m) 2022(sh) 2008(vs) 1987(m) 1966(sh) 1925(s) 1915(sh) 1683(m) cm^{-1}. The colour of solution changed from yellow to orange after standing in air for 5 minutes. IR (THF) of the orange solution: ν(CO) 2088(vw) 2050(sh) 2020(sh) 2008(vs) 1987(m) 1965(w) 1927(vs) 1778(m) 1726(w) 1683(m) cm^{-1}. This change in the IR spectrum indicated that either decomposition or isomerization was occurring in solution.

25. Reaction of $HOsRe(CO)_9$ with CH_3I

$HOsRe(CO)_9$ (0.02 g, 0.03 mmol) was dissolved in THF (5 cm^3) and cooled to 0°C. CH_3I (0.002 cm^3, 0.03 mmol)

was added and the reaction mixture stirred for 18 hours while warming up to room temperature. Removal of the solvent and recrystallisation of the pale yellow residue from CH_2Cl_2/petroleum ether (bp 30°-40°C) yielded a pale yellow solid (0.02 g, 88%) mpt 105°-110°C, which was identified as $IOsRe(CO)_9$. The mass spectrum gave a molecular ion at m/e 758 correspnding to $[IOsRe(CO)_9]^+$ with sequential loss of nine carbonyl groups to give a positive ion at m/e 504 corresponding to $[IOsRe]^+$. Too small a quantity of product was available for identification by elemental analysis. IR (n-hexane): ν(CO) 2092(m) 2055(m) 2052(sh) 2041(s) 2024(vs) 2015(sh) 2005(m) 1988(s) cm^{-1}.

26. Reaction of $HOsRe(CO)_9$ with CBr_4

$HOsRe(CO)_9$ (0.01 g, 0.02 mmol) was dissolved in n-hexane (5 cm^3) and CBr_4 (0.05 g, 0.20 mmol) added in the solid state at room temperature and the reaction mixture stirred for 30 minutes. Removal of the solvent under reduced pressure, resulted in an oily, colourless product which was extracted with n-hexane (2 x 10 cm^3) to remove any unreacted CBr_4. Recrystallisation of the colourless residue from CH_2Cl_2/petroleum ether (bp 30°-40°C) yielded a white solid (0.01 g, 71%) mpt 105°-110°C, identified as $BrOsRe(CO)_9$. IR (n-hexane): ν(CO) 2094(m) 2055(m)

2042(s) 2032(sh) 2023(vs) 2015(sh) 2005(m) 1988(s) cm^{-1}. A mass spectrum of the compound displayed a parent ion at m/e 708 corresponding to $[BrOsRe(CO)_9]^+$ with sequential loss of nine carbonyl groups, to give a positive ion at m/e 456 corresponding to $[BrOsRe]^+$. Too small a quantity of sample remained for identification by elemental analysis.

27. Reaction of $HOsRe(CO)_9$ with CCl_4

$HOsRe(CO)_9$ (0.05 g, 0.08 mmol) was dissolved in CCl_4 (5 cm^3) and the reaction mixture stirred at room temperature for 40 minutes. Removal of solvent and recrystallisation of the colourless product from CH_2Cl_2/ pet ether (bp 30°-40°C) yielded white needles of $ClOsRe(CO)_9$ (0.03 g, 75.3%) mpt 100°-105°C. IR (n-hexane): ν(CO) 2095(w) 2081(vw) 2068(vw,sh) 2056(m) 2044(s) 2023(vs) 2015(sh) 2004(m) 1986(s) cm^{-1}. A mass spectrum of the product displayed a parent ion at m/e 694 with the correct polyisotopic pattern corresponding to $[ClOsRe(CO)_9)^+$, with sequential loss of nine carbonyl groups to give a peak at m/e 415, corresponding to $[ClOsRe]^+$, as was observed previously.[126]

28. Reaction of $HOsRe(CO)_9$ with iodine

$HOsRe(CO)_9$ (0.01 g, 0.02 mmol) was dissolved in n-hexane (5 cm^3) and iodine (0.05 g, 0.20 mmol) added and the red

reaction mixture stirred at room temperature for 30 minutes. The solvent was removed to yield a yellow solid (0.01 g). IR (n-hexane): ν(CO) 2163(vw) 2147(vw) 2099(s) 2084(m) 2056(sh) 2049(s) 2043(vs) 2033(m) 2024(w) 2016(w) 2002(w) 1991(m) 1885(w,br) 1735(w,br) cm^{-1} which indicated a mixture of cis-$Os(CO)_4I_2$[114] and $Re(CO)_5I$. $Re_2(CO)_{10}$ was treated with iodine in CCl_4[215] and the IR spectrum in n-hexane of the product was found to be in agreement with some of the ν(CO) bands observed in the mixture. The two components were not separated due to the small amounts of material obtained.

29. Reaction of [$HOsRe(CO)_8Br$]PPN with CF_3COOH

[$HOsRe(CO)_8Br$]PPN (0.03 g, 0.03 mmol) was dissolved in CH_3CN (3 cm^3) and CF_3COOH (0.2 cm^3) added to the solution with stirring at room temperature. The reaction was monitored by IR spectroscopy and after 2 hours the reaction was judged to be complete. The solvent was removed in vacuo (0.01 mm Hg) and collected together with any volatile products at -196°C. IR (CH_3CN) of volatile products: ν(CO) 2144(w) 2070(sh) 2055(sh) 2048(s) 1977(br) 1789(vs) the latter band being attributable to excess CF_3COOH. NMR: ^1H (CH_3CN) 19.07(s) τ. These data were consistent with the product being $H_2Os(CO)_4$ by comparison with the IR and ^1H nmr spectra run on an authentic sample of $H_2Os(CO)_4$ in CH_3CN. The remaining white involatile product was identified as $[Re(CO)_4Br]_2$. IR (CH_3CN): ν(CO)

2119(vw) 2021(vs) 2000(m) 1947(s) cm^{-1} in agreement with the ν(CO) bands of an authentic sample of $[Re(CO)_4Br]_2$ in CH_3CN.

30. Reaction between $[HOsRe(CO)_8Br]PPN$ and CH_3I

$[HOsRe(CO)_8Br]PPN$ (0.03 g, 0.03 mmol) was dissolved in THF (10 cm^3) and CH_3I (0.02 cm^3, 0.03 mmol) added and the reaction mixture stirred at room temperature. After 20 hours reaction time, no change in the IR spectrum from that of the starting anionic product was observed. A further aliquot of CH_3I (0.02 cm^3, 0.03 mmol) was added and after a total reaction time of 56 hours with stirring at room temperature, reaction was judged to be complete. Evaporation of the solvent in vacuo and collection of the volatile products at -196°C which contained no carbonyl containing products, yielded an off-white solid (0.02 g, 65 %) mpt 110°-120°C (decomp) which was recrystallised by slow evaporation of a methanol/ether solvent system. This product was believed to be $[IOsRe(CO)_8Br]PPN$, on the basis that the IR spectrum was very similar to that obtained for $[BrOsRe(CO)_8Br]PPN$; however, too small an amount of product was available for positive identification by elemental analysis. IR (THF): ν(CO) 2093(vw) 2062(vw) 2054(w) 2018(sh) 2005(sh) 1993(vs) 1963(s) 1910(s) cm^{-1}.

31. Reaction between $[HOsRe(CO)_8Br]PPN$ and CBr_4

$[HOsRe(CO)_8Br]PPN$ (0.03 g, 0.03 mmol) was dissolved in THF (3 cm^3) and CBr_4 (0.08 g, 0.03 mmol) added and the reaction mixture stirred at room temperature for 45 minutes. The colour of the reaction mixture was seen to change from yellow to yellow-orange. Removal of the solvent under reduced pressure and trituration of the orange-brown oily residue with n-hexane (2 x 10 cm^3) yielded an orange crystalline solid. This was identified as $[BrOsRe(CO)_8Br]PPN$ (0.02 g, 51%) mpt 80°-90°C (decomposed to a brown solid which melted at 130°-150°C) and was recrystallised from a methanol/ether solvent system. (Found: C,42.5; H,3.2; N,1.2; $C_{44}Br_2H_{30}NO_8OsP_2Re$ requires: C,40.7; H.2.3; N,1.1). IR (THF): ν(CO) 2180(vw) 2109(m) 2097(m) 2055(w) 2022(m) 1995(vs) 1961(s) 1908(s) cm^{-1}.

32. Reaction of $[HOsRe(CO)_8Br]PPN$ with 2 moles $AuPPh_3Cl$

$[HOsRe(CO)_8Br]PPN$ (0.09 g, 0.07 mmol) was dissolved in THF (3 cm^3). $AuPPh_3Cl$ (0.07 g, 0.14 mmol) was added to the solution, with stirring, at room temperature. After 53 hours, the solvent was removed and the oily, brown residue triturated with n-hexane (2 x 10 cm^3) to leave a purple-brown hexane insoluble solid and a colourless solution. No carbonyl-containing product was observed in the hexane

extract. The hexane insoluble solid was recrystallised by slow evaporation of an ether/n-hexane solvent system. A brown microcrystalline solid (0.07 g, 59%) mpt 165°-190°C which crystallised from solution first was believed to be $[Os(CO)_4(AuPPh_3)ClRe(CO)_4]PPN.2C_4H_{10}O$ (Found: C,47.6; H,3.3; N,0.9. $C_{70}AuClH_{65}NO_{10}OsP_3Re$ requires: C,47.2; H,3.7; N,0.8). IR (THF): ν(CO) 2013(s) 1993(m) 1959(m) 1906(vs) 1871(m) cm^{-1}. NMR: ^1H (CD_3CN) 2.54(m) τ (phenyl protons). A purple-black crystalline product which formed after several days of slow evaporation of the mother liquors was believed to be a high nuclearity complex, possibly $[Os_2Re_2(CO)_{12}(AuPPh_3)_2]PPN$ (0.02 g, 10%) mpt 200°C (decomp). (Found: C,39.3; H,3.4; N,0.6. $C_{84}Au_2H_{60}NO_{12}Os_2P_4Re_2$ requires: C,39.6; H,2.4; N,0.6). IR (THF): ν(CO) 2105(vw) 2069(w) 2031(s) 2020(s) 2010(m,sh) 1989(m) 1960(sh) 1944(m) 1913(vs) 1880(sh) cm^{-1}. NMR: ^1H (CD_3CN) 2.54 (m) τ (phenyl protons).

33. Reaction between $[HOsRe(CO)_8Br]PPN$ and 1 mole PPh_3

$[HOsRe(CO)_8Br]PPN$ (0.05 g, 0.04 mmol) was dissolved in THF (5 cm^3) and solid PPh_3 (0.01 g, 0.04 mmol) added at room temperature, with stirring. After 4 days no reaction had occurred as monitored by IR spectroscopy. The temperature was raised to 60°C and after 3 days at that temperature the

reaction was judged to be complete, by the disappearance of ν(CO) bands of the starting material in the IR spectrum of the reaction mixture. Removal of the solvent under reduced pressure yielded an oily residue which was extracted with n-hexane (2 x 10 cm^3) to give a clear solution and a pale yellow solid. No carbonyl-containing compound was found in the hexane extract. The hexane insoluble solid (0.06 g, 91%) mpt 65°-75°C was believed to be $[Os(CO)_3H(PPh_3)Re(CO)_4Br]PPN$. (Found: C,49.9; H,3.8; N,0.9. $C_{61}BrH_{46}NO_7OsP_3Re$ requires: C,50.4; H,3.2; N,1.0). IR (THF): ν(CO) 2078(vw) 2043(m) 2018(sh) 2005(s) 1992(vs) 1955(m) 1946(m) 1887(vs) cm^{-1}. NMR: ^1H (CD_3OD) 18.12(d) τ, [$J(^{31}P-^1H)$ = 14 Hz]; 2.54(m) τ (phenyl protons).

34. Reaction between $[HOsRe(CO)_8Br]PPN$ and 1 mole pyridine

$[HOsRe(CO)_8Br]PPN$ (0.05 g, 0.04 mmol) was dissolved in THF (3 cm^3) and pyridine (0.02 cm^3, 0.04 mmol) added, at room temperature, to the solution with stirring. After 4 days, no reaction was observed to have occurred. The temperature was raised to 60°C and only after 3 days of stirring at that temperature was reaction judged to be complete. Removal of the solvent and extraction of the oily, brown residue with n-hexane (2 x 10 cm^3) with subsequent filtration, yielded a clear solution and a brown hexane insoluble solid. No

carbonyl-containing compound was observed to be present in the hexane extract. The brown solid (0.03 g, 54%) mpt 78°-88°C was believed to be $[Os(CO)_3H(py)Re(CO)_4Br]PPN$. (Found: C,44.9; H,3.5; N,2.3; $C_{48}BrH_{36}N_2O_7OsP_2Re$ requires: C,45.4; H,2.9; N,2.2). IR (THF): ν(CO) 2095(vw) 2043(m) 2025(sh) 2010(s) 1996(s) 1958(w) 1940(sh) 1924(m) 1895(sh) 1870(vs) cm^{-1}. NMR: ^1H (CD_3CN) 2.42(m) (phenyl protons); 1.34(m)τ , 1.13(m)τ (pyridine protons). A high field singlet was not observed in the spectrum due to the small amount of product available.

APPENDIX I

OBSERVED AND CALCULATED STRUCTURE FACTORS

FOR $Os_3(CO)_{12}Cl_2$

OBSERVED AND CALCULATED STRUCTURE FACTORS FOR OS 3 (CO) 12 CL 2

H	K	L	FO	FC	H	K	L	FO	FC	H	K	L	FO	FC	H	K	L	FO	FC	H	K	L	FO	FC
2	0	0	129	-122	4	8	0	175	171	-13	3	1	40	-41	5	7	1	52	-53	3	1	2	52	54
4	0	0	244	244	8	8	0	58	57	-11	3	1	132	135	7	7	1	151	147	5	1	2	79	79
6	0	0	52	52	1	9	0	79	79	-9	3	1	21	-14	-10	8	1	99	97	7	1	2	111	108
8	0	0	108	103	5	9	0	147	150	-7	3	1	138	142	-8	8	1	36	-37	11	1	2	132	134
10	0	0	105	106	7	9	0	53	-54	-5	3	1	123	128	-6	8	1	165	175	-12	2	2	149	151
12	0	0	27	-26	0	10	0	200	205	-3	3	1	97	-88	-4	8	1	67	-71	-10	2	2	67	-65
1	1	0	220	220	2	10	0	41	-39	-1	3	1	319	311	-2	8	1	186	179	-8	2	2	205	202
3	1	0	44	-40	4	10	0	136	139	1	3	1	96	81	2	8	1	95	95	-4	2	2	118	117
5	1	0	257	250	6	10	0	19	19	3	3	1	319	305	4	8	1	98	93	-2	2	2	140	135
7	1	0	61	-63	1	11	0	83	87	5	3	1	119	-112	8	8	1	124	125	0	2	2	69	-68
9	1	0	217	217	5	11	0	128	127	7	3	1	202	203	-7	9	1	83	93	2	2	2	272	256
11	1	0	35	-37	0	12	0	134	137	9	3	1	27	28	-5	9	1	65	69	4	2	2	92	-92
0	2	0	350	370	2	12	0	33	-34	11	3	1	41	35	-3	9	1	36	-31	6	2	2	261	250
2	2	0	125	-119	-12	0	1	24	25	-10	4	1	141	153	-1	9	1	187	184	8	2	2	53	-51
4	2	0	265	260	-10	0	1	193	187	-8	4	1	56	-62	1	9	1	52	-49	10	2	2	117	115
8	2	0	82	82	-8	0	1	74	-77	-6	4	1	286	306	3	9	1	193	188	-13	3	2	51	51
10	2	0	95	95	-6	0	1	327	311	-4	4	1	95	-95	5	9	1	69	-64	-11	3	2	76	77
1	3	0	144	134	-4	0	1	84	74	-2	4	1	272	264	7	9	1	123	116	-9	3	2	23	24
3	3	0	37	-32	-2	0	1	334	342	0	4	1	52	52	-8	10	1	31	-30	-7	3	2	180	187
5	3	0	328	325	2	0	1	185	183	2	4	1	166	161	-6	10	1	157	166	-5	3	2	96	-95
7	3	0	108	-104	4	0	1	178	175	4	4	1	128	125	-4	10	1	42	-41	-3	3	2	449	475
9	3	0	202	196	6	0	1	32	25	6	4	1	40	-36	-2	10	1	145	145	-1	3	2	155	-142
11	3	0	22	-24	8	0	1	186	184	8	4	1	211	204	2	10	1	83	87	1	3	2	249	239
0	4	0	384	394	10	0	1	50	-50	10	4	1	56	-54	4	10	1	75	79	3	3	2	46	46
2	4	0	72	-70	12	0	1	147	149	-11	5	1	125	133	-5	11	1	58	64	5	3	2	92	89
4	4	0	254	249	-13	1	1	51	-49	-9	5	1	126	127	-1	11	1	135	131	7	3	2	135	129
6	4	0	44	34	-11	1	1	173	168	-5	5	1	101	101	1	11	1	30	-30	9	3	2	51	-45
8	4	0	58	62	-9	1	1	23	-20	-1	5	1	270	259	3	11	1	151	146	-12	4	2	136	136
10	4	0	97	94	-7	1	1	129	128	1	5	1	111	-108	-4	12	1	39	-42	-10	4	2	38	-39
1	5	0	158	154	-5	1	1	151	150	3	5	1	311	293	-2	12	1	116	118	-8	4	2	197	200
3	5	0	18	-15	-3	1	1	30	-29	5	5	1	60	-58	2	12	1	48	49	-6	4	2	30	-27
5	5	0	218	212	-1	1	1	354	381	7	5	1	168	159	-12	0	2	161	159	-4	4	2	170	174
7	5	0	79	-76	1	1	1	146	-137	11	5	1	39	41	-10	0	2	73	-72	-2	4	2	156	146
9	5	0	197	192	3	1	1	399	404	-10	6	1	137	138	-8	0	2	265	258	0	4	2	26	-22
11	5	0	35	-39	5	1	1	80	-75	-8	6	1	60	-63	-6	0	2	28	24	2	4	2	303	285
0	6	0	382	381	7	1	1	199	201	-6	6	1	221	230	-4	0	2	175	166	4	4	2	65	-66
2	6	0	77	-75	9	1	1	23	20	-4	6	1	38	-41	-2	0	2	141	129	6	4	2	240	232
4	6	0	183	175	11	1	1	48	44	-2	6	1	252	248	2	0	2	467	522	8	4	2	37	-37
6	6	0	23	23	-10	2	1	143	144	2	6	1	115	108	4	0	2	136	-133	10	4	2	103	101
8	6	0	85	85	-8	2	1	64	-65	4	6	1	159	146	6	0	2	248	249	-11	5	2	66	64
10	6	0	77	79	-6	2	1	287	297	8	6	1	160	151	10	0	2	116	123	-7	5	2	199	208
1	7	0	148	147	-4	2	1	164	-170	10	6	1	45	-43	-13	1	2	67	72	-5	5	2	92	-93
3	7	0	29	-29	-2	2	1	308	312	-11	7	1	131	129	-11	1	2	60	60	-3	5	2	291	279
5	7	0	198	196	2	2	1	151	138	-7	7	1	73	80	-7	1	2	242	235	-1	5	2	82	-79
7	7	0	39	-40	4	2	1	150	141	-5	7	1	110	117	-5	1	2	72	-71	1	5	2	267	251
9	7	0	157	153	6	2	1	75	-70	-1	7	1	235	230	-3	1	2	315	354	3	5	2	41	39
0	8	0	253	237	8	2	1	201	199	1	7	1	49	-51	-1	1	2	120	-110	5	5	2	78	74
2	8	0	80	-81	10	2	1	54	-55	3	7	1	268	254	1	1	2	338	348	7	5	2	102	101

OBSERVED AND CALCULATED STRUCTURE FACTORS FOR OS 3 (CO) 12 CL 2

H	K	L	FO	FC	H	K	L	FO	FC	H	K	L	FO	FC	H	K	L	FO	FC	H	K	L	FO	FC
9	5	2	26	-25	-4	12	2	46	49	9	3	3	171	167	-9	9	3	122	127	8	2	4	153	154
-12	6	2	123	125	-2	12	2	45	49	-10	4	3	65	69	-7	9	3	36	-42	-13	3	4	48	-51
-10	6	2	53	-58	-14	0	3	102	106	-8	4	3	116	126	-5	9	3	152	157	-11	3	4	129	129
-8	6	2	169	179	-12	0	3	27	-23	-6	4	3	12	-10	-1	9	3	51	50	-7	3	4	108	106
-6	6	2	22	23	-10	0	3	129	125	-4	4	3	299	290	1	9	3	116	114	-5	3	4	107	102
-4	6	2	104	104	-8	0	3	155	144	-2	4	3	105	-99	3	9	3	21	-16	-1	3	4	352	348
-2	6	2	97	94	-6	0	3	44	-40	0	4	3	315	298	5	9	3	133	133	1	3	4	151	-145
2	6	2	294	284	-4	0	3	335	340	2	4	3	32	-32	-8	10	3	67	71	3	3	4	244	233
4	6	2	91	-86	-2	0	3	90	76	4	4	3	216	208	-4	10	3	152	158	7	3	4	130	128
6	6	2	198	186	0	0	3	323	316	6	4	3	22	22	-2	10	3	43	-43	-10	4	4	141	145
-11	7	2	35	39	2	0	3	91	-86	8	4	3	35	36	0	10	3	169	163	-8	4	4	43	-44
-9	7	2	20	21	4	0	3	257	268	-13	5	3	87	90	2	10	3	21	-23	-6	4	4	276	261
-7	7	2	159	162	6	0	3	45	42	-11	5	3	42	-42	4	10	3	123	117	-4	4	4	99	-94
-5	7	2	41	-41	8	0	3	54	55	-9	5	3	180	190	-5	11	3	105	117	-2	4	4	285	275
-3	7	2	262	256	10	0	3	76	80	-7	5	3	64	-67	-1	11	3	67	64	0	4	4	23	29
-1	7	2	84	-85	-13	1	3	108	111	-5	5	3	246	238	1	11	3	73	73	2	4	4	73	72
1	7	2	236	225	-11	1	3	58	-58	-1	5	3	115	111	-2	12	3	36	-42	4	4	4	126	129
3	7	2	34	37	-9	1	3	256	247	1	5	3	137	128	-14	0	4	68	71	8	4	4	144	144
5	7	2	56	53	-7	1	3	89	-84	3	5	3	41	-40	-10	0	4	170	153	-11	5	4	127	131
7	7	2	94	92	-5	1	3	269	265	5	5	3	208	202	-8	0	4	71	-64	-7	5	4	77	79
-10	8	2	46	-50	-3	1	3	45	46	7	5	3	55	-54	-6	0	4	371	368	-5	5	4	142	141
-8	8	2	134	143	-1	1	3	113	116	9	5	3	144	138	-4	0	4	70	-72	-3	5	4	42	-39
-4	8	2	77	82	1	1	3	174	165	-10	6	3	89	94	-2	0	4	254	257	-1	5	4	233	221
-2	8	2	105	108	3	1	3	61	-62	-8	6	3	92	96	0	0	4	42	44	1	5	4	74	-78
0	8	2	35	-35	5	1	3	259	253	-6	6	3	31	-29	2	0	4	109	108	3	5	4	239	233
2	8	2	200	190	7	1	3	65	-68	-4	6	3	242	237	4	0	4	206	199	7	5	4	112	113
4	8	2	70	-69	9	1	3	159	162	-2	6	3	40	-39	6	0	4	58	-60	-10	6	4	117	122
6	8	2	167	166	-10	2	3	93	89	0	6	3	260	248	8	0	4	160	162	-8	6	4	53	-58
8	8	2	32	-35	-8	2	3	93	92	2	6	3	76	-75	-13	1	4	36	-36	-6	6	4	251	244
-7	9	2	111	117	-6	2	3	22	-15	4	6	3	201	183	-11	1	4	164	151	-4	6	4	50	-50
-5	9	2	51	-53	-4	2	3	275	267	6	6	3	42	39	-7	1	4	124	125	-2	6	4	188	175
-3	9	2	192	198	-2	2	3	180	-176	8	6	3	31	34	-5	1	4	160	152	0	6	4	23	18
-1	9	2	57	-54	0	2	3	351	342	-11	7	3	42	-46	-1	1	4	270	262	2	6	4	89	88
1	9	2	135	136	2	2	3	69	-65	-9	7	3	179	184	1	1	4	104	-102	4	6	4	125	129
3	9	2	16	16	4	2	3	217	221	-7	7	3	47	-53	3	1	4	288	294	6	6	4	39	-35
5	9	2	72	67	8	2	3	30	32	-5	7	3	165	162	5	1	4	32	-33	-11	7	4	102	108
7	9	2	67	69	10	2	3	92	92	-3	7	3	45	45	7	1	4	124	132	-7	7	4	100	103
-8	10	2	109	117	-13	3	3	111	115	-1	7	3	86	88	-14	2	4	50	48	-5	7	4	110	107
-4	10	2	86	90	-11	3	3	62	-65	1	7	3	125	122	-12	2	4	19	-13	-1	7	4	219	204
-2	10	2	92	90	-9	3	3	208	207	5	7	3	188	181	-10	2	4	169	160	1	7	4	77	-77
2	10	2	165	166	-7	3	3	43	-46	7	7	3	51	-51	-8	2	4	84	-83	3	7	4	212	206
4	10	2	36	-37	-5	3	3	263	258	-10	8	3	60	64	-6	2	4	268	264	5	7	4	25	-28
6	10	2	138	135	-3	3	3	22	-14	-8	8	3	58	63	-4	2	4	79	-76	-10	8	4	103	111
-7	11	2	103	112	-1	3	3	81	78	-4	8	3	159	159	-2	2	4	253	244	-8	8	4	54	-58
-5	11	2	40	-42	1	3	3	177	175	-2	8	3	76	-74	0	2	4	22	25	-6	8	4	180	181
-3	11	2	154	158	3	3	3	35	31	0	8	3	216	203	2	2	4	60	60	-4	8	4	45	-48
-1	11	2	40	-43	5	3	3	189	189	2	8	3	45	-45	4	2	4	120	119	-2	8	4	154	149
1	11	2	138	132	7	3	3	78	-75	4	8	3	146	143	6	2	4	29	-28	0	8	4	23	25

OBSERVED AND CALCULATED STRUCTURE FACTORS FOR OS 3 (CO) 12 CL 2

H	K	L	FO	FC	H	K	L	FO	FC	H	K	L	FO	FC	H	K	L	FO	FC	H	K	L	FO	FC
2	8	4	40	39	-11	3	5	88	83	-2	8	5	92	88	-7	3	6	44	-46	-4	0	7	51	-55
4	8	4	98	99	-9	3	5	42	-43	0	8	5	29	-27	-5	3	6	175	169	-2	0	7	186	177
6	8	4	25	-23	-7	3	5	221	217	2	8	5	147	150	-1	3	6	85	93	0	0	7	70	71
-7	9	4	59	58	-5	3	5	46	-44	4	8	5	44	-47	1	3	6	151	156	2	0	7	61	59
-5	9	4	65	69	-3	3	5	267	261	-9	9	5	17	-18	3	3	6	66	-66	4	0	7	88	94
-1	9	4	164	164	-1	3	5	85	-86	-7	9	5	122	126	5	3	6	149	155	-13	1	7	29	-34
1	9	4	68	-65	1	3	5	198	195	-5	9	5	39	-42	-10	4	6	69	76	-11	1	7	126	119
3	9	4	146	145	3	3	5	46	48	-3	9	5	159	165	-8	4	6	95	96	-7	1	7	63	65
-6	10	4	146	147	5	3	5	58	59	-1	9	5	51	-51	-4	4	6	216	213	-5	1	7	138	133
-4	10	4	38	-42	7	3	5	82	88	1	9	5	112	110	-2	4	6	92	-88	-3	1	7	42	-39
-2	10	4	141	142	-12	4	5	161	156	3	9	5	35	34	0	4	6	248	247	-1	1	7	205	209
2	10	4	43	47	-10	4	5	53	-54	-6	10	5	26	27	2	4	6	39	-41	1	1	7	50	-51
-5	11	4	78	78	-8	4	5	152	145	-4	10	5	52	58	4	4	6	111	117	3	1	7	168	169
-1	11	4	124	133	-6	4	5	48	53	-2	10	5	87	96	-11	5	6	38	-41	-10	2	7	154	151
1	11	4	42	-43	-4	4	5	91	90	-3	11	5	129	133	-9	5	6	173	169	-8	2	7	76	-75
-14	0	5	33	-36	-2	4	5	164	159	-14	0	6	90	89	-7	5	6	45	-46	-6	2	7	213	199
-12	0	5	162	159	0	4	5	40	-41	-12	0	6	39	40	-5	5	6	162	154	-4	2	7	51	-53
-10	0	5	64	-59	2	4	5	209	207	-10	0	6	85	84	-3	5	6	47	45	-2	2	7	173	165
-8	0	5	230	222	4	4	5	50	-51	-8	0	6	89	88	-1	5	6	48	49	0	2	7	31	30
-6	0	5	34	32	6	4	5	165	165	-6	0	6	16	9	1	5	6	109	114	2	2	7	25	28
-4	0	5	86	88	-13	5	5	55	60	-4	0	6	291	295	5	5	6	142	148	4	2	7	110	112
-2	0	5	212	213	-11	5	5	59	61	-2	0	6	96	-101	-12	6	6	22	24	-13	3	7	45	-45
0	0	5	35	33	-7	5	5	179	178	0	0	6	245	235	-10	6	6	54	57	-11	3	7	143	142
2	0	5	200	194	-5	5	5	79	-75	4	0	6	142	142	-8	6	6	70	73	-9	3	7	145	143
4	0	5	81	-79	-3	5	5	264	260	6	0	6	50	51	-4	6	6	212	206	-1	3	7	178	178
6	0	5	211	210	-1	5	5	58	-56	-13	1	6	118	120	-2	6	6	69	-70	1	3	7	75	-77
-13	1	5	58	59	1	5	5	179	177	-11	1	6	44	-41	0	6	6	176	179	3	3	7	170	176
-11	1	5	79	82	3	5	5	29	24	-9	1	6	207	197	4	6	6	112	114	-10	4	7	154	154
-9	1	5	21	-17	5	5	5	39	41	-7	1	6	81	-77	-11	7	6	28	-25	-8	4	7	64	-63
-7	1	5	244	234	-12	6	5	116	122	-5	1	6	212	215	-9	7	6	139	140	-6	4	7	171	173
-5	1	5	91	-95	-10	6	5	40	-46	-3	1	6	42	42	-7	7	6	58	-60	-4	4	7	17	-15
-3	1	5	296	292	-8	6	5	166	166	-1	1	6	72	71	-5	7	6	167	164	-2	4	7	146	149
-1	1	5	35	-35	-4	6	5	64	63	1	1	6	131	128	-1	7	6	59	60	0	4	7	38	41
1	1	5	198	203	-2	6	5	154	153	3	1	6	36	-36	1	7	6	105	104	2	4	7	28	34
3	1	5	31	35	2	6	5	173	165	5	1	6	170	175	3	7	6	30	-27	4	4	7	94	104
5	1	5	36	40	4	6	5	60	-62	-14	2	6	102	96	-10	8	6	35	40	-11	5	7	115	111
7	1	5	116	120	6	6	5	159	159	-10	2	6	54	55	-8	8	6	71	73	-7	5	7	59	61
-14	2	5	33	-35	-11	7	5	64	68	-8	2	6	106	105	-4	8	6	154	152	-5	5	7	105	103
-12	2	5	161	155	-7	7	5	171	176	-6	2	6	38	-38	-2	8	6	51	-50	-3	5	7	34	-29
-10	2	5	68	-65	-5	7	5	58	-60	-4	2	6	224	214	0	8	6	153	154	-1	5	7	181	190
-8	2	5	181	175	-3	7	5	200	189	-2	2	6	81	-81	-5	9	6	102	101	1	5	7	52	-56
-4	2	5	102	97	-1	7	5	19	-18	0	2	6	248	240	-1	9	6	55	55	3	5	7	148	153
-2	2	5	139	137	1	7	5	139	139	2	2	6	41	-41	1	9	6	79	85	-10	6	7	127	126
0	2	5	82	-77	3	7	5	27	26	4	2	6	108	120	-4	10	6	119	125	-8	6	7	44	-45
2	2	5	227	227	5	7	5	39	38	6	2	6	24	33	-2	10	6	37	-42	-6	6	7	171	175
4	2	5	69	-68	-10	8	5	34	-40	-13	3	6	111	102	-10	0	7	173	169	-4	6	7	49	-49
6	2	5	177	179	-8	8	5	120	120	-11	3	6	54	-53	-8	0	7	59	-55	-2	6	7	134	132
-13	3	5	73	79	-4	8	5	69	71	-9	3	6	188	186	-6	0	7	238	229	0	6	7	57	52

OBSERVED AND CALCULATED STRUCTURE FACTORS FOR OS 3 (CO) 12 CL 2

H	K	L	FO	FC	H	K	L	FO	FC	H	K	L	FO	FC	H	K	L	FO	FC	H	K	L	FO	FC
2	6	7	40	37	-13	1	8	41	37	-12	4	8	118	117	-4	8	8	23	26	-5	3	9	106	102
-9	7	7	19	26	-11	1	8	85	85	-8	4	8	130	136	-10	0	9	25	31	-3	3	9	50	48
-7	7	7	41	45	-7	1	8	178	168	-4	4	8	48	49	-8	0	9	115	120	-1	3	9	34	34
-5	7	7	107	106	-5	1	8	80	-79	-2	4	8	115	114	-4	0	9	162	162	-10	4	9	45	42
-3	7	7	18	-23	-3	1	8	206	210	0	4	8	34	-31	-2	0	9	63	-63	-8	4	9	93	97
-1	7	7	143	147	1	1	8	115	114	2	4	8	153	159	0	0	9	166	165	-6	4	9	28	-26
1	7	7	33	-33	-12	2	8	131	123	-11	5	8	73	74	-11	1	9	39	-44	-4	4	9	128	137
-8	8	7	42	-46	-10	2	8	41	-43	-7	5	8	139	146	-9	1	9	145	141	-2	4	9	33	-33
-6	8	7	137	139	-8	2	8	122	121	-5	5	8	52	-53	-7	1	9	24	-23	-9	5	9	127	129
-4	8	7	39	-39	-6	2	8	29	26	-3	5	8	158	163	-5	1	9	117	119	-5	5	9	103	105
-2	8	7	112	114	-4	2	8	34	37	1	5	8	91	94	-3	1	9	34	32	-4	6	9	126	128
0	8	7	19	18	-2	2	8	114	114	-8	6	8	97	100	-1	1	9	27	30	-8	0	10	27	-29
-5	9	7	78	82	2	2	8	151	158	-4	6	8	56	55	-10	2	9	46	42	-6	0	10	140	138
-3	9	7	17	-13	-11	3	8	60	60	-2	6	8	102	110	-8	2	9	95	93	-9	1	10	30	29
-12	0	8	129	127	-9	3	8	18	-9	0	6	8	30	-32	-4	2	9	150	154	-7	1	10	39	37
-8	0	8	137	135	-7	3	8	173	166	-7	7	8	119	122	-2	2	9	52	-54	-5	1	10	93	96
-6	0	8	18	17	-5	3	8	67	-68	-5	7	8	54	-60	0	2	9	141	147	-8	2	10	48	-49
-4	0	8	82	80	-3	3	8	173	168	-3	7	8	151	161	-11	3	9	46	-46	-6	2	10	134	137
-2	0	8	146	147	-1	3	8	18	-23	-1	7	8	24	-24	-9	3	9	160	154	-7	3	10	46	45
0	0	8	42	-46	1	3	8	119	122	-6	8	8	23	19	-7	3	9	40	-41	-5	3	10	89	94
2	0	8	153	155																				

APPENDIX II

OBSERVED AND CALCULATED STRUCTURE FACTORS

FOR $Os_2(CO)_6I_2$

H	K	L	FO	FC	H	K	L	FO	FC	H	K	L	FO	FC	H	K	L	FO	FC	H	K	L	FO	FC
1	0	0	144	-126	1	5	0	215	219	1	10	0	87	87	1	0	1	210	-253	-7	3	1	16	17
2	0	0	146	-122	2	5	0	44	36	2	10	0	118	107	2	0	1	14	11	-6	3	1	29	30
3	0	0	17	-12	3	5	0	192	-172	4	10	0	110	-90	3	0	1	273	278	-5	3	1	38	-38
4	0	0	148	133	4	5	0	51	-46	5	10	0	39	-33	4	0	1	89	-77	-4	3	1	41	39
5	0	0	72	67	5	5	0	210	190	6	10	0	126	105	5	0	1	130	-123	-3	3	1	138	-127
6	0	0	161	-161	6	5	0	46	-43	1	11	0	137	132	6	0	1	29	29	-2	3	1	186	180
7	0	0	27	22	7	5	0	66	-58	2	11	0	12	-4	7	0	1	78	72	-1	3	1	129	-150
1	1	0	252	-259	0	6	0	41	35	3	11	0	136	-119	-7	1	1	15	9	0	3	1	50	-49
2	1	0	15	9	1	6	0	99	93	4	11	0	16	10	-6	1	1	100	98	1	3	1	104	99
3	1	0	199	179	2	6	0	241	-233	5	11	0	66	53	-5	1	1	12	-4	2	3	1	11	-9
4	1	0	50	-45	3	6	0	11	-7	6	11	0	35	29	-4	1	1	230	-219	3	3	1	115	104
5	1	0	79	-69	4	6	0	193	169	0	12	0	111	113	-3	1	1	174	155	4	3	1	114	-102
6	1	0	69	-65	5	6	0	39	-33	1	12	0	51	-51	-2	1	1	44	30	5	3	1	31	31
7	1	0	118	113	6	6	0	70	-61	2	12	0	50	-43	-1	1	1	42	33	6	3	1	13	13
1	2	0	151	132	7	6	0	38	-31	4	12	0	36	30	0	1	1	183	-248	-7	4	1	37	36
2	2	0	45	34	1	7	0	79	-75	5	12	0	33	26	1	1	1	20	-19	-6	4	1	20	-11
3	2	0	10	-7	2	7	0	11	-13	5	13	0	27	24	3	1	1	136	-126	-5	4	1	100	-97
4	2	0	26	-19	3	7	0	79	70	0	14	0	14	8	4	1	1	83	-71	-3	4	1	199	199
5	2	0	61	-54	4	7	0	47	42	1	14	0	52	38	5	1	1	28	-26	-2	4	1	51	-53
6	2	0	90	82	5	7	0	98	-84	2	14	0	97	-85	6	1	1	111	109	-1	4	1	123	-158
7	2	0	27	-22	6	7	0	35	32	4	14	0	74	62	7	1	1	16	-15	0	4	1	45	46
1	3	0	51	-42	0	8	0	150	163	1	15	0	85	-80	-7	2	1	61	62	1	4	1	191	192
2	3	0	21	-18	1	8	0	70	-65	3	15	0	90	73	-6	2	1	27	-28	2	4	1	87	-79
3	3	0	44	37	2	8	0	24	24	0	16	0	47	-44	-5	2	1	60	-55	3	4	1	106	-92
4	3	0	31	27	4	8	0	11	-8	1	16	0	20	-22	-4	2	1	41	36	4	4	1	42	-36
5	3	0	110	-98	5	8	0	42	36	2	16	0	100	84	-3	2	1	42	40	5	4	1	140	125
6	3	0	43	40	6	8	0	48	-42	1	17	0	37	35	-2	2	1	29	-25	7	4	1	107	-99
0	4	0	76	-75	7	8	0	25	22	-7	0	1	121	-124	-1	2	1	77	-74	-7	5	1	36	-37
1	4	0	219	-215	1	9	0	144	-142	-6	0	1	58	55	0	2	1	22	23	-6	5	1	100	-102
2	4	0	240	224	3	9	0	113	100	-5	0	1	160	161	1	2	1	58	55	-5	5	1	58	56
4	4	0	191	-170	4	9	0	24	-22	-4	0	1	99	-93	2	2	1	78	70	-4	5	1	104	101
5	4	0	45	43	5	9	0	44	-33	-3	0	1	186	-168	3	2	1	179	-167	-3	5	1	55	57
6	4	0	52	46	6	9	0	43	-36	-2	0	1	19	-15	4	2	1	82	76	-2	5	1	236	-301
7	4	0	26	25	0	10	0	212	-233	-1	0	1	271	268	5	2	1	26	21	-1	5	1	106	132

H	K	L	FO	FC	H	K	L	FO	FC	H	K	L	FO	FC	H	K	L	FO	FC	H	K	L	FO	FC
0	5	1	198	225	-6	8	1	14	16	-4	11	1	100	128	-2	15	1	90	110	2	1	2	39	-37
1	5	1	120	-117	-5	8	1	25	27	-3	11	1	57	-89	-1	15	1	33	-36	3	1	2	176	-170
2	5	1	117	-106	-4	8	1	17	-20	-2	11	1	46	-59	0	15	1	85	-83	4	1	2	17	5
3	5	1	85	-74	-1	8	1	29	22	-1	11	1	16	-18	1	15	1	36	33	5	1	2	180	178
4	5	1	245	230	0	8	1	12	-12	0	11	1	127	128	2	15	1	62	52	6	1	2	98	-94
5	5	1	59	-51	1	8	1	18	-16	2	11	1	173	-159	3	15	1	16	13	7	1	2	38	-35
6	5	1	104	-93	2	8	1	39	-32	3	11	1	70	65	-2	16	1	14	-16	-7	2	2	41	-42
-7	6	1	45	-46	3	8	1	91	82	4	11	1	79	65	-1	16	1	66	-74	-6	2	2	23	19
-5	6	1	98	100	4	8	1	49	-42	6	11	1	89	-77	1	16	1	86	77	-5	2	2	45	-47
-4	6	1	17	-3	-6	9	1	56	62	-5	12	1	28	39	2	16	1	31	-26	-4	2	2	130	121
-3	6	1	149	-162	-4	9	1	103	-128	-4	12	1	18	-29	-1	17	1	23	24	-3	2	2	64	-56
-2	6	1	53	65	-3	9	1	65	84	-3	12	1	30	-46	0	17	1	34	36	-2	2	2	147	-136
-1	6	1	148	186	-2	9	1	26	30	-1	12	1	53	61	-7	0	2	78	79	-1	2	2	175	185
0	6	1	50	-50	-1	9	1	24	28	1	12	1	52	-46	-6	0	2	60	58	0	2	2	100	-112
1	6	1	207	-215	0	9	1	120	-126	2	12	1	13	-18	-4	0	2	236	-228	1	2	2	133	137
2	6	1	84	79	1	9	1	23	-20	3	12	1	99	83	-3	0	2	126	111	2	2	2	159	-163
3	6	1	107	93	2	9	1	185	173	4	12	1	44	-38	-2	0	2	252	229	3	2	2	48	43
4	6	1	41	36	3	9	1	101	-87	5	12	1	37	-33	-1	0	2	208	-195	5	2	2	49	-44
5	6	1	145	-131	4	9	1	44	-40	-3	13	1	29	43	0	0	2	90	-94	6	2	2	23	-20
7	6	1	105	98	5	9	1	17	-16	-2	13	1	41	-52	2	0	2	245	275	-7	3	2	32	35
-7	7	1	23	24	6	9	1	82	70	-1	13	1	35	34	3	0	2	112	-109	-6	3	2	53	-52
-6	7	1	38	41	-6	10	1	24	-30	1	13	1	22	-20	4	0	2	208	-207	-4	3	2	15	-8
-5	7	1	41	-44	-5	10	1	83	-99	2	13	1	34	30	5	0	2	55	55	-3	3	2	49	46
-4	7	1	13	6	-4	10	1	32	43	3	13	1	40	-31	6	0	2	94	91	-2	3	2	46	-43
-3	7	1	62	-73	-3	10	1	62	93	4	13	1	41	34	7	0	2	16	-15	-1	3	2	85	-80
-2	7	1	132	197	-2	10	1	14	-25	5	13	1	21	-16	-7	1	2	48	47	0	3	2	64	-71
-1	7	1	69	-80	-1	10	1	131	-149	-4	14	1	13	3	-6	1	2	23	-19	1	3	2	92	94
0	7	1	66	-69	0	10	1	33	35	-3	14	1	44	-64	-5	1	2	149	-143	2	3	2	87	-84
1	7	1	48	45	1	10	1	149	143	-2	14	1	16	24	-4	1	2	91	85	3	3	2	50	-49
2	7	1	15	-13	2	10	1	12	3	-1	14	1	57	59	-3	1	2	158	141	4	3	2	59	56
3	7	1	51	45	4	10	1	52	44	0	14	1	15	-15	-2	1	2	113	-94	5	3	2	39	-36
4	7	1	118	-108	5	10	1	97	82	1	14	1	73	-68	-1	1	2	234	-241	6	3	2	50	51
5	7	1	35	30	6	10	1	20	-14	2	14	1	27	24	0	1	2	98	105	7	3	2	70	-67
6	7	1	48	40	-6	11	1	56	-65	3	14	1	44	36	1	1	2	88	91	-7	4	2	14	-9

H	K	L	FO	FC	H	K	L	FO	FC	H	K	L	FO	FC	H	K	L	FO	FC	H	K	L	FO	FC
-6	4	2	124	-125	0	6	2	253	-297	-5	9	2	78	-87	-1	12	2	73	-78	1	0	3	218	247
-5	4	2	112	107	1	6	2	165	168	-3	9	2	79	82	2	12	2	100	90	2	0	3	183	-196
-4	4	2	57	53	2	6	2	97	93	-2	9	2	29	-35	3	12	2	26	-22	3	0	3	48	-44
-3	4	2	27	-26	3	6	2	38	-35	-1	9	2	102	-111	4	12	2	56	-48	5	0	3	161	169
-2	4	2	107	-107	4	6	2	113	-101	0	9	2	77	78	5	12	2	30	25	6	0	3	69	-69
-1	4	2	26	-28	5	6	2	24	20	1	9	2	69	64	1	13	2	28	-26	7	0	3	100	-106
0	4	2	227	275	6	6	2	113	105	2	9	2	25	-25	2	13	2	26	22	-7	1	3	70	-74
1	4	2	180	-186	7	6	2	34	-34	5	9	2	120	108	3	13	2	18	11	-6	1	3	48	-51
2	4	2	97	-87	-7	7	2	44	48	6	9	2	62	-55	4	13	2	22	-19	-5	1	3	94	90
3	4	2	60	56	-6	7	2	42	-46	-6	10	2	35	-37	-4	14	2	19	-25	-4	1	3	52	45
4	4	2	133	124	-4	7	2	13	10	-4	10	2	125	135	-2	14	2	40	44	-3	1	3	30	26
6	4	2	102	-94	-3	7	2	60	69	-3	10	2	64	-71	0	14	2	95	-93	-2	1	3	282	-279
7	4	2	37	37	-2	7	2	14	-16	-2	10	2	117	-146	1	14	2	59	56	-1	1	3	193	211
-7	5	2	77	-83	-1	7	2	38	-39	-1	10	2	100	110	2	14	2	45	37	0	1	3	125	119
-6	5	2	75	77	0	7	2	22	24	0	10	2	72	69	4	14	2	47	-40	1	1	3	128	-137
-5	5	2	96	93	1	7	2	144	145	1	10	2	14	7	-3	15	2	51	68	2	1	3	73	-74
-4	5	2	50	-47	2	7	2	59	-55	2	10	2	172	-161	-2	15	2	25	-30	3	1	3	34	29
-3	5	2	157	-163	3	7	2	64	-58	3	10	2	55	49	-1	15	2	70	-69	4	1	3	164	164
-2	5	2	87	88	4	7	2	63	55	4	10	2	122	108	0	15	2	25	25	5	1	3	92	-91
-1	5	2	147	182	6	7	2	48	41	5	10	2	54	-48	1	15	2	109	97	6	1	3	73	-70
0	5	2	32	-33	7	7	2	72	-68	6	10	2	78	-67	2	15	2	43	-38	7	1	3	16	19
1	5	2	228	-243	-6	8	2	20	-20	-5	11	2	72	85	3	15	2	74	-63	-6	2	3	14	11
2	5	2	132	130	-5	8	2	35	40	-4	11	2	51	-55	-2	16	2	44	-50	-5	2	3	37	34
3	5	2	183	175	-4	8	2	61	-66	-3	11	2	83	-96	0	16	2	107	99	-4	2	3	26	-22
4	5	2	87	-84	-3	8	2	20	22	-2	11	2	40	46	1	16	2	64	-56	-3	2	3	64	-62
5	5	2	82	-73	-2	8	2	48	58	-1	11	2	102	108	2	16	2	56	-49	-2	2	3	30	28
6	5	2	22	-16	-1	8	2	77	-87	0	11	2	79	-82	-7	0	3	40	41	-1	2	3	89	90
7	5	2	123	117	0	8	2	76	78	1	11	2	95	-91	-6	0	3	61	-58	0	2	3	65	-64
-6	6	2	109	116	1	8	2	77	-75	3	11	2	114	98	-5	0	3	108	-106	1	2	3	71	-74
-5	6	2	107	-112	2	8	2	76	72	4	11	2	21	-15	-4	0	3	109	103	2	2	3	106	107
-4	6	2	59	-59	3	8	2	35	-33	5	11	2	124	-111	-3	0	3	149	131	3	2	3	24	-26
-3	6	2	44	45	4	8	2	45	-38	-4	12	2	62	-66	-2	0	3	120	-107	4	2	3	45	44
-2	6	2	118	120	5	8	2	23	17	-3	12	2	28	35	-1	0	3	251	-260	5	2	3	89	-85
-1	6	2	22	27	-6	9	2	14	-13	-2	12	2	62	71	0	0	3	156	155	6	2	3	29	26

H	K	L	FO	FC	H	K	L	FO	FC	H	K	L	FO	FC	H	K	L	FO	FC	H	K	L	FO	FC
-7	2	3	45	46	0	5	3	186	-206	1	8	3	39	36	2	11	3	72	65	0	16	3	41	-41
-6	3	3	38	-38	1	5	3	84	87	2	8	3	66	-62	3	11	3	24	-20	1	16	3	62	-58
-4	3	3	103	97	2	5	3	201	206	3	8	3	45	45	4	11	3	114	-103	-7	0	4	45	-45
-3	3	3	123	-118	3	5	3	146	-144	4	8	3	42	-39	5	11	3	59	54	-6	0	4	111	-118
-2	3	3	78	76	4	5	3	98	-93	5	8	3	49	45	-5	12	3	29	-27	-5	0	4	163	169
-1	3	3	71	-66	5	5	3	53	49	-6	9	3	24	-34	-4	12	3	25	24	-4	0	4	14	15
0	3	3	65	67	6	5	3	113	109	-5	9	3	51	53	-3	12	3	39	41	-3	0	4	123	-112
1	3	3	9	6	7	5	3	55	-56	-4	9	3	23	17	-2	12	3	24	-27	-2	0	4	138	-126
2	3	3	103	-106	-7	6	3	64	71	-2	9	3	163	-165	-1	12	3	54	-55	-1	0	4	39	37
3	3	3	109	106	-6	6	3	64	-67	-1	9	3	110	120	0	12	3	47	48	0	0	4	268	267
4	3	3	11	-12	-5	6	3	75	-79	0	9	3	71	75	1	12	3	67	62	1	0	4	256	-270
6	3	3	51	-50	-4	6	3	81	82	1	9	3	78	-75	2	12	3	57	-53	2	0	4	77	-77
7	3	3	23	24	-3	6	3	113	114	2	9	3	51	-47	3	12	3	21	-9	3	0	4	93	96
-7	4	3	60	-67	-1	6	3	99	-105	3	9	3	15	16	5	12	3	60	53	4	0	4	104	111
-6	4	3	64	64	0	6	3	75	76	4	9	3	97	92	-4	13	3	28	-27	5	0	4	101	-101
-5	4	3	75	74	1	6	3	110	108	5	9	3	58	-54	-3	13	3	41	46	6	0	4	83	-84
-4	4	3	82	-76	2	6	3	43	-41	6	9	3	47	-41	-2	13	3	40	-32	7	0	4	49	59
-3	4	3	112	-112	3	6	3	199	-198	-5	10	3	67	70	-1	13	3	28	28	-7	1	4	46	-52
-2	4	3	129	132	4	6	3	138	131	-4	10	3	65	-63	0	13	3	14	-18	-6	1	4	74	77
-1	4	3	118	107	5	6	3	65	58	-3	10	3	100	-93	2	13	3	31	28	-5	1	4	56	54
0	4	3	68	-72	6	6	3	36	-37	-2	10	3	54	58	3	13	3	28	-27	-4	1	4	102	-95
1	4	3	110	-112	-5	7	3	21	21	-1	10	3	124	131	4	13	3	15	12	-3	1	4	81	-75
3	4	3	198	203	-4	7	3	73	77	0	10	3	89	-86	-3	14	3	39	47	-2	1	4	133	129
4	4	3	144	-145	-3	7	3	124	-120	1	10	3	131	-122	-2	14	3	36	-40	-1	1	4	83	85
5	4	3	47	-44	-2	7	3	35	29	2	10	3	126	120	-1	14	3	34	-36	0	1	4	60	-52
6	4	3	40	40	-1	7	3	18	-18	3	10	3	52	50	0	14	3	26	27	1	1	4	205	-222
7	4	3	48	44	0	7	3	86	90	4	10	3	17	-12	1	14	3	45	37	2	1	4	181	194
-7	5	3	26	27	1	7	3	21	-17	5	10	3	119	-107	3	14	3	85	-75	4	1	4	103	-109
-6	5	3	87	89	2	7	3	125	-121	-5	11	3	47	-51	-2	15	3	26	-28	5	1	4	25	-18
-5	5	3	63	-61	3	7	3	86	84	-3	11	3	19	13	-1	15	3	22	21	7	1	4	96	105
-4	5	3	174	-176	6	7	3	51	-49	-2	11	3	125	145	0	15	3	82	76	-6	2	4	64	70
-3	5	3	204	210	-3	8	3	23	18	-1	11	3	105	-114	1	15	3	43	-40	-5	2	4	103	-102
-2	5	3	46	37	-1	8	3	50	-54	0	11	3	83	-80	2	15	3	91	-80	-4	2	4	40	39
-1	5	3	28	-25	0	8	3	25	22	1	11	3	85	80	-1	16	3	46	48	-3	2	4	15	1

H	K	L	FO	FC	H	K	L	FO	FC	H	K	L	FO	FC	H	K	L	FO	FC	H	K	L	FO	FC
-2	2	4	30	29	0	5	4	186	201	-4	8	4	46	-43	0	11	4	47	47	2	0	5	101	105
0	2	4	148	-141	1	5	4	49	48	-2	8	4	18	-14	1	11	4	123	120	3	0	5	171	185
1	2	4	121	128	2	5	4	64	-61	-1	8	4	35	-35	2	11	4	110	-104	4	0	5	175	-197
3	2	4	20	-22	3	5	4	138	-136	0	8	4	82	82	3	11	4	61	-57	-6	1	5	60	65
4	2	4	45	-47	4	5	4	72	71	1	8	4	79	-80	4	11	4	80	76	-5	1	5	82	-83
5	2	4	35	35	5	5	4	136	137	2	8	4	17	14	-3	12	4	24	-16	-4	1	5	93	-93
6	2	4	35	23	6	5	4	121	-126	4	8	4	13	11	-2	12	4	27	-27	-3	1	5	193	198
-5	3	4	25	24	-6	6	4	14	-9	5	8	4	23	-19	-1	12	4	13	15	-2	1	5	26	-24
-4	3	4	25	-20	-5	6	4	19	16	-5	9	4	38	34	0	12	4	75	74	-1	1	5	64	-60
-3	3	4	35	-31	-4	6	4	125	129	-4	9	4	65	-58	1	12	4	75	-71	0	1	5	135	-120
-2	3	4	41	43	-3	6	4	138	-125	-3	9	4	59	-48	2	12	4	21	-14	2	1	5	107	112
-1	3	4	87	75	-2	6	4	119	-99	-2	9	4	81	70	3	12	4	33	29	3	1	5	124	-136
0	3	4	123	-119	-1	6	4	199	184	-1	9	4	54	54	4	12	4	41	40	4	1	5	49	-51
1	3	4	49	52	0	6	4	35	35	0	9	4	30	-25	-3	13	4	17	10	5	1	5	70	74
3	3	4	63	66	1	6	4	42	-40	1	9	4	129	-127	-1	13	4	16	-20	-6	2	5	30	-32
5	3	4	64	-67	2	6	4	149	-150	2	9	4	117	112	0	13	4	31	29	-5	2	5	21	-18
6	3	4	74	77	3	6	4	109	110	3	9	4	45	44	1	13	4	29	-28	-4	2	5	38	36
-4	4	4	124	-130	4	6	4	82	81	4	9	4	74	-73	2	13	4	23	24	-3	2	5	58	59
-3	4	4	146	143	5	6	4	60	-62	5	9	4	16	-12	-3	14	4	48	-46	-2	2	5	109	-113
-2	4	4	145	132	6	6	4	64	-67	-5	10	4	105	-103	-2	14	4	43	-40	-1	2	5	37	35
-1	4	4	192	-174	-6	7	4	25	27	-4	10	4	31	-24	-1	14	4	69	70	0	2	5	21	15
0	4	4	14	10	-5	7	4	31	32	-3	10	4	72	59	1	14	4	22	-9	1	2	5	20	20
1	4	4	23	18	-4	7	4	39	-40	-2	10	4	70	61	2	14	4	62	-56	2	2	5	23	21
2	4	4	157	159	-3	7	4	58	-51	-1	10	4	56	-59	-1	15	4	62	59	3	2	5	116	-127
3	4	4	103	-105	-2	7	4	48	41	0	10	4	153	-156	0	15	4	82	-77	4	2	5	117	127
4	4	4	67	-70	-1	7	4	82	74	1	10	4	148	144	1	15	4	36	-32	5	2	5	27	-30
5	4	4	72	71	0	7	4	108	-109	2	10	4	59	56	-6	0	5	90	93	-5	3	5	26	-26
6	4	4	69	65	1	7	4	19	19	3	10	4	70	-66	-5	0	5	62	66	-4	3	5	29	31
-6	5	4	57	-58	3	7	4	56	54	4	10	4	83	-78	-4	0	5	108	-111	-3	3	5	46	-46
-5	5	4	81	-83	4	7	4	29	-27	5	10	4	63	61	-3	0	5	93	-90	-1	3	5	133	-119
-4	5	4	99	102	5	7	4	81	-81	-5	11	4	44	-42	-2	0	5	204	202	1	3	5	41	41
-3	5	4	109	109	6	7	4	64	63	-4	11	4	77	66	-1	0	5	33	30	4	3	5	26	-28
-2	5	4	159	-137	-6	8	4	44	-47	-2	11	4	83	-77	0	0	5	145	-133	5	3	5	36	35
-1	5	4	175	-160	-5	8	4	51	56	-1	11	4	51	-52	1	0	5	109	-100	-6	4	5	60	-60

H	K	L	FO	FC	H	K	L	FO	FC	H	K	L	FO	FC	H	K	L	FO	FC	H	K	L	FO	FC
-5	4	5	43	-44	-2	7	5	128	103	2	11	5	66	-65	3	2	6	57	62	3	6	6	93	-100
-4	4	5	80	80	-1	7	5	128	-112	-3	12	5	42	-35	4	2	6	15	9	-3	7	6	27	-17
-3	4	5	28	29	1	7	5	66	64	-2	12	5	80	67	-4	3	6	58	58	-2	7	6	63	-52
-2	4	5	77	-65	2	7	5	16	17	0	12	5	26	-27	-2	3	6	17	-15	1	7	6	89	96
-1	4	5	136	-120	3	7	5	38	-35	1	12	5	23	-20	-1	3	6	33	25	2	7	6	107	-114
0	4	5	171	161	4	7	5	38	-39	-2	13	5	41	-38	0	3	6	34	-31	-3	8	6	53	42
1	4	5	79	80	-5	8	5	16	13	-1	13	5	35	34	1	3	6	108	107	-2	8	6	23	14
2	4	5	160	-166	-3	8	5	36	-27	0	13	5	24	-12	2	3	6	111	-119	-1	8	6	51	-45
4	4	5	16	10	-2	8	5	69	56	-1	14	5	44	45	3	3	6	26	24	0	8	6	43	37
5	4	5	94	101	-1	8	5	36	-32	0	14	5	59	-58	4	3	6	36	40	2	8	6	27	30
-6	5	5	15	-19	2	8	5	24	-22	1	14	5	33	-31	-4	4	6	27	-28	-2	9	6	93	-77
-5	5	5	85	88	3	8	5	74	76	-4	0	6	94	-98	-3	4	6	71	-64	-1	9	6	60	-56
-4	5	5	29	27	4	8	5	72	-71	-3	0	6	168	179	-2	4	6	43	-38	0	9	6	136	130
-3	5	5	64	-57	-5	9	5	58	-52	-2	0	6	51	53	-1	4	6	85	76	1	9	6	24	-28
-2	5	5	181	-157	-4	9	5	66	-58	-1	0	6	191	-192	0	4	6	89	84	2	9	6	27	-29
-1	5	5	240	209	-3	9	5	136	113	1	0	6	147	132	1	4	6	161	-161	-1	10	6	135	122
0	5	5	66	63	-2	9	5	18	-15	2	0	6	93	91	2	4	6	31	-30	-3	0	7	19	-19
1	5	5	152	-158	-1	9	5	40	-33	3	0	6	127	-145	3	4	6	74	84	-2	0	7	74	-71
2	5	5	69	-67	1	9	5	81	81	4	0	6	30	-36	4	4	6	42	48	-1	0	7	107	-104
3	5	5	91	95	2	9	5	76	72	-4	1	6	75	75	-4	5	6	138	-134	0	0	7	207	201
4	5	5	86	91	3	9	5	84	-84	-3	1	6	72	73	-3	5	6	25	-18	1	0	7	23	17
-6	6	5	63	63	-4	10	5	95	80	-2	1	6	120	-123	-2	5	6	143	124	2	0	7	185	-193
-5	6	5	34	36	-3	10	5	82	65	-1	1	6	71	-72	-1	5	6	24	16	3	0	7	49	53
-4	6	5	102	-99	-2	10	5	145	-124	0	1	6	235	216	0	5	6	88	-80	-3	1	7	51	-53
-3	6	5	48	-37	-1	10	5	32	-29	1	1	6	54	-50	1	5	6	137	-139	-2	1	7	83	-78
-2	6	5	85	69	0	10	5	88	82	2	1	6	47	-46	2	5	6	191	208	-1	1	7	169	166
-1	6	5	140	127	1	10	5	63	62	3	1	6	78	-87	3	5	6	17	19	0	1	7	15	0
0	6	5	158	-154	2	10	5	64	-63	4	1	6	90	98	4	5	6	106	-117	1	1	7	129	-128
1	6	5	86	-88	3	10	5	106	-106	-4	2	6	69	75	-3	6	6	85	70	3	1	7	101	117
2	6	5	156	162	-4	11	5	69	61	-3	2	6	84	-83	-2	6	6	43	34	-3	2	7	28	27
3	6	5	14	-7	-3	11	5	144	-117	-2	2	6	25	-25	-1	6	6	97	-81	-2	2	7	14	-12
4	6	5	23	-22	-1	11	5	53	52	-1	2	6	109	102	0	6	6	94	-90	-1	2	7	78	77
-5	7	5	42	-43	0	11	5	69	67	0	2	6	53	-47	1	6	6	152	158	0	2	7	113	-106
-3	7	5	21	-21	1	11	5	82	-81	2	2	6	46	-48	2	6	6	17	20	2	2	7	78	86

H	K	L	FO	FC	H	K	L	FO	FC	H	K	L	FO	FC	H	K	L	FO	FC	H	K	L	FO	FC
3	2	7	47	-55	3	3	7	26	30	2	4	7	58	63	-2	6	7	174	-157	-1	7	7	17	20
-3	3	7	89	-84	-3	4	7	44	-48	-2	5	7	42	-36	-1	6	7	52	47	0	7	7	23	22
-2	3	7	49	50	-2	4	7	176	162	-1	5	7	103	-93	0	6	7	82	75	1	7	7	52	-51
-1	3	7	15	-6	-1	4	7	53	-52	0	5	7	37	-35	1	6	7	26	26	0	0	8	27	24
0	3	7	20	21	0	4	7	59	-56	1	5	7	133	134	2	6	7	67	-77	0	1	8	56	-52
1	3	7	36	-37	1	4	7	20	-19	2	5	7	21	24										

APPENDIX III

OBSERVED AND CALCULATED STRUCTURE FACTORS

FOR $Os_2(CO)_8Cl_2$

OBSERVED AND CALCULATED STRUCTURE FACTORS FOR OS2 (CO)8 CL2

H	K	L	FO	FC	H	K	L	FO	FC	H	K	L	FO	FC	H	K	L	FO	FC	H	K	L	FO	FC
2	0	0	63	63	1	6	0	104	105	11	1	1	74	75	6	6	1	42	42	2	1	2	121	120
4	0	0	172	167	2	6	0	42	42	0	2	1	60	62	7	6	1	46	44	3	1	2	171	163
6	0	0	175	170	3	6	0	103	104	1	2	1	155	152	8	6	1	25	29	4	1	2	145	141
8	0	0	86	88	4	6	0	47	48	2	2	1	123	121	0	7	1	138	138	5	1	2	58	59
10	0	0	28	25	6	6	0	92	93	3	2	1	137	135	1	7	1	41	43	6	1	2	162	160
1	1	0	334	343	8	6	0	74	70	4	2	1	263	261	2	7	1	34	37	7	1	2	71	73
4	1	0	49	50	1	7	0	124	125	5	2	1	39	38	3	7	1	144	138	8	1	2	74	75
5	1	0	55	53	4	7	0	99	106	6	2	1	43	42	4	7	1	101	97	9	1	2	67	69
7	1	0	248	254	5	7	0	21	25	7	2	1	48	47	5	7	1	88	92	10	1	2	15	14
8	1	0	15	13	6	7	0	55	55	8	2	1	47	49	6	7	1	19	20	11	1	2	16	12
11	1	0	59	64	7	7	0	108	108	10	2	1	96	96	7	7	1	61	62	0	2	2	150	158
0	2	0	439	480	8	7	0	48	50	0	3	1	100	100	0	8	1	100	102	1	2	2	181	178
1	2	0	47	50	0	8	0	154	145	1	3	1	48	47	1	8	1	43	38	2	2	2	30	31
2	2	0	29	30	1	8	0	108	106	2	3	1	109	101	2	8	1	89	92	3	2	2	38	34
3	2	0	72	73	3	8	0	114	115	3	3	1	289	284	3	8	1	64	64	4	2	2	71	68
4	2	0	98	95	5	8	0	31	34	4	3	1	162	163	4	8	1	112	110	5	2	2	87	84
6	2	0	175	178	6	8	0	75	79	5	3	1	120	123	6	8	1	45	46	6	2	2	88	87
7	2	0	15	17	7	8	0	26	29	6	3	1	70	70	7	8	1	52	54	7	2	2	192	191
8	2	0	126	125	8	8	0	52	55	7	3	1	61	62	0	9	1	67	69	8	2	2	83	86
10	2	0	32	30	1	9	0	94	94	8	3	1	60	60	1	9	1	23	24	10	2	2	46	51
1	3	0	154	157	4	9	0	62	66	9	3	1	35	35	2	9	1	45	43	0	3	2	352	363
3	3	0	37	35	6	9	0	33	31	10	3	1	61	63	3	9	1	86	89	1	3	2	131	125
4	3	0	72	71	7	9	0	61	64	0	4	1	145	146	4	9	1	45	42	2	3	2	49	48
5	3	0	31	30	0	10	0	95	92	1	4	1	139	131	5	9	1	57	57	3	3	2	136	134
6	3	0	52	52	1	10	0	59	57	2	4	1	118	122	6	9	1	35	40	4	3	2	131	125
7	3	0	227	234	2	10	0	49	51	3	4	1	177	174	7	9	1	36	39	5	3	2	100	102
8	3	0	44	45	3	10	0	61	67	4	4	1	226	228	0	10	1	64	63	6	3	2	120	112
9	3	0	27	23	1	11	0	56	56	6	4	1	41	42	1	10	1	27	26	7	3	2	86	84
10	3	0	33	34	1	0	1	213	212	7	4	1	78	79	2	10	1	53	52	8	3	2	77	78
0	4	0	488	512	2	0	1	121	117	8	4	1	46	48	3	10	1	34	33	9	3	2	74	73
1	4	0	169	175	3	0	1	293	293	10	4	1	78	77	4	10	1	58	61	0	4	2	109	114
2	4	0	60	63	4	0	1	285	285	0	5	1	101	104	0	11	1	57	60	1	4	2	165	166
3	4	0	125	120	5	0	1	36	35	1	5	1	33	35	1	11	1	33	36	2	4	2	84	95
4	4	0	115	106	7	0	1	49	51	2	5	1	44	44	3	11	1	38	41	3	4	2	53	52
5	4	0	32	34	8	0	1	59	61	3	5	1	226	223	0	0	2	199	203	4	4	2	102	102
6	4	0	149	151	10	0	1	103	102	4	5	1	122	119	1	0	2	241	238	5	4	2	78	73
7	4	0	32	26	11	0	1	40	41	5	5	1	83	85	2	0	2	174	172	6	4	2	84	83
8	4	0	86	86	0	1	1	50	49	6	5	1	41	43	3	0	2	195	190	7	4	2	163	162
10	4	0	33	32	1	1	1	80	77	7	5	1	68	69	4	0	2	36	34	8	4	2	77	79
1	5	0	236	245	2	1	1	27	22	8	5	1	46	50	5	0	2	107	104	10	4	2	47	49
3	5	0	25	21	3	1	1	356	361	9	5	1	33	31	6	0	2	55	55	0	5	2	265	273
4	5	0	79	83	4	1	1	191	186	10	5	1	45	46	7	0	2	217	218	1	5	2	150	152
5	5	0	31	32	5	1	1	87	86	0	6	1	101	99	8	0	2	69	69	2	5	2	74	74
6	5	0	49	49	6	1	1	80	81	1	6	1	89	83	9	0	2	19	22	3	5	2	135	126
7	5	0	156	158	7	1	1	53	51	2	6	1	89	95	10	0	2	34	36	4	5	2	87	86
8	5	0	46	45	8	1	1	71	70	3	6	1	99	98	11	0	2	61	62	5	5	2	44	42
10	5	0	38	40	9	1	1	19	19	4	6	1	155	161	0	1	2	427	490	6	5	2	107	111
0	6	0	307	305	10	1	1	70	73	5	6	1	54	59	1	1	2	172	170	7	5	2	53	52

OBSERVED AND CALCULATED STRUCTURE FACTORS FOR OS2 (CO)8 CL2

H	K	L	FO	FC	H	K	L	FO	FC	H	K	L	FO	FC	H	K	L	FO	FC	H	K	L	FO	FC
8	5	2	56	55	6	0	3	203	200	3	5	3	51	50	2	0	4	303	300	0	5	4	96	95
9	5	2	45	47	7	0	3	63	62	4	5	3	198	192	3	0	4	137	133	1	5	4	43	44
0	6	2	121	123	8	0	3	91	92	5	5	3	106	112	4	0	4	121	123	2	5	4	145	138
1	6	2	114	116	9	0	3	34	39	6	5	3	34	35	5	0	4	125	129	3	5	4	81	76
2	6	2	82	92	0	1	3	13	12	7	5	3	48	49	6	0	4	99	93	4	5	4	75	74
3	6	2	26	26	1	1	3	242	238	8	5	3	30	26	7	0	4	101	102	5	5	4	79	74
4	6	2	86	89	2	1	3	155	150	0	6	3	70	75	9	0	4	111	117	6	5	4	100	98
5	6	2	30	25	3	1	3	109	105	1	6	3	34	32	0	1	4	120	116	7	5	4	76	76
6	6	2	71	73	4	1	3	294	295	2	6	3	75	74	1	1	4	57	54	8	5	4	99	99
7	6	2	101	104	5	1	3	136	139	3	6	3	190	182	2	1	4	212	205	9	5	4	37	39
8	6	2	65	68	6	1	3	27	26	4	6	3	15	20	3	1	4	145	141	0	6	4	59	63
0	7	2	147	141	7	1	3	38	36	5	6	3	94	99	4	1	4	42	44	1	6	4	156	148
1	7	2	133	132	8	1	3	58	60	6	6	3	79	79	5	1	4	127	130	2	6	4	73	71
2	7	2	50	50	9	1	3	25	26	7	6	3	66	69	6	1	4	112	116	3	6	4	89	86
3	7	2	113	110	10	1	3	82	80	8	6	3	34	38	7	1	4	116	119	4	6	4	37	32
4	7	2	25	24	0	2	3	29	32	9	6	3	37	39	8	1	4	108	109	5	6	4	71	70
5	7	2	48	49	1	2	3	41	37	0	7	3	83	83	9	1	4	76	76	6	6	4	41	42
6	7	2	62	61	2	2	3	149	138	1	7	3	67	64	10	1	4	55	61	7	6	4	69	70
7	7	2	53	53	3	2	3	267	266	2	7	3	141	140	0	2	4	108	102	8	6	4	16	17
8	7	2	46	47	4	2	3	44	43	3	7	3	30	31	1	2	4	328	329	9	6	4	69	68
0	8	2	55	57	5	2	3	100	98	4	7	3	130	121	2	2	4	99	91	0	7	4	131	132
1	8	2	94	93	6	2	3	143	142	5	7	3	51	48	3	2	4	106	99	1	7	4	55	53
2	8	2	37	41	7	2	3	60	63	6	7	3	46	46	4	2	4	119	122	2	7	4	113	109
4	8	2	73	77	8	2	3	75	77	7	7	3	52	57	5	2	4	108	106	3	7	4	21	20
5	8	2	18	21	0	3	3	136	136	0	8	3	85	88	6	2	4	40	39	4	7	4	74	72
6	8	2	60	64	1	3	3	234	229	1	8	3	26	21	7	2	4	82	78	5	7	4	45	43
7	8	2	64	65	2	3	3	122	116	2	8	3	44	47	9	2	4	98	99	6	7	4	86	87
8	8	2	60	66	4	3	3	241	234	3	8	3	109	106	10	2	4	24	28	7	7	4	28	28
0	9	2	104	103	5	3	3	98	100	4	8	3	43	42	0	3	4	215	225	8	7	4	77	78
1	9	2	82	86	6	3	3	38	39	5	8	3	82	80	1	3	4	99	90	0	8	4	37	40
2	9	2	25	17	7	3	3	36	36	6	8	3	51	50	2	3	4	230	230	1	8	4	138	138
3	9	2	85	85	8	3	3	45	45	7	8	3	44	45	3	3	4	79	72	2	8	4	34	34
5	9	2	28	30	9	3	3	25	28	0	9	3	73	72	4	3	4	56	54	3	8	4	95	93
6	9	2	44	46	10	3	3	71	71	1	9	3	58	59	5	3	4	145	144	4	8	4	30	32
7	9	2	36	38	0	4	3	100	101	2	9	3	72	69	6	3	4	112	109	5	8	4	64	61
0	10	2	60	62	1	4	3	42	43	4	9	3	92	91	7	3	4	79	80	6	8	4	39	37
1	10	2	42	42	2	4	3	104	101	5	9	3	41	42	8	3	4	89	95	7	8	4	50	50
2	10	2	48	46	3	4	3	243	237	6	9	3	32	31	9	3	4	63	64	0	9	4	74	74
4	10	2	57	57	4	4	3	66	69	0	10	3	57	59	10	3	4	52	57	1	9	4	33	32
5	10	2	22	22	5	4	3	113	114	1	10	3	20	23	0	4	4	138	142	2	9	4	72	72
1	11	2	58	61	6	4	3	130	128	2	10	3	20	23	1	4	4	224	211	4	9	4	42	43
2	11	2	39	40	7	4	3	59	61	3	10	3	67	65	2	4	4	159	151	5	9	4	34	37
3	11	2	52	53	8	4	3	68	69	4	10	3	30	32	3	4	4	144	137	6	9	4	58	61
1	0	3	58	54	9	4	3	50	54	5	10	3	64	63	4	4	4	126	120	1	10	4	72	73
2	0	3	80	80	10	4	3	23	24	0	11	3	34	31	5	4	4	102	105	2	10	4	23	28
3	0	3	357	365	0	5	3	83	80	2	11	3	58	60	6	4	4	58	59	3	10	4	44	42
4	0	3	109	105	1	5	3	158	149	0	0	4	231	229	7	4	4	79	80	5	10	4	34	31
5	0	3	94	92	2	5	3	122	118	1	0	4	173	173	9	4	4	88	87	0	11	4	53	56

OBSERVED AND CALCULATED STRUCTURE FACTORS FOR OS2 (CO)8 CL2

H	K	L	FO	FC	H	K	L	FO	FC	H	K	L	FO	FC	H	K	L	FO	FC	H	K	L	FO	FC
1	0	5	364	364	9	4	5	39	43	0	0	6	70	71	8	4	6	75	73	5	0	7	67	68
3	0	5	28	27	10	4	5	36	37	2	0	6	216	208	9	4	6	94	92	6	0	7	199	204
4	0	5	141	137	0	5	5	46	45	3	0	6	100	92	0	5	6	35	37	8	0	7	84	90
5	0	5	251	254	1	5	5	58	53	4	0	6	62	61	1	5	6	136	131	0	1	7	26	24
6	0	5	19	14	2	5	5	145	141	5	0	6	189	193	2	5	6	157	149	1	1	7	254	248
8	0	5	51	51	3	5	5	106	102	6	0	6	67	62	3	5	6	68	66	2	1	7	77	75
9	0	5	49	52	4	5	5	71	70	7	0	6	29	28	4	5	6	97	93	3	1	7	25	25
10	0	5	40	42	5	5	5	61	63	8	0	6	79	79	5	5	6	88	83	4	1	7	26	25
0	1	5	34	33	6	5	5	132	135	9	0	6	134	135	6	5	6	46	47	5	1	7	217	221
1	1	5	85	83	7	5	5	46	48	10	0	6	46	46	7	5	6	39	38	6	1	7	56	55
2	1	5	198	194	8	5	5	62	60	0	1	6	92	89	8	5	6	60	63	7	1	7	29	27
3	1	5	144	139	9	5	5	42	44	1	1	6	142	135	9	5	6	59	62	8	1	7	36	34
4	1	5	67	69	0	6	5	73	71	2	1	6	271	266	0	6	6	56	57	9	1	7	45	47
5	1	5	54	52	1	6	5	136	127	3	1	6	81	73	1	6	6	74	77	0	2	7	19	18
6	1	5	210	215	2	6	5	85	85	4	1	6	112	114	2	6	6	108	107	1	2	7	57	54
7	1	5	32	32	3	6	5	65	62	5	1	6	113	113	3	6	6	59	58	2	2	7	200	194
8	1	5	88	95	4	6	5	91	86	7	1	6	42	41	4	6	6	54	52	3	2	7	36	30
9	1	5	22	25	5	6	5	122	116	8	1	6	70	72	5	6	6	83	79	4	2	7	76	71
0	2	5	38	36	7	6	5	47	46	9	1	6	80	84	6	6	6	75	79	5	2	7	66	68
1	2	5	240	236	9	6	5	29	32	10	1	6	47	50	8	6	6	66	64	6	2	7	167	171
2	2	5	70	68	0	7	5	40	44	0	2	6	88	90	0	7	6	45	45	7	2	7	23	22
3	2	5	52	50	2	7	5	100	96	1	2	6	114	114	1	7	6	128	123	8	2	7	76	80
4	2	5	119	114	3	7	5	77	77	2	2	6	180	173	2	7	6	93	92	0	3	7	54	53
5	2	5	188	189	4	7	5	69	66	3	2	6	135	127	3	7	6	71	69	1	3	7	219	217
6	2	5	15	18	5	7	5	88	88	4	2	6	53	52	5	7	6	63	62	2	3	7	125	120
7	2	5	32	35	6	7	5	86	85	5	2	6	125	121	6	7	6	51	50	3	3	7	63	59
8	2	5	45	44	7	7	5	36	34	6	2	6	48	49	7	7	6	31	30	4	3	7	63	61
9	2	5	50	51	8	7	5	20	26	8	2	6	67	66	8	7	6	40	40	5	3	7	189	177
10	2	5	40	42	0	8	5	66	61	9	2	6	103	107	0	8	6	48	51	6	3	7	47	47
0	3	5	76	76	1	8	5	63	63	10	2	6	39	42	1	8	6	78	83	7	3	7	30	31
1	3	5	42	38	2	8	5	104	103	0	3	6	22	19	2	8	6	72	75	8	3	7	35	31
2	3	5	195	195	3	8	5	46	44	1	3	6	185	173	3	8	6	49	47	9	3	7	46	45
3	3	5	133	130	4	8	5	71	72	2	3	6	256	251	5	8	6	44	48	1	4	7	84	81
4	3	5	64	60	5	8	5	89	88	3	3	6	108	105	6	8	6	67	65	2	4	7	196	186
5	3	5	51	47	7	8	5	32	32	4	3	6	61	59	0	9	6	28	27	3	4	7	68	66
6	3	5	172	170	0	9	5	50	53	5	3	6	109	105	1	9	6	80	82	4	4	7	53	48
7	3	5	49	49	1	9	5	19	24	6	3	6	42	45	2	9	6	61	60	5	4	7	82	80
8	3	5	76	80	2	9	5	57	61	7	3	6	26	26	3	9	6	40	40	6	4	7	148	144
9	3	5	39	40	3	9	5	68	64	8	3	6	48	49	4	9	6	20	21	7	4	7	31	32
0	4	5	87	84	4	9	5	56	56	9	3	6	65	68	5	9	6	48	48	8	4	7	68	69
1	4	5	234	230	5	9	5	47	44	10	3	6	30	37	6	9	6	36	33	0	5	7	41	44
2	4	5	146	140	6	9	5	48	49	0	4	6	36	38	0	10	6	38	42	1	5	7	166	165
3	4	5	18	18	0	10	5	29	25	1	4	6	107	110	1	10	6	50	47	2	5	7	107	104
4	4	5	107	102	1	10	5	36	39	2	4	6	170	173	2	10	6	46	45	3	5	7	32	27
5	4	5	181	189	2	10	5	67	68	3	4	6	92	89	0	11	6	42	40	4	5	7	61	61
6	4	5	33	36	3	10	5	44	47	4	4	6	56	51	1	11	6	54	56	5	5	7	148	141
7	4	5	29	29	5	10	5	52	48	5	4	6	136	130	1	0	7	131	126	6	5	7	33	32
8	4	5	33	29	2	11	5	31	32	6	4	6	71	73	2	0	7	235	228	7	5	7	17	16

OBSERVED AND CALCULATED STRUCTURE FACTORS FOR OS2 (CO)8 CL2

H	K	L	FO	FC	H	K	L	FO	FC	H	K	L	FO	FC	H	K	L	FO	FC	H	K	L	FO	FC
9	5	7	30	34	4	1	8	58	55	3	6	8	42	43	6	2	9	78	74	1	10	9	26	21
0	6	7	31	31	5	1	8	157	151	4	6	8	48	45	1	3	9	68	67	2	10	9	54	51
1	6	7	38	35	6	1	8	45	45	5	6	8	53	48	2	3	9	109	106	0	0	10	232	241
2	6	7	107	100	7	1	8	24	20	6	6	8	54	55	3	3	9	123	111	1	0	10	99	99
3	6	7	56	53	9	1	8	120	121	8	6	8	69	67	4	3	9	42	36	2	0	10	53	52
4	6	7	57	56	10	1	8	16	16	0	7	8	28	31	5	3	9	131	121	3	0	10	140	129
5	6	7	83	79	0	2	8	43	42	1	7	8	96	96	6	3	9	104	103	4	0	10	63	59
6	6	7	92	94	1	2	8	58	55	2	7	8	49	51	7	3	9	32	32	5	0	10	84	77
7	6	7	33	35	2	2	8	237	240	3	7	8	68	66	8	3	9	65	64	6	0	10	66	64
8	6	7	36	35	3	2	8	26	26	4	7	8	28	25	9	3	9	38	41	7	0	10	22	21
0	7	7	83	84	4	2	8	68	63	5	7	8	54	53	0	4	9	112	110	8	0	10	49	53
1	7	7	60	63	5	2	8	77	75	6	7	8	63	59	1	4	9	168	166	9	0	10	81	81
2	7	7	104	102	6	2	8	59	60	7	7	8	36	37	2	4	9	128	125	1	1	10	124	119
3	7	7	57	56	7	2	8	26	31	0	8	8	46	48	3	4	9	50	46	2	1	10	206	205
4	7	7	63	62	8	2	8	90	93	1	8	8	80	83	4	4	9	125	120	4	1	10	86	80
5	7	7	100	95	9	2	8	33	40	2	8	8	81	78	5	4	9	99	92	5	1	10	28	27
6	7	7	25	24	0	3	8	99	102	3	8	8	40	39	6	4	9	60	58	7	1	10	106	108
7	7	7	23	24	1	3	8	131	135	4	8	8	29	28	8	4	9	25	18	8	1	10	58	60
0	8	7	18	15	2	3	8	66	66	5	8	8	60	56	1	5	9	55	54	0	2	10	157	163
1	8	7	28	29	3	3	8	140	132	6	8	8	43	41	2	5	9	87	81	1	2	10	57	60
2	8	7	80	77	4	3	8	79	76	1	9	8	69	70	3	5	9	86	82	2	2	10	36	30
3	8	7	58	56	5	3	8	133	124	2	9	8	39	40	5	5	9	98	93	3	2	10	88	85
4	8	7	62	62	6	3	8	42	41	3	9	8	40	37	6	5	9	87	81	4	2	10	39	33
5	8	7	59	58	7	3	8	23	23	5	9	8	41	39	7	5	9	39	41	5	2	10	105	96
6	8	7	67	65	8	3	8	35	36	0	10	8	49	50	8	5	9	45	44	6	2	10	66	64
7	8	7	20	29	9	3	8	100	102	1	10	8	51	52	0	6	9	48	47	8	2	10	54	55
0	9	7	32	31	0	4	8	47	44	2	10	8	49	45	1	6	9	79	76	9	2	10	80	83
1	9	7	57	61	1	4	8	96	94	1	0	9	249	251	2	6	9	114	112	1	3	10	119	118
2	9	7	85	85	2	4	8	233	228	2	0	9	130	128	3	6	9	22	15	2	3	10	134	138
3	9	7	52	50	3	4	8	72	68	3	0	9	107	102	4	6	9	87	81	3	3	10	48	47
4	9	7	43	42	4	4	8	101	92	4	0	9	112	109	5	6	9	59	56	4	3	10	95	85
5	9	7	68	61	5	4	8	81	75	5	0	9	127	123	6	6	9	53	48	5	3	10	51	50
2	10	7	46	46	6	4	8	46	44	6	0	9	74	72	1	7	9	28	33	6	3	10	48	45
3	10	7	44	42	7	4	8	35	37	8	0	9	24	12	2	7	9	41	41	7	3	10	101	97
4	10	7	46	45	8	4	8	89	88	1	1	9	72	68	3	7	9	95	98	8	3	10	71	66
2	0	8	323	321	9	4	8	28	28	2	1	9	111	106	5	7	9	79	76	0	4	10	151	157
3	0	8	129	117	0	5	8	35	34	3	1	9	112	109	6	7	9	42	43	1	4	10	85	92
4	0	8	142	129	1	5	8	133	130	4	1	9	51	48	7	7	9	47	48	2	4	10	45	40
5	0	8	55	56	2	5	8	93	95	5	1	9	122	117	0	8	9	70	70	3	4	10	83	82
6	0	8	41	38	3	5	8	94	90	6	1	9	130	126	1	8	9	40	43	4	4	10	53	52
7	0	8	57	61	4	5	8	40	37	7	1	9	23	24	2	8	9	101	97	5	4	10	79	78
8	0	8	106	111	5	5	8	100	95	8	1	9	75	78	4	8	9	86	81	6	4	10	69	64
9	0	8	30	30	6	5	8	68	66	9	1	9	26	25	5	8	9	34	35	8	4	10	59	53
10	0	8	48	52	7	5	8	29	30	1	2	9	142	141	6	8	9	36	37	1	5	10	105	102
0	1	8	85	81	8	5	8	34	29	2	2	9	136	135	1	9	9	28	30	2	5	10	143	139
1	1	8	138	140	0	6	8	52	49	3	2	9	54	52	2	9	9	30	37	3	5	10	37	34
2	1	8	127	122	1	6	8	81	81	4	2	9	122	118	3	9	9	57	54	4	5	10	63	59
3	1	8	148	138	2	6	8	144	135	5	2	9	112	100	0	10	9	40	46	5	5	10	41	35

OBSERVED AND CALCULATED STRUCTURE FACTORS FOR OS2 (CO)8 CL2

H	K	L	FO	FC	H	K	L	FO	FC	H	K	L	FO	FC	H	K	L	FO	FC	H	K	L	FO	FC
7	5	10	77	74	2	3	11	93	93	4	1	12	58	55	4	0	13	68	62	0	1	14	103	113
8	5	10	51	51	3	3	11	119	116	5	1	12	55	52	7	0	13	36	37	1	1	14	77	82
0	6	10	112	117	4	3	11	123	117	6	1	12	84	77	1	1	13	18	22	3	1	14	25	27
1	6	10	71	71	6	3	11	60	56	7	1	12	46	43	2	1	13	33	33	4	1	14	40	39
2	6	10	35	33	7	3	11	23	22	8	1	12	58	59	3	1	13	51	50	5	1	14	36	32
3	6	10	79	78	1	4	11	40	40	0	2	12	51	51	4	1	13	161	156	6	1	14	57	50
4	6	10	31	23	2	4	11	28	26	1	2	12	129	130	5	1	13	33	31	7	1	14	101	97
5	6	10	41	38	3	4	11	97	97	2	2	12	73	72	6	1	13	40	37	0	2	14	140	150
6	6	10	58	55	4	4	11	91	89	3	2	12	29	21	8	1	13	52	53	1	2	14	55	55
7	6	10	19	14	5	4	11	100	89	4	2	12	50	46	0	2	13	38	38	3	2	14	28	29
0	7	10	24	29	6	4	11	51	48	7	2	12	127	127	1	2	13	44	47	4	2	14	59	60
1	7	10	89	89	7	4	11	50	54	8	2	12	26	23	3	2	13	153	151	6	2	14	44	44
2	7	10	62	61	8	4	11	56	52	0	3	12	170	182	4	2	13	57	53	7	2	14	72	65
3	7	10	40	37	0	5	11	62	62	1	3	12	33	31	7	2	13	36	31	0	3	14	74	77
4	7	10	52	50	1	5	11	86	86	3	3	12	60	58	3	3	13	53	53	1	3	14	82	86
5	7	10	44	43	2	5	11	85	87	5	3	12	41	35	4	3	13	132	128	3	3	14	31	30
6	7	10	42	40	3	5	11	99	94	6	3	12	81	77	5	3	13	37	37	4	3	14	36	32
0	8	10	59	59	4	5	11	102	98	7	3	12	47	43	7	3	13	37	39	5	3	14	43	44
1	8	10	56	55	5	5	11	21	20	8	3	12	68	69	0	4	13	51	58	6	3	14	59	52
2	8	10	29	33	6	5	11	59	52	0	4	12	58	60	1	4	13	63	66	0	4	14	112	121
3	8	10	45	47	0	6	11	35	37	1	4	12	111	114	2	4	13	55	55	1	4	14	60	66
5	8	10	41	38	1	6	11	35	36	2	4	12	66	62	3	4	13	145	141	2	4	14	25	24
0	9	10	23	27	3	6	11	84	85	3	4	12	38	38	4	4	13	57	58	3	4	14	42	44
1	9	10	60	62	4	6	11	55	55	4	4	12	70	65	5	4	13	18	21	4	4	14	57	54
2	9	10	48	47	5	6	11	81	79	5	4	12	28	30	6	4	13	27	32	6	4	14	53	51
1	0	11	47	50	6	6	11	25	25	6	4	12	31	29	7	4	13	31	33	0	5	14	76	82
2	0	11	39	38	7	6	11	48	45	7	4	12	109	105	1	5	13	24	28	1	5	14	50	53
3	0	11	115	114	0	7	11	84	86	0	5	12	149	155	2	5	13	29	30	3	5	14	29	26
4	0	11	143	128	1	7	11	40	43	1	5	12	35	40	3	5	13	43	43	4	5	14	40	42
5	0	11	107	104	2	7	11	74	79	3	5	12	45	48	4	5	13	111	107	5	5	14	19	15
6	0	11	81	80	3	7	11	47	48	4	5	12	48	47	5	5	13	40	41	0	6	14	75	86
8	0	11	68	71	4	7	11	79	79	5	5	12	37	35	0	6	13	75	79	1	6	14	54	56
0	1	11	24	25	6	7	11	39	33	6	5	12	62	60	2	6	13	31	31	3	6	14	45	45
1	1	11	142	147	3	8	11	58	57	7	5	12	22	19	3	6	13	98	96	4	6	14	19	24
2	1	11	82	86	4	8	11	36	36	0	6	12	29	31	4	6	13	50	52	0	7	14	35	40
3	1	11	154	152	0	9	11	51	53	1	6	12	97	97	1	7	13	30	34	1	7	14	48	53
4	1	11	130	125	2	9	11	57	55	2	6	12	33	30	2	7	13	33	33	2	7	14	23	19
5	1	11	37	35	3	9	11	32	31	3	6	12	28	27	3	7	13	33	36	1	0	15	48	47
6	1	11	65	62	0	0	12	106	110	4	6	12	51	53	4	7	13	61	61	2	0	15	21	21
1	2	11	48	51	1	0	12	170	169	6	6	12	34	30	0	8	13	60	63	4	0	15	131	130
3	2	11	106	106	2	0	12	83	82	0	7	12	90	95	2	8	13	45	47	6	0	15	33	24
4	2	11	100	95	3	0	12	20	9	1	7	12	42	42	0	0	14	162	173	1	1	15	51	56
5	2	11	91	90	4	0	12	84	76	3	7	12	49	52	1	0	14	68	72	2	1	15	31	30
6	2	11	58	57	5	0	12	48	48	1	8	12	68	69	2	0	14	57	56	3	1	15	146	148
7	2	11	31	30	6	0	12	17	19	4	8	12	46	41	4	0	14	55	53	6	1	15	28	31
8	2	11	61	63	7	0	12	126	128	0	9	12	63	63	5	0	14	25	27	1	2	15	30	32
0	3	11	70	71	0	1	12	217	234	1	0	13	90	90	6	0	14	69	69	2	2	15	24	27
1	3	11	108	106	3	1	12	41	37	3	0	13	203	202	7	0	14	67	63	3	2	15	24	21

OBSERVED AND CALCULATED STRUCTURE FACTORS FOR OS2 (CO)8 CL2

H	K	L	FO	FC	H	K	L	FO	FC	H	K	L	FO	FC	H	K	L	FO	FC	H	K	L	FO	FC
4	2	15	115	114	3	5	15	97	97	4	1	16	53	49	0	5	16	52	58	1	3	17	45	51
5	2	15	24	23	4	5	15	29	28	0	2	16	100	109	1	5	16	60	62	4	3	17	57	51
0	3	15	53	58	0	6	15	18	9	1	2	16	20	18	2	5	16	42	44	0	4	17	40	43
1	3	15	38	42	1	6	15	19	22	2	2	16	31	33	3	5	16	34	37	1	4	17	43	47
2	3	15	37	37	2	6	15	36	34	3	2	16	33	30	0	6	16	56	56	2	4	17	50	55
3	3	15	116	118	3	6	15	29	29	5	2	16	44	41	1	0	17	68	70	3	4	17	60	63
4	3	15	34	36	0	7	15	48	52	0	3	16	64	73	2	0	17	52	54	0	0	18	51	59
1	4	15	42	45	0	0	16	102	112	1	3	16	77	83	3	0	17	83	84	1	0	18	33	37
2	4	15	20	24	3	0	16	43	47	2	3	16	53	55	1	1	17	52	52	2	0	18	75	77
4	4	15	101	99	5	0	16	50	47	3	3	16	41	35	4	1	17	60	59	0	1	18	59	65
5	4	15	37	34	6	0	16	69	68	4	3	16	44	47	1	2	17	50	53	3	1	18	43	42
0	5	15	52	60	0	1	16	84	92	0	4	16	89	93	2	2	17	48	50	1	2	18	38	41
1	5	15	28	30	1	1	16	65	72	3	4	16	32	33	3	2	17	59	62	2	2	18	69	73
2	5	15	30	33	2	1	16	74	77	4	4	16	29	30	4	2	17	34	31	0	3	18	52	57

APPENDIX IV

OBSERVED AND CALCULATED STRUCTURE FACTORS

FOR $Os_2(CO)_8I_2$

H	K	L	FO	FC	H	K	L	FO	FC	H	K	L	FO	FC	H	K	L	FO	FC	H	K	L	FO	FC
0	2	0	380	371	1	4	1	165	162	1	5	2	67	61	4	5	3	65	57	0	6	4	344	353
2	2	0	147	172	3	4	1	194	193	3	5	2	458	466	1	6	3	237	249	2	6	4	115	106
1	3	0	552	574	2	5	1	345	371	5	5	2	556	560	3	6	3	400	411	4	6	4	273	287
0	4	0	279	283	4	5	1	185	184	0	6	2	277	281	5	6	3	295	311	6	6	4	148	143
2	4	0	194	198	1	6	1	324	336	2	6	2	150	154	2	7	3	247	237	1	7	4	123	131
4	4	0	975	1016	3	6	1	188	188	4	6	2	171	184	4	7	3	157	161	3	7	4	298	324
1	5	0	734	740	5	6	1	290	291	1	7	2	323	338	6	7	3	133	146	5	7	4	268	288
3	5	0	80	87	2	7	1	113	126	3	7	2	97	93	1	8	3	86	67	0	8	4	544	539
0	6	0	129	143	6	7	1	269	271	5	7	2	93	112	3	8	3	264	259	2	8	4	273	281
2	6	0	52	51	1	8	1	229	232	7	7	2	223	200	5	8	3	217	210	4	8	4	78	71
4	6	0	209	210	5	8	1	124	112	0	8	2	161	152	2	9	3	258	249	6	8	4	158	154
6	6	0	154	141	7	8	1	135	115	2	8	2	226	215	6	9	3	172	180	8	8	4	218	230
1	7	0	196	182	2	9	1	282	286	4	8	2	497	500	8	9	3	79	84	1	9	4	91	92
3	7	0	286	291	4	9	1	96	95	6	8	2	170	185	1	10	3	192	189	3	9	4	253	256
5	7	0	206	200	6	9	1	223	233	1	9	2	387	374	3	10	3	152	143	5	9	4	257	267
0	8	0	729	707	8	9	1	107	120	7	9	2	131	129	5	10	3	151	169	0	10	4	97	82
2	8	0	274	273	1	10	1	207	201	9	9	2	211	187	7	10	3	215	211	2	10	4	115	102
8	8	0	270	253	3	10	1	228	241	0	10	2	127	113	9	10	3	154	137	4	10	4	120	109
3	9	0	288	274	5	10	1	156	163	4	10	2	142	118	2	11	3	146	149	8	10	4	77	62
5	9	0	358	339	7	10	1	175	177	1	11	2	146	139	4	11	3	76	47	1	11	4	163	157
0	10	0	160	148	9	10	1	118	121	3	11	2	127	115	6	11	3	185	178	3	11	4	94	84
2	10	0	62	60	2	11	1	158	161	5	11	2	81	80	8	11	3	105	81	5	11	4	67	71
1	11	0	89	78	6	11	1	140	158	0	12	2	226	198	1	12	3	155	150	7	11	4	84	80
3	11	0	132	124	3	12	1	126	104	2	12	2	182	176	7	12	3	113	96	0	12	4	133	142
5	11	0	108	107	5	12	1	116	111	4	12	2	119	111	2	13	3	149	146	2	12	4	159	147
7	11	0	104	89	7	12	1	77	38	6	12	2	80	80	0	0	4	1372	1421	4	12	4	162	157
0	12	0	177	161	2	13	1	178	147	1	13	2	87	83	0	2	4	465	452	6	12	4	114	110
2	12	0	157	155	4	13	1	88	53	3	13	2	132	112	2	2	4	208	199	1	13	4	108	127
4	12	0	179	159	1	1	2	893	874	5	13	2	125	123	1	3	4	593	580	1	2	5	318	296
6	12	0	103	112	0	2	2	329	327	1	2	3	446	437	0	4	4	106	121	2	3	5	406	372
1	13	0	181	163	1	3	2	144	134	2	3	3	238	221	2	4	4	408	404	1	4	5	150	144
0	14	0	101	57	3	3	2	434	432	1	4	3	346	326	4	4	4	881	919	3	4	5	312	297
1	2	1	310	326	0	4	2	1398	1441	3	4	3	90	76	1	5	4	555	552	2	5	5	323	323
2	3	1	363	386	2	4	2	302	311	2	5	3	354	373	3	5	4	92	105	4	5	5	219	207

H	K	L	FO	FC	H	K	L	FO	FC	H	K	L	FO	FC	H	K	L	FO	FC	H	K	L	FO	FC
1	6	5	363	373	4	6	6	308	308	4	9	7	102	88	3	9	8	202	206	1	12	9	115	122
5	6	5	219	211	1	7	6	420	425	6	9	7	149	164	5	9	8	115	103	3	12	9	143	151
2	7	5	207	199	7	7	6	206	198	1	10	7	139	128	7	9	8	84	79	5	12	9	86	96
4	7	5	101	106	0	8	6	123	133	3	10	7	95	67	2	10	8	105	101	2	13	9	125	110
6	7	5	303	310	2	8	6	302	304	5	10	7	124	133	4	10	8	122	106	1	1	10	529	520
1	8	5	292	293	4	8	6	350	363	7	10	7	167	163	1	11	8	182	188	0	2	10	738	725
3	8	5	115	118	6	8	6	174	170	9	10	7	122	134	0	12	8	141	137	1	3	10	81	81
5	8	5	82	65	1	9	6	212	217	2	11	7	149	155	2	12	8	144	143	3	3	10	528	519
7	8	5	201	200	3	9	6	120	133	4	11	7	87	61	4	12	8	139	145	0	4	10	359	368
2	9	5	218	212	7	9	6	172	171	6	11	7	159	158	1	2	9	122	124	2	4	10	485	474
4	9	5	69	45	9	9	6	101	107	1	12	7	166	155	2	3	9	307	297	1	5	10	119	119
6	9	5	221	222	0	10	6	161	158	3	12	7	118	118	1	4	9	171	168	3	5	10	391	396
8	9	5	119	112	3	11	6	137	135	5	12	7	83	61	3	4	9	223	228	5	5	10	215	217
1	10	5	140	134	5	11	6	151	152	2	13	7	140	120	2	5	9	102	107	0	6	10	324	302
3	10	5	213	205	0	12	6	195	193	0	0	8	743	717	4	5	9	144	146	2	6	10	139	142
5	10	5	138	145	2	12	6	162	159	0	2	8	703	683	1	6	9	171	160	4	6	10	355	351
7	10	5	103	100	6	12	6	102	85	2	2	8	137	117	3	6	9	175	181	1	7	10	396	394
2	11	5	167	170	1	13	6	119	119	1	3	8	593	570	5	6	9	110	109	5	7	10	95	62
4	11	5	108	93	1	2	7	449	414	0	4	8	96	82	2	7	9	271	275	7	7	10	165	153
6	11	5	122	123	2	3	7	184	173	2	4	8	611	596	4	7	9	118	124	0	8	10	137	144
3	12	5	193	164	1	4	7	302	300	4	4	8	418	400	6	7	9	219	218	2	8	10	300	304
5	12	5	125	122	3	4	7	168	162	1	5	8	371	372	1	8	9	254	260	4	8	10	230	224
2	13	5	160	141	2	5	7	150	139	3	5	8	152	151	3	8	9	201	209	6	8	10	133	144
1	1	6	551	518	4	5	7	65	70	0	6	8	425	428	5	8	9	112	114	1	9	10	151	153
0	2	6	778	761	3	6	7	271	266	2	6	8	79	84	7	8	9	203	205	3	9	10	128	134
1	3	6	101	90	5	6	7	229	224	4	6	8	242	239	2	9	9	151	157	5	9	10	86	87
3	3	6	549	539	2	7	7	328	340	6	6	8	155	153	6	9	9	167	179	7	9	10	158	154
0	4	6	790	776	4	7	7	183	190	3	7	8	362	360	1	10	9	93	78	0	10	10	121	116
2	4	6	505	491	6	7	7	175	172	5	7	8	334	333	3	10	9	103	105	6	10	10	83	78
1	5	6	100	108	1	8	7	183	180	0	8	8	322	327	5	10	9	121	118	3	11	10	143	136
3	5	6	476	461	3	8	7	281	297	2	8	8	292	306	7	10	9	105	110	5	11	10	138	152
5	5	6	362	367	5	8	7	183	184	6	8	8	191	198	2	11	9	190	176	0	12	10	162	147
0	6	6	277	281	7	8	7	128	142	8	8	8	140	157	4	11	9	91	92	2	12	10	141	135
2	6	6	192	183	2	9	7	214	220	1	9	8	138	155	6	11	9	128	134	4	12	10	120	108

H	K	L	FO	FC	H	K	L	FO	FC	H	K	L	FO	FC	H	K	L	FO	FC	H	K	L	FO	FC
1	13	10	120	124	3	5	12	98	103	5	8	13	119	134	0	12	14	105	105	4	8	16	86	72
1	2	11	97	98	0	6	12	374	358	7	8	13	117	108	1	2	15	61	62	6	8	16	117	106
2	3	11	321	324	2	6	12	72	69	2	9	13	107	119	2	3	15	214	214	8	8	16	93	118
1	4	11	192	192	4	6	12	220	211	6	9	13	120	109	1	4	15	61	64	3	9	16	150	156
3	4	11	165	168	6	6	12	106	109	1	10	13	96	104	3	4	15	113	118	5	9	16	147	170
2	5	11	76	85	3	7	12	281	273	5	10	13	90	99	2	5	15	170	172	0	10	16	98	96
4	5	11	86	91	5	7	12	259	257	7	10	13	124	136	4	5	15	103	115	1	2	17	175	173
1	6	11	160	151	0	8	12	225	237	2	11	13	156	156	1	6	15	180	187	2	3	17	54	38
3	6	11	136	133	2	8	12	239	246	1	12	13	103	115	5	6	15	108	110	1	4	17	98	113
5	6	11	127	117	4	8	12	89	99	3	12	13	102	98	2	7	15	151	150	2	5	17	138	135
2	7	11	243	234	6	8	12	182	176	1	1	14	443	435	6	7	15	192	210	1	6	17	91	93
4	7	11	138	143	8	8	12	113	115	0	2	14	466	449	1	8	15	148	156	3	6	17	162	168
6	7	11	207	217	1	9	12	115	116	3	3	14	372	355	3	8	15	79	68	5	6	17	152	151
1	8	11	192	202	3	9	12	166	180	0	4	14	523	516	7	8	15	77	86	2	7	17	158	169
3	8	11	197	203	5	9	12	124	132	2	4	14	326	310	2	9	15	107	115	6	7	17	83	111
5	8	11	126	124	0	10	12	93	82	3	5	14	334	325	6	9	15	120	129	3	8	17	84	97
7	8	11	132	134	4	10	12	108	112	5	5	14	296	289	1	10	15	100	99	5	8	17	111	116
2	9	11	117	115	1	11	12	164	158	0	6	14	215	209	3	10	15	131	137	2	9	17	134	136
6	9	11	136	132	3	11	12	72	42	2	6	14	97	96	5	10	15	124	104	6	9	17	99	95
1	10	11	63	81	0	12	12	143	144	4	6	14	230	233	2	11	15	153	150	1	10	17	118	111
3	10	11	101	121	2	12	12	113	128	1	7	14	252	252	0	0	16	750	732	3	10	17	76	104
5	10	11	133	114	4	12	12	98	102	7	7	14	123	123	0	2	16	299	273	1	1	18	362	342
7	10	11	89	90	1	2	13	211	215	0	8	14	162	146	1	3	16	340	316	0	2	18	194	180
2	11	11	172	174	2	3	13	189	182	2	8	14	219	217	0	4	16	62	53	3	3	18	239	233
6	11	11	117	128	1	4	13	166	173	4	8	14	206	214	2	4	16	251	244	0	4	18	517	523
1	12	11	111	116	3	4	13	135	127	6	8	14	103	110	4	4	16	415	433	2	4	18	165	162
3	12	11	141	129	1	6	13	79	65	1	9	14	197	200	1	5	16	347	349	3	5	18	208	234
0	0	12	499	484	3	6	13	253	260	3	9	14	84	68	0	6	16	178	185	5	5	18	255	272
0	2	12	528	504	5	6	13	138	138	5	9	14	71	45	4	6	16	130	142	0	6	18	156	155
2	2	12	50	75	2	7	13	224	235	7	9	14	92	109	1	7	16	83	72	4	6	18	95	103
1	3	12	491	479	4	7	13	91	103	0	10	14	108	114	3	7	16	183	178	1	7	18	159	157
2	4	12	474	463	6	7	13	118	127	4	10	14	68	78	5	7	16	138	158	7	7	18	118	94
4	4	12	361	368	1	8	13	134	130	3	11	14	105	101	0	8	16	266	275	0	8	18	83	81
1	5	12	356	358	3	8	13	151	159	5	11	14	101	104	2	8	16	165	165	2	8	18	112	122

H	K	L	FO	FC	H	K	L	FO	FC	H	K	L	FO	FC	H	K	L	FO	FC	H	K	L	FO	FC
4	8	18	207	225	0	0	20	516	548	1	2	21	62	77	2	4	22	142	137	1	3	24	179	184
1	9	18	166	182	0	2	20	145	150	1	4	21	73	51	3	5	22	177	174	2	4	24	105	113
1	2	19	107	92	1	3	20	230	237	2	5	21	133	123	5	5	22	174	177	4	4	24	216	221
2	3	19	79	74	2	4	20	104	113	1	6	21	70	97	0	6	22	89	96	1	5	24	165	157
3	4	19	59	51	4	4	20	368	380	5	6	21	115	114	1	7	22	137	131	4	6	24	69	80
2	5	19	160	146	1	5	20	248	257	2	7	21	67	71	2	8	22	93	92	2	5	25	73	74
1	6	19	144	141	0	6	20	80	64	6	7	21	98	96	1	2	23	73	62	1	6	25	65	61
3	6	19	115	109	4	6	20	123	116	1	8	21	70	64	1	4	23	71	57	1	1	26	165	165
5	6	19	130	109	1	7	20	68	56	3	8	21	57	44	2	5	23	81	95	0	2	26	124	121
2	7	19	92	81	3	7	20	130	135	2	9	21	109	114	3	6	23	81	81	3	3	26	128	139
6	7	19	123	132	5	7	20	103	104	1	1	22	217	236	5	6	23	75	85	0	4	26	200	198
1	8	19	87	91	0	8	20	234	242	0	2	22	136	130	0	0	24	343	345	2	4	26	105	108
2	9	19	111	118	2	8	20	117	119	3	3	22	182	193	0	2	24	140	142	0	0	28	189	182
1	10	19	88	90	3	9	20	95	119	0	4	22	341	365										

APPENDIX V

OBSERVED AND CALCULATED STRUCTURE FACTORS

FOR [$HOsRe(CO)_8Br$]PPN

OBSERVED AND CALCULATED STRUCTURE FACTORS FOR H OS RE (CO)8 BR PPN

H	K	L	FO	FC	H	K	L	FO	FC	H	K	L	FO	FC	H	K	L	FO	FC	H	K	L	FO	FC
-4	12	1	60	-56	-8	-8	2	83	-77	4	-5	2	48	-47	1	-2	2	335	-338	-2	1	2	25	-31
1	12	1	44	39	-7	-8	2	57	53	6	-5	2	67	-68	2	-2	2	46	43	1	1	2	46	37
2	12	1	55	-57	-3	-8	2	71	77	7	-5	2	32	33	3	-2	2	38	45	2	1	2	158	-158
3	12	1	33	35	-2	-8	2	150	-155	9	-5	2	36	-42	4	-2	2	49	-50	3	1	2	312	318
0	13	1	51	55	-1	-8	2	125	121	-12	-4	2	35	16	6	-2	2	51	51	4	1	2	253	-259
1	13	1	35	-37	0	-8	2	91	-92	-9	-4	2	77	84	7	-2	2	64	-60	5	1	2	165	162
1	-14	2	52	46	1	-8	2	27	24	-8	-4	2	150	-145	8	-2	2	127	128	6	1	2	31	33
2	-14	2	59	-51	4	-8	2	35	-37	-7	-4	2	105	105	9	-2	2	76	-77	10	1	2	61	-57
-4	-13	2	56	-57	5	-8	2	53	59	-6	-4	2	62	-61	10	-2	2	58	61	11	1	2	45	49
-3	-13	2	56	56	6	-8	2	87	-86	-4	-4	2	54	-52	-12	-1	2	64	61	12	1	2	55	-49
2	-13	2	67	-65	7	-8	2	68	67	-1	-4	2	66	64	-11	-1	2	78	-76	-10	2	2	56	-57
4	-13	2	70	-74	8	-8	2	74	-76	0	-4	2	249	-248	-7	-1	2	50	-52	-9	2	2	103	99
5	-13	2	35	27	9	-8	2	38	40	1	-4	2	266	269	-6	-1	2	202	202	-8	2	2	40	-41
-6	-12	2	32	33	10	-8	2	38	39	2	-4	2	189	-194	-5	-1	2	134	-141	-7	2	2	34	-34
1	-12	2	54	-59	-6	-7	2	27	-25	3	-4	2	86	84	-4	-1	2	133	131	-6	2	2	71	74
2	-12	2	50	51	-4	-7	2	68	69	5	-4	2	72	-72	-3	-1	2	96	-90	-5	2	2	99	-98
-5	-11	2	74	-70	-3	-7	2	76	-83	6	-4	2	168	-168	-2	-1	2	54	54	-4	2	2	56	-61
-4	-11	2	102	98	-2	-7	2	144	158	7	-4	2	118	121	-1	-1	2	43	-45	-3	2	2	124	118
-3	-11	2	87	-85	-1	-7	2	97	-97	8	-4	2	152	-156	1	-1	2	86	-79	-2	2	2	165	-160
2	-11	2	54	54	2	-7	2	52	-54	9	-4	2	65	64	2	-1	2	203	194	-1	2	2	92	84
3	-11	2	66	-62	3	-7	2	47	-51	10	-4	2	28	-37	3	-1	2	174	-181	0	2	2	78	77
4	-11	2	103	104	4	-7	2	91	93	11	-4	2	32	26	4	-1	2	220	223	1	2	2	28	36
5	-11	2	75	-75	5	-7	2	97	-96	-12	-3	2	58	-47	5	-1	2	81	-81	2	2	2	77	76
6	-11	2	47	46	6	-7	2	110	111	-11	-3	2	37	33	7	-1	2	48	43	3	2	2	21	-22
-8	-10	2	40	37	12	-7	2	39	44	-9	-3	2	31	-29	10	-1	2	101	100	5	2	2	36	37
-4	-10	2	28	-31	-9	-6	2	77	-74	-7	-3	2	46	48	11	-1	2	38	-46	6	2	2	87	-89
-3	-10	2	48	-50	-8	-6	2	124	125	-6	-3	2	170	-164	-9	0	2	47	-45	7	2	2	57	56
-2	-10	2	96	100	-7	-6	2	67	-70	-5	-3	2	165	172	-7	0	2	67	69	9	2	2	56	-49
-1	-10	2	61	-62	-3	-6	2	82	-85	-4	-3	2	51	-49	-6	0	2	116	-116	10	2	2	67	70
0	-10	2	43	41	-2	-6	2	157	155	-3	-3	2	49	-58	-5	0	2	92	96	-11	3	2	75	-74
1	-10	2	38	39	-1	-6	2	189	-186	-2	-3	2	113	110	-4	0	2	33	33	-10	3	2	42	44
2	-10	2	55	-56	0	-6	2	165	164	1	-3	2	70	70	-3	0	2	115	-119	-9	3	2	61	-59
5	-10	2	50	-60	1	-6	2	114	-115	2	-3	2	257	-256	-2	0	2	67	69	-5	3	2	70	-71
6	-10	2	48	49	2	-6	2	72	70	3	-3	2	99	97	-1	0	2	51	-51	-4	3	2	186	190
7	-10	2	35	-36	3	-6	2	41	-36	4	-3	2	88	-88	0	0	2	201	-192	-3	3	2	211	-207
10	-10	2	43	-37	6	-6	2	122	126	6	-3	2	61	59	1	0	2	170	165	-2	3	2	104	104
-5	-9	2	63	63	7	-6	2	135	-139	7	-3	2	71	-73	2	0	2	168	-161	-1	3	2	56	55
-4	-9	2	83	-80	8	-6	2	135	135	10	-3	2	63	-55	3	0	2	80	78	0	3	2	109	-111
-3	-9	2	88	90	9	-6	2	46	-51	11	-3	2	56	57	8	0	2	65	-68	2	3	2	99	101
-2	-9	2	90	-93	12	-6	2	36	-7	-8	-2	2	61	64	9	0	2	53	49	3	3	2	162	-173
-1	-9	2	56	60	-6	-5	2	80	83	-7	-2	2	111	-116	10	0	2	75	-79	4	3	2	179	177
3	-9	2	68	70	-5	-5	2	63	-67	-6	-2	2	118	118	-12	1	2	70	-62	5	3	2	176	-171
4	-9	2	149	-148	-2	-5	2	167	-175	-5	-2	2	90	-100	-11	1	2	97	96	6	3	2	69	72
5	-9	2	103	105	-1	-5	2	67	67	-4	-2	2	64	63	-7	1	2	46	46	7	3	2	59	-57
6	-9	2	91	-96	0	-5	2	35	33	-3	-2	2	37	42	-6	1	2	110	-110	8	3	2	28	27
10	-9	2	37	-19	1	-5	2	107	-111	-2	-2	2	112	-115	-5	1	2	97	98	10	3	2	42	37
11	-9	2	47	52	2	-5	2	94	97	-1	-2	2	156	-147	-4	1	2	176	-174	-10	4	2	88	92
-10	-8	2	53	-49	3	-5	2	41	42	0	-2	2	259	256	-3	1	2	269	265	-9	4	2	142	-140

OBSERVED AND CALCULATED STRUCTURE FACTORS FOR H OS RE (CO)8 BR PPN

H	K	L	FO	FC	H	K	L	FO	FC	H	K	L	FO	FC	H	K	L	FO	FC	H	K	L	FO	FC
1	0	0	211	-204	-6	3	0	113	-112	11	5	0	55	-55	-7	9	0	38	42	3	-11	1	49	-49
2	0	0	128	121	-5	3	0	157	154	-10	6	0	67	69	-6	9	0	45	49	8	-11	1	44	46
3	0	0	37	40	-4	3	0	189	-194	-9	6	0	65	-65	-4	9	0	110	111	9	-11	1	52	-54
4	0	0	49	44	-3	3	0	78	79	-8	6	0	26	-26	-3	9	0	101	-100	-5	-10	1	103	-103
5	0	0	73	-75	-2	3	0	93	-91	-6	6	0	64	-64	-2	9	0	60	63	-4	-10	1	86	84
6	0	0	96	96	-1	3	0	143	-141	-3	6	0	47	-45	-1	9	0	83	-82	-3	-10	1	75	-77
7	0	0	112	-114	0	3	0	35	41	-2	6	0	85	84	4	9	0	94	97	2	-10	1	74	75
8	0	0	113	115	1	3	0	87	84	0	6	0	42	34	5	9	0	93	-91	3	-10	1	127	-129
9	0	0	61	-60	2	3	0	249	-263	1	6	0	73	71	6	9	0	63	63	4	-10	1	63	68
10	0	0	59	57	3	3	0	140	141	2	6	0	113	-115	8	9	0	36	-28	5	-10	1	104	-109
-10	1	0	55	-56	4	3	0	143	-143	3	6	0	119	120	-10	10	0	30	41	-5	-9	1	44	49
-7	1	0	94	-95	6	3	0	58	60	5	6	0	83	-86	-9	10	0	43	-42	-2	-9	1	93	92
-6	1	0	126	125	9	3	0	41	37	6	6	0	60	56	-8	10	0	66	66	-1	-9	1	55	-53
-5	1	0	50	-50	10	3	0	48	-57	7	6	0	28	-28	-7	10	0	54	-53	1	-9	1	65	63
-4	1	0	58	56	-12	4	0	30	7	8	6	0	57	-52	-2	10	0	102	97	2	-9	1	88	-82
-3	1	0	112	110	-10	4	0	38	-41	9	6	0	37	39	-1	10	0	129	-125	5	-9	1	54	-50
-2	1	0	57	-52	-9	4	0	39	37	-11	7	0	66	58	0	10	0	72	73	6	-9	1	29	29
-1	1	0	65	60	-8	4	0	81	84	-10	7	0	74	-69	1	10	0	27	-31	7	-9	1	26	-25
0	1	0	43	20	-7	4	0	105	-107	-9	7	0	34	28	6	10	0	47	50	9	-9	1	45	43
1	1	0	50	-46	-6	4	0	137	136	-8	7	0	46	-45	7	10	0	49	-50	-5	-8	1	109	116
2	1	0	194	197	-5	4	0	60	-62	-5	7	0	106	108	-4	11	0	34	-41	-4	-8	1	85	-90
3	1	0	102	-108	-4	4	0	40	-46	-4	7	0	167	-172	-3	11	0	44	43	-3	-8	1	147	144
5	1	0	27	25	-2	4	0	34	30	-3	7	0	180	182	-2	11	0	63	-64	-2	-8	1	81	-86
6	1	0	147	-147	-1	4	0	53	-57	-2	7	0	46	-47	-1	11	0	59	57	-1	-8	1	59	57
7	1	0	62	63	0	4	0	127	122	1	7	0	44	47	4	11	0	54	-50	0	-8	1	49	-48
9	1	0	58	-54	1	4	0	167	-158	2	7	0	92	-95	5	11	0	51	53	2	-8	1	40	-38
10	1	0	63	67	2	4	0	223	225	3	7	0	93	97	6	11	0	45	-49	3	-8	1	102	101
-8	2	0	93	-96	3	4	0	68	-69	4	7	0	160	-162	-7	12	0	58	56	4	-8	1	178	-181
-7	2	0	156	158	8	4	0	91	92	5	7	0	99	97	-2	12	0	51	-48	5	-8	1	164	163
-6	2	0	140	-139	9	4	0	110	-115	6	7	0	71	-68	-1	12	0	63	61	6	-8	1	41	-43
-5	2	0	73	76	10	4	0	49	48	7	7	0	31	35	0	12	0	64	-62	10	-8	1	41	-41
-4	2	0	113	114	-12	5	0	71	69	8	7	0	37	34	1	12	0	69	68	11	-8	1	56	57
-3	2	0	51	-53	-11	5	0	57	-52	10	7	0	36	-32	-5	13	0	46	41	-9	-7	1	82	79
-1	2	0	193	196	-10	5	0	47	50	-10	8	0	62	-63	-2	13	0	42	36	-7	-7	1	62	60
0	2	0	327	-322	-6	5	0	81	83	-9	8	0	55	58	2	13	0	46	-43	-5	-7	1	45	-53
1	2	0	150	148	-5	5	0	119	-118	-8	8	0	39	-39	2	-14	1	35	29	-3	-7	1	72	73
2	2	0	199	-202	-4	5	0	194	200	-6	8	0	33	24	3	-14	1	44	-44	-2	-7	1	168	-168
3	2	0	133	137	-3	5	0	186	-189	-3	8	0	50	52	0	-13	1	53	-52	-1	-7	1	145	137
4	2	0	50	-50	-2	5	0	75	73	-2	8	0	90	-88	2	-13	1	49	-46	0	-7	1	35	-39
5	2	0	42	42	-1	5	0	49	51	-1	8	0	120	121	3	-13	1	30	30	2	-7	1	58	57
6	2	0	51	-51	0	5	0	24	-24	0	8	0	52	-49	-5	-12	1	70	70	5	-7	1	68	60
7	2	0	75	76	1	5	0	64	-67	1	8	0	24	-21	-4	-12	1	59	-60	6	-7	1	66	-63
8	2	0	125	-128	2	5	0	176	186	2	8	0	73	74	-3	-12	1	43	33	7	-7	1	104	107
9	2	0	111	113	3	5	0	131	-139	3	8	0	52	-54	-1	-12	1	29	-22	10	-7	1	29	29
10	2	0	47	-45	4	5	0	146	155	5	8	0	50	49	3	-12	1	68	71	11	-7	1	45	-42
-12	3	0	72	-74	5	5	0	53	-52	6	8	0	49	-55	0	-11	1	41	47	-11	-6	1	47	-48
-11	3	0	37	36	9	5	0	35	-23	-10	9	0	43	45	1	-11	1	71	-67	-10	-6	1	42	36
-7	3	0	78	80	10	5	0	41	36	-9	9	0	31	-19	2	-11	1	83	79	-4	-6	1	32	29

OBSERVED AND CALCULATED STRUCTURE FACTORS FOR H OS RE (CO)8 BR PPN

H	K	L	FO	FC	H	K	L	FO	FC	H	K	L	FO	FC	H	K	L	FO	FC	H	K	L	FO	FC
-3	-6	1	200	-206	6	-3	1	157	-159	4	0	1	129	137	1	3	1	52	-49	-11	7	1	44	42
-2	-6	1	153	152	7	-3	1	190	194	6	0	1	64	-62	2	3	1	79	80	-10	7	1	54	-51
-1	-6	1	122	-126	8	-3	1	103	-111	7	0	1	83	81	3	3	1	131	-134	-9	7	1	72	73
1	-6	1	47	53	9	-3	1	93	94	9	0	1	91	-89	4	3	1	49	49	-8	7	1	84	-88
3	-6	1	111	-117	-7	-2	1	104	106	10	0	1	63	65	5	3	1	67	69	-2	7	1	80	-81
4	-6	1	193	199	-6	-2	1	112	-115	11	0	1	59	-56	6	3	1	46	-51	-1	7	1	157	161
5	-6	1	123	-126	-5	-2	1	151	154	-10	1	1	33	37	8	3	1	61	58	0	7	1	129	-128
6	-6	1	77	77	-3	-2	1	49	-55	-8	1	1	42	-43	9	3	1	91	-88	2	7	1	53	51
11	-6	1	50	-52	-1	-2	1	102	-99	-7	1	1	96	98	10	3	1	75	71	3	7	1	37	-34
12	-6	1	55	57	0	-2	1	83	-86	-6	1	1	137	-143	-11	4	1	57	-59	5	7	1	70	65
-9	-5	1	93	-92	1	-2	1	104	103	-5	1	1	98	96	-10	4	1	49	43	6	7	1	79	-79
-8	-5	1	95	91	2	-2	1	72	-69	-4	1	1	53	51	-5	4	1	161	-152	8	7	1	34	-39
-7	-5	1	101	-104	5	-2	1	46	-41	-3	1	1	132	-137	-4	4	1	215	226	-10	8	1	43	31
-3	-5	1	115	-118	6	-2	1	86	83	-1	1	1	180	183	-3	4	1	234	-237	-6	8	1	46	-41
-2	-5	1	122	124	7	-2	1	56	-64	0	1	1	145	-141	-2	4	1	90	98	-4	8	1	86	83
-1	-5	1	220	-216	8	-2	1	45	39	1	1	1	273	276	0	4	1	113	-111	-3	8	1	63	-64
0	-5	1	121	123	9	-2	1	70	68	2	1	1	105	-98	2	4	1	86	90	-2	8	1	98	99
1	-5	1	83	-81	10	-2	1	58	-53	3	1	1	79	78	3	4	1	212	-218	-1	8	1	28	-29
2	-5	1	94	95	-9	-1	1	65	-62	4	1	1	56	-61	4	4	1	108	114	4	8	1	32	34
5	-5	1	58	-53	-8	-1	1	106	108	5	1	1	23	16	5	4	1	91	-95	5	8	1	78	-74
6	-5	1	91	91	-7	-1	1	115	-118	8	1	1	86	-86	6	4	1	81	82	6	8	1	82	81
7	-5	1	185	-182	-6	-1	1	181	178	9	1	1	127	121	11	4	1	73	-76	-9	9	1	57	-62
8	-5	1	70	69	-5	-1	1	114	-116	10	1	1	81	-83	-10	5	1	79	73	-8	9	1	78	84
9	-5	1	38	-45	-4	-1	1	59	57	11	1	1	30	23	-9	5	1	69	-65	-7	9	1	77	-76
-7	-4	1	36	-38	-3	-1	1	76	-71	-12	2	1	72	-74	-8	5	1	64	67	-6	9	1	52	54
-6	-4	1	55	60	-2	-1	1	33	24	-8	2	1	52	-51	-7	5	1	37	33	-2	9	1	86	90
-5	-4	1	74	-82	-1	-1	1	272	-265	-7	2	1	57	55	-3	5	1	69	-74	-1	9	1	136	-135
-3	-4	1	185	194	0	-1	1	247	242	-6	2	1	103	-101	-2	5	1	71	72	0	9	1	119	116
-2	-4	1	178	-179	1	-1	1	325	-321	-5	2	1	174	171	-1	5	1	128	-131	1	9	1	56	-55
-1	-4	1	86	93	2	-1	1	287	278	-4	2	1	146	-149	0	5	1	56	63	6	9	1	46	46
2	-4	1	77	-74	3	-1	1	104	110	-3	2	1	122	125	2	5	1	34	-44	7	9	1	65	-61
4	-4	1	86	-88	6	-1	1	65	65	-2	2	1	178	-180	3	5	1	91	94	8	9	1	60	58
5	-4	1	121	114	7	-1	1	113	-113	1	2	1	85	-90	4	5	1	31	31	-7	10	1	42	-38
6	-4	1	132	-139	8	-1	1	93	93	2	2	1	180	-180	5	5	1	90	-90	-6	10	1	49	53
7	-4	1	41	44	9	-1	1	126	-123	3	2	1	344	354	6	5	1	85	86	-3	10	1	25	28
10	-4	1	36	32	10	-1	1	60	56	4	2	1	162	-170	7	5	1	52	-55	-2	10	1	65	-67
-10	-3	1	65	-58	-12	0	1	73	69	6	2	1	24	-29	-12	6	1	29	-25	0	10	1	31	-22
-9	-3	1	120	122	-9	0	1	62	56	9	2	1	67	64	-11	6	1	61	63	2	10	1	57	53
-8	-3	1	123	-124	-7	0	1	77	-76	10	2	1	45	-47	-10	6	1	58	-61	3	10	1	63	58
-7	-3	1	108	109	-6	0	1	145	148	11	2	1	65	67	-7	6	1	33	-31	-8	11	1	67	-63
-6	-3	1	74	-71	-5	0	1	194	-188	-10	3	1	73	-75	-5	6	1	96	94	-7	11	1	59	55
-5	-3	1	58	60	-4	0	1	59	57	-7	3	1	109	-109	-4	6	1	171	-176	-6	11	1	57	-51
-2	-3	1	35	-35	-3	0	1	68	-61	-6	3	1	139	132	-3	6	1	136	143	-2	11	1	39	-38
-1	-3	1	223	222	-1	0	1	47	39	-5	3	1	76	-74	-2	6	1	126	-130	-1	11	1	67	63
0	-3	1	225	-230	0	0	1	45	19	-4	3	1	24	-19	3	6	1	88	93	0	11	1	83	-82
1	-3	1	220	223	1	0	1	99	-94	-3	3	1	56	61	4	6	1	110	-110	2	11	1	50	-46
2	-3	1	148	-148	2	0	1	138	127	-1	3	1	47	41	5	6	1	111	112	-6	12	1	53	-51
3	-3	1	199	-195	3	0	1	160	-163	0	3	1	40	-38	6	6	1	86	-86	-5	12	1	38	39

OBSERVED AND CALCULATED STRUCTURE FACTORS FOR H OS RE (CO)8 BR PPN

H	K	L	FO	FC	H	K	L	FO	FC	H	K	L	FO	FC	H	K	L	FO	FC	H	K	L	FO	FC
-8	4	2	67	70	5	7	2	55	-56	-2-13	3	41	-37	4	-8	3	48	48	-12	-4	3	55	-56
-7	4	2	64	62	6	7	2	84	81	-1-13	3	34	39	5	-8	3	116	-118	-11	-4	3	55	48
-3	4	2	76	-73	-10	8	2	35	35	3-13	3	45	-46	6	-8	3	37	34	-6	-4	3	122	-122
-2	4	2	139	138	-9	8	2	37	-43	6-13	3	39	-31	7	-8	3	36	-39	-5	-4	3	161	161
-1	4	2	150	-145	-8	8	2	74	74	-5-12	3	49	-49	-9	-7	3	52	-54	-4	-4	3	175	-174
0	4	2	58	60	-7	8	2	120	-124	-4-12	3	84	82	-8	-7	3	88	89	-1	-4	3	58	-49
1	4	2	127	-123	-6	8	2	56	56	-3-12	3	72	-73	-7	-7	3	119	-120	0	-4	3	95	-95
2	4	2	67	-66	-5	8	2	33	-35	-2-12	3	46	39	-6	-7	3	60	55	1	-4	3	164	161
3	4	2	61	62	-2	8	2	89	87	-1-12	3	26	-20	-5	-7	3	31	33	2	-4	3	150	-150
4	4	2	31	-30	-1	8	2	130	-130	3-12	3	61	-56	-2	-7	3	95	99	3	-4	3	152	148
5	4	2	97	-100	0	8	2	142	141	4-12	3	66	68	-1	-7	3	118	-118	4	-4	3	126	-126
6	4	2	150	154	1	8	2	91	-92	5-12	3	86	-85	0	-7	3	154	163	5	-4	3	34	36
7	4	2	76	-79	6	8	2	49	43	6-12	3	52	51	1	-7	3	167	-167	7	-4	3	52	-56
-10	5	2	63	-56	7	8	2	68	-64	-5-11	3	31	18	2	-7	3	99	106	9	-4	3	33	30
-9	5	2	69	65	8	8	2	61	58	-3-11	3	48	-53	3	-7	3	34	-41	10	-4	3	97	-92
-7	5	2	47	-47	-7	9	2	40	-46	-1-11	3	128	-125	6	-7	3	49	51	11	-4	3	69	63
-4	5	2	118	-117	-6	9	2	55	57	0-11	3	59	63	7	-7	3	126	-126	-11	-3	3	42	45
-3	5	2	157	163	-5	9	2	74	-79	3-11	3	41	43	8	-7	3	139	141	-10	-3	3	29	-23
-2	5	2	119	-117	-1	9	2	49	45	4-11	3	31	25	9	-7	3	68	-69	-7	-3	3	76	-77
-1	5	2	46	-45	1	9	2	43	-43	5-11	3	28	-31	-7	-6	3	44	-47	-6	-3	3	80	80
1	5	2	37	-37	2	9	2	65	63	6-11	3	59	60	-6	-6	3	91	97	-5	-3	3	123	-114
2	5	2	44	-43	3	9	2	77	-81	7-11	3	66	-59	-5	-6	3	98	-98	-3	-3	3	106	105
4	5	2	87	-89	6	9	2	40	-40	8-11	3	35	25	-4	-6	3	121	120	-2	-3	3	106	-109
5	5	2	113	113	7	9	2	29	22	-4-10	3	44	-43	-1	-6	3	104	105	-1	-3	3	65	69
6	5	2	76	-74	-7	10	2	61	69	-3-10	3	78	83	0	-6	3	57	57	1	-3	3	235	-240
7	5	2	61	55	-6	10	2	47	-51	-2-10	3	54	-56	1	-6	3	169	-174	2	-3	3	192	193
-10	6	2	61	-59	-5	10	2	34	22	-1-10	3	33	43	2	-6	3	130	133	4	-3	3	68	-70
-9	6	2	91	96	-2	10	2	40	-41	2-10	3	52	52	3	-6	3	95	-95	5	-3	3	29	33
-8	6	2	62	-66	-1	10	2	70	69	4-10	3	59	-63	4	-6	3	56	52	7	-3	3	81	-80
-7	6	2	105	105	0	10	2	66	-64	5-10	3	134	134	5	-6	3	81	83	8	-3	3	30	32
-2	6	2	135	-132	1	10	2	90	86	-9 -9	3	64	53	9	-6	3	35	-31	9	-3	3	97	-102
-1	6	2	184	176	2	10	2	57	-57	-8 -9	3	77	-75	10	-6	3	44	51	10	-3	3	64	52
0	6	2	155	-160	-7	11	2	32	27	-7 -9	3	45	52	11	-6	3	37	-45	-12	-2	3	82	75
1	6	2	102	101	-5	11	2	91	80	-6 -9	3	44	-40	-9	-5	3	51	57	-11	-2	3	65	-68
5	6	2	80	84	-4	11	2	46	-47	-2 -9	3	109	-104	-8	-5	3	69	-70	-10	-2	3	56	55
6	6	2	73	-72	-3	11	2	51	48	-1 -9	3	185	194	-7	-5	3	104	105	-7	-2	3	59	-66
7	6	2	85	82	1	11	2	50	46	0 -9	3	129	-127	-6	-5	3	55	-57	-6	-2	3	157	155
8	6	2	30	-47	2	11	2	68	-62	1 -9	3	54	60	-5	-5	3	33	32	-5	-2	3	209	-202
9	6	2	33	36	3	11	2	71	64	6 -9	3	79	-83	-1	-5	3	46	40	-4	-2	3	219	218
-10	7	2	47	45	1	12	2	59	-58	7 -9	3	88	93	0	-5	3	208	-207	-2	-2	3	169	167
-9	7	2	43	-31	-3-14	3	50	51	8 -9	3	81	-79	1	-5	3	286	284	0	-2	3	65	69
-7	7	2	34	39	-2-14	3	31	-14	-5 -8	3	40	42	2	-5	3	145	-152	2	-2	3	154	155
-6	7	2	56	-50	2-14	3	49	-38	-4 -8	3	28	-22	3	-5	3	44	42	3	-2	3	274	-282
-3	7	2	62	-62	3-14	3	67	66	-3 -8	3	44	-43	4	-5	3	63	63	4	-2	3	234	235
-2	7	2	50	47	4-14	3	47	-48	-2 -8	3	99	100	6	-5	3	37	-44	5	-2	3	123	-127
1	7	2	54	54	5-14	3	41	43	-1 -8	3	59	-64	7	-5	3	134	133	7	-2	3	28	31
3	7	2	47	46	6-14	3	46	-40	1 -8	3	114	124	8	-5	3	118	-120	8	-2	3	35	-40
4	7	2	44	44	-3-13	3	45	38	2 -8	3	59	-53	9	-5	3	89	87	9	-2	3	73	-76

OBSERVED AND CALCULATED STRUCTURE FACTORS FOR H OS RE (CO)8 BR PPH

H	K	L	FO	FC	H	K	L	FO	FC	H	K	L	FO	FC	H	K	L	FO	FC	H	K	L	FO	FC
10	-2	3	83	77	1	1	3	74	78	0	4	3	51	52	2	8	3	100	99	-1	-10	4	127	132
-11	-2	3	65	-68	2	1	3	55	-54	1	4	3	45	-46	3	8	3	77	-77	0	-10	4	147	-152
12	-2	3	59	56	3	1	3	37	-39	4	4	3	46	-47	4	8	3	46	45	1	-10	4	67	68
-11	-1	3	40	-32	4	1	3	24	20	5	4	3	74	75	-7	9	3	65	64	2	-10	4	57	-59
-10	-1	3	57	55	5	1	3	89	95	6	4	3	100	-96	-6	9	3	52	-56	7	-10	4	59	61
-9	-1	3	59	-57	6	1	3	120	-118	7	4	3	33	31	-1	9	3	40	37	8	-10	4	78	-83
-8	-1	3	54	54	7	1	3	109	109	-10	5	3	53	-46	0	9	3	75	-79	9	-10	4	63	58
-6	-1	3	75	-77	8	1	3	54	-51	-9	5	3	61	66	1	9	3	69	66	-6	-9	4	45	-49
-5	-1	3	88	89	9	1	3	66	-62	-8	5	3	109	-111	2	9	3	54	-59	-5	-9	4	57	61
-4	-1	3	30	35	10	1	3	33	40	-7	5	3	63	67	3	9	3	43	46	-2	-9	4	41	40
-3	-1	3	77	-78	-12	2	3	35	38	-6	5	3	95	-95	-6	10	3	57	-49	1	-9	4	67	66
-2	-1	3	272	264	-10	2	3	63	62	-5	5	3	59	63	-5	10	3	75	74	2	-9	4	96	-98
-0	-1	3	26	22	-7	2	3	38	41	-2	5	3	45	-48	-4	10	3	101	-98	3	-9	4	80	80
1	-1	3	100	104	-6	2	3	56	-54	-1	5	3	187	191	-3	10	3	58	54	5	-9	4	36	-27
2	-1	3	58	-56	-5	2	3	33	-37	0	5	3	255	-254	1	10	3	33	33	6	-9	4	65	75
5	-1	3	56	-55	-4	2	3	139	135	1	5	3	121	125	2	10	3	67	-69	10	-9	4	39	-48
6	-1	3	26	26	-3	2	3	159	-166	2	5	3	49	-51	3	10	3	67	62	-8	-8	4	82	81
7	-1	3	24	-9	-2	2	3	229	230	3	5	3	36	-37	4	10	3	60	-59	-7	-8	4	72	-78
9	-1	3	70	73	-1	2	3	54	-60	6	5	3	93	-91	2	11	3	32	40	-6	-8	4	41	43
10	-1	3	77	-72	1	2	3	31	32	7	5	3	87	87	-3	12	3	48	-51	-5	-8	4	36	-43
-12	0	3	75	-73	2	2	3	78	78	8	5	3	68	-68	-2	12	3	31	29	-4	-8	4	53	-57
-11	0	3	61	58	3	2	3	159	-157	9	5	3	47	43	2-15		4	36	-26	-2	-8	4	54	51
-10	0	3	58	-59	4	2	3	182	187	-7	6	3	72	71	3-15		4	46	48	-1	-8	4	76	-75
-7	0	3	42	43	5	2	3	141	-140	-6	6	3	115	-116	-2-14		4	41	-45	0	-8	4	127	132
-5	0	3	139	127	6	2	3	96	95	-5	6	3	61	66	-1-14		4	57	55	1	-8	4	127	-127
-4	0	3	204	-197	7	2	3	29	-31	-2	6	3	59	61	6-14		4	57	-53	2	-8	4	127	126
-3	0	3	302	293	11	2	3	46	-44	1	6	3	37	37	-4-13		4	59	48	3	-8	4	62	-61
-2	0	3	191	-187	-10	3	3	74	72	2	6	3	88	-86	-3-13		4	59	-55	6	-8	4	48	50
-1	0	3	200	193	-9	3	3	98	-98	3	6	3	38	34	-2-13		4	53	50	7	-8	4	74	-77
0	0	3	68	63	-8	3	3	142	153	4	6	3	46	-44	4-13		4	64	69	8	-8	4	105	105
2	0	3	93	-92	-7	3	3	44	-48	6	6	3	67	70	5-13		4	66	-69	9	-8	4	73	-70
3	0	3	206	216	-3	3	3	107	-106	7	6	3	33	-34	-2-12		4	75	72	-7	-7	4	32	-26
4	0	3	226	-238	-2	3	3	98	92	9	6	3	56	47	-1-12		4	87	-87	-6	-7	4	88	92
5	0	3	131	129	-1	3	3	127	-134	-8	7	3	80	82	0-12		4	66	69	-5	-7	4	155	-166
6	0	3	41	-42	0	3	3	230	231	-7	7	3	63	-66	1-12		4	37	-43	-4	-7	4	113	113
9	0	3	32	35	1	3	3	91	-100	-6	7	3	112	108	3-12		4	41	-46	-3	-7	4	90	-90
11	0	3	67	67	2	3	3	36	43	-5	7	3	28	-16	6-12		4	72	74	-1	-7	4	52	55
12	0	3	61	-57	4	3	3	34	-32	-1	7	3	120	-124	8-12		4	48	48	0	-7	4	50	53
-10	1	3	83	-79	5	3	3	79	-83	0	7	3	168	166	-2-11		4	39	-41	1	-7	4	86	-90
-9	1	3	103	105	6	3	3	133	132	1	7	3	113	-111	1-11		4	44	-40	2	-7	4	196	200
-8	1	3	94	-91	7	3	3	143	-144	2	7	3	47	53	3-11		4	34	-33	3	-7	4	91	-99
-6	1	3	69	69	8	3	3	49	50	3	7	3	27	-32	4-11		4	64	-63	10	-7	4	67	79
-5	1	3	51	-51	-10	4	3	45	-46	7	7	3	56	-49	5-11		4	57	55	11	-7	4	45	-46
-4	1	3	52	-50	-7	4	3	53	-58	8	7	3	66	66	6-11		4	72	-69	-8	-6	4	84	-84
-3	1	3	145	151	-6	4	3	86	88	-6	8	3	78	83	-8-10		4	61	-60	-7	-6	4	70	68
-2	1	3	290	-275	-3	4	3	119	120	-5	8	3	75	-72	-7-10		4	86	80	-5	-6	4	29	29
-1	1	3	79	76	-2	4	3	90	-93	-4	8	3	81	82	-6-10		4	42	-39	-2	-6	4	26	23
0	1	3	202	-200	-1	4	3	66	67	-3	8	3	46	-43	-2-10		4	110	-111	0	-6	4	133	-127

OBSERVED AND CALCULATED STRUCTURE FACTORS FOR H OS RE (CO)8 BR PPN

H	K	L	FO	FC	H	K	L	FO	FC	H	K	L	FO	FC	H	K	L	FO	FC	H	K	L	FO	FC
1	-6	4	148	151	3	-3	4	240	-242	1	0	4	108	104	5	3	4	39	40	3	7	4	130	-129
2	-6	4	184	-188	4	-3	4	257	263	2	0	4	52	-58	6	3	4	54	-54	4	7	4	61	69
3	-6	4	86	86	5	-3	4	200	-203	5	0	4	31	36	7	3	4	64	58	-7	8	4	46	46
5	-6	4	63	-63	6	-3	4	69	67	6	0	4	109	-113	-9	4	4	64	67	-6	8	4	47	-46
7	-6	4	63	65	10	-3	4	53	52	7	0	4	154	158	-8	4	4	77	-75	-5	8	4	38	35
8	-6	4	106	-110	11	-3	4	86	-85	8	0	4	56	-57	-7	4	4	122	120	-3	8	4	52	-53
9	-6	4	73	77	12	-3	4	46	45	9	0	4	33	32	-6	4	4	92	-90	0	8	4	43	-40
10	-6	4	43	-41	-10	-2	4	72	67	-11	1	4	45	-43	-5	4	4	44	47	1	8	4	46	49
-11	-5	4	67	60	-9	-2	4	90	-89	-9	1	4	53	-48	-4	4	4	68	-64	2	8	4	46	-48
-6	-5	4	93	-95	-8	-2	4	77	78	-7	1	4	47	50	-3	4	4	44	-41	-5	9	4	68	65
-5	-5	4	191	195	-6	-2	4	33	-25	-6	1	4	35	-36	-2	4	4	91	-90	-4	9	4	91	-88
-4	-5	4	167	-167	-3	-2	4	161	-151	-5	1	4	36	36	-1	4	4	138	141	-3	9	4	89	84
-3	-5	4	99	105	-2	-2	4	165	168	-4	1	4	75	74	0	4	4	155	-152	-2	9	4	48	-52
-1	-5	4	51	50	-1	-2	4	170	-173	-3	1	4	223	-219	1	4	4	170	170	2	9	4	47	-49
0	-5	4	111	-108	1	-2	4	83	84	-2	1	4	165	164	2	4	4	64	-67	3	9	4	91	89
1	-5	4	96	98	2	-2	4	55	-55	-1	1	4	49	-51	6	4	4	85	-86	4	9	4	46	-48
2	-5	4	185	-185	3	-2	4	74	68	0	1	4	22	17	7	4	4	84	85	-2	10	4	43	-42
3	-5	4	154	150	5	-2	4	68	-63	1	1	4	23	35	8	4	4	85	-86	-1	10	4	45	39
4	-5	4	151	-155	6	-2	4	60	67	4	1	4	134	136	9	4	4	64	66	-5	11	4	49	-49
5	-5	4	82	87	7	-2	4	93	-95	5	1	4	129	-127	10	4	4	37	-36	-4	11	4	57	52
10	-5	4	91	-88	10	-2	4	28	-38	6	1	4	64	58	-7	5	4	42	36	-3	11	4	42	-43
11	-5	4	84	79	11	-2	4	38	33	7	1	4	26	-32	-6	5	4	96	-105	-2	11	4	58	46
12	-5	4	52	-51	-11	-1	4	75	79	-10	2	4	47	49	-5	5	4	125	129	-1	15	5	52	57
-9	-4	4	33	44	-10	-1	4	29	-33	-9	2	4	113	-117	-4	5	4	52	-51	0	15	5	56	-49
-8	-4	4	41	41	-8	-1	4	90	-88	-8	2	4	99	99	1	5	4	65	66	-3	14	5	43	-44
-5	-4	4	45	-47	-5	-1	4	42	40	-7	2	4	95	-96	2	5	4	55	-53	5	14	5	32	-37
-3	-4	4	50	55	-4	-1	4	125	-123	-4	2	4	75	73	3	5	4	114	113	6	14	5	38	38
-2	-4	4	109	-110	-3	-1	4	211	200	-3	2	4	43	-47	4	5	4	60	-61	-2	13	5	37	39
-1	-4	4	94	98	-2	-1	4	256	-248	-2	2	4	54	55	7	5	4	39	-45	-1	13	5	93	-90
1	-4	4	123	-130	-1	-1	4	88	88	-1	2	4	229	-222	9	5	4	35	39	0	13	5	93	87
2	-4	4	96	98	0	-1	4	81	83	0	2	4	180	179	-8	6	4	28	21	1	13	5	58	-52
3	-4	4	69	-68	1	-1	4	87	-87	1	2	4	174	-186	-7	6	4	85	-91	5	13	5	40	-34
4	-4	4	45	-51	3	-1	4	78	78	2	2	4	73	73	-6	6	4	68	72	6	13	5	56	53
5	-4	4	77	79	4	-1	4	216	-226	3	2	4	29	28	-5	6	4	48	-51	7	13	5	65	-64
7	-4	4	22	22	5	-1	4	161	162	5	2	4	39	-38	-3	6	4	43	39	8	13	5	47	51
8	-4	4	54	52	6	-1	4	64	-60	6	2	4	141	149	-1	6	4	76	-72	-7	12	5	42	-47
9	-4	4	31	-33	11	-1	4	49	48	7	2	4	135	-135	0	6	4	107	106	-6	12	5	50	45
11	-4	4	40	-39	12	-1	4	60	-51	8	2	4	66	73	1	6	4	142	-149	-5	12	5	30	-31
-11	-3	4	91	-85	-10	0	4	53	-57	9	2	4	52	-48	2	6	4	52	46	2	12	5	51	52
-10	-3	4	55	50	-9	0	4	118	118	-9	3	4	56	50	7	6	4	35	-29	6	12	5	58	-52
-6	-3	4	82	84	-8	0	4	122	-120	-7	3	4	59	-64	8	6	4	55	53	9	12	5	45	-44
-5	-3	4	180	-180	-7	0	4	92	89	-6	3	4	102	104	-7	7	4	33	-42	-8	11	5	42	-51
-4	-3	4	156	152	-5	0	4	58	-56	-5	3	4	104	-106	-6	7	4	89	85	-7	11	5	52	56
-3	-3	4	161	-153	-4	0	4	70	-71	-3	3	4	101	101	-5	7	4	96	-93	-6	11	5	51	-53
-2	-3	4	84	81	-3	0	4	206	203	-2	3	4	32	-36	-4	7	4	85	85	-1	11	5	118	113
-1	-3	4	118	-121	-2	0	4	316	-300	-1	3	4	23	23	-3	7	4	61	-60	0	11	5	109	-110
0	-3	4	54	52	-1	0	4	222	219	0	3	4	63	66	-2	7	4	34	40	1	11	5	78	83
2	-3	4	56	55	0	0	4	93	-89	1	3	4	89	-88	2	7	4	89	85	2	11	5	45	-46

OBSERVED AND CALCULATED STRUCTURE FACTORS FOR H OS RE (CO)8 BR PPN

H	K	L	FO	FC	H	K	L	FO	FC	H	K	L	FO	FC	H	K	L	FO	FC	H	K	L	FO	FC
7	-11	5	73	72	-5	-6	5	164	163	-7	-3	5	58	-59	-5	0	5	32	37	-1	3	5	31	33
8	-11	5	66	-61	-4	-6	5	201	-207	-5	-3	5	57	56	-3	0	5	125	-126	0	3	5	223	-222
-7	-10	5	45	42	-3	-6	5	126	128	-4	-3	5	46	-46	-2	0	5	167	165	1	3	5	139	145
-6	-10	5	60	-58	-2	-6	5	64	-64	-3	-3	5	96	-96	-1	0	5	85	-82	2	3	5	103	-106
-5	-10	5	52	56	1	-6	5	108	109	-2	-3	5	179	182	0	0	5	47	-42	6	3	5	40	-38
-4	-10	5	83	-86	2	-6	5	91	-90	-1	-3	5	212	-216	1	0	5	113	115	7	3	5	94	98
1	-10	5	72	68	3	-6	5	126	127	0	-3	5	78	76	2	0	5	67	-67	8	3	5	79	-81
2	-10	5	134	-134	4	-6	5	177	-184	1	-3	5	59	61	4	0	5	54	54	9	3	5	49	55
3	-10	5	79	79	5	-6	5	105	109	2	-3	5	56	-56	5	0	5	29	-33	10	3	5	38	-36
4	-10	5	63	-67	6	-6	5	79	-81	3	-3	5	39	-36	6	0	5	52	59	-7	4	5	73	72
10	-10	5	36	-35	10	-6	5	58	-59	4	-3	5	86	80	10	0	5	29	-30	-6	4	5	126	-126
-8	-9	5	53	45	11	-6	5	86	83	5	-3	5	71	-68	-9	1	5	74	-75	-5	4	5	110	111
-7	-9	5	69	-70	-11	-5	5	40	38	6	-3	5	111	114	-8	1	5	115	120	-4	4	5	97	-103
-6	-9	5	75	77	-10	-5	5	59	-66	7	-3	5	75	-73	-7	1	5	103	-103	-1	4	5	33	36
-1	-9	5	68	-70	-9	-5	5	44	36	8	-3	5	99	101	-6	1	5	26	24	2	4	5	113	-115
0	-9	5	88	92	-5	-5	5	27	-36	-12	-2	5	35	-29	-3	1	5	68	-64	3	4	5	131	131
1	-9	5	137	-136	-3	-5	5	107	105	-10	-2	5	59	-60	-2	1	5	121	122	4	4	5	84	-86
2	-9	5	115	114	-2	-5	5	142	-142	-8	-2	5	27	29	-1	1	5	76	-72	5	4	5	50	51
3	-9	5	44	-45	-1	-5	5	70	73	-5	-2	5	41	38	0	1	5	239	240	6	4	5	27	34
5	-9	5	43	40	0	-5	5	76	-72	-4	-2	5	101	-99	1	1	5	190	-196	7	4	5	27	-19
7	-9	5	48	-51	1	-5	5	50	-48	-3	-2	5	109	103	2	1	5	134	138	9	4	5	52	48
8	-9	5	83	90	2	-5	5	102	102	-2	-2	5	186	-191	4	1	5	33	-27	-9	5	5	29	24
9	-9	5	65	-63	3	-5	5	49	-44	0	-2	5	46	41	6	1	5	92	99	-6	5	5	68	71
-6	-8	5	73	72	4	-5	5	99	-99	1	-2	5	85	-90	7	1	5	122	-119	-5	5	5	46	-40
-5	-8	5	114	-120	5	-5	5	105	107	2	-2	5	78	80	8	1	5	134	136	-4	5	5	40	-38
-4	-8	5	155	153	6	-5	5	85	-82	3	-2	5	56	59	-10	2	5	31	-14	-3	5	5	53	48
-3	-8	5	77	-76	10	-5	5	55	50	4	-2	5	155	-150	-7	2	5	68	-68	-2	5	5	75	-74
1	-8	5	120	-118	-12	-4	5	37	45	5	-2	5	139	139	-6	2	5	159	158	-1	5	5	28	-23
2	-8	5	179	183	-11	-4	5	67	-65	6	-2	5	104	-103	-5	2	5	115	-117	0	5	5	103	103
3	-8	5	144	-145	-10	-4	5	67	71	-10	-1	5	46	-47	-4	2	5	72	70	1	5	5	51	-54
4	-8	5	113	110	-8	-4	5	37	-45	-9	-1	5	114	113	-2	2	5	85	-87	2	5	5	79	78
11	-8	5	62	-63	-6	-4	5	45	46	-8	-1	5	152	-152	-1	2	5	35	38	-7	6	5	34	-41
-10	-7	5	61	46	-5	-4	5	119	-119	-7	-1	5	113	117	0	2	5	52	55	-6	6	5	45	54
-7	-7	5	65	59	-4	-4	5	135	136	-6	-1	5	32	-35	1	2	5	107	-112	-5	6	5	92	-96
-6	-7	5	43	-43	-3	-4	5	128	-121	-3	-1	5	117	120	2	2	5	83	82	-4	6	5	125	128
-3	-7	5	32	-29	-2	-4	5	137	133	-2	-1	5	276	-265	3	2	5	62	-62	-3	6	5	90	-91
-2	-7	5	69	72	-1	-4	5	73	-75	-1	-1	5	164	177	4	2	5	46	43	-2	6	5	54	56
1	-7	5	108	112	0	-4	5	67	65	0	-1	5	159	-157	5	2	5	26	-25	2	6	5	120	118
2	-7	5	118	-127	3	-4	5	142	-147	1	-1	5	76	77	6	2	5	57	-58	3	6	5	86	-88
3	-7	5	35	32	4	-4	5	199	210	2	-1	5	50	-53	9	2	5	31	-27	4	6	5	119	113
5	-7	5	48	-43	5	-4	5	176	-175	3	-1	5	64	61	10	2	5	68	61	5	6	5	53	-50
6	-7	5	38	44	6	-4	5	92	89	4	-1	5	60	61	-9	3	5	49	49	-9	7	5	52	-54
8	-7	5	57	-53	10	-4	5	58	59	5	-1	5	53	51	-8	3	5	67	-71	-6	7	5	41	-43
9	-7	5	63	66	11	-4	5	58	-56	6	-1	5	131	-135	-7	3	5	81	81	-3	7	5	64	-64
10	-7	5	42	-42	12	-4	5	59	60	7	-1	5	141	140	-6	3	5	68	-69	-2	7	5	103	105
-11	-6	5	50	46	-10	-3	5	52	52	8	-1	5	115	-113	-5	3	5	84	83	0	7	5	41	-37
-10	-6	5	49	-48	-9	-3	5	91	-91	-7	0	5	28	28	-4	3	5	38	38	6	7	5	47	37
-8	-6	5	77	-72	-8	-3	5	125	129	-6	0	5	110	-108	-3	3	5	52	-47	7	7	5	31	-21

OBSERVED AND CALCULATED STRUCTURE FACTORS FOR H OS RE (CO)8 BR PPN

H	K	L	FO	FC	H	K	L	FO	FC	H	K	L	FO	FC	H	K	L	FO	FC	H	K	L	FO	FC
-5	8	5	52	50	2	-10	6	65	66	-3	-6	6	38	40	1	-3	6	111	-111	-10	1	6	31	30
-4	8	5	84	-82	3	-10	6	58	-52	-2	-6	6	133	-138	2	-3	6	73	75	-6	1	6	101	100
-3	8	5	99	93	4	-10	6	28	-25	-1	-6	6	196	198	4	-3	6	98	-99	-5	1	6	212	-207
-2	8	5	33	-33	8	-10	6	45	38	0	-6	6	86	-85	5	-3	6	141	142	-4	1	6	108	107
2	8	5	52	-51	9	-10	6	65	-67	1	-6	6	37	40	6	-3	6	89	-93	-3	1	6	40	-38
3	8	5	58	53	10	-10	6	36	40	2	-6	6	57	56	-10	-2	6	34	-30	0	1	6	76	77
4	8	5	87	-87	-5	-9	6	111	-114	3	-6	6	26	-31	-9	-2	6	84	86	1	1	6	141	-136
5	8	5	44	42	-4	-9	6	128	130	5	-6	6	122	123	-8	-2	6	134	-131	2	1	6	126	126
-3	9	5	34	46	-3	-9	6	109	-115	6	-6	6	91	-89	-7	-2	6	155	153	3	1	6	109	-111
-2	9	5	61	-69	-2	-9	6	37	37	7	-6	6	64	68	-6	-2	6	26	-28	4	1	6	68	70
-1	9	5	56	56	1	-9	6	55	-54	-11	-5	6	48	-49	-4	-2	6	40	42	5	1	6	34	-35
0	9	5	62	-56	2	-9	6	150	148	-10	-5	6	49	46	-3	-2	6	95	95	7	1	6	30	27
3	9	5	29	-20	3	-9	6	171	-178	-7	-5	6	60	55	-2	-2	6	90	-93	9	1	6	62	-61
-4	10	5	51	53	4	-9	6	70	74	-5	-5	6	85	-85	-1	-2	6	195	190	10	1	6	46	51
-3	10	5	74	-75	5	-9	6	89	-87	-4	-5	6	102	100	0	-2	6	141	-136	-7	2	6	60	63
2	10	5	31	19	10	-9	6	55	53	-3	-5	6	148	-142	1	-2	6	72	71	-6	2	6	62	-61
1	-15	6	30	22	-10	-8	6	41	34	-2	-5	6	52	49	2	-2	6	118	-116	-4	2	6	36	30
-2	-14	6	29	33	-9	-8	6	43	-47	-1	-5	6	111	-108	6	-2	6	78	-78	-2	2	6	82	84
-1	-14	6	54	-52	-5	-8	6	48	49	0	-5	6	41	51	7	-2	6	155	157	-1	2	6	38	41
0	-14	6	77	72	-4	-8	6	58	60	1	-5	6	78	73	8	-2	6	107	-107	0	2	6	75	-76
1	-14	6	77	-71	-3	-8	6	36	-39	4	-5	6	145	147	9	-2	6	66	69	1	2	6	185	185
6	-14	6	53	50	-2	-8	6	64	62	5	-5	6	181	-182	-7	-1	6	49	51	2	2	6	105	-103
-5	-13	6	38	-42	-1	-8	6	61	-67	6	-5	6	68	66	-6	-1	6	82	-80	5	2	6	42	-44
1	-13	6	42	-35	0	-8	6	47	40	7	-5	6	39	-38	-5	-1	6	136	138	7	2	6	52	47
3	-13	6	55	-57	2	-8	6	59	-55	8	-5	6	33	-30	-4	-1	6	61	-62	8	2	6	53	-49
-7	-12	6	55	58	3	-8	6	47	56	11	-5	6	45	-48	-3	-1	6	52	-48	9	2	6	49	60
-6	-12	6	37	-45	4	-8	6	40	43	-9	-4	6	95	-94	-2	-1	6	35	41	-11	3	6	51	45
-1	-12	6	40	45	5	-8	6	84	-84	-8	-4	6	82	80	-1	-1	6	106	-100	-9	3	6	36	-30
0	-12	6	66	-60	6	-8	6	62	59	-7	-4	6	104	-101	0	-1	6	67	-66	-7	3	6	40	35
1	-12	6	91	91	9	-8	6	51	56	-5	-4	6	65	63	1	-1	6	130	128	-6	3	6	71	-66
3	-12	6	34	29	-10	-7	6	40	-38	-3	-4	6	37	-30	2	-1	6	182	-172	-5	3	6	157	159
7	-12	6	45	40	-9	-7	6	33	25	-2	-4	6	178	180	3	-1	6	82	80	-4	3	6	125	-123
8	-12	6	64	-66	-5	-7	6	121	127	-1	-4	6	205	-213	5	-1	6	45	-50	-3	3	6	66	66
9	-12	6	63	62	-4	-7	6	148	-150	0	-4	6	170	168	-9	0	6	40	-41	0	3	6	48	-49
-6	-11	6	59	-57	-3	-7	6	144	147	1	-4	6	81	-77	-8	0	6	90	88	1	3	6	40	45
-5	-11	6	54	64	0	-7	6	51	-54	4	-4	6	39	46	-7	0	6	95	-94	2	3	6	95	-96
-4	-11	6	70	-75	2	-7	6	49	-56	5	-4	6	96	-96	-6	0	6	60	62	3	3	6	151	162
-3	-11	6	59	63	3	-7	6	123	119	6	-4	6	93	90	-5	0	6	47	-43	4	3	6	143	-152
1	-11	6	54	55	4	-7	6	120	-122	7	-4	6	155	-150	-3	0	6	29	-32	5	3	6	51	53
2	-11	6	91	-89	5	-7	6	171	172	8	-4	6	66	63	-1	0	6	147	-141	7	3	6	30	-29
3	-11	6	132	133	6	-7	6	74	-75	9	-4	6	44	-45	0	0	6	141	139	9	3	6	32	34
4	-11	6	53	-54	7	-7	6	30	35	-7	-3	6	64	-56	1	0	6	221	-218	-6	4	6	56	60
8	-11	6	35	-39	10	-7	6	58	-55	-6	-3	6	41	39	2	0	6	134	130	-3	4	6	123	121
-7	-10	6	50	-49	11	-7	6	52	58	-4	-3	6	59	59	5	0	6	27	34	-2	4	6	78	-77
-6	-10	6	42	47	-11	-6	6	47	36	-3	-3	6	107	107	6	0	6	51	49	-1	4	6	26	30
-3	-10	6	62	60	-10	-6	6	50	-46	-2	-3	6	64	-64	7	0	6	113	-115	1	4	6	115	-113
0	-10	6	46	49	-9	-6	6	77	81	-1	-3	6	127	123	8	0	6	89	89	2	4	6	33	34
1	-10	6	67	-67	-7	-6	6	33	41	0	-3	6	79	74	9	0	6	79	-72	4	4	6	31	-30

OBSERVED AND CALCULATED STRUCTURE FACTORS FOR H OS RE (CO)8 BR PPN

H	K	L	FO	FC	H	K	L	FO	FC	H	K	L	FO	FC	H	K	L	FO	FC	H	K	L	FO	FC
5	4	6	31	41	-2	-11	7	54	-58	-4	-6	7	59	60	7	-3	7	85	82	4	1	7	74	71
-10	5	6	41	43	1	-11	7	46	-41	-3	-6	7	59	-59	8	-3	7	127	-125	5	1	7	64	-62
-6	5	6	36	39	6	-11	7	52	-48	-2	-6	7	49	52	9	-3	7	57	58	8	1	7	49	-53
-5	5	6	72	-83	9	-11	7	45	-41	-1	-6	7	38	-38	-7	-2	7	32	28	-11	2	7	68	65
-4	5	6	89	88	-5	-10	7	61	-67	0	-6	7	47	-44	-6	-2	7	120	-119	-6	2	7	96	-95
-3	5	6	95	-98	-4	-10	7	93	93	2	-6	7	99	-102	-5	-2	7	121	121	-5	2	7	107	106
-2	5	6	74	76	-3	-10	7	106	-104	4	-6	7	95	90	-4	-2	7	139	-135	-4	2	7	130	-128
-1	5	6	26	-31	-2	-10	7	53	48	5	-6	7	90	-97	-3	-2	7	65	66	-3	2	7	101	100
2	5	6	43	43	1	-10	7	39	-37	6	-6	7	113	110	-2	-2	7	80	80	-2	2	7	77	-74
3	5	6	121	-124	2	-10	7	77	77	11	-6	7	35	-22	0	-2	7	66	-68	-1	2	7	59	61
4	5	6	103	103	3	-10	7	77	-77	-10	-5	7	39	40	1	-2	7	138	135	0	2	7	28	-31
5	5	6	65	-57	4	-10	7	128	138	-8	-5	7	111	109	2	-2	7	160	-161	1	2	7	58	60
-9	6	6	40	-42	5	-10	7	52	-50	-7	-5	7	91	-87	3	-2	7	87	87	2	2	7	86	-91
-8	6	6	56	64	6	-10	7	31	34	-6	-5	7	63	63	4	-2	7	61	-58	3	2	7	122	119
-3	6	6	92	-91	-9	-9	7	50	-46	-4	-5	7	44	-43	10	-2	7	61	-54	4	2	7	129	-127
-2	6	6	57	62	-3	-9	7	61	-62	-3	-5	7	39	-44	-8	-1	7	61	61	5	2	7	109	110
-1	6	6	65	-65	-2	-9	7	102	102	-2	-5	7	188	188	-7	-1	7	76	-75	-10	3	7	53	-58
0	6	6	40	42	-1	-9	7	77	-80	-1	-5	7	225	-232	-6	-1	7	75	75	-9	3	7	59	56
7	6	6	57	-50	0	-9	7	100	98	0	-5	7	177	178	0	-1	7	83	81	-5	3	7	46	-38
-4	7	6	74	-71	5	-9	7	57	-57	1	-5	7	74	-72	1	-1	7	163	-166	-3	3	7	102	102
-3	7	6	82	80	6	-9	7	91	95	3	-5	7	24	-27	2	-1	7	106	105	-2	3	7	106	-110
-2	7	6	80	-75	7	-9	7	49	-48	6	-5	7	102	96	3	-1	7	57	-66	-1	3	7	104	106
3	7	6	61	61	-10	-8	7	59	-53	7	-5	7	84	-87	4	-1	7	29	-33	2	3	7	51	54
4	7	6	71	-69	-4	-8	7	120	-116	8	-5	7	121	114	5	-1	7	35	32	4	3	7	51	-53
6	7	6	38	-40	-3	-8	7	109	109	9	-5	7	69	-71	7	-1	7	41	-48	6	3	7	43	-47
-3	8	6	58	55	-2	-8	7	60	-63	-8	-4	7	31	36	8	-1	7	107	105	7	3	7	36	30
-2	8	6	56	-53	1	-8	7	47	41	-7	-4	7	67	-71	9	-1	7	49	-55	-5	4	7	48	-47
-1	8	6	84	80	2	-8	7	32	-32	-6	-4	7	70	71	-11	0	7	58	-56	-4	4	7	76	77
0	8	6	72	-67	3	-8	7	64	62	-5	-4	7	70	-69	-6	0	7	133	137	-3	4	7	97	-93
1	8	6	33	32	4	-8	7	139	-133	-3	-4	7	41	-38	-5	0	7	208	-203	-2	4	7	78	78
-4	9	6	34	26	5	-8	7	90	91	-2	-4	7	70	-70	-4	0	7	164	164	3	4	7	101	-97
-2	9	6	38	44	6	-8	7	94	-99	-1	-4	7	35	34	-3	0	7	105	-101	4	4	7	108	103
-1	-15	7	45	-41	-10	-7	7	59	-59	1	-4	7	77	-81	0	0	7	41	42	5	4	7	89	-88
0	-15	7	80	72	-9	-7	7	54	52	2	-4	7	158	157	1	0	7	84	-86	-9	5	7	72	-75
1	-15	7	36	-45	-8	-7	7	64	-71	5	-4	7	79	80	2	0	7	144	136	-8	5	7	55	55
-4	-14	7	37	33	-7	-7	7	57	50	6	-4	7	79	-76	3	0	7	101	-100	-4	5	7	52	44
2	-14	7	74	66	-3	-7	7	57	51	-9	-3	7	34	39	4	0	7	97	97	-3	5	7	52	-52
4	-14	7	48	49	-2	-7	7	127	-125	-8	-3	7	117	-115	5	0	7	68	-66	-2	5	7	123	126
0	-13	7	63	-62	-1	-7	7	161	157	-7	-3	7	88	83	9	0	7	45	-36	-1	5	7	100	-104
1	-13	7	44	34	0	-7	7	153	-157	-6	-3	7	81	-83	10	0	7	66	62	6	5	7	71	73
2	-13	7	47	-51	1	-7	7	45	48	-3	-3	7	28	29	-10	1	7	45	38	7	5	7	52	-50
-7	-12	7	38	35	5	-7	7	99	98	-2	-3	7	74	-74	-5	1	7	23	9	-4	6	7	54	-57
-5	-12	7	59	66	6	-7	7	125	-129	-1	-3	7	158	160	-3	1	7	74	-78	-3	6	7	58	62
-4	-12	7	63	-65	7	-7	7	54	56	0	-3	7	133	-134	-2	1	7	70	69	-2	6	7	70	-70
-2	-12	7	41	-43	8	-7	7	42	-42	1	-3	7	137	135	-1	1	7	42	-43	1	6	7	40	-40
2	-12	7	104	-100	-10	-6	7	56	51	2	-3	7	96	-97	0	1	7	77	-75	4	6	7	58	-60
3	-12	7	100	97	-8	-6	7	38	-37	3	-3	7	34	35	1	1	7	92	92	5	6	7	54	53
4	-12	7	84	-89	-6	-6	7	40	-37	6	-3	7	56	-55	2	1	7	93	-95	-7	7	7	47	48

OBSERVED AND CALCULATED STRUCTURE FACTORS FOR H OS RE (CO)8 BR PPN

H	K	L	FO	FC	H	K	L	FO	FC	H	K	L	FO	FC	H	K	L	FO	FC	H	K	L	FO	FC
-2	7	7	81	-80	0	-8	8	145	-148	0	-4	8	107	-103	-10	0	8	50	43	-1	4	8	74	-78
-1	7	7	84	91	1	-8	8	89	88	1	-4	8	134	131	-9	0	8	49	-53	0	4	8	129	123
0	7	7	74	-69	3	-8	8	31	-24	2	-4	8	66	-67	-3	0	8	74	-76	2	4	8	29	27
1	7	7	75	70	4	-8	8	44	-50	3	-4	8	72	65	-2	0	8	128	127	5	4	8	44	-49
-6	8	7	44	-44	5	-8	8	54	54	7	-4	8	86	81	-1	0	8	92	-93	6	4	8	49	53
-2	8	7	32	27	6	-8	8	86	-88	8	-4	8	88	-83	1	0	8	60	60	7	4	8	79	-74
-2	9	7	47	38	7	-8	8	89	93	9	-4	8	84	82	2	0	8	97	-96	-3	5	8	47	53
3-15		8	58	-60	8	-8	8	68	-66	-7	-3	8	58	50	4	0	8	38	41	-2	5	8	51	-54
1-14		8	38	42	-7	-7	8	90	92	-6	-3	8	89	-90	5	0	8	82	-85	0	5	8	47	45
-5-13		8	37	43	-6	-7	8	91	-90	-5	-3	8	131	127	6	0	8	62	70	1	5	8	51	-50
-3-13		8	72	73	-3	-7	8	39	-41	-4	-3	8	182	-187	-11	1	8	47	48	4	5	8	36	-27
2-13		8	56	-57	-2	-7	8	38	36	-3	-3	8	62	62	-10	1	8	38	-39	-7	6	8	47	46
-3-13		8	100	100	1	-7	8	52	53	-2	-3	8	27	-24	-5	1	8	109	108	-2	6	8	46	-44
4-13		8	86	-83	2	-7	8	72	-67	-1	-3	8	59	-58	-4	1	8	139	-134	-1	6	8	50	52
5-13		8	40	45	3	-7	8	47	43	1	-3	8	174	169	-3	1	8	111	105	0	6	8	83	-90
-3-12		8	70	70	5	-7	8	90	-91	2	-3	8	167	-167	-2	1	8	99	-100	-6	7	8	63	-63
-2-12		8	45	-37	6	-7	8	44	47	3	-3	8	165	162	0	1	8	43	-44	0	7	8	41	-29
5-12		8	44	50	9	-7	8	73	72	4	-3	8	66	-64	2	1	8	54	-50	2	7	8	49	-52
-4-11		8	77	82	-9	-6	8	59	-55	5	-3	8	31	30	3	1	8	111	111	0	8	8	67	61
-3-11		8	95	-96	-8	-6	8	61	61	6	-3	8	30	-26	4	1	8	131	-131	-2-15		9	45	47
-2-11		8	53	44	-7	-6	8	94	-101	10	-3	8	53	-59	5	1	8	97	94	-4-14		9	51	-54
3-11		8	91	-96	-6	-6	8	86	86	-10	-2	8	33	-37	-10	2	8	44	-44	-2-14		9	44	-43
4-11		8	58	58	-2	-6	8	85	90	-7	-2	8	70	-70	-9	2	8	59	58	3-14		9	63	61
6-11		8	61	52	-1	-6	8	165	-164	-3	-2	8	68	67	-8	2	8	58	-57	4-14		9	73	-68
-8-10		8	52	57	0	-6	8	168	164	-2	-2	8	30	-32	-7	2	8	27	32	-1-13		9	66	68
-3-10		8	77	-78	1	-6	8	134	-134	0	-2	8	68	65	-3	2	8	59	58	5-13		9	32	33
-2-10		8	74	66	5	-6	8	35	-37	1	-2	8	88	-90	-2	2	8	165	-163	6-13		9	75	-72
-1-10		8	115	-114	6	-6	8	75	80	2	-2	8	123	119	-1	2	8	95	96	7-13		9	43	40
0-10		8	75	73	7	-6	8	98	-95	3	-2	8	44	-43	0	2	8	69	-69	-3-12		9	50	-44
1-10		8	43	-57	8	-6	8	97	98	5	-2	8	62	61	1	2	8	31	-36	-2-12		9	58	59
3-10		8	48	44	9	-6	8	53	-54	6	-2	8	40	-40	2	2	8	32	32	4-12		9	68	64
5-10		8	77	-72	-7	-5	8	82	-79	7	-2	8	50	-49	4	2	8	32	-31	5-12		9	65	-66
6-10		8	74	71	-6	-5	8	106	103	8	-2	8	55	50	5	2	8	62	60	-2-11		9	83	81
7-10		8	58	-62	-5	-5	8	79	-77	9	-2	8	61	-63	6	2	8	53	-57	-1-11		9	80	-78
-6	-9	8	51	46	-4	-5	8	75	77	-11	-1	8	49	-52	7	2	8	40	38	0-11		9	96	85
-4	-9	8	84	-81	1	-5	8	116	-114	-10	-1	8	38	37	-10	3	8	49	51	1-11		9	72	-62
-3	-9	8	78	78	2	-5	8	129	129	-6	-1	8	67	65	-7	3	8	29	21	5-11		9	53	-54
-2	-9	8	54	-55	3	-5	8	100	-98	-5	-1	8	162	-162	-3	3	8	77	-79	6-11		9	93	88
3	-9	8	40	45	4	-5	8	48	49	-4	-1	8	194	198	-2	3	8	74	73	7-11		9	73	-76
5	-9	8	102	102	5	-5	8	60	61	-3	-1	8	85	-87	1	3	8	52	50	8-11		9	52	51
6	-9	8	38	-41	8	-5	8	65	65	1	-1	8	48	-53	3	3	8	37	-40	-6-10		9	75	65
9	-9	8	44	-35	9	-5	8	57	-54	2	-1	8	105	105	4	3	8	104	105	-3-10		9	58	55
-9	-8	8	54	57	-8	-4	8	45	-42	3	-1	8	122	-118	5	3	8	75	-71	0-10		9	48	41
-8	-8	8	73	-74	-7	-4	8	114	114	4	-1	8	106	108	6	3	8	49	52	3-10		9	43	-41
-7	-8	8	37	44	-6	-4	8	43	-48	5	-1	8	77	-78	-9	4	8	59	-63	5-10		9	40	37
-6	-8	8	52	-59	-3	-4	8	29	-32	6	-1	8	40	43	-8	4	8	84	83	6-10		9	39	-43
-2	-8	8	102	-99	-2	-4	8	33	-30	10	-1	8	75	64	-7	4	8	63	-60	7-10		9	32	33
-1	-8	8	180	179	-1	-4	8	106	106	-11	0	8	47	-49	-2	4	8	111	113	-9	-9	9	47	46

OBSERVED AND CALCULATED STRUCTURE FACTORS FOR H OS RE (CO)8 BR PPN

H	K	L	FO	FC	H	K	L	FO	FC	H	K	L	FO	FC	H	K	L	FO	FC	H	K	L	FO	FC
-8	-9	9	52	-47	1	-5	9	73	74	2	-1	9	46	-48	-5	4	9	39	-44	-5	-9	10	76	77
-7	-9	9	53	57	2	-5	9	59	-61	4	-1	9	56	53	-2	4	9	31	-29	-4	-9	10	42	-39
-2	-9	9	71	-73	5	-5	9	35	-39	5	-1	9	88	-93	0	4	9	31	33	1	-9	10	44	49
-1	-9	9	120	118	8	-5	9	79	-75	6	-1	9	37	40	1	4	9	83	-79	2	-9	10	94	-95
0	-9	9	168	-165	9	-5	9	73	71	7	-1	9	56	-50	2	4	9	58	66	3	-9	10	62	61
1	-9	9	104	103	-5	-4	9	136	136	9	-1	9	29	4	3	4	9	33	-29	4	-9	10	79	-76
6	-9	9	76	-80	-4	-4	9	124	-124	-10	0	9	40	-40	5	4	9	40	44	9	-9	10	62	61
7	-9	9	71	72	-3	-4	9	171	167	-7	0	9	44	-37	-7	5	9	44	45	-6	-8	10	60	63
9	-9	9	36	40	-2	-4	9	29	-28	-5	0	9	72	70	-2	5	9	36	-25	-3	-8	10	28	28
-7	-8	9	61	64	1	-4	9	79	79	-4	0	9	85	-86	-1	5	9	55	55	-2	-8	10	40	-41
-6	-8	9	63	-67	2	-4	9	163	-160	-3	0	9	98	99	0	5	9	67	-65	-1	-8	10	90	-87
-5	-8	9	75	72	3	-4	9	152	156	-2	0	9	46	-48	1	5	9	66	66	0	-8	10	66	72
1	-8	9	62	66	4	-4	9	97	-100	-1	0	9	51	49	2	5	9	31	-32	1	-8	10	83	-79
2	-8	9	82	-77	5	-4	9	64	64	4	0	9	100	-99	-6	6	9	45	-43	2	-8	10	58	61
3	-8	9	120	118	9	-4	9	35	29	5	0	9	92	88	-5	6	9	72	73	7	-8	10	40	-38
6	-8	9	51	54	10	-4	9	47	-51	6	0	9	68	-67	-4	6	9	43	-40	9	-8	10	57	-52
-10	-8	9	52	-45	-10	-3	9	45	-42	-10	1	9	52	-50	1	6	9	43	44	-7	-7	10	50	-51
-8	-7	9	45	44	-9	-3	9	59	51	-9	1	9	66	66	0	7	9	36	32	-6	-7	10	74	75
-7	-7	9	100	-96	-6	-3	9	51	55	-8	1	9	67	-60	3	-15	10	45	33	-5	-7	10	86	-89
-5	-7	9	53	-56	-4	-3	9	63	-67	-7	1	9	49	50	-2	-14	10	66	-59	-4	-7	10	75	79
-2	-7	9	50	54	-3	-3	9	75	68	-3	1	9	55	60	-1	-14	10	49	50	-3	-7	10	89	-91
-1	-7	9	91	-92	-2	-3	9	47	-49	-2	1	9	115	-122	0	-14	10	54	-56	-2	-7	10	45	48
0	-7	9	148	146	-1	-3	9	39	38	-1	1	9	153	154	1	-14	10	33	35	1	-7	10	58	-58
1	-7	9	79	-80	1	-3	9	54	-49	0	1	9	88	-90	5	-14	10	49	51	2	-7	10	123	125
2	-7	9	58	60	2	-3	9	86	87	5	1	9	64	57	-3	-13	10	58	-53	3	-7	10	117	-120
3	-7	9	41	-43	3	-3	9	49	-42	6	1	9	64	-67	4	-13	10	31	26	4	-7	10	121	116
7	-7	9	70	-73	4	-3	9	26	-25	7	1	9	65	63	-2	-12	10	35	32	5	-7	10	28	-32
8	-7	9	79	82	5	-3	9	83	84	-7	2	9	49	54	-1	-12	10	69	-61	9	-7	10	46	-54
9	-7	9	72	-68	6	-3	9	56	-55	-5	2	9	36	25	0	-12	10	92	86	-10	-6	10	50	45
-7	-6	9	42	-46	8	-3	9	38	41	-3	2	9	44	-46	1	-12	10	58	-57	-7	-6	10	41	29
-6	-6	9	79	78	-10	-2	9	47	38	-2	2	9	29	27	2	-12	10	51	47	-6	-6	10	73	-71
-5	-6	9	109	-111	-6	-2	9	43	38	-1	2	9	56	-59	5	-12	10	39	-37	-5	-6	10	37	-30
-4	-6	9	84	82	-5	-2	9	99	-102	0	2	9	31	-32	6	-12	10	56	54	-4	-6	10	44	43
-3	-6	9	53	-55	-4	-2	9	125	127	1	2	9	57	52	7	-12	10	85	-87	-3	-6	10	72	-74
-1	-6	9	27	23	-3	-2	9	123	-116	4	2	9	66	61	-7	-11	10	48	-44	-2	-6	10	66	68
1	-6	9	60	-62	1	-2	9	45	-42	5	2	9	73	-66	-6	-11	10	59	53	1	-6	10	46	52
2	-6	9	150	157	2	-2	9	95	97	6	2	9	35	39	0	-11	10	43	45	2	-6	10	39	-43
3	-6	9	174	-171	3	-2	9	93	-98	-9	3	9	59	-58	2	-11	10	55	61	5	-6	10	38	-39
4	-6	9	44	46	4	-2	9	131	126	-8	3	9	87	79	-7	-10	10	40	42	6	-6	10	42	40
5	-6	9	31	-29	5	-2	9	96	-95	-7	3	9	61	-57	-6	-10	10	51	-50	8	-6	10	42	-47
6	-6	9	39	-39	6	-2	9	33	48	-3	3	9	36	-38	-1	-10	10	95	98	-5	-5	10	87	90
10	-6	9	64	63	-10	-1	9	52	58	-2	3	9	70	67	0	-10	10	107	-108	-4	-5	10	122	-121
-8	-5	9	40	-37	-9	-1	9	56	-62	-1	3	9	118	-121	1	-10	10	78	84	-3	-5	10	118	117
-7	-5	9	66	68	-7	-1	9	45	-47	0	3	9	76	76	2	-10	10	30	-34	-2	-5	10	54	-57
-6	-5	9	32	-32	-3	-1	9	74	-71	1	3	9	82	-80	7	-10	10	73	76	0	-5	10	34	31
-5	-5	9	55	52	-2	-1	9	106	103	2	3	9	44	48	8	-10	10	60	-54	1	-5	10	63	67
-4	-5	9	66	66	-1	-1	9	134	-135	6	3	9	50	48	-7	-9	10	66	62	2	-5	10	107	-104
0	-5	9	84	-83	0	-1	9	78	73	-7	4	9	37	-44	-6	-9	10	83	-83	3	-5	10	122	126

OBSERVED AND CALCULATED STRUCTURE FACTORS FOR H OS RE (CO)8 BR PPN

H	K	L	FO	FC	H	K	L	FO	FC	H	K	L	FO	FC	H	K	L	FO	FC	H	K	L	FO	FC
4	-5	10	104	-104	0	0	10	113	-115	2	-10	11	66	-71	5	-4	11	78	-81	2	3	11	31	-36
6	-5	10	51	-49	1	0	10	45	43	3	-10	11	88	86	-9	-3	11	67	-64	-5	4	11	79	77
9	-5	10	29	28	6	0	10	64	-67	4	-10	11	76	-74	-8	-3	11	54	52	-4	4	11	68	-66
-10	-4	10	71	-70	7	0	10	36	48	-4	-9	11	28	-23	-7	-3	11	60	-63	-3	4	11	30	41
-9	-4	10	43	35	-7	1	10	47	45	-3	-9	11	76	76	-2	-3	11	101	101	2	4	11	46	-53
-5	-4	10	30	28	1	1	10	47	47	1	-9	11	72	-76	-1	-3	11	129	-131	0	-14	12	53	54
-3	-4	10	81	80	2	1	10	98	-98	8	-9	11	38	32	0	-3	11	111	114	1	-14	12	52	-47
-2	-4	10	115	-117	5	1	10	57	-57	-6	-8	11	50	50	1	-3	11	67	-63	-4	-13	12	65	64
-1	-4	10	67	69	-8	2	10	63	60	-5	-8	11	72	-69	4	-3	11	40	35	1	-13	12	70	-65
2	-4	10	28	25	-7	2	10	71	-65	-4	-8	11	75	74	5	-3	11	53	-56	2	-13	12	53	46
3	-4	10	35	-32	-6	2	10	31	34	-3	-8	11	88	-90	6	-3	11	80	88	3	-13	12	52	-56
5	-4	10	74	77	-2	2	10	73	70	1	-8	11	30	-33	7	-3	11	66	-67	0	-12	12	46	-47
6	-4	10	85	-86	-1	2	10	83	-83	2	-8	11	67	69	8	-3	11	41	51	1	-12	12	48	44
-10	-3	10	46	38	0	2	10	99	98	3	-8	11	148	-153	-7	-2	11	74	-70	-6	-11	12	45	-41
-5	-3	10	47	-50	1	2	10	69	-71	4	-8	11	85	87	-6	-2	11	60	61	-2	-11	12	29	-23
-4	-3	10	128	129	-8	3	10	69	69	5	-8	11	34	-37	-3	-2	11	36	39	3	-11	12	67	69
-3	-3	10	66	-69	-5	3	10	63	-60	-9	-7	11	38	-39	1	-2	11	72	-72	4	-11	12	71	-72
-2	-3	10	61	62	-4	3	10	46	52	-4	-7	11	50	49	5	-2	11	68	68	5	-11	12	40	43
1	-3	10	43	-39	0	3	10	38	29	-3	-7	11	90	-89	-8	-1	11	58	-57	-6	-10	12	36	27
3	-3	10	83	-90	1	3	10	69	-77	-2	-7	11	53	56	-7	-1	11	75	80	-4	-10	12	34	-26
4	-3	10	106	106	2	3	10	84	76	-1	-7	11	68	-70	-6	-1	11	38	-39	-3	-10	12	66	61
5	-3	10	63	-62	3	3	10	45	-43	6	-7	11	67	63	-2	-1	11	71	-70	-2	-10	12	61	-65
6	-3	10	77	75	-7	4	10	42	41	-4	-6	11	88	-93	-1	-1	11	102	106	4	-10	12	35	-15
-10	-2	10	67	59	0	4	10	66	-62	-3	-6	11	129	128	0	-1	11	105	-103	6	-10	12	45	-37
-9	-2	10	64	-67	1	4	10	49	49	-2	-6	11	42	-47	1	-1	11	82	81	-7	-9	12	31	-24
-8	-2	10	55	55	2	4	10	50	-41	2	-6	11	75	-77	5	-1	11	46	40	-6	-9	12	32	23
-5	-2	10	26	-29	-5	5	10	70	69	3	-6	11	123	129	6	-1	11	48	-44	-5	-9	12	41	-45
-3	-2	10	65	-68	-4	5	10	57	-54	4	-6	11	67	-70	7	-1	11	71	70	-4	-9	12	79	82
-2	-2	10	112	110	1	5	10	47	50	5	-6	11	74	79	-7	0	11	69	68	-3	-9	12	64	-62
-1	-2	10	133	-135	2	5	10	54	-59	-9	-5	11	68	72	-6	0	11	72	-76	-2	-9	12	64	65
0	-2	10	115	116	-1	6	10	28	12	-8	-5	11	41	-45	-5	0	11	38	44	2	-9	12	39	40
2	-2	10	24	-26	-1	-13	11	53	-56	-4	-5	11	69	-69	-4	0	11	38	-36	3	-9	12	77	-73
4	-2	10	40	38	0	-13	11	66	59	-3	-5	11	75	73	1	0	11	52	63	4	-9	12	79	80
5	-2	10	74	-68	1	-13	11	75	-73	-2	-5	11	78	-75	2	0	11	79	-79	5	-9	12	50	-53
6	-2	10	91	97	-6	-12	11	63	57	-1	-5	11	115	117	3	0	11	70	68	-8	-8	12	38	35
-4	-1	10	54	-56	-5	-12	11	63	-59	0	-5	11	57	-58	-8	1	11	42	41	-4	-8	12	28	31
-3	-1	10	42	45	1	-12	11	52	-51	1	-5	11	52	45	-7	1	11	65	-70	-3	-8	12	78	-78
-2	-1	10	56	-54	2	-12	11	62	66	4	-5	11	28	-33	-1	1	11	67	-66	-2	-8	12	102	106
2	-1	10	35	43	3	-12	11	47	-42	5	-5	11	82	82	0	1	11	73	77	-1	-8	12	47	-48
4	-1	10	58	-58	-1	-11	11	38	44	6	-5	11	82	-84	1	1	11	58	-61	1	-8	12	19	-27
5	-1	10	59	59	0	-11	11	64	-61	7	-5	11	69	69	-7	2	11	38	-46	5	-8	12	54	-53
6	-1	10	58	-56	1	-11	11	89	86	-7	-4	11	41	41	-6	2	11	54	56	6	-8	12	62	61
-9	0	10	56	53	3	-11	11	28	15	-4	-4	11	53	55	-5	2	11	82	-81	7	-8	12	44	-45
-8	0	10	88	-86	4	-11	11	38	33	-3	-4	11	86	-87	-4	2	11	71	68	-5	-7	12	29	23
-7	0	10	43	53	-6	-10	11	70	-73	-2	-4	11	38	40	0	2	11	33	24	-4	-7	12	46	-51
-6	0	10	40	-51	-5	-10	11	75	78	2	-4	11	38	31	1	2	11	63	-63	-3	-7	12	53	51
-2	0	10	98	-100	-4	-10	11	48	-50	3	-4	11	50	-53	2	2	11	102	98	-2	-7	12	65	-66
-1	0	10	157	156	1	-10	11	40	43	4	-4	11	49	44	3	2	11	75	-72	2	-7	12	33	-43

OBSERVED AND CALCULATED STRUCTURE FACTORS FOR H OS RE (CO)8 BR PPN

H	K	L	FO	FC	H	K	L	FO	FC	H	K	L	FO	FC	H	K	L	FO	FC	H	K	L	FO	FC
3	-7	12	28	24	-4	-2	12	28	27	5	-9	13	44	-47	-7	-2	13	45	44	-1	-6	14	40	-39
4	-7	12	92	-96	-1	-2	12	79	84	6	-9	13	47	53	-6	-2	13	69	-68	0	-6	14	75	70
5	-7	12	35	36	0	-2	12	104	-110	-4	-8	13	35	-31	-5	-2	13	54	55	1	-6	14	75	-68
-7	-6	12	39	35	1	-2	12	63	60	1	-8	13	34	-30	-4	-2	13	52	-57	2	-6	14	31	29
-3	-6	12	62	61	2	-2	12	30	-35	3	-8	13	37	41	1	-2	13	50	56	-6	-5	14	68	66
-2	-6	12	107	-105	6	-2	12	45	-41	4	-8	13	45	-47	2	-2	13	66	-70	-5	-5	14	67	-72
-1	-6	12	80	86	-7	-1	12	47	49	-3	-7	13	43	35	3	-2	13	91	91	-4	-5	14	38	43
0	-6	12	106	-105	-6	-1	12	60	-62	-2	-7	13	29	-36	4	-2	13	56	-58	2	-5	14	60	72
1	-6	12	57	55	-5	-1	12	64	66	-1	-7	13	91	92	-3	-1	13	55	55	3	-5	14	89	-88
2	-6	12	29	-21	2	-1	12	109	-109	0	-7	13	90	-91	-5	0	13	54	-57	4	-5	14	43	42
5	-6	12	52	54	3	-1	12	64	68	1	-7	13	74	67	-4	0	13	81	80	-4	-4	14	35	41
6	-6	12	95	-92	0	0	12	40	39	5	-7	13	34	39	-3	0	13	44	-46	0	-4	14	52	-51
7	-6	12	67	66	1	0	12	50	-53	6	-7	13	71	-65	-2	0	13	38	37	1	-4	14	42	42
-7	-5	12	48	49	2	0	12	29	27	-7	-6	13	40	41	1	0	13	31	-34	-5	-3	14	62	61
-3	-5	12	62	-62	-6	1	12	45	56	-6	-6	13	62	-56	2	0	13	47	49	-3	-3	14	48	49
-2	-5	12	39	40	-5	1	12	75	-78	-5	-6	13	43	45	3	0	13	73	-73	2	-3	14	64	-62
-1	-5	12	37	17	-4	1	12	71	76	0	-6	13	42	-48	-3	1	13	35	-43	3	-3	14	89	89
0	-5	12	61	-64	-3	1	12	59	-64	1	-6	13	70	69	-1	1	13	38	-37	-3	-2	14	51	49
1	-5	12	34	25	2	1	12	74	80	2	-6	13	42	-41	-2	-12	14	71	-67	-2	-2	14	47	-49
4	-5	12	35	39	3	1	12	74	-71	5	-6	13	37	-32	-1	-12	14	57	57	-4	-1	14	47	45
5	-5	12	33	-30	-3	2	12	41	-47	6	-6	13	29	15	-2	-11	14	42	34	-3	-1	14	61	-60
-8	-4	12	56	60	-3	3	12	49	48	-7	-5	13	36	-40	1	-11	14	31	20	0	-11	15	49	48
-7	-4	12	37	-31	-2	3	12	27	-16	-6	-5	13	52	47	4	-11	14	50	45	2	-10	15	48	45
-5	-4	12	44	-40	-2	-13	13	31	31	-1	-5	13	86	-87	-2	-10	14	67	69	0	-9	15	53	-57
-2	-4	12	45	50	-3	-12	13	49	41	0	-5	13	76	77	-1	-10	14	59	-60	1	-9	15	47	40
-1	-4	12	95	-98	3	-12	13	69	71	1	-5	13	79	-76	0	-10	14	49	48	-4	-8	15	45	-46
0	-4	12	139	141	4	-12	13	56	-60	-6	-4	13	81	81	-2	-9	14	42	-44	1	-8	15	49	48
1	-4	12	54	-59	-3	-11	13	51	54	-5	-4	13	51	-57	1	-9	14	60	-53	2	-8	15	54	-63
5	-4	12	44	-43	-2	-11	13	58	-62	-4	-4	13	31	33	2	-9	14	42	51	3	-8	15	38	38
6	-4	12	90	84	-1	-11	13	58	57	0	-4	13	40	38	-2	-8	14	58	-56	1	-7	15	54	-56
7	-4	12	51	-53	5	-11	13	43	43	1	-4	13	64	-75	-1	-8	14	53	56	-4	-6	15	52	51
-7	-3	12	54	-54	3	-10	13	53	-55	2	-4	13	59	60	0	-8	14	77	-76	2	-6	15	52	56
-6	-3	12	63	64	4	-10	13	68	66	3	-4	13	65	-57	1	-8	14	65	64	3	-6	15	51	-52
-5	-3	12	60	-62	5	-10	13	46	-47	4	-4	13	52	50	-6	-7	14	57	-64	-3	-5	15	40	-46
2	-3	12	85	88	-3	-9	13	74	-74	-7	-3	13	49	45	-5	-7	14	59	55	-2	-5	15	49	52
3	-3	12	54	-60	-2	-9	13	71	67	-1	-3	13	42	47	0	-7	14	36	-36	1	-5	15	35	27
6	-3	12	36	-37	-1	-9	13	91	-91	0	-3	13	67	-65	1	-7	14	64	69	-3	-4	15	42	41
-8	-2	12	46	-57	0	-9	13	42	47	1	-3	13	77	75	3	-7	14	44	47	-2	-3	15	61	-63
-7	-2	12	47	51	4	-9	13	31	24															

REFERENCES

REFERENCES

1. C MASTERS. "Homogeneous Transition-metal Catalysis - A Gentle Art", London: Chapman & Hall (1981), p 20.

2. E L MUETTERTIES. Bull Soc Chim Belg, (1975) 84, 959.

3. B F G JOHNSON. "Transition Metal Clusters", Chichester: Wiley (1980).

4. E L MUETTERTIES. Science, (1977) 196, 839.

5. (a) R UGO. Catal Rev, (1975) 11, 225.

   (b) J A CONNOR. J Organometal Chem, (1975), 94, 195.

   (c) P J GARDNER, A CARTNER, R G CUNNINGHAME & B H ROBINSON. J Chem Soc (Dalton), (1975), 2582.

6. F A COTTON & G WILKINSON. "Advanced Inorganic Chemistry", 4th ed, New York: John Wiley (1980), p 1081.

7. G L GEOFFROY. Acc Chem Res, (1980), 13, 469.

8. R B KING. Prog Inorg Chem, (1972), 15, 287.

9. F A COTTON. Quart Revs, (1966), 389.

10. D L KEPERT & K VRIEZE. In: "Comprehensive Inorganic Chemistry", 4, Pergamon Press, New York (1973), p 97.

11. H VAHRENKAMP. In: "Structure and Bonding", 32, Berlin: Springer-Verlag (1977), p 1.

12. H VAHRENKAMP. Angew Chem, Int Ed Engl, (1978), 17, 379.

13. C J COMMONS & B F HOSKINS. Aust J Chem, (1975), 28, 1663.

14. J R SHAPLEY, J B KEISTER, M R CHURCHILL & B G DE BOER. J Amer Chem Soc, (1975), 97, 4145.

15. F A COTTON. Inorg Chem, (1966), 5, 1083.

16. C M COMRIE & W H WEINBERG. J Chem Phys, (1976), 64, 250.

17. C MASTERS. Adv Organomet Chem, (1979), 17, 61.

18. G HENRICI-OLIVÈ & S OLIVÈ. Angew Chem, Int Ed Engl, (1976), 15, 136.

19. (a) R C BRADY & R PETTIT. J Amer Chem Soc, (1980), 102, 6181.

(b) R C BRADY & R PETTIT. J Amer Chem Soc, (1981), 103, 1287.

20. W A HERRMANN. Angew Chem, Int Ed Engl, (1982), 21, 117.

21. I A OXTON, D B POWELL, N SHEPPHARD, K BURGESS, B F G JOHNSON & J LEWIS. J C S Chem Comm, (1982), 719.

22. E L MUETTERTIES & J STEIN. Chem Revs, (1979), 79, 479.

23. P DAY. Chemistry in Britain, (1983), 308.

24. I M FRITH. In: "Superconductivity", J G Cook, ed, London: Mills & Boon Ltd (1972), p 8.

25. R SPAL & A J HEEGER. Phys Rev Lett, (1977), 39, 650.

26. K KROGMANN. Angew Chem, Int Ed Engl, (1969), 8, 35.

27. J S MILLER & A J EPSTEIN. Prog Inorg Chem, (1976), 20, 1.

28. L V INTERRANTE. In: "Extended Interactions between Metal Ions in Transition Metal Complexes, Amer Chem Soc Symp Ser, (1974), no 5.

29. H J KELLER. "Low Dimensional Cooperative Phenomena", Nato Advanced Study Series, Physics, 7, New York: Plenum Press (1974).

30. M N AHMAD & A E UNDERHILL. J Chem Soc (Dalton), (1982), 1065.

31. A P GINSBERG, J W KOEPKE, J J HAUSER, K W WEST, F J DI SALVO, C R SPRINKLE & R L COHEN. Inorg Chem, (1976), 15, 514.

32. F A COTTON & G WILKINSON. "Advanced Inorganic Chemistry". 4th ed, New York: John Wiley (1980), p 1110-11.

33. Y-N CHIU & F E WANG. Inorg Chem, (1982), 21, 4264.

34. B F G JOHNSON & J LEWIS. Adv In Inorg Chem Radiochem, (1981), 24, 225.

35. J E YATES. Honours project, Chemistry Department, Rhodes University (1979).

36. J P COLLMAN, D W MURPHY, E B FLEISCHER & D SWIFT. Inorg Chem, (1974), 13, 1.

37. E W ABEL, R D McLEAN & S MOORHOUSE. Inorg Nucl Chem Lett, (1971), 7, 587.

38. A C WILLIS, G N VAN BUUREN, R K POMEROY & F W B EINSTEIN. Inorg Chem, (1983), 22, 1162.

39. M R CHURCHILL & B G DE BOER. Inorg Chem, (1977), 16, 878.

40. N COOK, L SMART & P WOODWARD. J Chem Soc (Dalton), (1977), 1744.

41. R BAU, S W KIRTLEY, T N SORRELL & S WINARKO. J Amer Chem Soc, (1974), 96, 988.

42. G O EVANS & R K SHELINE. J Inorg Nucl Chem, (1968), 30, 2862.

43. P CHINI. Pure & Appl Chem, (1970), 23, 489.

44. R USÓN, A LAGUNA, M LAGUNA, P G JONES & G M SHELDRICK. J Chem Soc (Dalton), (1981), 366.

45. R N BRIER, A A CHALMERS, J LEWIS & S B WILD. J Chem Soc (A), (1967), 1889.

46. J L BLUNDELL & H M POWELL. J Chem Soc (A), (1971), 1685.

47. D MORAS, J DEHAND & R WEISS. Compt rend, (1968), 267C, 1471.

48. P BRAUNSTEIN & J DEHAND. Bull Soc Chim Fr, (1975), 1997.

49. P BRAUNSTEIN, J DEHAND & J F NENNIG. J Organometal Chem, (1975), 92, 117.

50. J FISCHER, A MITSCHLER, R WEISS, J DEHAND & J F NENNIG. J Organometal Chem, (1975), 91, C37.

51. J P BARBIER & P BRAUNSTEIN.
J Chem Res (S), (1978), 412.
J Chem Res (M), (1978), 5029.

52. A GIRAUDEAU, P LEMOINE, M GROSS & P BRAUNSTEIN. J Organometal Chem, (1980), 202, 455.

53. P BRAUNSTEIN, D MATT, O BARS, M LOUËR, D GRANDJEAN, J FISCHER & A MITSCHLER. J Organometal Chem, (1981), 213, 79.

54. P LEMOINE, A GIRAUDEAU, M GROSS, R BENDER & P BRAUNSTEIN. J Chem Soc (Dalton), (1981), 2059.

55. P H M BUDZELAAR, J BOERSMA & G J M VAN DER KERK, J Organometal Chem, (1980), 202, C71.

56. J M BURLITCH & R C WINTERTON. Inorg Chem, (1979), 18, 2309.

57. H HOCK & H STUHLMAN. Chem Ber, (1928), 61, 2097.

58. C G PIERPONT, R G SHONG & B A SOSINSKY. Inorg Chem, (1982), 21, 3247.

59. J J HABEEB, D G TUCK & Z ZHANDIRE. Can J Chem, (1979), 57, 2196.

60. P H M BUDZELAAR, J BOERSMA, G J M VAN DER KERK, A L SPEK & A J M DUISENBERG. Inorg Chem, (1982), 21, 3777.

61. B LEE, J M BURLITCH & J L HOARD. J Amer Chem Soc, (1967), 89, 6363.

62. G E COATES, M L H GREEN, P POWELL & K WADE. "Principles of Organometallic Chemistry". London: Methuen (1971), p 150.

63. P H M BUDZELAAR, H J ALBERTS-JANSEN, J BOERSMA & G J M VAN DER KERK. Polyhedron, (1982), 1 (6), 563.

64. S N TITOVA, V T BYCHKOV, G A DOMRACHEV, G A RAZUVAEV, YU T STRUCHKOV & L N ZAKHAROV. J Organometal Chem, (1980), 187, 167.

65. R B KING & F G A STONE. Inorg Synth, (1963), 1, 99.

66. M J ALBRIGHT & J P OLIVER. J Organometal Chem, (1979), 172, 99.

67. F GLOCKLING, V B MAHALE & J J SWEENEY. J Chem Soc (Dalton), (1979), 767.

68. H W BAIRD & L F DAHL. J Organometal Chem, (1967), 7, 503.

69. B L BOOTH, G C CASEY & R N HASZELDINE. J Chem Soc (Dalton), (1980), 403.

70. D SEYFERTH & R J SPOHN. J Amer Chem Soc, (1969), 91, 3037.

71. M N BOCHKAREV, L P MAIOROVA & G A RAZUVAEV. Zh Obshch Khim, (1980), 50, 903.

72. T N TEPLOVA, L G KUZMINA, YU T STRUCHKOV, V I SOKOLOV, V V BASHILOV, M N BOCHKAREV, L P MAIOROVA & P V PETROVSKI. Koord Khim, (1980), 6, 134.

73. R B KING. Inorg Chem, (1970), 9, 1936.

74. J RAJARAM & J A IBERS. Inorg Chem, (1973), 12, 1313.

75. H VAHRENKAMP. Chem Ber, (1974), 107, 3867.

76. H PREUT, W WOLFES & H-J HAUPT. Z anorg chem, (1975), 412, 121.

77. K D BOS, E J BULTEN, J G NOLTES & A L SPEK. J Organometal Chem, (1975), 92, 33.

78. W KÖDEL, F HUBER & H-J HAUPT. Z anorg chem, (1979) 448, 126.

79. I NODA, S KATO, M MIZULA, W YASNAKA & N KASAI. Angew Chem, Int Ed Engl, (1979), 18, 83.

80. J A K HOWARD, S C KELLETT & P WOODWARD. J Chem Soc (Dalton), (1975), 2332.

81. F A COTTON & W T EDWARDS. J Amer Chem Soc, (1968), 90, 5412.

82. S P GUBIN, D M CHENTSOVA, G V BURMAKINA & A A IOGANSON. Izves Akad Nauk SSSR, Ser Khim, (1981), 12, 2790.

83. J R MOSS & W A G GRAHAM. J Organometal Chem, (1969), 18, P24.

84. F P BOER & J J FLYNN. J Amer Chem Soc, (1971), 93, 6495.

85. F P BOER, J H TSAI & J J FLYNN. J Amer Chem Soc, (1970), 92, 6094.

86. F GLOCKLING & A F CLEMMIT. J Chem Soc (A), (1971), 1164.

87. F GLOCKLING & R J I POLLOCK. J Chem Soc (Dalton), (1975), 497.

88. C EABORN, K KUNDU & A PIDCOCK. J Chem Soc (Dalton), (1981), 1223.

89. C EABORN, A PIDCOCK & B R STEELE. J Chem Soc (Dalton), (1975), 809.

90. H BEHRENS, K GÖRTUNG, P MERBACH & M MOLL. Z anorg chem, (1979), 454, 67.

91. F H CARRE, R J P CORRIU & B J L HENNER. J Organometal Chem, (1982), 228, 139.

92. A N NESMEYANOV, K N ANISIMOV, N E KOLOBOVA & M YA ZAKHAROV. Proc Acad Sci USSR, Chem Sect, (1964), 156, 532.

93. L K THOMPSON, E EISNER & M J NEWLANDS. J Organometal Chem, (1973), 56, 327.

94. P HACKETT & A R MANNING. J Chem Soc (Dalton), (1974), 2257.

95. M MOLL, H BEHRENS, P MERBACH, K GÖRTUNG, G LIEHR & R BÖHMA. Z Naturforsch B, (1980), 35b, 1115.

96. K JONAS. Angew Chem, Int Ed Engl, (1975), 14, 752.

97. D J BRAUER, C KRÜGER & J C SEKUTOWSKI. J Organometal Chem, (1979), 178, 249.

98. M GOCHIN. Personal communication.

99. W R WADT. J Amer Chem Soc, (1981), 103, 6053.

100. K TATSUMI & R HOFFMANN. Inorg Chem, (1980), 19, 2656.

101. F A COTTON & G WILKINSON. "Advanced Inorganic Chemistry", 4th ed, New York: John Wiley (1980), p 210.

102. J P COLLMAN, R K ROTHROCK, R G FINKE, E J MOORE & F ROSE-MUNCH. Inorg Chem, (1982), 21, 146.

103. E L MUETTERTIES. J Organometal Chem, (1980), 200, 177.

104. V W DAY, M F FREDRICH, G S REDDY, A J SIVAK, W R PRETZER & E L MUETTERTIES. J Amer Chem Soc, (1977), 99, 8091.

105. H W CHOI & E L MUETTERTIES. Inorg Chem, (1981), 20, 2664.

106. W A HERRMANN. Pure & Appl Chem, (1982), 54, 65.

107. C E SUMNER, P E RILEY, R E DAVIS & R PETTIT. J Amer Chem Soc, (1980), 102, 1754.

108. D L DAVIES, A F DYKE, S A R KNOX & M J MORRIS. J Organometal Chem, (1981), 215, C30.

109. K M MOTYL, J R NORTON, C K SCHAUER & O P ANDERSON. J Amer Chem Soc, (1982), 104, 7325.

110. K H THEOPOLD & R G BERGMAN. J Amer Chem Soc, (1981), 103, 2489.

111(a) L BREWER. Science, (1968), 161, 115.

(b) Values represent the heats of atomisation of the element per bonding electron per atom at 298.15 K or at the melting points, whichever temperature is lower.

112. W MANCHOT & J KÖNIG. Ber, (1925), 58, 229.

113. W HIEBER & H STALLMAN. Ber, (1942), 75, 1472.

114. L A W HALES & R J IRVING. J Chem Soc (A), (1967), 1932.

115. M I BRUCE, M COOKE, M GREEN & D J WESTLAKE. J Chem Soc (A), (1969), 987.

116. G BRACA, S SBRANA, P PINO & E BENEDETTI. Chimica o Industria, (1967), 49, 1381.

117. S MERLINO & G MONTAGNOLI. Acta Cryst, (1968), B24, 424.

118. M I BRUCE & F G A STONE. J Chem Soc (A), (1967), 1238.

119. B F G JOHNSON, J LEWIS & P A KILTY. J Chem Soc (A), (1968), 2859.

120. D R TYLER, M ALTOBELLI & H B GRAY. J Amer Chem Soc, (1980), 102, 3022.

121. R PSARO & C DOSSI. Inorg Chim Acta, (1983), 77, L255.

122. E W ABEL, G B HARGREAVES & G WILKINSON. J Chem Soc (A), (1958), 3149.

123. J P MAHER. Personal communication.

124. J P CANDLIN & J COOPER. J Organometal Chem, (1968), 15, 230.

125. S ROSENBERG, A W HERLINGER, W S MAHONEY & G L GEOFFROY. Submitted for publication, 1985.

126. J R MOSS & W A G GRAHAM. J Chem Soc (Dalton), (1977), 89.

127. J R MOSS & W A G GRAHAM. Inorg Chem, (1977), 16, 75.

128. R D ADAMS & J P SELEGUE. In: "Comprehensive Organometallic Chemistry", G Wilkinson, F G A Stone & E W Abel, eds. Oxford: Pergamon Press (1982), 4, p 967-71.

129. F L'EPLATTENIER & F CALDERAZZO. Inorg Chem, (1967), 6, 2092.

130. M PANKOWSKI & M BIGORGNE. J Organometal Chem, (1969), 19, 393.

131. E BENEDETTI, G BRACA, G SBRANA, F SALVETTI & B GRASSI. J Organometal Chem, (1972), 37, 361.

132. B F G JOHNSON, R D JOHNSTON & J LEWIS. J Chem Soc (A), (1969), 792.

133. A J DEEMING, B F G JOHNSON & J LEWIS. J Organometal Chem, (1969), 17, 40.

134. E E SUTTON, M L NIVEN & J R MOSS. Inorg Chim Acta, (1983), 70, 207.

135. F R HARTLEY. In: "Comprehensive Organometallic Chemistry", G Wilkinson, F G A Stone & E W Abel, eds, Oxford: Pergamon Press, (1982), 6, p 488.

136. D J ROBINSON. M.Sc Thesis, University of the Witwatersrand, Johannesburg, South Africa.

137. G W HARRIS, J C A BOEYENS & N J COVILLE. **Organometallics**, (1985), 4, 914.

138. E W ABEL & G WILKINSON. J **Chem Soc (A)**, (1959), 1501.

139. G H STOUT & J L JENSEN. "X-Ray Structure Determination, A Practical Guide". London: MacMillan (1968).

140. M J BUERGER. "Crystal Structure Analysis". New York: J Wiley and Sons, Inc (1967).

141. J P GLUSKER & K N TRUEBLOOD. "Crystal Structure Analysis - A Primer". London: Oxford University Press (1972).

142. J S KASPER & K LONSDALE, eds. International Tables for X-Ray Crystallography, Vols I, II, III, IV. Birmingham: Kynock Press.

143. G M SHELDRICK. The SHELX program system. Univ Chem Lab, Cambridge (1976).

144. L PAULING. "The Nature of the Chemical Bond". New York, Ithaca: Cornell Univ Press (1960).

145. D T CROMER & J B MANN. **Acta Cryst**, (1968), A24, 321.

146. D T CROMER & D LIBERMAN. J **Chem Phys**, (1970), 53, 1891.

147. M H DU PLESSIS. University of Cape Town. Unpublished programme. (1981).

148. W D S MOTHERWELL. Cambridge. Unpublished programme.

149. M R CHURCHILL. Personal communication quoted in: J W KELLAND & J R NORTON. J Organometal Chem, (1978), 149, 185.

150. A C T NORTH, D C PHILLIPS & F S MATHEWS. Acta Cryst, (1968), A24, 351.

151. W J A M PETERSE & J H PALM. Acta Cryst, (1966), 20, 147.

152. M R CHURCHILL, K N AMOH, H J WASSERMAN. Inorg Chem, (1981), 20, 1609.

153. M F BAILEY & L F DAHL. Inorg Chem, (1965), 4, 1140.

154. M G BENNETT & R MASON. Nature (London), (1965), 205, 760.

155. W A G GRAHAM. Inorg Chem, (1968), 7, 315.

156. P A AGRON, R D ELLISON & H A LEVY, Acta Cryst, (1967), 23, 1079.

157. S F KETTLE. Inorg Chem, (1965), 4, 1661.

158. R MASON, K M THOMAS, D F GILL & B L SHAW. J Organometal Chem, (1972), 40, C67.

159. G G SUMNER, H P KLUG & L E ALEXANDER. Acta Cryst, (1964), 17, 732.

160. B K TEO, M B HALL, R F FENSKE & L F DAHL. Inorg Chem, (1975), 14, 3103.

161. A F WELLS. "Structural Inorganic Chemistry", 3rd edition. London: Oxford University Press (1962), p 84.

162. J G BULLIT & F A COTTON. **Inorg Chim Acta**, (1971), 5, 406.

163. R P DODGE, O S MILLS & V SCHOMAKER. **Proc Chem Soc**, (1963), 380.

164. M R CHURCHILL, F J HOLLANDER & J P HUTCHINSON. **Inorg Chem**, (1977), 16, 2697.

165. J PUGA, R SÁNCHEZ-DELGADO, A ANDRIOLLO, J ASCANIO & D BRAGA. **Organometallics**, (1985), 4, 2064.

166. S F WATKINS, F R FRONCZEK, K A ABBOUD, T J DELORD, J T DONNER, T A EKMAN, M A GUTIERREZ, H W LEE, J H MEDLEY, M A OLIVER, R V PICCIONE, W E PUCKETT, D R SALINOVICH, E M SKELLY, R D SNELLING & M M SOROCZAK. **Am Cryst Assoc, Series 2**, (1981), 9, 21.

167. D H FARRAR, P G JACKSON, B F G JOHNSON, J LEWIS, W J H NELSON & M D VARGAS. J C S **Chem Comm**, (1981), 1009.

168. B F G JOHNSON, J LEWIS, W J H NELSON, M VARGAS, D BRAGA & M McPARTLIN. **J Organometal Chem**, (1983), 249, C21.

169. P DONALDSON & M J BENNETT. Personal Communication.

170. W C HAMILTON. **Acta Cryst**, (1965), C8, 502.

171. F A COTTON & J L THOMPSON. **J Amer Chem Soc**, (1980), 102, 6437.

172. G R CLARK, K MARSDEN, W R ROPER & L J WRIGHT. **J Amer Chem Soc**, (1980), 102, 6570.

173. J A IGGO, D P MARKHAM, B L SHAW & M THORNTON-PETT. J C S Chem Comm, (1985), 432.

174. A V RIVERA, G M SHELDRICK & M B HURSTHOUSE. Acta Crystallogr (B), (1978), 34, 3376.

175. B F G JOHNSON, J LEWIS, P R RAITHBY, K WONG & K D ROUSSE. J Chem Soc (Dalton), (1980), 1248.

176. A BONDI. J Phys Chem, (1964), 68, 441.

177. D W HART, R BAU & T F KOETZLE. J Amer Chem Soc, (1977), 99, 7557.

178. T BERINGHELLI, G CIANI, G D'ALFONSO, L GHIDORSI, H MOLINARI, A SIRONI & M FRENI. Poster 506, XII, ICOMC, Vienna, September, 1985.

179. R POLI, G WILKINSON, M MOTEVALLI & M B HURSTHOUSE. J Chem Soc (Dalton), (1985), 931.

180. M R CHURCHILL & F J HOLLANDER. Inorg Chem, (1977), 16, 2493.

181. M R CHURCHILL, F J HOLLANDER, R A LASHEWYCZ, G A PEARSON & J R SHAPLEY. J Amer Chem Soc, (1981), 103, 2430.

182. R BAU , B FONTAL, H D KAESZ & M R CHURCHILL. J Amer Chem Soc, (1967), 89, 6374.

183. L-Y HSU, N BHATTACHARYYA, S G SHORE. Organometallics, (1985), 4, 1483.

184. R W BROACH & J M WILLIAMS. Inorg Chem, (1979), 18, 374.

185. M C COULDWELL & J SIMPSON. Cryst Struct Comm, (1977), 6, 1.

186. E J DITZEL, B F G JOHNSON, J LEWIS, P R RAITHBY & M J TAYLOR. **J Chem Soc (Dalton)**, (1985), 555.

187. R L LINTVEDT, B TOMLONOVIC, D E FENTON & M D GLICK. **Adv Chem Ser**, (1976), 150 (Inorg Compd Unusual Prop, Symp, 1975), 407.

188. M D GLICK & R L LINTVEDT. **Prog Inorg Chem**, (1976), 21, 233.

189. U CASELLATO, P A VIGATO, D E FENTON & M VIDALI. **Chem Soc Rev**, (1979), 8, 199.

190. D A WROBLESKI & T B RAUCHFUSS. **J Amer Chem Soc**, (1982), 104, 2314.

191. D A ROBERTS & G L GEOFFROY. In: "Comprehensive Organometallic Chemistry", G Wilkinson, F G A Stone and E W Abel, eds. Oxford: Pergamon Press (1982), Chapter 40, 5, p 763.

192. W L GLADFELTER & G L GEOFFROY. **Adv Organometal Chem**, (1980), 18, 207.

193. N S VYAZANKIN, G A RAZUVAEV & O A KRUGLAYA. **Organometal Chem Rev**, (1968), 3A, 323.

194. D A ROBERTS, W C MERCER, S M ZAHURAK, G L GEOFFROY, C W DE BROSSE, M E CASS & C G PIERPONT. **J Amer Chem Soc**, (1982), 104, 910.

195. T J MEYER. **Prog Inorg Chem**, (1975), 19, 1.

196. F A COTTON & G WILKINSON. "Advanced Inorganic Chemistry", 4th edition. New York: John Wiley, (1980), p 1062-63.

197. J E ELLIS & E A FLOM. **J Organometal Chem**, (1975), 99, 263.

198. R B KING. Acc Chem Res, (1970), 3, 417.

199. R D GEORGE, S A R KNOX & F G A STONE. J Chem Soc (Dalton), (1973), 972.

200. F L'EPLATTENIER. Inorg Chem, (1969), 8, 965.

201. J E ELLIS. J Organometal Chem, (1975), 86, 1.

202. H W WALKER & P C FORD. J Organometal Chem, (1981), 214, C43.

203. R G PEARSON, H W WALKER, H MAUERMANN & P C FORD. Inorg Chem, (1981), 20, 2741.

204. J B KEISTER. J Organometal Chem, (1983), 245, 409.

205. W HIEBER & G BRENDEL. Z anorg chem, (1957), 289, 324.

206. C R EADY, B F G JOHNSON, J LEWIS & M C MALATESTA. J Chem Soc (Dalton), (1978), 1358.

207. C C NAGEL, J C BRICKER, D G ALWAY & S G SHORE. J Organometal Chem, (1981), 219, C9.

208. W J CARTER, J W KELLAND, S J OKRASINSKI, K E WARNER & J R NORTON. Inorg Chem, (1982), 21, 3955.

209. R F JORDAN & J R NORTON. J Amer Chem Soc, (1982), 104, 1255.

210. J K RUFF. Inorg Chem, (1968), 7, 1818.

211. R J M CLARK & B C CROSSE. J Chem Soc (A), (1969), 224.

212. C P CASEY & S M NEUMANN. J Amer Chem Soc, (1978), 100, 2544.

213. G O EVANS, J P HARGADEN & R K SHELINE. Chem Comm, (1967), 186.

214. W HIEBER, W BECK & G ZEITLER. Angew Chem, (1961), 73, 364.

215. G M WHITESIDES & G MAGLIO. J Amer Chem Soc, (1969), 91, 4980.

216. W HIEBER & H BEUTNER. Z Anorg allg chem, (1962), 317, 63.

217. J KNIGHT & M J MAYS. J Chem Soc (Dalton), (1972), 1022.

218. H D KAESZ & R B SAILLANT. Chem Revs, (1972), 72, 231.

219. D H GIBSON, W-L HSU & F U AHMED. J Organometal Chem, (1981), 215, 379.

220. R B KING. 'Transition Metal Compounds Organometallic Synthesis', Vol 1, New York: Academic Press (1965).

221. C W BRADFORD, W VAN BRONSWIJK, R J H CLARK & R S NYHOLM. J Chem Soc (A), (1970), 2889.

222. K WADE. In: "Transition Metal Clusters", ed B F G Johnson. New York: Wiley (1980), Chapter 3.

223. D G EVANS & D M P MINGOS. J Organometal Chem, (1982), 232, 171.

224. J A K HOWARD, L FARRUGIA, C FOSTER, F G A STONE & P WOODWARD. Eur Cryst Meeting, (1980), 6, 73.

225. B F G JOHNSON, D A KANER, J LEWIS, P R RAITHBY & M J TAYLOR. Polyhedron, (1982), 1, 105.

226. J LEWIS & B F G JOHNSON. **Pure & Appl Chem**, (1982), **54**, 97.

227. R A FALTYNEK & M S WRIGHTON. **J Amer Chem Soc**, (1978), **100**, 159.

228. F ZINGALES, M GRAZIANI, F FARAONE & U BELLUCO. **Inorg Chim Acta**, (1967), 1, 1972.

229. G C DEMITRAS & E L MUETTERTIES. **J Amer Chem Soc**, (1977), **99**, 2796.

230. C UNGERMAN, V LANDIS, S A MOYA, H COHEN, H WALKER, R G PEARSON, R G RINKER & P C FORD. **J Amer Chem Soc**, (1979), **101**, 5922.

231. J A CONNER. **Top Curr Chem**, (1977), 71, 71.

232. A CERIOTTI, G LONGONI, R D PERGOLA, B T HEATON & D O SMITH. **J Chem Soc (Dalton)**, (1983), 1433.

233. G L GEOFFROY. **Prog Inorg Chem**, (1980), 27, 123.

234. G A THOMLINSON. Consiglio Nazionale Delle Ricerche, Rome: study in progress.

235. D CRAWFORD. University of Cape Town: study in progress.

236. B K TEO & D C JOY, eds. "EXAFS Spectroscopy", New York: Plenum Press (1981).

237. T E WOLFF, J M BENG, K O HODGSON, R B FRANKEL & R H HOLM. **J Amer Chem Soc**, (1979), **101**, 4140.

238. R PSARO, R UGO, G M ZANDERIGHI, B BESSON, A K SMITH & J M BASSET. **J Organometal Chem**, (1981), 213, 215.

239. S L COOK, J EVANS, G N GREAVES, B F G JOHNSON, J LEWIS, P R RAITHBY, P B WELLS & P WORTHINGTON. J C S Chem Comm, (1983), 777.

240. J R MOSS & W A G GRAHAM. J C S Chem Comm, (1969), 800.

241. J R MOSS & W A G GRAHAM. J Organometal Chem, (1970), 23, C47.

242. R K HARRIS & B E MANN, eds . "NMR and the Periodic Table", Academic Press, London (1978).

243. L VANCEA & W A G GRAHAM. J Organometal Chem, (1977), 134, 219.

244. E C CONSTABLE, B F G JOHNSON, J LEWIS, G N PAIN & M J TAYLOR. J C S Chem Comm, (1982), 754.

245. B E MANN, C MASTERS & B L SHAW. J C S Chem Comm, (1970), 1041.

246. P F JACKSON, B F G JOHNSON, J LEWIS, M McPARTLIN & W J H NELSON. J C S Chem Comm, (1982), 49.

247. B F G JOHNSON, J LEWIS, P R RAITHBY, G M SHELDRICK, K WONG & M McPARTLIN. J Chem Soc (Dalton), (1978), 673.

248. G A WEBB. In: "NMR and the Periodic Table". R K Harris & B E Mann, eds, London: Academic Press (1978).

249. K A K EBRAHEEM & G A WEBB. Prog NMR Spectry, (1977), 9; (1977), 11, 149.

250. A CARRINGTON & A D McLACHLAN. "Introduction to Magnetic Resonance", New York: Harper & Row (1967), Chapter 5.

251. T F BOLLES & R S DRAGO. J Amer Chem Soc, (1966), 88, 5730.

252. P W ATKINS, J C GREEN & M L H GREEN. J Chem Soc (A), (1968), 2275.

253. B DEUBZER & H D KAESZ. J Amer Chem Soc, (1968), 90, 3276.

254. D A STANISLAWSKI & R WEST. J Organometal Chem, (1981), 204, 295.

255. P W FROST, J A K HOWARD, J L SPENCER & D G TURNER. J C S Chem Comm, (1981), 1104.

256. R H HILL, P DE MAYO & R J PUDDEPHATT. Inorg Chem, (1982), 21, 3642.

257. A A KORIDZE, O A KIZAS, N M ASTAKHOVA, P V PETROVSKII & Y K GRISHIN, J C S Chem Comm, (1981), 853.

258. Calculated mass spectra were obtained using a computer program originally prepared by Drs R S Gray and E H Brooks, University of Alberta, Edmonton, Alberta, Canada, and modified for use on the University of Cape Town computer by Dr M L Niven.

259. D C PERRIN. "Purification of Laboratory Chemicals", Oxford: Pergamon Press (1966).

260. J C HILEMAN, D K HUGGINS & H D KAESZ. Inorg Chem, (1962), 1, 933.

261. L VANCEA & W A G GRAHAM. J Organometal Chem, (1977), 134, 219.

262. H D KAESZ, R BAU, D HENDRICKSON & J M SMITH. J Amer Chem Soc, (1967), 89, 2844.